NSEL Report Series
Report No. NSEL-016
August 2009

Seismic Performance of Anchored Brick Veneer

Dziugas Reneckis
and
James M. LaFave

NEWMARK STRUCTURAL ENGINEERING LABORATORY

Department of Civil and Environmental Engineering
University of Illinois at Urbana-Champaign

UILU-ENG-2009-1804

ISSN: 1940-9826

The Newmark Structural Engineering Laboratory (NSEL) of the Department of Civil and Environmental Engineering at the University of Illinois at Urbana-Champaign has a long history of excellence in research and education that has contributed greatly to the state-of-the-art in civil engineering. Completed in 1967 and extended in 1971, the structural testing area of the laboratory has a versatile strong-floor/wall and a three-story clear height that can be used to carry out a wide range of tests of building materials, models, and structural systems. The laboratory is named for Dr. Nathan M. Newmark, an internationally known educator and engineer, who was the Head of the Department of Civil Engineering at the University of Illinois [1956-73] and the Chair of the Digital Computing Laboratory [1947-57]. He developed simple, yet powerful and widely used, methods for analyzing complex structures and assemblages subjected to a variety of static, dynamic, blast, and earthquake loadings. Dr. Newmark received numerous honors and awards for his achievements, including the prestigious National Medal of Science awarded in 1968 by President Lyndon B. Johnson. He was also one of the founding members of the National Academy of Engineering.

Contact:
Prof. B.F. Spencer, Jr.
Director, Newmark Structural Engineering Laboratory
2213 NCEL, MC-250
205 North Mathews Ave.
Urbana, IL 61801
Telephone (217) 333-8630
E-mail: bfs@illinois.edu

This technical report is based on the first author's doctoral dissertation of the same title, which was completed in May 2009. The second author served as the dissertation advisor for this work.

Financial support for this research was provided by State Farm Insurance (through Laird Macdonald, Superintendent of their Building Technology Lab) and also by the Mid-America Earthquake (MAE) Center (under a grant from the Earthquake Engineering Research Centers program of the National Science Foundation per Award No. EEC-9701785).

The cover photographs are used with permission. The Trans-Alaska Pipeline photograph was provided by Terra Galleria Photography (http://www.terragalleria.com/).

ABSTRACT

A study was conducted on the out-of-plane seismic performance of anchored brick veneer with wood-frame backup wall systems, to evaluate prescriptive design requirements and current construction practices. Prescriptive requirements for the design and construction of anchored brick veneer are currently provided by the Masonry Standards Joint Committee (MSJC) Building Code, the International Residential Code (IRC) for One- and Two-Family Dwellings, and the Brick Industry Association (BIA) Technical Notes. Laboratory tests were conducted on brick-tie-wood subassemblies, comprising two bricks with a corrugated sheet metal tie either nail- or screw-attached to a wood stud, permitting an evaluation of the stiffness, strength, and failure modes for a local portion of a veneer wall system, rather than just of a single tie by itself. Then, full-scale brick veneer wall specimens (two one-story solid walls, as well as a one-and-a-half story wall with a window opening and a gable region) were tested under static and dynamic out-of-plane loading on a shake table. The shake table tests captured the performance of brick veneer wall systems, including interaction and load-sharing between the brick veneer, corrugated sheet metal ties, and wood-frame backup. Finally, all of these test results were used to develop finite element models of brick veneer wall systems, including nonlinear inelastic properties for the tie connections. The experimental and analytical studies showed that the out-of-plane seismic performance of residential anchored brick veneer walls is generally governed by: tensile stiffness and strength properties of the tie connections, as controlled by tie installation details; overall grid spacing of the tie connections, especially for tie installation along the edges and in the upper regions of walls; and, overall wall geometric variations. Damage limit states for single-story residential brick veneer wall systems were established from the experimental and analytical studies as a function of tensile failure of key tie connections, and the seismic fragility of this form of construction was then evaluated. Based on the overall findings, it is recommended that codes incorporate specific requirements for tie connection installation along all brick veneer wall edges, as well as for tie connection installation at reduced spacings in the upper regions of wall panels and near stiffer regions of the backup. Residential anchored brick veneer construction should as a minimum be built in accordance with the current prescriptive code requirements and recommendations, throughout low to moderate seismicity regions of the central and eastern U.S., whereas non-compliant methods of construction commonly substituted in practice are generally not acceptable.

TABLE OF CONTENTS

INTRODUCTION

1.1 Overview of Residential Anchored Brick Veneer Design and Construction

Wood frame buildings with anchored brick masonry veneer are a common type of residential construction throughout the United States (U.S.), particularly in regions of moderate seismicity and/or high wind. Brick veneer construction is valued for its pleasant appearance, excellent thermal performance, and ability to accommodate water penetration. As shown in Figure 1.1, this type of construction typically comprises an exterior masonry wall and an interior wood frame backup (separated by an air cavity), both of which are supported vertically on a foundation. Regularly spaced corrugated sheet metal ties are used to connect the brick masonry to the backup through the cavity, which acts as a thermal barrier and provides for drainage as well as weather resistance (Drysdale et al. 1999). Commonly used residential brick veneer ties and a typical repair anchor, as well as their installation details, are shown in Figure 1.2.

Wood frame homes with exterior brick veneer may incorporate a variety of architectural styles, as shown in Figure 1.3, consisting of the following wall and corner configurations: brick veneer built over the front wall only (open corners), utilizing alternate siding material on the remaining walls; continuous brick veneer enclosing all of the exterior wood frame walls (closed corners); and/or brick veneer built in sections, with expansion joints at the wall corners (open corners) and near the edges of openings. In addition to window and door openings, other geometric variations (such as gable ends) are also common in the exterior walls of residential buildings. Exterior brick veneer walls can also extend over more than one story, depending on the layout of the particular wood frame home structure. The architectural style of a residential building may affect the strength performance of its brick veneer.

During design and construction of brick veneer walls, a number of performance requirements must be considered. The masonry veneer should be able to carry its own weight and to transfer out-of-plane inertial loads (due to earthquakes and wind) through the tie connections across the wall cavity to the wood frame backup. Therefore, the wood frame backup walls need to be designed to resist all of the exterior lateral loading, as well as any gravity loads from the home structure floor or roof framing (Drysdale et al. 1999). In reality, however, such brick veneer walls often carry some of the transverse horizontal loads, due to the relatively higher stiffness of the masonry than that of typical wood frame backup construction (BIA 2002). For adequate performance of brick veneer wall systems, the design and construction details should also account for differential movement between the masonry and backup walls, as well as for water penetration of the exterior masonry wall (Drysdale et al. 1999). Prescriptive requirements for residential brick veneer design and construction are provided by the Masonry Standards Joint Committee (MSJC) Building Code (MSJC 2008), the International Residential Code

(IRC) for One- and Two-Family Dwellings (ICC 2003), and the Brick Industry Association (BIA) Technical Note 28 (BIA 2002). In addition to the prescriptive requirements, MSJC (2008) provides an alternative design method, involving load and deflection analysis of brick veneer walls. The strength and serviceability design requirements for brick veneer wall systems are described in greater detail in Chapter 2.

1.2 Motivation and Scope of the Research Project

Over the years, residential brick veneer wall damage (including cracking, relative movement, and collapse) has been observed on a number of occasions resulting from moderate earthquakes and severe wind storms, as shown respectively in Figures 1.4 and 1.5 (IMI et al. 1990; Page 1991; EERI 1996; Hamilton et al. 2001; Kjolseth 2008; Sparks 1986; McGinley et al. 1996; FEMA 1999; Bryja and Bennett 2004; FEMA 2006). Damage of brick veneer walls has been mainly attributed to their vulnerability to out-of-plane loading, as the brick veneer moves away from the wood backup, placing a high demand on the tensile force and displacement capacity of the tie connections. Brick veneer wall damage has often also been a result of improper material use and/or poor workmanship during construction. Certain architectural variations in brick veneer walls, such as window openings and gables, can affect wall performance as well, sometimes making them even more susceptible to damage (Page 1991; Exponent 2001). Various experimental and analytical studies have been conducted on the strength performance of brick veneer wall systems subjected to earthquake and wind loads, to understand the inter-relationship between the masonry, ties, and backup (wood or metal stud, or concrete masonry walls). However, the majority of these studies have focused on typical brick veneer wall systems used in commercial construction – those with metal stud or concrete masonry backups. For wood frame backup construction, the studies have mainly focused on veneer systems built using older construction practices, and they did not fully explore the strength limits of the tie connections. Some of these studies, as well as reports of existing residential brick veneer building performance, are summarized in greater detail in Chapter 2.

To address more current and widespread residential brick veneer construction practice, a study has been undertaken here at the University of Illinois to evaluate the out-of-plane seismic performance of brick veneer with wood frame backup wall systems. The first phase of the study, described in Chapter 3, involved laboratory testing of brick-tie-wood subassemblies, comprising two bricks with a corrugated sheet metal tie either nail- or screw-attached to a wood stud. The subassemblies were built to represent prescriptive design requirements and current construction practices for installation of brick veneer ties, capturing workmanship variability. The tie connection subassemblies were subjected to monotonic and cyclic in-plane and out-of-plane loads (tension, compression, and shear), permitting an evaluation of the stiffness, strength, and failure modes for a local portion of a veneer wall system, rather than just of a single tie by itself. Another phase of the study involved static and dynamic out-of-plane load testing of two full-scale single-story solid brick veneer wall panel specimens, as described in the first part of Chapter 4. The second part of that chapter describes out-of-plane static and dynamic load tests on a one-and-a-half story brick veneer wall specimen, with a window opening,

representing the gable-end wall of a typical residential home structure. The experimental studies were used to evaluate the overall performance of brick veneer wall systems, including interaction and load-sharing between the brick veneer, corrugated sheet metal ties, and wood frame backup. The progression of system damage was noted up until partial collapse of the veneer walls; tie connection stiffness and strength were found to significantly affect wall performance at all stages of behavior.

The experimental results were then used to develop detailed finite element (FE) models of brick veneer wall panels, as described in Chapter 5. Parametric studies were conducted with the FE models to further explore the effects on out-of-plane seismic performance of brick veneer walls from different tie connection details, as well as geometric variations in wall design and construction. Damage limit states for residential brick veneer wall systems were established during these experimental and analytical studies. In the final phase of this study, described in Chapter 6, simplified brick veneer with wood frame backup models were established, and they were utilized to evaluate the seismic fragility of residential brick veneer wall systems. Additionally, the seismic vulnerability of this form of construction was evaluated for certain regions of the U.S. Finally, Chapter 7 contains the summary and conclusions from the experimental and analytical studies, as well as recommendations for future study.

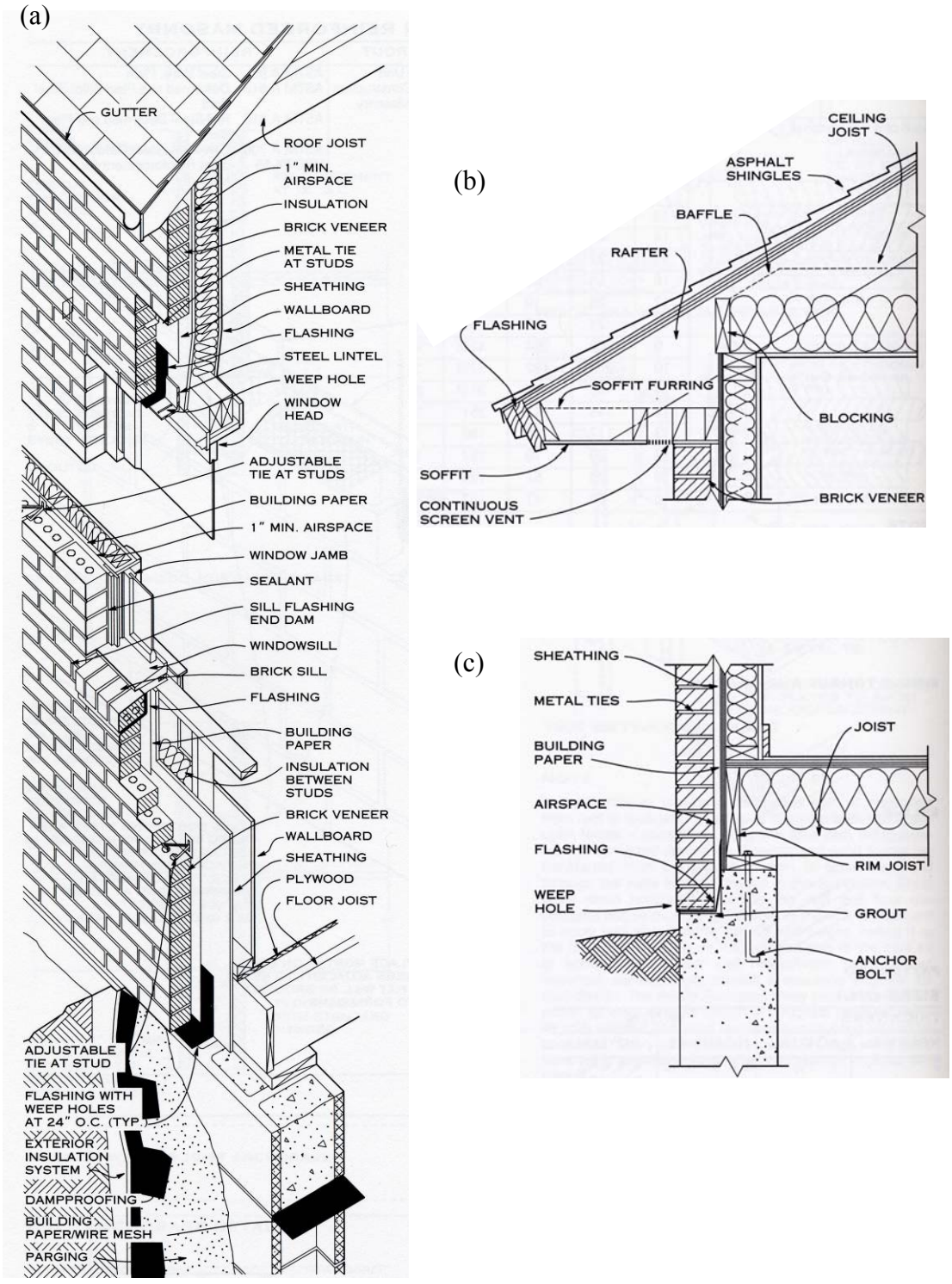

Figure 1.1 – Typical details of brick veneer on wood frame home construction (Rumbarger and Vitullo 2003).

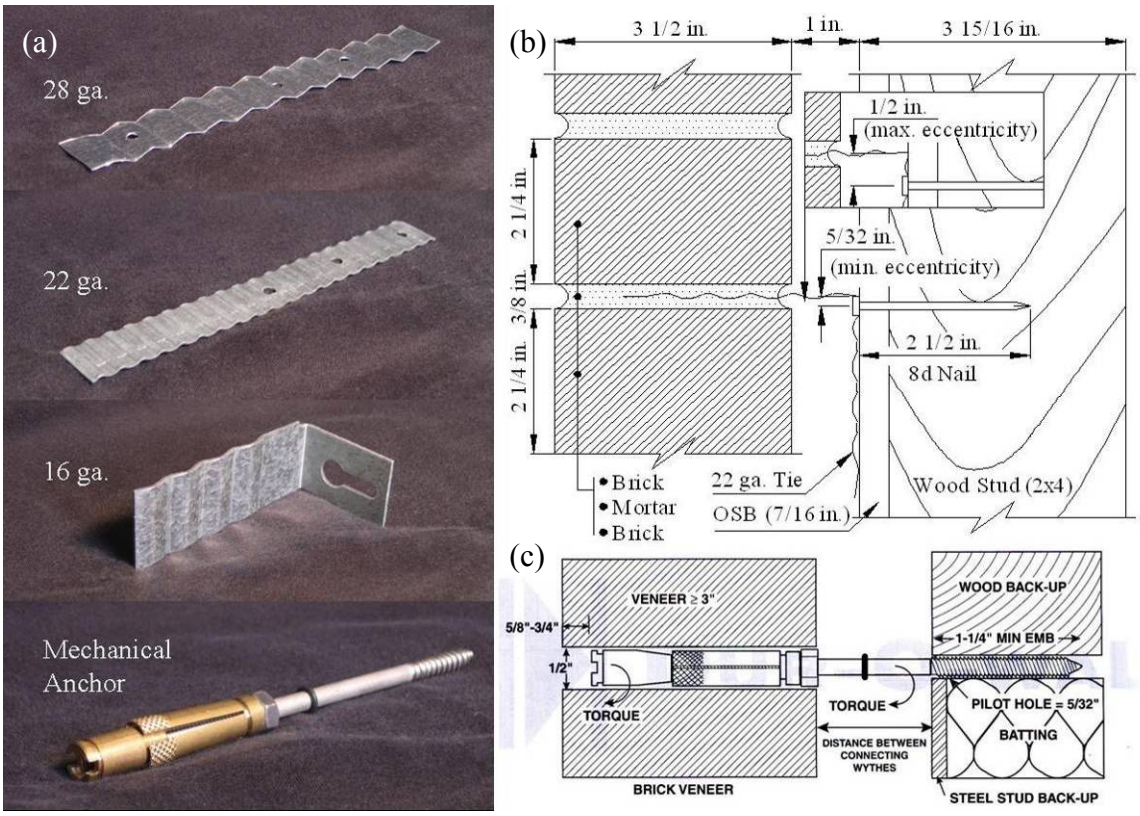

Figure 1.2 – Residential brick veneer wall connectors: (a) corrugated sheet metal ties of three different thicknesses and Series 5300 Dur-O-Wal mechanical repair anchor; (b) tie connection installation details meeting the MSJC (2008) code requirements; and (c) mechanical repair anchor installation details (Dur-O-Wal 1998).

Figure 1.3 – Typical architectural styles for brick veneer construction: (a) front wall only brick veneer, (b) continuous around corners and multi-story brick veneer, and (c) expansion joint (open) wall corner details (corner detail sketches from Lapish (1988)).

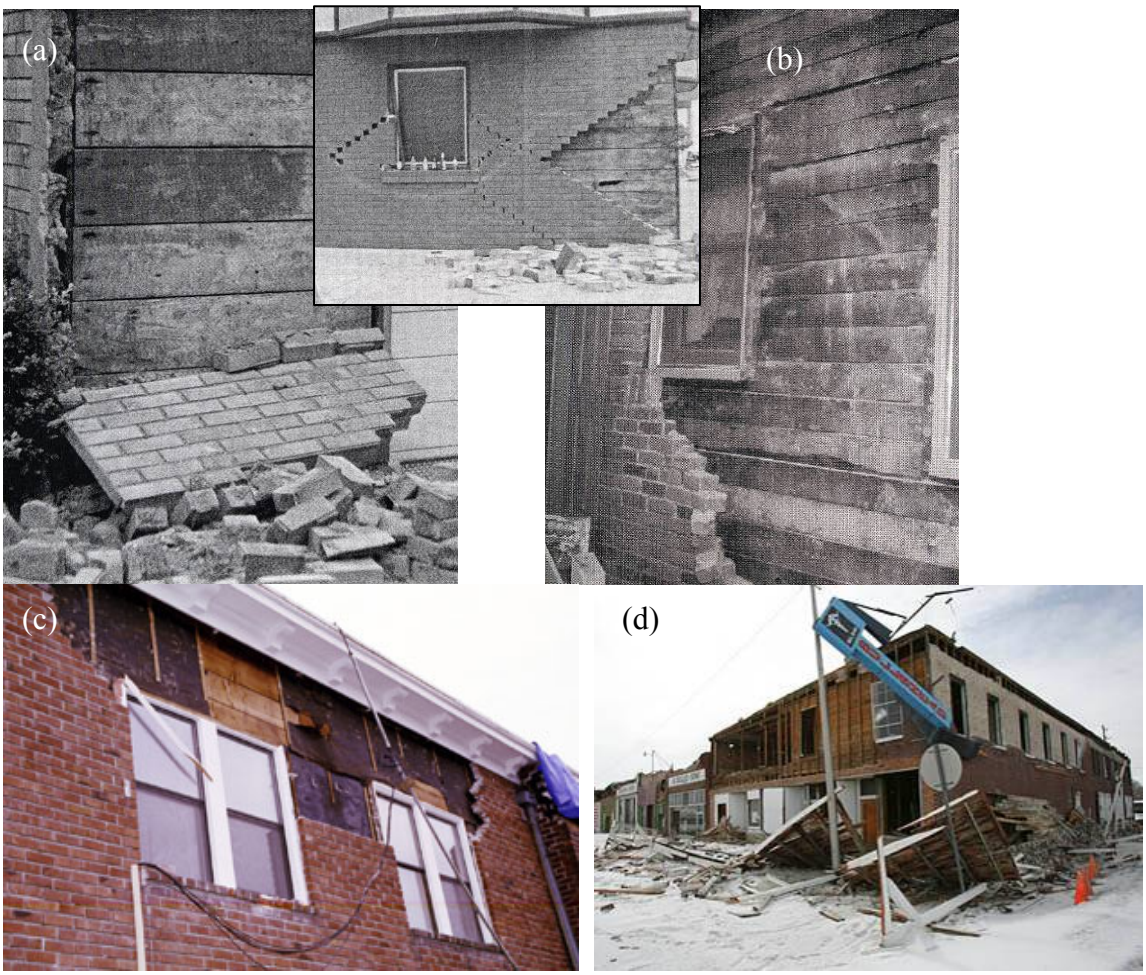

Figure 1.4 – Earthquake damage to brick veneer with wood frame backup: (a) Loma Prieta, California (IMI et al. 1990); (b) Northridge, California (EERI 1996); (c) Nisqually, Washington (Exponent 2001); and (d) Wells, Nevada (Kjolseth 2008).

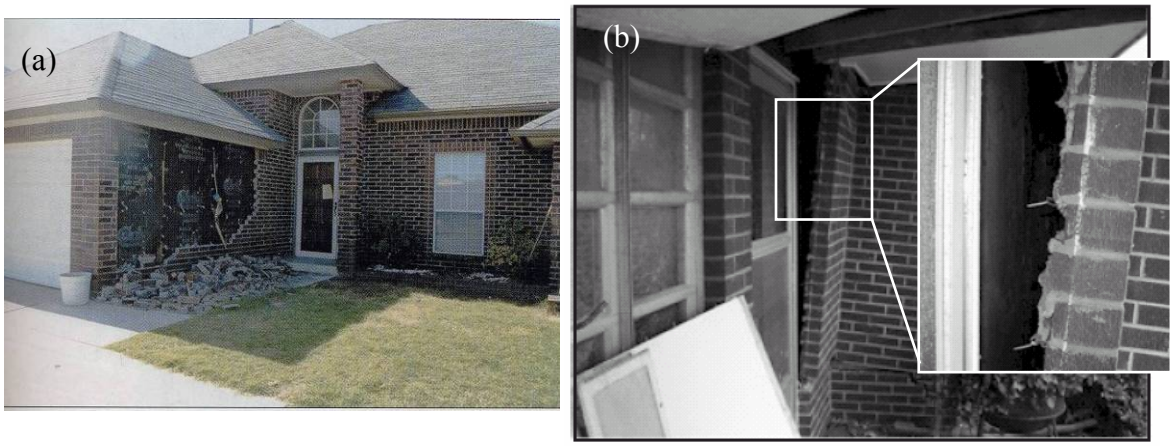

Figure 1.5 – Severe wind storm damage to brick veneer with wood frame backup: (a) Oklahoma (FEMA 1999), and (b) Eastern Tennessee (Bryja and Bennett 2004).

BACKGROUND INFORMATION

Typical U.S. design requirements for strength and serviceability of brick veneer on wood frame home structures are summarized in the first section of this chapter. These requirements have in part been based on a number of earlier experimental and analytical studies, investigating the strength performance of brick veneer wall systems. Load tests were performed on a variety of tie connections used in brick veneer wall construction, as described in Section 2.2. Residential and commercial brick veneer walls have been tested and analyzed under simulated earthquake and wind pressure loads, as summarized in Section 2.3. All of these studies have helped toward gaining some basic understanding of the interrelationship between the masonry, ties, and backup components of brick veneer wall systems. The studies have been conducted on brick veneer wall systems following common construction practices in the U.S., Canada, United Kingdom, New Zealand, and Australia, with most of the North American studies mainly focusing on the commercial type of brick veneer construction. Reports of earthquake and wind damage to existing brick veneer homes, as well as other serviceability problems, have been summarized in Section 2.4. Finally, Section 2.5 provides a brief overview for seismic performance and fragility evaluation of residential wood frame homes and for low-rise unreinforced masonry buildings, which will pave the way toward evaluating the seismic fragility of brick veneer walls.

2.1 Design and Construction of Anchored Brick Veneer

During design and construction of residential brick veneer walls, a number of performance requirements must be considered. The masonry veneer should be able to carry its own weight and to transfer out-of-plane inertial body loads (due to earthquakes and wind) through the tie connections across the wall cavity to the wood frame backup and then eventually into the foundation. Therefore, the wood frame backup walls need to be designed to resist all of the exterior lateral loading, as well as any gravity loads from the home structure floor or roof framing (Drysdale et al. 1999). In reality, however, such brick veneer walls often carry some of the lateral loads, due to the relatively higher stiffness of the masonry than that of typical wood frame backup construction (BIA 2002). For adequate performance of brick veneer wall systems, the design and construction details should also account for possible differential movement between the masonry and backup walls, as well as for water penetration of the exterior masonry wall (Drysdale et al. 1999). Prescriptive requirements for strength and serviceability design of brick veneer built over wood frame home structures are provided by the Masonry Standards Joint Committee (MSJC) Building Code (MSJC 2008), the International Residential Code (IRC) for One- and Two-Family Dwellings (ICC 2003), and the Brick Industry Association (BIA) Technical Note 28 (BIA 2002). In addition to the prescriptive requirements, MSJC (2008) provides an alternative design method involving load and deflection analysis of brick veneer walls.

2.1.1 General Requirements

Residential wood frame home structures with exterior brick masonry veneer are typically built in one or two story configurations, as shown earlier in Figure 1.3. The wood frame structure and the brick veneer must be supported by a noncombustible foundation, usually made of concrete or masonry. The wood backup structure typically comprises floor framing, walls built of 2x4 (1-1/2 in. x 3-1/2 in. [38 mm x 89 mm]) studs spaced at 16 in. (406 mm) on center (with exterior sheathing and interior gypsum wallboard), and roof/ceiling framing (Figure 1.1). The IRC (ICC 2003) provides design and construction requirements for all structural components of a home. On the other hand, MSJC (2008) simply recommends that such designs comply with the ACI 318 Building Code Requirements for Structural Concrete (ACI 2005) for the concrete foundation, and with the National Design Specification (NDS) for Wood Construction (NDS 2001) for the wood frame structure; MSJC would be referenced for the case of designing a masonry foundation.

The MSJC (2008) code and BIA Technical Note 28 (BIA 2002) present requirements for design and construction of brick masonry veneer walls. The out-of-plane stability of a brick masonry veneer wall is controlled by the masonry wall materials, its height and thickness, and also by the layout and properties of the corrugated sheet metal tie connections that anchor it to the wood frame backup. The brick masonry units in brick veneer should be at least 2-5/8 in. (66.7 mm) thick; however, the mortar mix as well as strength of brick masonry materials are generally not specified in brick veneer walls because, under service loading, there is no consideration for stresses in the veneer and cracking of the veneer can be tolerated. For seismic design category C or below (and for typical wind exposure conditions, with wind speeds of up to 110 mph [177 km/h]), brick masonry with Type N mortar is usually used, which is adequate for carrying the self-weight, transferring loads to the tie connections, and limiting flexural cracking of the brick veneer. Type S or M mortars are recommended if a higher masonry flexural strength is needed, as with seismic design categories D and above (and/or in areas of high wind). Additionally, to ensure stability of exterior brick veneer and to control cracking in the masonry, MSJC (2008) requires limiting the out-of-plane service load deflections of the backup wall; however, deflection limits are not specified for wood frame backup walls. Prescriptive requirements for the installation of tie connections, as well as for dimensioning residential brick veneer walls, are summarized in the next sub-section, followed by an overview of an alternative design approach for such wall systems.

Brick veneer wall systems also require detailing to protect the building materials from water damage (including corrosion of the tie connections) and to account for material dimensional changes. Wind driven rainwater can penetrate the exterior masonry, so flashing and weep ropes should be installed along the edges of the wall to provide drainage out of the wall cavity, and the exterior of the wood backup wall must be waterproofed to prevent moisture from entering the building interior (Figure 1.1). Additionally, mortar droppings into the wall cavity, as shown in Figure 2.1, should be limited during masonry construction because they could provide a conduit for water movement across the cavity, prevent drainage of water out of the cavity, and cause water

to collect on the ties (thereby accelerating their corrosion). Finally, expansion joints should be installed in a brick masonry wall, as needed, to account for differential movement between the backup and masonry walls, as well as for any dimensional changes in the masonry itself (MSJC 2008; ICC 2003; BIA 2002).

2.1.2 Prescriptive Requirements and Recommendations

Prescriptive installation requirements for corrugated sheet metal ties used to connect brick veneer to a wood frame backup are summarized in Table 2.1, as specified by MSJC (2008), the IRC (ICC 2003), and BIA Technical Notes. The tie connections should ideally satisfy a set of performance requirements such as: a) sufficient strength and stiffness (in tension and compression) to transfer lateral loads to the backup, b) adequate transverse flexibility to accommodate differential vertical movements between exterior and interior walls, and c) resistance to corrosion and moisture transfer across the air cavity (BIA 2003). As can be seen from Table 2.1, it is typically assumed that these performance requirements are met if a properly spaced grid of galvanized 22 ga. corrugated sheet metal ties are employed, attached to the wood backup with at least 8d (2-1/2 in. [63.5 mm] long and 0.131 in. [3.3 mm] diameter) galvanized nails and also adequately embedded into the mortar joints. The required tie connection horizontal and vertical spacing limits vary somewhat; however, the maximum veneer wall area to be supported by a tie connection is 2.67 ft^2 (0.25 m^2) for building construction in seismic design category C and below (and for typical wind exposure conditions), generally resulting in a tie spacing of 16 in. (406 mm) horizontally (one at every stud) and 24 in. (610 mm) vertically. Also, the codes require that ties be installed within 12 in. (305 mm) of the wall edges and openings, with maximum 36 in. (914 mm) tie spacing around the perimeter of such an opening; to be safer, the BIA Technical Note 44B recommends that ties be installed within 8 in. (203 mm) of wall edges. The height of a brick veneer wall is typically limited to be 30 ft (9.14 m) above its support, with an additional 8 ft (2.44 m) permitted at gable ends of a home structure.

The codes prescribe stricter requirements for brick veneer construction in more severe seismic and wind regions of the U.S. (Table 2.1). The tributary wall area per tie must be reduced to 2 ft^2 (0.19 m^2) for construction with seismic design category D (or higher) per MSJC (2008) and the IRC (ICC 2003), as well as where wind pressures exceed 30 psf (1.44 kN/m^2) per the IRC; additionally, MSJC requires lowering the wall area per tie to 1.87 ft^2 (0.17 m^2) where wind speeds are above 110 mph (177 km/h). For more severe seismic conditions, the IRC also specifies reducing the brick veneer wall height limit by 10 ft (3.05 m), as well as isolating brick veneer walls from one another. Furthermore, the MSJC code requires the use of horizontal joint reinforcement (with ties mechanically attached to the reinforcement) in all brick masonry for buildings with seismic design categories E and higher, as well as supporting the brick veneer independently at each level of the building. (The requirement for horizontal reinforcement has been questioned by Bennett and Bryja (2003), based on satisfactory performance of unreinforced brick veneer construction during some earthquakes and severe wind storms, as well as on experimental test results and an assessment of the relative hazard of earthquakes vs. severe wind events in certain regions of the U.S.) Other suggestions that have been proposed for improving the strength of residential brick veneer construction are to use

ring or screw-shank nails for attaching ties to the wood framing, in order to increase nail pullout resistance (FEMA 2004), and also to use adjustable wire ties such as those typically employed in light-commercial construction (Krogstad 2003; FEMA 2006). However, these measures are seldom prescribed or used in actual residential brick veneer construction, possibly due in part to perceived higher construction costs. Overall, most of the design requirements and recommendations described above are based on various studies of brick veneer wall system performance; a number of those studies have been outlined in a later section of this chapter.

2.1.3 Alternative Requirements

An alternative strength design approach is provided by MSJC (2008) for anchored brick veneer wall systems. Seismic and wind design forces must be computed, followed by a structural analysis and design of the brick veneer wall and its connection to the wood backup. The masonry veneer should be able to carry its own weight and to transfer out-of-plane face loads, through the tie connections, back to the wood frame home structure. (On the other hand, brick veneer walls will generally have adequate shear strength and overturning resistance to withstand their own in-plane seismic inertial loads or lateral wind loading.) The out-of-plane deflection of the backup should also be limited to maintain brick veneer stability. The brick veneer itself is not required to resist flexural tensile stresses, and therefore a strength review of the masonry is generally not required for walls subjected to out-of-plane loading. Finally, the design of the brick veneer wall has to meet certain prescriptive design and construction requirements for walls with seismic design category C and above, as described earlier.

Seismic design forces for architectural and other non-structural components, including brick veneer wall systems, can be determined from FEMA (2003) and ASCE (2005). The strength (resistance) of the tie connections (fasteners) is the key design variable in a brick veneer wall system. According to the minimum design load provisions, architectural and nonstructural components connected to more than one point on the supporting structure should be able to accommodate relative movements between their supports when subjected to seismic loading. However, limits on relative displacements generally would not apply to typical designs of brick veneer wall systems; according to MSJC (2008), brick veneer is not required to resist loading other than its self-weight, and cracking is generally expected. As shown in Table 2.2, the out-of-plane seismic design loads have been computed for veneer and fasteners, with design categories A through D. (Design loads were not computed for seismic design categories E and F because the short period spectral accelerations are dependent on site specific conditions for these higher categories.)

Wind design forces for brick veneer wall systems can also be determined per ASCE 7 (2005), as shown in Table 2.3. In this tabular example from FEMA (2006), out-of-plane wind load pressures were evaluated for a brick veneer wall of a low-rise building, by treating the veneer as a component and cladding located on the corner of the building. Wind design pressures of up to 26.6 psf (1.28 kN/m^2) were evaluated for brick veneer wall construction in typical wind exposure conditions, with wind speeds up to 110 mph (177 km/h). The design wind loads were then compared with the nominal resistance of

brick veneer tie connections, which were assumed to be equal to the withdrawal strength of an 8d nail (minimum required fastener by the codes for corrugated sheet metal ties), with an estimated allowable strength of approximately 65 lbs (290 N) per NDS (2001). (As seen from Table 2.3, the nail withdrawal strength calculations incorporated a thermal reduction coefficient of 0.8; without this coefficient, the allowable withdrawal strength of an 8d nail would be approximately 80 lbs [356 N].)

Based on these calculations, a wall area of 2.67 ft^2 (0.25 m^2) per tie connection was found to be generally acceptable for brick veneer wall construction in zones with wind speeds of up to 110 mph (177 km/h), consistent with current code provisions (i.e., in a wall panel with a stud spacing of 16 in. [406 mm] with ties at every stud, a maximum vertical spacing of 24 in. [610 mm] would be acceptable). (Note that in Table 2.3, a maximum vertical tie spacing of 18 in. [457 mm] is provided by FEMA (2006) because the results of the study were being compared to an earlier version (2005) of the MSJC code, where the maximum permitted vertical tie spacing was 18 in.) As seen from this example, a reduced tie spacing would be required for brick veneer design in higher wind speed zones. The seismic design loads in Table 2.2 also indicate that, for fasteners with seismic design category C, the maximum wall area per tie should be 2.67 ft^2 (0.25 m^2), based on the same estimated strength for tie connections. Overall, Bennett and Bryja (2003) have shown that wind loads will typically result in higher lateral design loads than earthquakes will, for brick veneer homes built throughout most regions of the U.S. (especially in hurricane-prone coastal regions).

2.2 Strength Performance of Brick Veneer Tie Connections

Corrugated sheet metal ties are ordinarily used in residential brick veneer construction (Figure 1.2), although a wide variety of connectors are currently available. Tie connection ultimate strength (capacity), under tensile or compressive loading, was the primary focus during most early studies. Grimm (1976) provided strength estimates for corrugated sheet metal tie connections, among many other types of metal connectors, based on four controlling factors of connection performance – the metal tie itself, the length of the tie (across the wall cavity), the embedment (length) of the tie into the masonry mortar joint, and the type of tie attachment (nail or screw) to the wood studs. For a 22 ga. tie connected to a wood backup with an 8d nail, the tensile and compressive strengths were estimated to be 80 lbs (356 N); therefore, the author recommended a tributary brick veneer wall area of 2.67 ft^2 (0.25 m^2) to be supported per tie, for a design wind pressure load of 30 psf (1.44 kN/m^2). (This tributary area recommendation is the same as that prescribed by the current codes for building construction with seismic design category C or lower, as well as for non-coastal wind exposure regions.)

In another study, by performing tension and compression load tests to failure on brick veneer tied to concrete masonry, steel, and wood stud backups, Hatzinikolas et al. (1982) showed that the pullout strength from masonry of corrugated sheet metal ties can be improved by utilizing stronger mortars; however, the ties connected to wood studs typically failed in tension by nail pullout from the studs or by tearing of the tie at its hole, and they failed in compression by bending or buckling. Burnett and Postma (1995)

showed that the tie pullout strength from masonry mortar joints can also increase significantly by virtue of the pre-compression load from the masonry wall self-weight on the embedded part of the tie (primarily at or below the mid-height of a brick veneer wall). The length and diameter of the nail, as well as the tree species of the studs, has been found to govern the tie connection capacity at its point of attachment to the backup (Chrysler 1995). Finally, the stiffness of corrugated sheet metal tie connections typically depends on the thickness of the tie material, as well as on the distance of the 90 degree bend of the tie from the nail (Arumala and Brown 1982). Arumala and Brown tested several types of tie connections as part of their experimental program for full-scale commercial brick veneer walls; numerous other load tests have been conducted on brick veneer tie connections as part of other brick veneer wall testing programs, some of which are mentioned in Section 2.3.

These earlier studies described above provided valuable information about the key factors controlling residential (as well as commercial) brick veneer tie connection performance; however, they did not necessarily provide stiffness, strength, and cyclic load-displacement results for the types of corrugated sheet metal tie connections that are most commonly utilized in current U.S. residential construction practice. More recently, Simundic et al. (1999) tested brick-tie-wood subassemblies, representing Australian construction methods. The tests captured the performance of both the ties and their attachments to the brick and the wood stud, under monotonic and cyclic loading. Choi and LaFave (2004) also performed an experimental study on brick-tie-wood subassemblies, each consisting of two standard bricks, one 2x4 stud, and one corrugated sheet metal tie either nail or screw attached to the stud, representing current U.S. construction practice. These subassemblies represented a localized portion of a brick veneer wall system, and they therefore captured the interaction between each component of the system (rather than just the behavior of the tie itself). The test specimens comprised a variety of possible tie installation conditions that could occur in actual brick veneer construction. The tie subassembly strengths, stiffnesses, and failure modes were determined for different types of loading, including: monotonic tension, monotonic compression, cyclic (low-cycle) tension-compression, monotonic shear, and cyclic shear. This experimental study by Choi and LaFave (2004) kicked off the greater experimental and analytical investigation at Illinois on the performance of residential brick veneer wall construction, and their results are described in greater detail later on in this thesis.

In general, the loading on and deformations of the tie connections situated within brick veneer walls can be affected by: the relative stiffness between the facing and backing materials, the tie connection spacing and stiffness, the support conditions of the brick veneer and the backup, the location of wall edges and openings, the cavity width, and the type of loading applied to the wall (BIA 2003). Workmanship during construction of brick veneer, particularly with respect to installation of the ties, also plays an important role on the overall wall system performance. Some of these effects have been explained by experimental and analytical studies of brick veneer walls, as well as in damage surveys of residential brick veneer construction following moderate earthquakes and severe wind storms, as described in more detail in the following sections.

2.3 Strength Performance of Brick Veneer Wall Systems

The key components, including design and construction details, of residential brick veneer wall systems have been described earlier and illustrated in Figures 1.1 through 1.3. In general, lateral wind and earthquake loads are mainly resisted by the exterior walls in residential home structures, therefore subjecting the brick veneer walls to out-of-plane and/or in-plane loads; the various architectural styles (Figure 1.3) of residential brick veneer wall construction will also have some effect on their behavior. Previous experimental and analytical studies have been conducted focusing not only on the performance of individual wall panels under out-of-plane and in-plane loads, but also on the interaction between exterior and interior walls. Described herein are a number of studies performed over the years on the structural performance of residential as well as commercial brick veneer wall systems. (Even though commercial wall systems differ somewhat from residential brick veneer construction, most of the observations from those studies described in this section are still relevant for general understanding of the out-of-plane performance of brick veneer with flexible backups.)

2.3.1 Walls Subjected to Out-of-Plane Loads

Moore (1978) performed one of the earliest experimental studies on residential brick veneer walls at the British Research Establishment (BRE), roughly identifying the response of these walls subjected to static out-of-plane positive and negative pressure loads; walls were also tested under in-plane shear loading, as described in the next sub-section. Uniform positive pressures were applied by inflating air-bags against a strong reaction surface in front of a one-story solid brick veneer wall, connected with 0.024 in. (0.6 mm) thick sheet metal ties (staggered at 23.6 in. (600 mm) horizontal and 14.8 in. (375 mm) vertical spacings) to a wood stud wall with interior plasterboard and exterior plywood, as shown in Figure 2.2(a). Negative (suction) pressure tests, however, were only conducted on brick veneer walls connected with the same types of ties to a rigid steel reaction wall, by inflating the air-bags inside the wall cavity to simulate the negative pressure loads (and these tests were not effective in capturing any effects of a flexible wood frame backup). The positive pressure loads were applied in increments up to 21 psf (1000 N/m^2), and the displacements of both the backup and the brick veneer were measured across the centerline. As shown in Figure 2.2(b), the masonry wall deflected towards the backup, rotating about its base as a rigid body. The backup deflected similar to a simply-supported beam, with some translation at the top of the wall, possibly due to a flexible support representing a roof/ceiling connection (the author, however, did not describe the backup wall support conditions in this test specimen). As shown in Figure 2.2(c), the negative pressure testing demonstrated that the masonry wall and ties exhibited substantial strength, with the first occurrence of masonry cracking approximately two-thirds of the way up the wall (Figure 2.2(a)) at a pressure of 50 psf (2400 N/m^2). The wall sustained 75 psf (3600 N/m^2) pressures without collapse; however, these negative pressure tests are not entirely practical. The author carried out separate load tests for the tie connections used in the wall specimen, and found their average ultimate strength to be 590 lbs (2.6 kN) when attached to the rigid metal backup, whereas tests of ties nailed to the wood studs exhibited a strength of only 23 lbs (100 N).

No other damage limit states besides masonry cracking were noted during these wall tests.

A year later, dynamic tests on brick veneer walls with wood backup framing were performed by Priestley et al. (1979), identifying the out-of-plane dynamic properties, acceleration response, and ultimate damage limit states of these walls. In their test specimens, the brick veneer was connected to wood stud walls with one of two types of ties commonly used in New Zealand construction practice at the time, which were identified as "special" (8 gauge wire) and "conventional" ties, as shown in Figure 2.3(a); in most of the specimens, the ties were installed at 13.4 in. (340 mm) vertical and at 23.6 in. (600 mm) horizontal spacings. The solid brick masonry veneer walls were constructed with and without vertical reinforcement; additionally, to simulate existing cracking in the brick veneer, un-bonded ("pre-cracked") mortar joints were positioned horizontally (at ¼, ½, and ¾ of the height of the wall) or diagonally (from corner to corner) in some of the wall specimens. (The wood stud backup walls, however, were not covered with either exterior wood sheathing or interior gypsum wallboard, which are commonly used in current construction.) Then the top and bottom of the wall panel specimens were connected to a loading frame, capable of generating harmonic excitation in their out-of-plane direction, as shown in Figure 2.3(b). The dynamic properties of the walls were identified by impact tests, exhibiting natural frequencies in the range of 10 to 12 Hz for the uncracked walls and approximately 5 Hz for the cracked walls; the damping ratios ranged from 6% up to almost 18% (the higher values being for the pre-cracked walls). Dynamic tests were conducted by subjecting the walls to increasing sinusoidal input accelerations of 5 Hz (representing a typical frequency of the major energy content in measured earthquakes). The researchers identified the peak acceleration response at mid-height of the brick veneer and the resulting damage from each dynamic test; changes in the natural frequencies and damping ratios were also noted as damage in the walls progressed. During these wall tests, initial damage was noted at the tie connections before developing any new cracks in the masonry, following an acceleration response of approximately 0.5g to 1.0g, as the ties deformed either at the nail attachment to the wood or at the mortar joint. Overall, the "special" ties exhibited better strength than the "conventional" ties. The unreinforced masonry walls collapsed in small pieces, at a wall mid-height response of approximately 2g to 3g following an input intensity somewhere in the range of 0.5g to 0.8g, after failure of a number of the tie connections, flexural failure of the wood studs, and/or shear failure of the wood stud supports. The horizontal or diagonal pre-cracks did not affect the ultimate capacity or the mode of failure of the walls, though they affected the dynamic properties at the earlier stages of testing. The reinforced brick veneers were not loaded to collapse because of the limited capacity of the testing equipment, but some tie damage was observed in those specimens. In addition to the dynamic tests, theoretical relationships for estimating the wall panel natural frequencies were derived based on the elastic properties of the wall components. The authors concluded that the seismic out-of-plane capacity of brick veneer walls built over wood frame studs was higher than expected.

The experimental studies described above provided some general information on the static and dynamic out-of-plane performance of residential brick veneer walls; those

studies, however, did not explore the relationships between the external out-of-plane face loads and the internal force/displacement response of particular tie connections at different locations in the walls. Lapish and Allen (1982) developed linear elastic models representing the geometry of one- and two-story (continuous) high brick veneer walls, and they explored the wall system behavior under distributed static loads, focusing in particular on the tie connections. As shown in Figure 2.4, the analysis results indicated that higher loads will be imposed on the ties located in the upper region of single story walls, or on the ties anchored near the floors in multi-story construction. Furthermore, their analysis results for continuous brick veneer walls showed that stiffer ties at the floor levels will attract more load, and consequently higher moments will develop in the exterior masonry wall at those locations. The authors concluded that strong and ductile tie connections should be utilized, in order to redistribute the loads to the other tie connections, away from the supports, and therefore lower the moments in the exterior masonry wall. Additionally, the authors considered that the supports at the top of the walls (representing floor or roof framing) can deform due to interstory drift or diaphragm flexibility, and they explained that those deformations will not much affect the magnitude of loading in the tie connections anchored near those locations. (However, Simsir (2004) showed that a flexible support at the top of a wall can definitely affect its out-of-plane response under dynamic loading, and therefore an effect on the seismic tie loads in a brick veneer wall should be expected.)

Since the 1980's, most of the experimental and analytical studies conducted in the U.S. and Canada focused on the out-of-plane performance of brick veneer walls anchored to light-gauge steel studs (a common form of wall construction in commercial buildings). As shown in Figure 2.5, these walls typically comprise a steel stud backup (anchored to a much heavier reinforced concrete or steel frame building structure) and a brick veneer panel supported on steel shelf angles at every floor level; the brick veneer is usually anchored to the backup with adjustable wire ties. The behavior of these wall systems has been effectively captured by experimental and analytical studies of one-story wall panels, with the steel stud backup designed to resist all of the lateral loading without exceeding a mid-span deflection of the stud height (span) divided by 360. The studies of wall panels typically showed that, when subjected to distributed out-of-plane loading (from wind or earthquake), the brick masonry veneer rotates about its base and moves towards or away from the backup, with the tie connections providing lateral restraint along the height (and across the width) of the wall panel (with some possible additional restraint at the very top of the masonry wall imposed by friction, generated by the gap filler in between the masonry and the shelf angle above); the backup wall then deflects in a way similar to a simply supported beam.

Brown and Arumala (1982) subjected such wall panels to positive and negative (suction) pressures, and they noticed that the brick masonry typically experienced cracking (forming a hinge) somewhere near the mid-height of the wall, sometimes at loading below the design capacity of the wall panel. Also, lower positive pressures were generally required to initiate cracking in the brick veneer mortar joints, possibly because under positive pressure the untooled (and therefore weaker) mortar joints were subjected to tensile stresses. Together with results from the wall tests, a more detailed analysis

showed that a composite model of a brick veneer wall panel should not only be based on the relative stiffnesses of the masonry and the backup, but also on the tie connection stiffness, the wall cavity width, and the wall component boundary conditions (Arumala 1991). The studies showed that, before masonry cracking, brick veneer can significantly increase the flexural resistance of an entire wall panel, due to its higher stiffness than that of the backup framing; also, it was shown that the tie forces are not uniform throughout brick veneer walls, with ties anchored near the supports of the backup resisting higher loads, as indicated in Figure 2.5. After masonry cracking, however, all of the lateral loading must be resisted by the steel studs, and ties near the wall mid-height will then experience higher loads than before. In this study, masonry cracking was designated as the ultimate damage limit state, without any damage to the tie connections.

Experimental and analytical studies were also conducted by McGinley et al. (1988) on sets of brick veneer wall panel specimens with varying wall system components, including different types of backup walls (steel stud or concrete masonry), as well as various steel stud sizes, stud wall covering materials, wall heights, and tie connection configurations. In general, the elastic behavior of these walls under simulated positive and negative pressures was similar to the behavior observed in the study mentioned above, however with evident effects due to differences in the wall system components. Additionally, these wall panels were loaded well past their design capacities, and a number of failure modes were identified beyond just masonry cracking, including: tension (or compression) failure of the tie connections, flexural failure of the backup studs, shear failure at the supports of the backup, excessive deflection of the backup, and partial collapse of the brick masonry. The authors noted that a majority of the wall specimens exhibited tie failure as the governing wall failure mode after masonry cracking under simulated negative pressures; these tie connections were most vulnerable at their screw attachment to the backup studs. However, under positive pressures, the backup components typically failed after cracking in the brick masonry. Based on this study, McGinley et al. (1989) presented a limit states design approach for commercial brick veneer construction, with masonry cracking considered as the governing limit state; those researchers further suggested that masonry cracking could be considered a serviceability limit state because the wall tests exhibited significant reserve capacity from the ties and the backup wall, providing brick veneer wall stability even after cracking. Therefore, tie connection and stud capacities would probably really govern the ultimate performance of these walls.

For some time there was widespread debate over the extent of masonry cracking that can be accepted in commercial brick veneer construction. Grimm and Klingner (1990) explained that masonry cracking should not be accepted in brick veneer wall design because the crack openings will allow more water to flow into the wall cavity, which can cause extensive damage to the wall materials, including: freeze-thaw spalling and splitting of the bricks, efflorescence, corrosion of the ties, and even collapse of the brick veneer. The probability of developing cracks in the masonry can be very high for loading well below the design capacity of the walls, particularly because of the unpredictable strength of mortars in brick veneer construction (since this form of construction is typically carried out without material inspection). Limiting the backup deflections will

not always prevent a masonry wall from cracking because the limits do not account for the flexural stresses in the brick veneer; even though the steel backup and its connections are designed to resist all of the applied loads, they typically deflect more than the brittle masonry can sustain without cracking. Grimm (1992) even suggested ending the use of light-gauge steel stud backups altogether for commercial brick veneer construction, after inspecting more than twenty wall collapses resulting from water damage. The author recommended using stiffer concrete masonry backup walls instead.

On the other hand, the earlier tests (mentioned above) showed that commercial brick veneer wall systems with steel stud backups exhibit significant strength beyond the first occurrence of masonry cracking. Therefore, during design of these walls, the backup deflections should be limited not necessarily to avoid masonry cracking, but rather to control the size of the crack openings and to limit the amount of water flow into the wall cavity (Wilson and Drysdale 1990). Then, corrosion-resistant materials and flashing must be utilized to avoid water damage; additionally, adequate tie connection strength has to be available after the masonry undergoes cracking, which could be achieved by installing horizontal joint reinforcement and by mechanically connecting the ties to the reinforcement (Kelly et al. 1990). Moreover, vertically reinforced brick veneer is sometimes currently used in commercial construction practice, anchored directly to the brick veneer wall support shelf angles (therefore rendering tie connections not necessary), making the interior wall independent of the exterior veneer; such walls exhibit more ductile behavior and perform well under out-of-plane loading (Liaw and Drysdale 1992; Tawresey 1995).

Currently, steel stud backups in commercial brick veneer construction are designed for a deflection limit of the wall height divided by 600, based in part on the studies mentioned above (BIA 2005). Over the years, there have been numerous additional comprehensive design recommendations and guidelines published for commercial brick veneer wall systems (McCavour and Laird 1995; Suter and Drysdale 1992; KPFF 1998). And, more recently, analytical studies have been conducted on commercial brick veneer walls subjected to wind and earthquake loading, proposing alternative ties and tie layouts (Memari et al. 2002; Yi et al. 2003).

Based on some of the earlier studies of commercial brick veneer walls, Page et al. (1996) developed analytical models to investigate loads in the tie connections, for commercial as well as residential wall systems. For residential wall construction, most of the findings were in agreement with Lapish and Allen (1982), as described above; however, Page et al. analyzed multi-story wall panels with and without cracks in the masonry. In multi-story brick veneer walls, cracks will typically occur at the floor levels, causing the exterior masonry wall to behave as single-story panels. The authors concluded that additional ties are preferred near the top and bottom of every floor in continuous veneers, and that ultimate tie forces should be checked for both uncracked and cracked masonry conditions during design.

Dynamic tests of older (turn of the 20th century) brick veneer wall construction were carried out by Paquette et al. (2001), for the case where the masonry was originally

anchored to the wood backup with nails only (nail head embedded into the mortar) and where the wood backup was made of horizontal 3 in. x 10 in. (75 mm x 250 mm) planks nailed to vertical heavy timber posts spaced at 12 ft (4 m). Three such wall panels were retrieved from an existing building in Montreal, Canada. Shake table tests were performed on one original wall and two retrofitted walls, either with additional anchors connecting the masonry wall to the backup along the mid-height or with fiberglass strips epoxied to the exterior of the masonry. The tests were conducted to evaluate the dynamic properties of the walls, along with their dynamic response and ultimate performance under earthquake loading; a synthetic ground motion proposed for the Montreal region was used, and it was scaled at increasing peak ground accelerations (PGAs) throughout these tests. In the earlier stages of testing, the retrofit methods proved to be effective, by increasing the out-of-plane stiffness of the walls. However, the exterior masonry walls in all the panels underwent significant cracking, exhibiting slippage at the nail (used to anchor the exterior masonry to the wood backup) embedment into the mortar, and finally bricks began falling off during an excitation of about 1.0g to 1.25g PGA. All of the walls ultimately collapsed after shaking scaled to a PGA of 1.75g, regardless of the retrofits; however, larger portions of brick masonry remained intact in the retrofitted specimens.

McGinley and Hamoush (2008) have recently conducted quasi-static out-of-plane load tests on solid brick veneer wall panels with wood backup framing. The brick veneer walls were built with 22 and 16 ga. corrugated sheet metal ties, nail or screw attached to the wood backup, with varying spacings (either 24 in. or 16 in. [610 mm or 406 mm] vertically, and 16 in. [406 mm] horizontally). The wall cavity widths were also varied, from 1 in. to 2 in. (25 mm to 50 mm). In some cases, the ties were mechanically attached to horizontal wire reinforcement embedded in the brick masonry, even meeting the code requirements for construction of brick veneer walls within seismic design category E. Overall, the tests further confirmed that the performance of brick veneer walls is closely related to properties and layouts of the tie connections, and that wall performance is ultimately controlled by tie connection deformation and damage limits in tension. For walls with 22 ga. ties connected to the backup with nails, the common failure mode at the tie connections was by nail pullout and/or fatigue fracture of the ties; on the other hand, for screw attached 16 ga. ties, failure was dominated by tie pullout from the mortar joints. The presence of horizontal wire reinforcement in the brick veneer did not appear to improve its strength performance. In general, the wall panels were able to sustain equivalent load pressures of up to approximately 78 psf to 110 psf (3.8 kN/m^2 to 5.3 kN/m^2), which are substantially higher than the current seismic and wind design loads for brick veneer walls.

2.3.2 Walls Subjected to In-Plane Loads

As mentioned above, Moore (1978) also investigated the in-plane shear performance of wood frame walls, both with and without an exterior brick veneer. The walls were loaded in one direction, by subjecting the top of the wood frame wall to a displacement of 0.16 in. (4 mm), representing a 1/600 drift. At this displacement, the wall panel without exterior brick veneer resisted 1.1 kips (5 kN); with the brick veneer, however, a load of 3.2 kips (14 kN) was resisted at a displacement of about 0.12 in. (3 mm). Loads were also applied to the masonry veneer, in order to observe the contribution to the load

resistance from the wood frame wall. Overall, these tests showed that for loads applied directly to the wood wall with brick veneer, there is a significant contribution to resistance (of approximately 70%) from the masonry veneer, whereas for loads applied directly to the masonry, the contribution from the wood framing was minimal (approximately 10%). No significant damage to the wall system was noted during these tests, except for horizontal cracking in the mortar joints near the bottom of the brick wall (Figure 2.2(a)). The contribution to in-plane load resistance from the brick veneer is controlled by the shear stiffness of the tie connections. Separate testing of individual ties nailed to the wood backup estimated their shear stiffness as only 35.7 lb/in. (6.25 N/mm).

Allen and Lapish (1982) also tested wall panels under in-plane shear loading. Wood stud wall panels were constructed with exterior plywood and interior wallboard, and brick veneer walls were tied to the wood backup with "stiff" ties, as shown in Figure 2.6(a); for comparison, wood frame wall panels were also tested without brick veneer. The wall panels were subjected to in-plane cyclic loads in displacement control at the wood frame top-plates (Figure 2.6(b)), up to and beyond the ultimate capacity of the walls. The tests showed that from the wood panel top-plate, the in-plane shear loads were distributed through the backup wall and transferred via the ties (in shear) into the brick veneer; for example, during 1 in. (25.4 mm) displacement cycles applied to a wood frame, the masonry wall was raised up off the foundation, breaking the mortar bond at the base of the walls. During the earlier cycles, some nail pullout was noted at the tie attachments to the backup, and some bending was observed in the top row of ties. Though not explored experimentally, the authors described that larger cavity widths could create a more ductile wall, since the in-plane stiffness of the tie connections would be governed by their length. (Information was not provided on the in-plane stiffness or strength of these tie connections; however, a higher shear stiffness can be expected from these particular ties because two nails are used to connect them to the backup.) Ultimately, the wall panels were loaded up to a displacement cycle of 1.6 in. (40 mm). The capacity of these wall panels was limited by the wood backup framing components; wall strength dropped significantly as the outside studs lifted off their supports, and then the wood wall ultimately failed as the exterior plywood buckled and pulled away from the studs after shearing failure of the nails. The cyclic force-displacement response from two of these wall tests are shown in Figure 2.6(c), for walls with and without brick veneer, demonstrating the relative increase in stiffness and strength in these wall panels provided by the masonry. Other experimental studies have been performed on the in-plane performance of residential brick veneer wall systems, as well as their interaction with the out-of-plane walls, as summarized below.

2.3.3 Brick Veneer Homes Subjected to Lateral Loads

Several studies have been conducted on the overall behavior of brick veneer home structures, focusing on the performance and the interaction of the exterior walls, and in some cases considering the interior walls as well. Based on earlier experimental and analytical findings (described above), Lapish (1988) fairly simply generalized the exterior brick veneer wall behavior and construction in residential home structures under earthquake loading as follows: the walls resisting in-plane loading are extremely stiff, and those resisting out-of-plane loading are quite flexible; therefore, brick veneer walls

should be constructed with open corners (Figure 1.3), allowing the walls to respond independently of one another (thus avoiding brittle failure of the masonry at the corners); finally, each one of the exterior walls must be detailed appropriately to resist the loading demand. Lapish further explained that the ductile properties of wood shear walls are preferable in resisting seismic loading, and therefore brick veneer tie connections should not transfer in-plane shear loads, thereby isolating the brick veneer from the backup. Brick veneer walls should be properly dimensioned to resist rocking and overturning by their own weight, therefore preventing them from imposing additional inertial loading onto a wood frame home structure by their mass, and conversely ensuring that the wood frame structure's ductility is not lost due to stiffening by the brick veneer. On the other hand, brick veneer walls subjected to out-of-plane loads must be attached well to the wood frame backup with stiff and ductile tie connections (in tension and compression) to maintain their stability. (Open corners in brick veneer walls, however, can undergo damage over time due to expansion of the masonry, as shown in Figure 2.7; therefore, expansion joints are typically recommended at some modest distance away from the corners (Chrysler 1995).)

The performance of brick veneer home structures comprising isolated brick veneer walls with open corners, comparable to those described above, has been studied by Gad et al. (1999). This study, however, focused on light-gauge steel frame home construction, which is common in Australia and Japan (although somewhat less so in the U.S.); these types of residential homes consist of light-gauge steel framing resembling the layout of a typical wood frame home structure, as shown in Figure 2.8. The authors conducted shake table tests on a single-story, one room, box-like structure, at different stages of construction (shown in Figure 2.9(a)), to determine the effects on the dynamic properties and performance of these stud walls with the addition of various "non-structural" covering materials, including plasterboard and brick veneer. The test structure was subjected to harmonic sine-sweep excitation, as well as to the El-Centro earthquake record (scaled to different PGAs). A modal analysis of this four-wall structure, with interior plasterboard and exterior strap braces (but without the exterior brick veneer), indicated a response governed by a single sway mode at a frequency of 4.5 Hz, as shown in Figure 2.9(b). However, after construction of the brick veneer walls, the first sway mode frequency was reduced to 4.0 Hz due to the added mass, and two additional higher modes (at frequencies of 7.0 and 7.3 Hz) were developed due to rocking of the out-of-plane walls (Figure 2.9(c)). The brick veneer walls were connected to the steel studs with clip-on ties (Figure 2.9(d)), which do not transfer in-plane shear loads; therefore, there was no observed contribution to the in-plane wall resistance after the construction of these brick walls (also because the brick veneer wall corners were left open). The box structure sustained a 100% PGA (0.32g) El-Centro earthquake, then it exhibited some minor damage during a test scaled to 200% PGA shaking; the structure finally collapsed during a 300% PGA run. The in-plane walls exhibited damage in the backup frame members (straps and plasterboard); one of the in-plane brick veneer walls slid about 1 in. (25 mm) along its support and became detached from the backup studs. The out-of-plane brick veneer walls cracked across their mid-height and then collapsed during the final test. Throughout these tests, the relative out-of-plane displacements between the brick

veneer and the steel stud backup were found to be from deformations of the stud flanges and not the ties, as shown in Figure 2.9(d).

Many brick veneer homes, however, are built with closed corners. As part of a wider study of light-gauge steel frame construction, Gad et al. (1998, 2001) performed modal tests on various residential structures, at different stages of construction, in Sydney, Australia. The field tests were performed by using impact hammers and portable data acquisition devices. The structures were subjected to from 0.2 to 0.9 kip (1 to 4 kN) pulses at a frequency range of 0 to 50 Hz, exciting the structure either in a sway or torsional vibration mode; the response of the structure was then measured with accelerometers positioned throughout the home (Figure 2.10). Overall, the natural frequencies of light-gauge steel framed home structures were about 3.0 Hz for walls without any covering materials; the addition of the brick veneer increased the free vibration frequency to 4.7 Hz, and the addition of interior wall covering materials increased it further to 12.4 Hz. These dynamic tests showed that brick veneer walls can generally increase the overall stiffness of a light-frame home structure, though they may keep its dynamic properties unchanged; the increase in the overall mass of the structure after construction of the brick veneer can outweigh its contribution to lateral stiffness.

In another study, laboratory tests were performed by DeVekey (1987) at the BRE on a full-scale two-story wood frame home structure with exterior brick veneer. Positive (push) pressure loads were applied to a gable-end wall of the test structure by inflating air-bags against a rigid reaction surface, as shown in Figure 2.11(a). The wood frame home was constructed following British construction practice, and the tests were conducted at different stages of construction of the exterior brick veneer walls, as follows: a) bare wood frame structure; b) wood frame structure with brick veneer on the gable-end face only; c) at different stages of construction of the return (in-plane) walls, with closed corners; and d) with brick veneer walls enclosing the entire wood frame structure. The brick veneer was anchored to the wood frame with "special" stiff ties, as shown in Figure 2.11(b), which are stronger in compression than typical ties. Displacements of the wood frame backup and the brick veneer were measured at various locations during the positive pressure tests. As shown in Figure 2.11(c), construction of the brick veneer just on the gable-end had a significant effect on the vertical deflection profile of the wood frame wall subjected to 17 psf (800 N/m^2) pressure. Under the same pressures, for the case without brick veneer, there was a visible effect on the second floor exterior wall horizontal deflection profile from the interior partitions (which acted as additional supports for that wall), as shown in Figure 2.11(d); after adding brick veneer on the gable-end face only, there was a significant increase in the out-of-plane wall stiffness, and the effects of the interior partitions were almost eliminated. Construction of the in-plane walls (with closed corners) further increased the stiffness of the overall structure (Figure 2.11(c,d)). The variation in tie connection loads was also traced by measuring the relative displacements between the masonry and the backup, which exhibited much higher closures of the wall cavity near the ceiling/floor framing, therefore subjecting the ties at those locations to higher loads.

Another set of tests on the structural performance of full-scale two-story homes subjected to simulated wind pressures was conducted at the BRE, as reported by Edgel and DeVekey (1983, 1985) and Templeton et al. (1988). The homes were concrete masonry with exterior brick veneer (cavity) wall construction, and the distributed pressure loads were applied by inflating air-bags against the test structures. Tests were conducted to evaluate the effects on building performance due to variations in construction methods, as well as the interaction between the exterior brick veneer, the interior concrete masonry walls, and other structural components of the building (such as floor and roof framing, interior walls, and lintels at window and door openings). The last phase of the study by Templeton et al. (1988) mainly focused on the gable portion of the home structure, showing that the concrete masonry and brick cavity wall, connected to a wood frame floor and roof truss, can sustain out-of-plane pressures of up to 26 psf (1.25 kN/m^2) before cracking and 63 psf (3 kN/m^2) leading to severe cracking and near collapse of the wall. Beyond this experimental study, there have been very few other studies on the seismic or wind performance of brick veneer walls with wood backup framing containing openings and/or gables. Other masonry wall systems with such architectural variations have been investigated. For example, Griffith et al. (2007) tested bare masonry walls with window openings under dynamic loads, and Bradford and Sen (2004) investigated the wind load resistance and bracing techniques of wood frame gables connected to concrete masonry walls.

It is apparent that closed brick veneer wall corners can play an important role in the overall behavior of residential home structures, so several studies have been conducted focusing on the performance of brick veneer and wood backup corners alone. Naguib and Suter (1986) performed an analytical study on brick veneer corner cracking due to external wind pressure loads and internal loads from expansion or contraction of the masonry (from mortar shrinkage, brick moisture expansion, and thermal effects). The authors explained that when two masonry walls are connected at a corner, an in-plane movement of one wall will generally cause an out-of-plane movement of the other. The resistance to these movements is then typically provided by the tie connections (loaded in tension) and friction between the masonry and its foundation, for movement away from the backup, as depicted in Figure 2.12(a); in the other direction, the motion is mainly resisted by the mortar droppings (loaded in compression), as shown in Figure 2.12(b). In the analytical models, these three controlling factors were represented by linear elastic spring supports for semi-infinite beams representing the masonry wall, with one fixed-end support representing wall corner fixity. Parametric studies were performed to capture the relative effects from each of the three restraining factors on the bending stresses at the wall corners. Vertical deflections were imposed to the fixed end of the beam, and the properties of the spring supports were varied, while tracing the bending stresses at that end support. For example, the analysis showed that walls restrained from movement by friction only (as may occur near the bottom of the wall) can undergo corner cracking at displacements as low as 0.034 in. (0.88 mm); walls restrained by the tie connections (higher up the wall) can crack at even lower displacements (0.0011 in. [0.28 mm]). For wall movement into the backup, the restraint provided by the mortar droppings can cause the masonry to crack at even lower displacements. Depending on the layout and properties of the tie connections, it was shown that some ties can fail

before the wall corner will crack. Finally, in a more recent experimental study of the structural performance of various components in residential structures, shake table tests were performed by Beattie (2004) to evaluate the behavior of brick veneer walls meeting at corners, on the test specimen shown in Figure 2.13(a). Dynamic tests proved that during relatively low level shaking, as the out-of-plane wall undergoes higher deformations than the in-plane wall, the corner will experience severe cracking near the foundation, which has commonly been observed following actual earthquakes, as shown in Figure 2.13(b). No tie damage was noticed in any of these test walls.

As seen from Sections 2.2 and 2.3, a number of experimental and analytical studies have been conducted on the strength performance of brick veneer wall systems subjected to earthquake and wind loads, to understand the inter-relationship between the masonry, the ties, and the backup (wood or metal stud, or concrete masonry walls). However, a majority of these studies have focused on typical commercial brick veneer wall systems – those containing metal stud or concrete masonry backups. For wood frame backup construction, the studies have mainly focused on veneer systems built using older non-U.S. construction practices, and they did not fully explore strength limits of the tie connections. Furthermore, there have been very few studies on the seismic and wind performance of brick veneer walls with wood backup framing containing openings and/or gables. Thus, to address the more current and widespread residential brick veneer construction practice, a study has been undertaken at the University of Illinois to evaluate the out-of-plane seismic performance of brick veneer with wood frame backup wall systems, as described in greater detail in the following chapters of this thesis.

2.4 Strength and Serviceability Performance of Existing Brick Veneer Homes

In addition to the various experimental and analytical studies of brick veneer wall performance, some other particularly beneficial examples of their strength and serviceability are from observations of in-service performance of existing homes with brick masonry veneer. Brick veneer wall damage has been observed on numerous occasions, following moderate earthquakes and severe wind storms, which often reveal poor workmanship during construction. Corrosion of tie connections is another factor affecting brick veneer wall performance under normal and severe loading conditions. Movement and cracking of brick veneer are also significant serviceability problems in existing brick veneer homes.

2.4.1 Brick Veneer in Earthquakes and Wind Storms

Over the years, residential brick veneer wall damage (including cracking, relative movement, and even collapse of masonry under out-of-plane loading) has been observed on a number of occasions resulting from moderate earthquakes and strong wind events (IMI et al. 1990; Page 1991; EERI 1996; Hamilton et al. 2001; Kjolseth 2008; Sparks 1986; McGinley et al. 1996; FEMA 1999; Bryja and Bennett 2004; FEMA 2006). During such events, out-of-plane wall damage, such as shown earlier in Figures 1.4 and 1.5, is most likely to occur as the brick veneer moves away from the backup, placing a high demand on the tensile force (and displacement) capacity of the tie connections, which typically ultimately exhibit one of three types of failure: tie fracture, tie pullout

from the mortar joint, or tie fastener (nail) pullout from the wood backup. In an earthquake, brick veneer wall damage is usually attributed to excessive inertial loads developed by the masonry veneer mass, where the tie connection tensile capacity cannot support the veneer displacements in the out-of-plane direction. In-plane load damage to brick veneer walls is less common during moderate earthquakes, but may occur as a result of low in-plane (shear) resistance of the tie connections and the masonry itself. In severe wind storms, brick veneer walls can typically experience damage as a result of excessive wind suction pressures. Furthermore, a number of residential brick veneer homes have also performed effectively during moderate earthquakes and severe wind storms, by presenting greater structural resistance than that of bare wood framing (Hamilton et al. 2001; IMI et al. 1990; Jalil et al. 1993; McGinley et al. 1996). Brick masonry walls can also protect residential structures and their contents from airborne debris during severe wind storms (McGinley et al. 1996).

After moderate earthquakes and severe wind storms, brick veneer wall failure has often been explained by improper material use and/or poor workmanship during construction, particularly as relates to the installation of the tie connections. A majority of the collapsed veneer walls referred to above revealed failed tie connections, which were often spaced further apart than permitted by codes. For example, in some cases the code requirements for tie installation have been completely ignored during construction, as shown in Figure 2.14(a) illustrating the required vs. actual tie layouts in a damaged home in the Hurricane Katrina affected zone of the U.S. In fairly modern construction, tie connections typically fail in either a tie pullout or nail pullout mode at their point of attachment (to either the masonry or the wood backup, respectively) before developing the full tensile strength capacity of the ties themselves. A leading source of damage noted in residential brick veneer construction is the low withdrawal strength of the tie connection fastener (nail) at its attachment to the wood frame backup. As was noted in most of the post-disaster damage surveys, and in a separate case study by Thomas (1988), low fastener withdrawal strength can be attributed to nails driven into only exterior wood sheathing (and not the studs), nails driven into edges of studs, and/or the use of inadequately sized nails. In particular, following the destructive Tennessee wind storms of the Fall of 2002, Bryja and Bennett (2004) noted the widespread use of thin 28 ga. ties attached only with 1-1/4 in. (32 mm) long roofing nails to the wood framing, which was identified as a fairly common construction practice in that region. Consequently, almost all observed veneer wall failures were accompanied by tie connection nail pullout from the wood backup (Figure 1.5(b)). Similarly, following the midwestern U.S. tornadoes in the Spring of 1999, FEMA (1999) reported on the common use of smaller 6d (2 in. [50.8 mm] long and 0.099 in. [2.5 mm] diameter) nails for brick veneer tie attachment to the wood backup. Brick veneer wall failures following Hurricane Katrina, in August of 2005, revealed the widespread use of smooth-shank 1-3/8 in. (34.9 mm) and 1-3/4 in. (44.5 mm) nails (FEMA 2006). Recent visits to local construction sites in central Illinois further confirm the common use of 28 ga. ties (as primarily distributed by local suppliers) with 1-1/4 in. (32 mm) roofing nails for attachment; however, it was noted that reduced tie spacings (such as 16 in. x 16 in. [406 mm x 406 mm]) have sometimes also been adopted.

Tie connection failures by tie pullout from the mortar joint were usually a product of poor mortars and/or too short of a tie embedment length into the mortar joint. Tie embedment length can be reduced significantly when veneer walls are constructed with the air cavity in excess of the code specified value (FEMA 1999), as well as when ties are installed at excessive slopes across the cavity due to tie misalignment with the mortar joint, as shown in Figure 2.14(b) (DeVekey et al. 1988; FEMA 2006). In one extreme case, a collapsed brick veneer wall following Hurricane Katrina revealed ties that were well attached to the wood backup, however without ever being set into the masonry mortar joints, as shown in Figure 2.14(c). In older construction, connection failures by tie fracture are also quite common, sometimes in part as a result of corrosion due to inadequate moisture drainage out of the wall cavity; a large number of brick veneer walls collapsed during the 1989 Newcastle (Australia) and the 1989 Loma Prieta (U.S.) earthquakes, as well as in Hurricane Katrina, as a result of corroded tie connections (Page 1991; IMI et al. 1990; FEMA 2006). Tie corrosion appears to be most common for brick veneer construction located in coastal regions.

2.4.2 Corrosion of Brick Veneer Tie Connections

As seen from a number of post-disaster surveys, corrosion of tie connections can be a major factor affecting the strength performance of brick veneer walls. Sudden brick veneer wall failure under "normal" load conditions can also occur in cases where corrosion goes undetected, resulting in complete deterioration of the tie connections. Corrosion of other metal components in masonry walls, such as shelf angles and lintels, as well as of metal stud backups, can also result in a loss of the supporting structure for the masonry (Heidersbach et al. 1987; Grimm 1992; Nelson et al. 2003).

Corrosion of metals is an electrochemical process, which involves both a chemical reaction and the flow of electricity. Metals coupled with electrolytes (which come about as a result of varying moisture concentrations, dissolved oxygen levels, or concentrations of other dissolved substances at different places along the same piece of metal) will develop an electric potential, which causes the base metal to break down (Catani 1985). Corrosion is most active when the metal is exposed to relative humidities of approximately 75 percent. In brick veneer walls, tie corrosion is often caused by an increase of corrosive pollutants in the air, presence of salts, and temperature and moisture variations, as well as from the use of calcium chloride in mortar as an accelerator; chlorides may also be present in cleaning materials used for the removal of efflorescence. As shown in Figure 2.15, the area of corrosion in a brick veneer tie connection is typically where moisture and contaminant concentrations are highest, such as at the embedded portion of the tie, as well as along the exposed portion of the tie within the wall cavity (which is often surrounded by mortar droppings). Additionally, galvanic corrosion may occur as a result of two dissimilar metals being connected. The two metallic surfaces will generate different electric potentials in the presence of moisture, which may result in a physical breakdown of at least one of the metals. In brick veneer walls, this may occur when two incompatible materials are connected together, such as by welding stainless steel ties to galvanized joint reinforcement, or by the use of stainless steel screws to fasten anchors to carbon steel studs (Catani 1985; Hagel et al. 2007).

To protect brick veneer ties from corrosion, the conditions that cause and accelerate it must be reduced. Brick veneer wall systems should be detailed for adequate ventilation and moisture drainage out of the wall cavity, and the use of chlorides in mortar mixes and in washing compounds must be avoided. Corrosion protection in the form of galvanizing zinc coatings, as well as the use of thicker ties, can also slow corrosion (Catani 1985; Heidersbach et al. 1987). However, zinc coatings alone cannot be relied upon; Hagel et al. (2007) showed that typical zinc-coated corrugated sheet metal ties can corrode in less than 12 years, whereas buildings with masonry cladding are expected to last well over 50 years. Overall, the use of stainless steel materials appears to be the best solution for connecting brick veneer to a wood frame backup. In existing brick veneer wall construction, tie corrosion can often be recognized early on in the form of cracking and bulging of the masonry, as well as from efflorescence forming on the outside face of the building. The condition of tie connections can also be investigated visually by removing brickwork at a few select locations, or by the use of metal detectors. It is recommended that potentially vulnerable brick veneer walls be inspected early and often, so that portions of brick veneer can be rebuilt with new tie connections, or that repair anchors could be post-installed. The wall cavity may even also be filled with high-strength/adherence foam (DeVekey 1979).

2.4.3 Movement and Cracking of Brick Veneer Walls

Brick masonry wall movement and cracking under "normal" load conditions are common serviceability problems in low-rise masonry buildings, including for brick veneer walls (Page 2001). Masonry is a brittle building material, with a relatively low tensile strength, and is particularly prone to cracking at the mortar joints. Wall cracking may not be structurally significant, but is often aesthetically unacceptable. The major causes of wall cracking have been classified into external and internal events. For example, external events may involve movement at the foundations, or interaction of masonry with other elements in a building, whereas internal events are dimensional changes of the masonry itself, such as expansion or shrinkage of masonry due to moisture and thermal variations (where clay brick masonry generally undergoes some irreversible expansion, while concrete masonry experiences contraction). In general, brick masonry walls must be designed and detailed to limit the locations and size of cracks, by using adequate masonry materials (with mortar mixes that provide good bond strength) and by providing expansion or control joints. The foundations supporting unreinforced masonry should be stiff enough to counteract movement in the soils (Page 2001).

Differential movement between the brick veneer and the wood frame backup is another form of distress often found in existing home construction. For example, Dickson (2007) studied a ten year old two-story wood frame building with brick veneer, where the brick veneer was undergoing outward movement (away from the wood backup structure) on the order of 0.38 in. to 1.25 in. (10 mm to 32 mm), developing significant gaps around window and door frames. The distress in the brick veneer was explained by the highly expansive bricks, which caused the outer face of the brick veneer wall to expand due to thermal and moisture changes, resulting in an overall outward bow and vertical movement in the veneer. Additionally, the lack of ties used to anchor the brick veneer to the wood frame backup further amplified the problem. (Some existing ties were observed

visually, as well as by employing a metal detector, indicating that tie connections were only present for 4.25 ft^2 to 12.5 ft^2 (0.39 m^2 to 1.16 m^2) of tributary wall area per tie, far fewer than required by codes.) Some distress was also noted in the foundation of this building; however, the distress in the brick veneer was not related to movement at the foundation.

2.5 Seismic Performance and Loss of Residential Construction

A majority of buildings in the U.S. are residential wood frame home structures. This form of construction can be quite vulnerable to earthquakes, as seen from the poor performance of many wood frame homes during the 1994 Northridge earthquake in California (Filiatrault et al. 2002). Unreinforced masonry buildings also make up a sizeable portion of low-rise residential construction throughout the U.S., and these buildings are particularly susceptible to damage and collapse by out-of-plane wall failure during earthquakes (Simsir 2004). Furthermore, a large number of building structures located throughout the central and eastern U.S. have been designed for gravity and wind loads only, without consideration for seismic loads. Most areas have not adopted earthquake resistant design practices or codes, and seismic vulnerability assessment of buildings in this region is not well established (Ellingwood et al. 2007).

Following the Northridge earthquake, a comprehensive study of wood frame home structural behavior was organized by the Consortium of Universities for Research in Earthquake Engineering (CUREE). Among various phases of this research, experiments were conducted on wood frame buildings and their components, analytical models were developed, and damage limits were established for building serviceability and safety in earthquakes (Isoda et al. 2001; Filiatrault et al. 2002). Fragility analyses were then conducted to predict the probabilistic performance of wood frame home structures, such as by Ellingwood et al. (2004), Li and Ellingwood (2006), and Liang (2007). Numerous studies have also been conducted on the seismic performance of unreinforced masonry structures located in the central and eastern U.S.; however, seismic fragilities of unreinforced masonry building construction based on analytical models are scarce. As part of a study by Park et al. (2009), fragility curves were developed analytically for several representative low-rise unreinforced masonry buildings, whereas most fragility functions for these types of buildings are based on expert opinion.

Following weak to moderate earthquakes, it is common to find residential wood frame buildings with very minor to no structural damage, but with significant damage to their architectural and/or nonstructural components, such as brick veneer walls (Figure 1.4), often resulting in high repair and replacement costs (Gillengerten 2001, Villaverde 2004). The seismic performance of brick veneer wall systems has been evaluated through a variety of experimental and analytical studies, as described above; however, there are no studies to date on the seismic fragility of this form of construction. Khudeira and Mohammadi (2006) performed a very general baseline study on the vulnerability of unreinforced low-rise masonry buildings located in northern Illinois. Ground accelerations were estimated for seismic activity in the New Madrid Seismic Zone, with a return period of 50 years, and basic (engineering judgment based) fragilities for

unreinforced masonry buildings from FEMA (1985) were employed, as shown in Figure 2.16. The damage limit states were identified to be as follows: nonstructural, slight structural, moderate structural, severe structural, and collapse. These fragility curves are very general in nature and may only act as a baseline case for fragility assessment of brick veneer construction. The seismic performance of brick veneer on wood frame homes is likely different from that of unreinforced masonry buildings, so a more detailed study with better data on the performance of wood frame homes with brick veneer should be used to assess the fragility of this form of construction.

Overall, brick veneer walls can make up a significant portion of the total cost of a residential home building, and the replacement costs of these components following an earthquake can be very high. Evaluating the seismic fragility of residential brick veneer construction can help home owners and insurers predict the costs of repair and replacement of brick veneer, as well as the need for retrofitting. Furthermore, these findings can be used to mitigate risk of injury to the building occupants and the general public. More specifically, owners and insurers might be interested in knowing the seismic vulnerability of brick veneer as a function of workmanship variability during construction, as well as the vulnerability of wall components that are most susceptible to out-of-plane seismic damage, such as gable-end walls. As described in the subsequent chapters of this thesis, experimental and analytical studies were conducted to evaluate the seismic performance of residential brick veneer wall systems. Brick veneer wall damage limit states were then identified and characterized in terms of seismic performance levels per ASCE 41-06 (ASCE 2006). In the final phase of the project, simplified brick veneer with wood frame backup models were established, and they were utilized to evaluate the seismic fragility of residential anchored brick veneer wall systems.

Table 2.1 – Prescriptive installation requirements for corrugated sheet metal ties.

Construction details	MSJC (2008)	ICC (2003)	BIA (2002)
Tie thickness (gage) [min.]	22	22	22
Tie width (in.) [min.]	0.875	0.875	0.875
Typical wall area per tie (ft^2) [max.]	2.67	2.67	2.67
Horizontal spacing (in.) [max.]	32	24	24
Vertical spacing (in.) [max.]	25	24	24
Wall area per tie in seismic areas (ft^2)[a] [max.]	2.00	2.00	n/a
Wall area per tie in severe wind zones (ft^2) [max.]	1.87[b]	2.00[c]	n/a
Fastener to wood backup [min.]	8d nail[d]	n/a	n/a
Bend distance from fastener (in.) [max.]	0.5	n/a	0.5
Embedment length into mortar (in.) [min.]	1.5	n/a	1.5[e]
Mortar cover on outside face (in.) [min.]	0.625	n/a	0.625
Air gap (in.) [min. and max.]	1.0	1.0	1.0

[a] With seismic design category D and above. MSJC (2008) also requires installation of horizontal joint reinforcement for seismic design categories E and F.

[b] For construction in areas where basic wind speed is between 110 mph and 130 mph (177 and 209 km/h); also, maximum horizontal spacing of ties is reduced to 18 in.

[c] Wind regions with more than 30 psf (1.45 kPa) design pressure.

[d] … or fastener having equivalent/greater pullout strength; should also be corrosion resistant.

[e] … or half the thickness of the brick veneer.

(1 in. = 25.4 mm; 1 ft^2 = 0.0929 m^2)

Table 2.2 – Seismic design loads for veneer and fasteners (FEMA 2003; ASCE 2005).

Seismic Design Category	Short Period Spectral Design Acceleration, S_{DS} (g)	Veneer[a] Design Pressure, F_p/A (psf)	Fasteners[b] Design Pressure, F_p/A (psf)
A	$S_{DS} < 0.167$	$F_p/A < 5$	$F_p/A < 10$
B	$0.167 \le S_{DS} < 0.33$	$5 \le F_p/A < 10$	$10 \le F_p/A < 19$
C	$0.33 \le S_{DS} < 0.50$	$10 \le F_p/A < 16$	$19 \le F_p/A < 29$
D	$0.50 < S_{DS}$	$16 < F_p/A$	$29 < F_p/A$

NOTES:

Design pressure: $F_p/A = 0.4a_pS_{DS}(W_p/A)I_p(1+2z/h)/R_p$

W_p/A = 39 psf (1.88 kN/m^3), with brick masonry density of 115 pcf (1.84 g/cm^3).

$z/h = 1$, $I_p = 1.0$

[a] Veneer - Low deformability elements and attachments: $a_p = 1.0$ and $R_p = 1.5$

[b] Exterior Nonstructural Wall Elements and Connections - Fasteners: $a_p = 1.25$ and $R_p = 1.0$

Table 2.3 – Wind design pressures and resulting tie connection spacing from FEMA (2006).

Wind Speed (mph) (3-Second Peak Gust)	Wind Pressure (psf)	Maximum Vertical Spacing for Ties	
		16" stud spacing	24" stud spacing
90	17.8	18.0[a]	16.0[a]
100	22.0	18.0[a]	16.0[a]
110	26.6	18.0[a]	14.8
120	31.6	18.0[a]	NA[b]
130	37.1	15.9	NA[b]
140	43.0	13.7	NA[b]
150	49.4	10.2	NA[b]

Notes:

1. The tie spacing is based on wind loads derived from Method 1 of ASCE 7-02, for the corner area of buildings up to 30' high, located in Exposure B with an importance factor (I) of 1.0 and no topographic influence. For other heights, exposure, or importance factor, an engineered design is recommended.
2. Fastener strength is for wall framing with a Specific Gravity G=0.55 with moisture contents less than 19% and the following adjustment factors, Ct=0.8; and CD, CM, Ceg, and Ctn=1.0.
3. Nail embedment depth of 2" for 2.5" long 8d common (0.131" diameter) ring-shank fasteners

[a] Maximum spacing allowed by ACI 530-05

[b] 24" stud spacing exceeds the maximum horizontal tie spacing of ACI 530-05 prescribed for wind speeds over 100 mph

Figure 2.1 – Residential brick veneer home during construction, with excessive mortar droppings in the wall cavity.

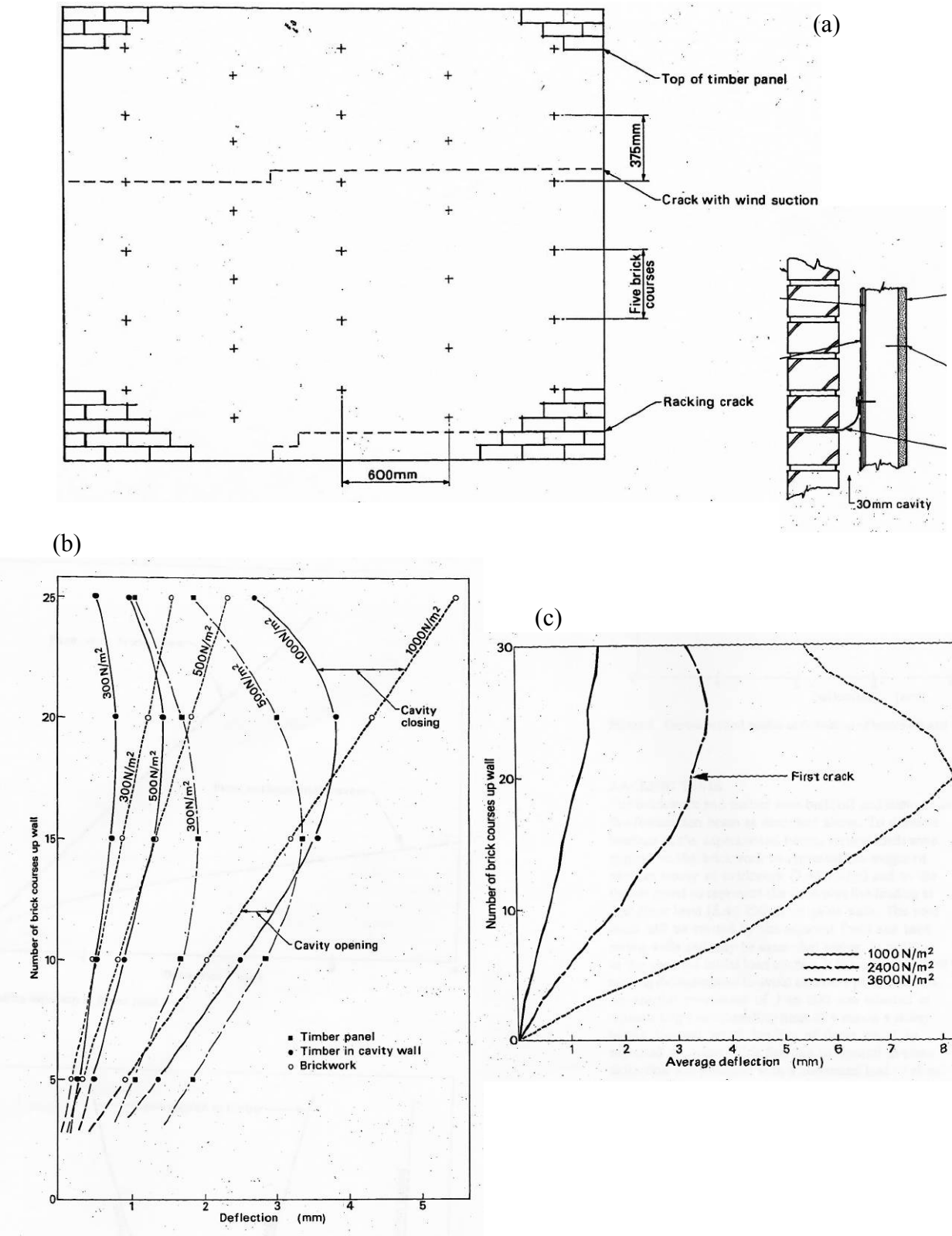

Figure 2.2 – Experimental test setup and results from a study by Moore (1978).

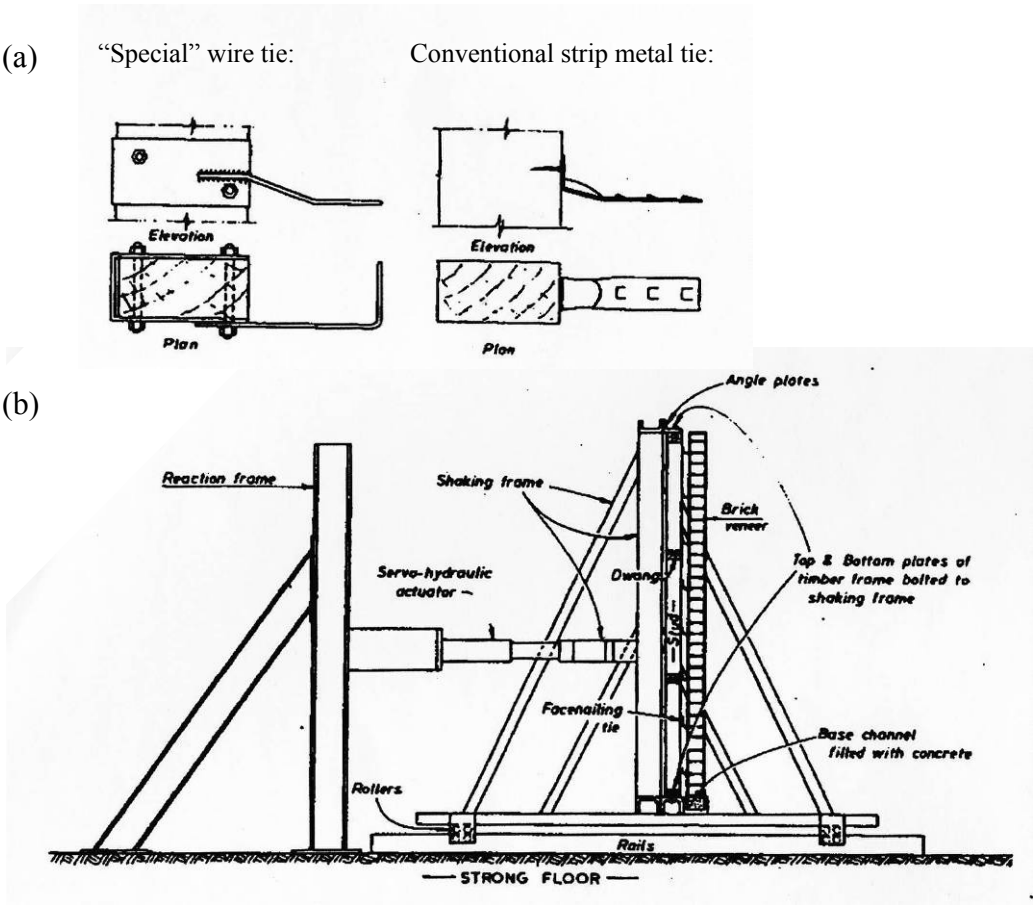

Figure 2.3 – (a) Tie connection details and (b) out-of-plane wall panel experimental setup from a study by Priestley et al. (1979).

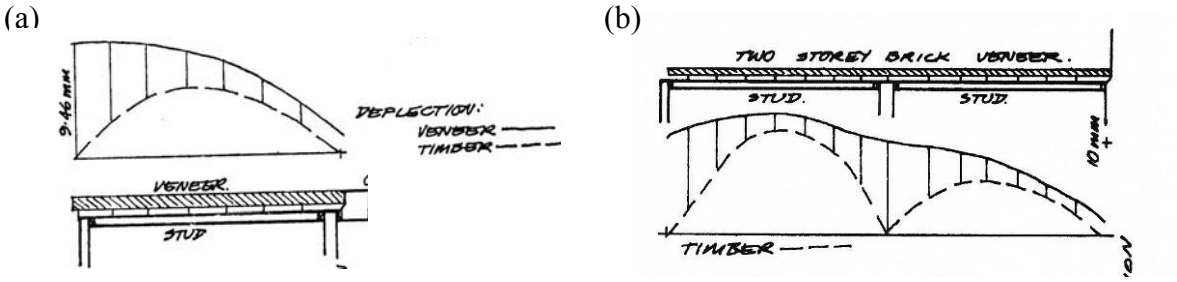

Figure 2.4 – Qualitative analysis results from a study by Lapish and Allen (1982) for the out-of-plane behavior of (a) single- and (b) multi-story brick veneer walls.

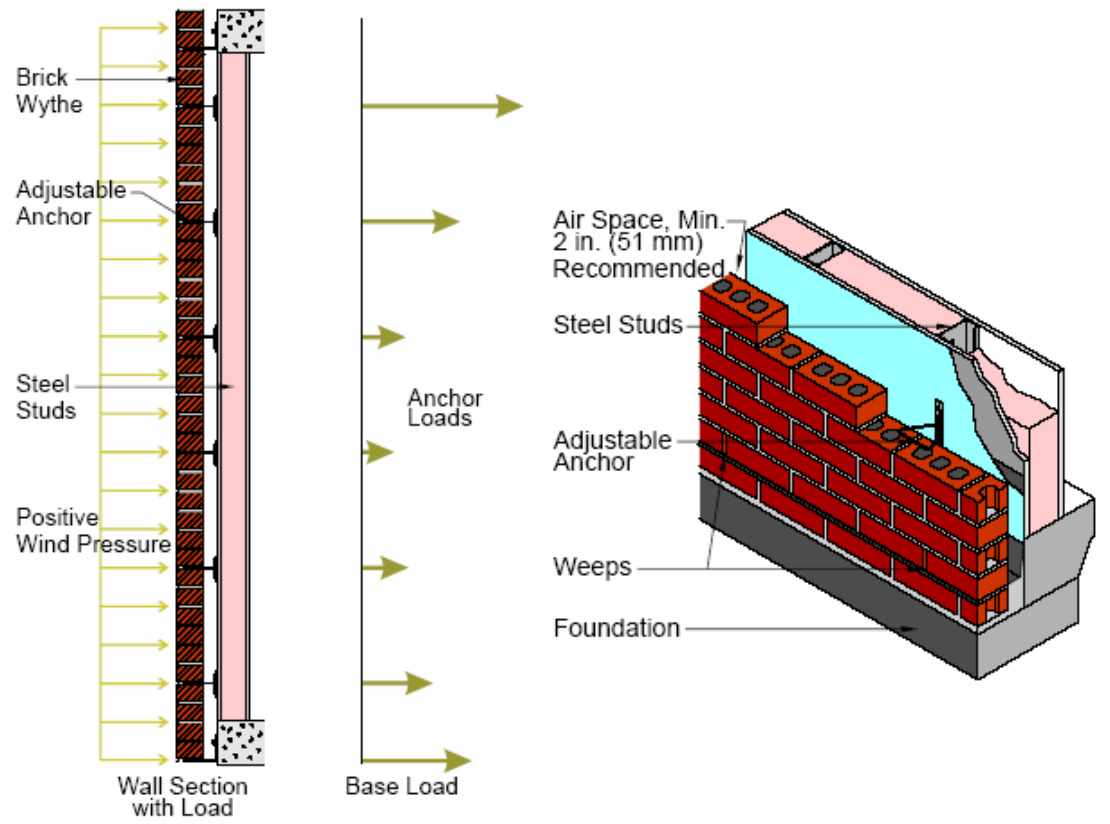

Figure 2.5 – Typical construction details of commercial brick veneer walls, including a qualitative depiction of the relative loads resisted by the tie connections (anchors) for a wall subjected to out-of-plane loading (BIA 2005).

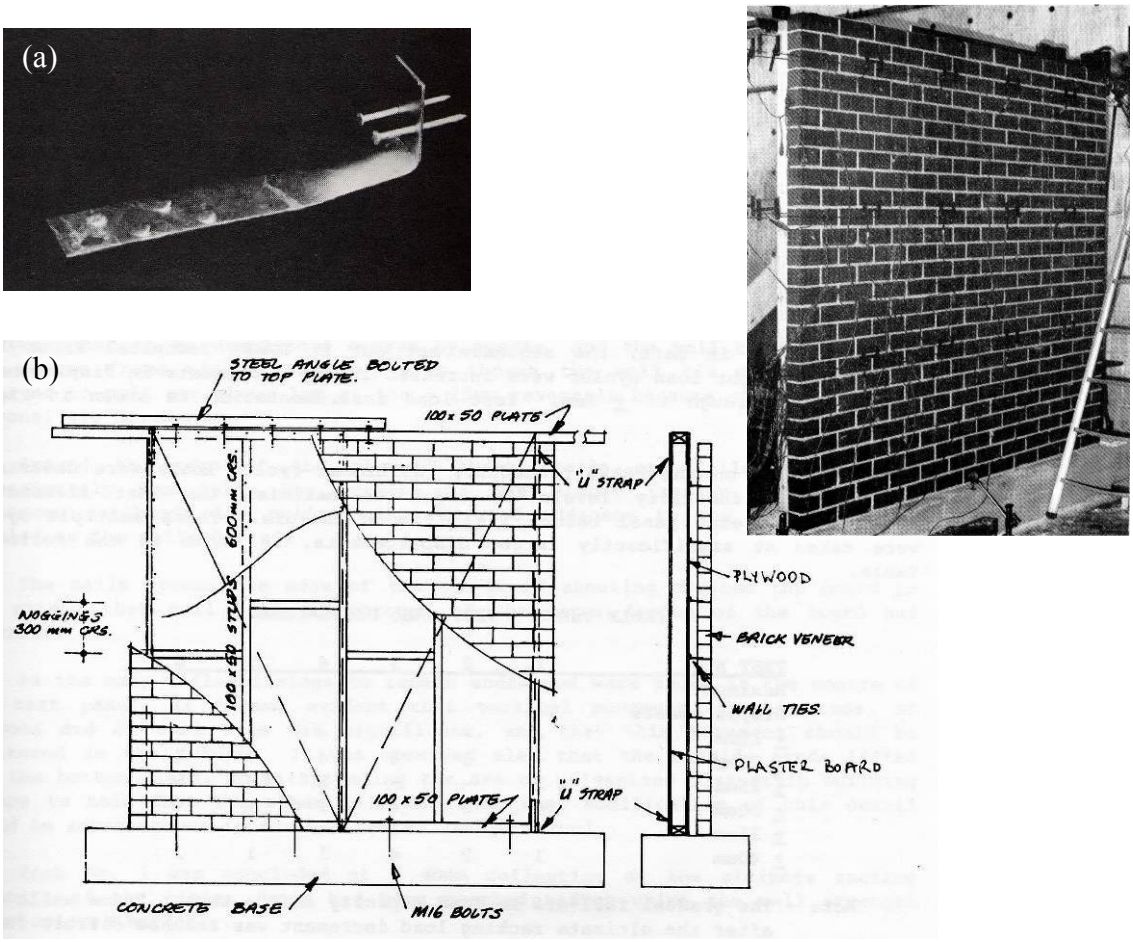

Figure 2.6 – Experimental test setup and results from a study by Allen and Lapish (1982).

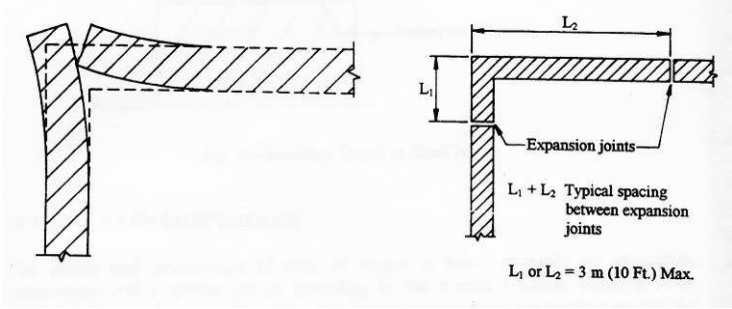

Figure 2.7 – A problem with locating expansion joints at corners of masonry walls and a simple solution (Chrysler 1995).

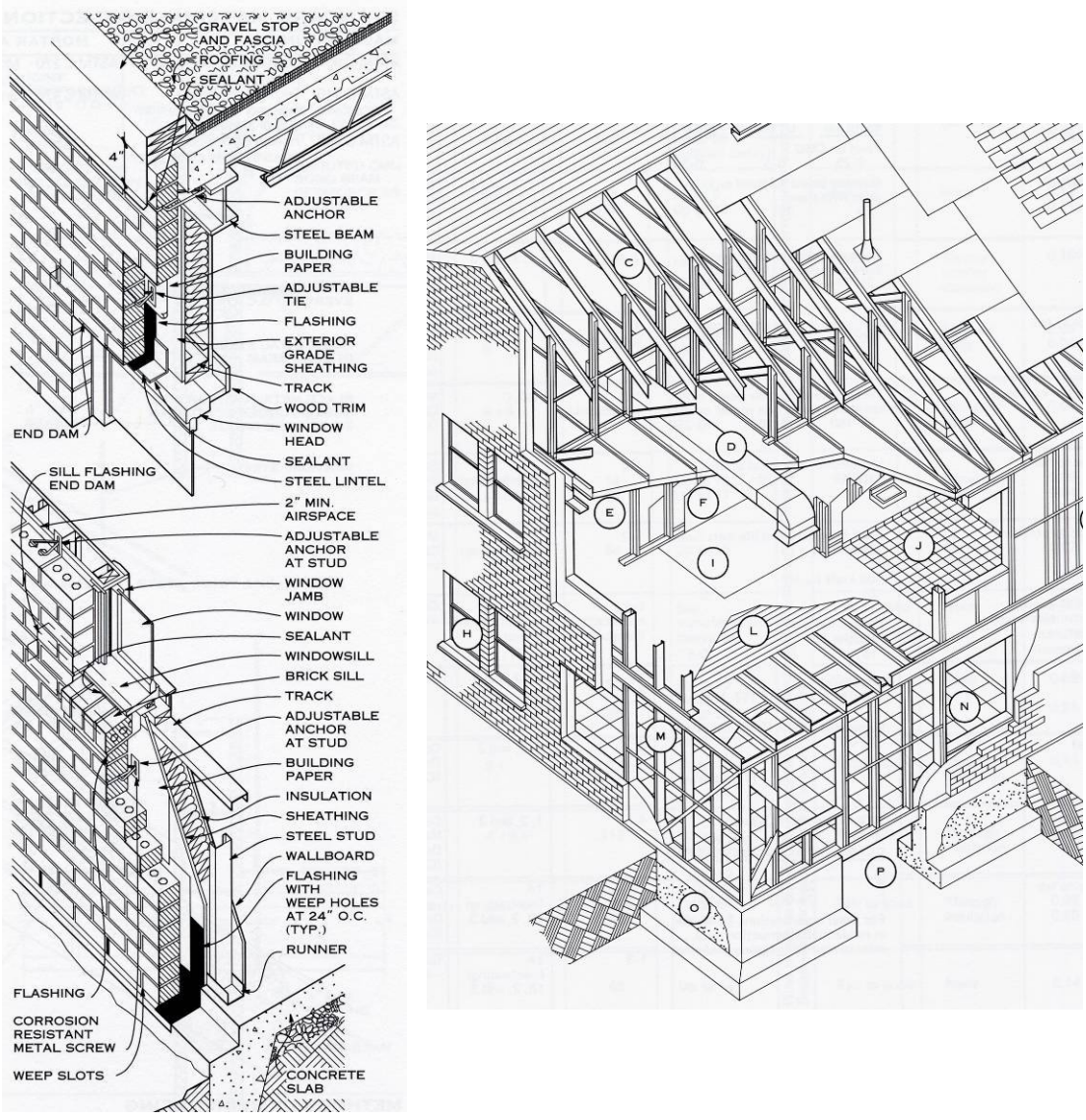

Figure 2.8 – Typical details of brick veneer on light-gauge steel frame home construction (Rumbarger and Vitullo 2003).

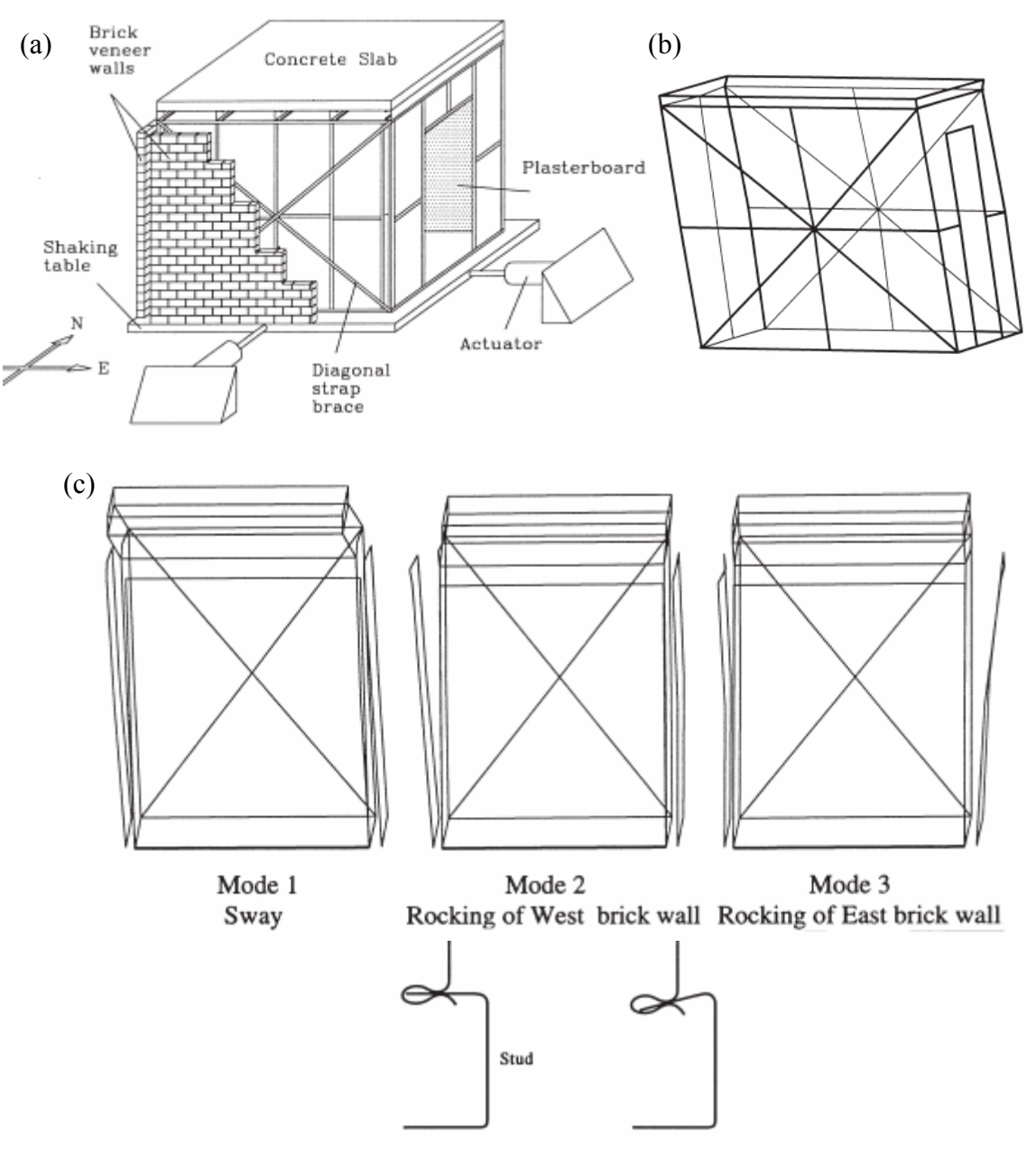

Figure 2.9 – Experimental test setup and analysis of results from a study by Gad et al. (1999).

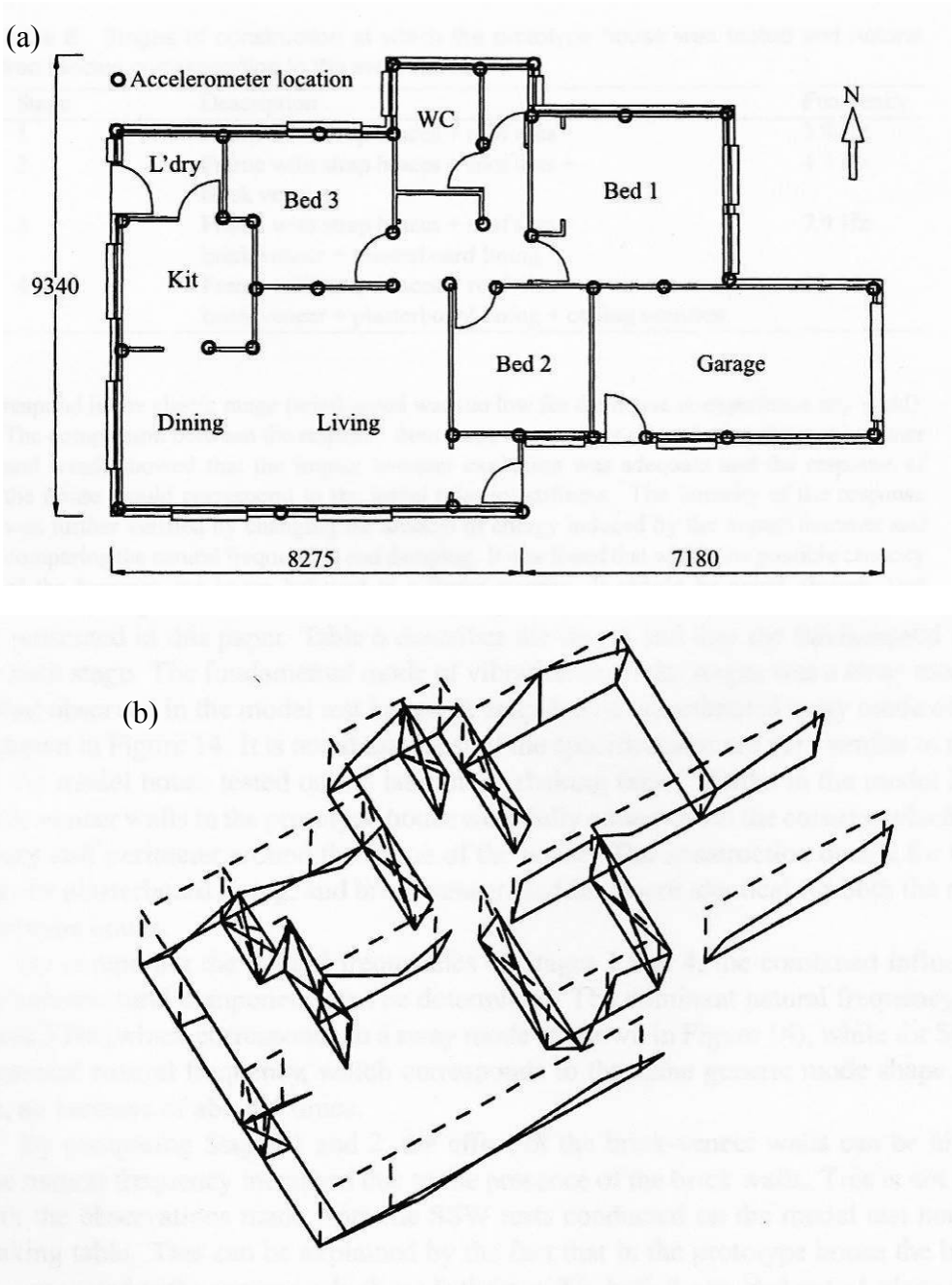

Figure 2.10 – (a) A typical floor plan layout and (b) modal response of a residential home structure, from field tests by Gad et al. (2001).

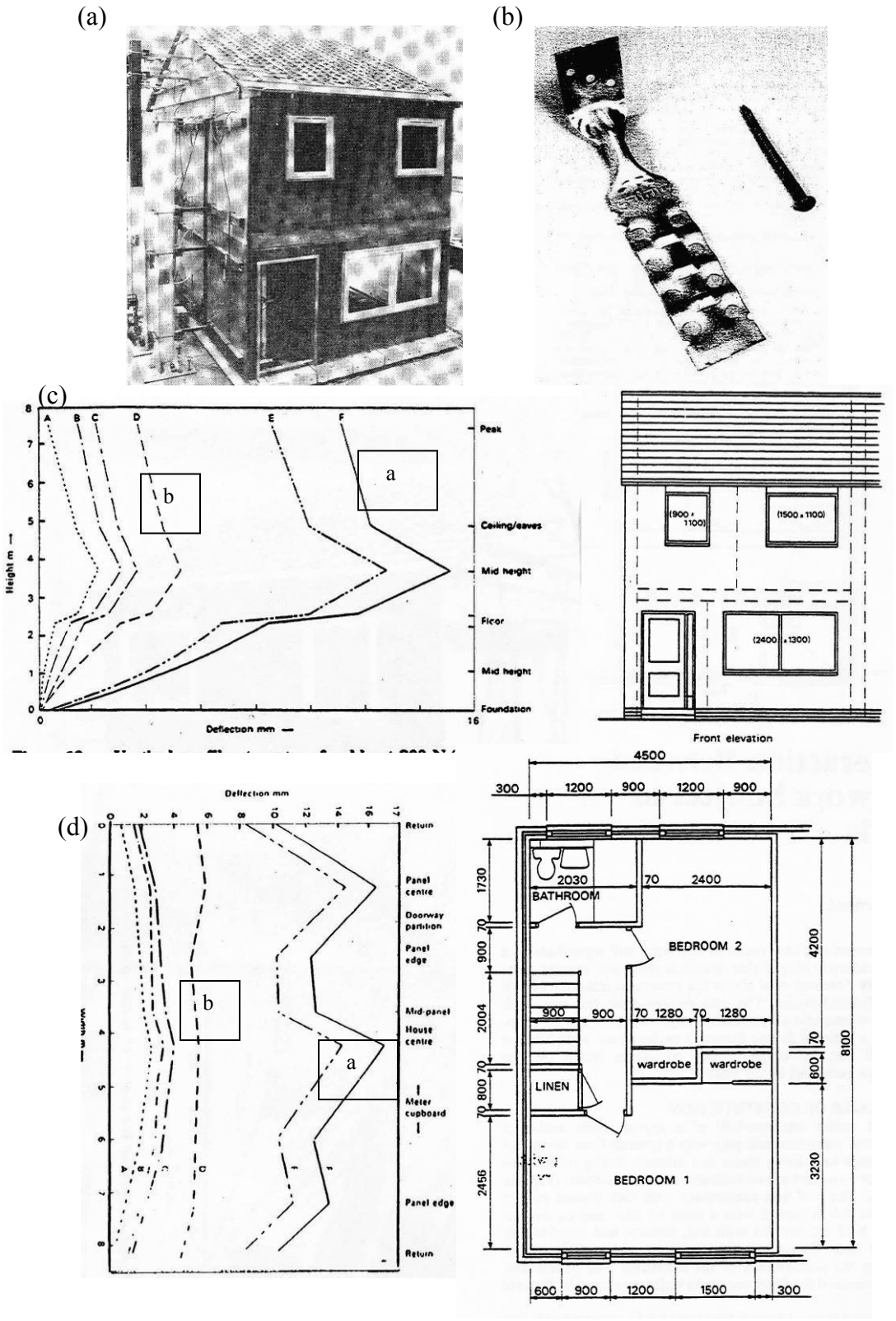

Figure 2.11 – Experimental test setup and results from a study by De Vekey (1987); labels "a" and "b" in the graphs indicate test results without brick veneer and with brick veneer, respectively.

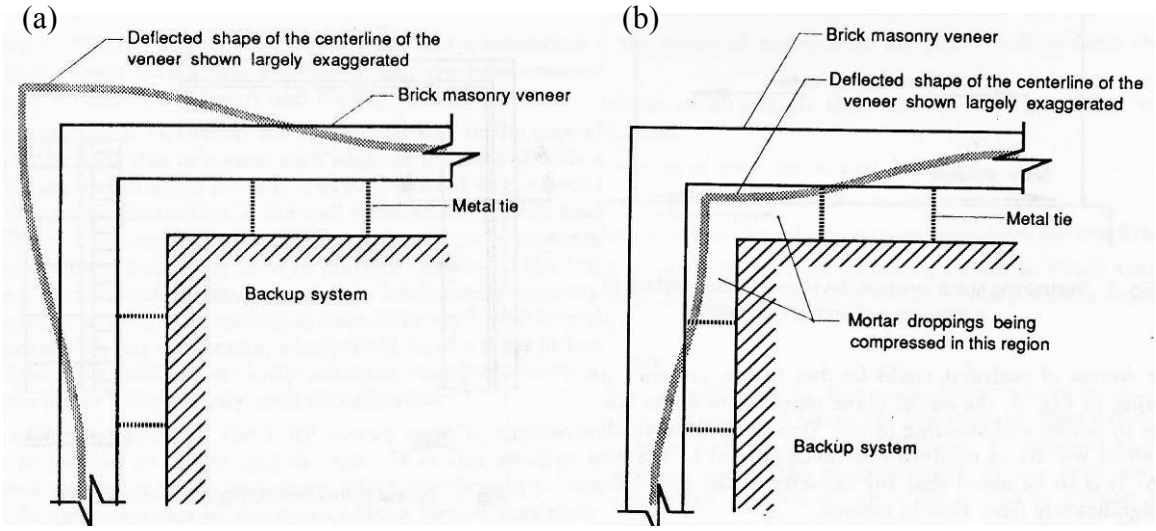

Figure 2.12 – Analytical modeling considerations for brick veneer wall corners by Naguib and Suter (1986).

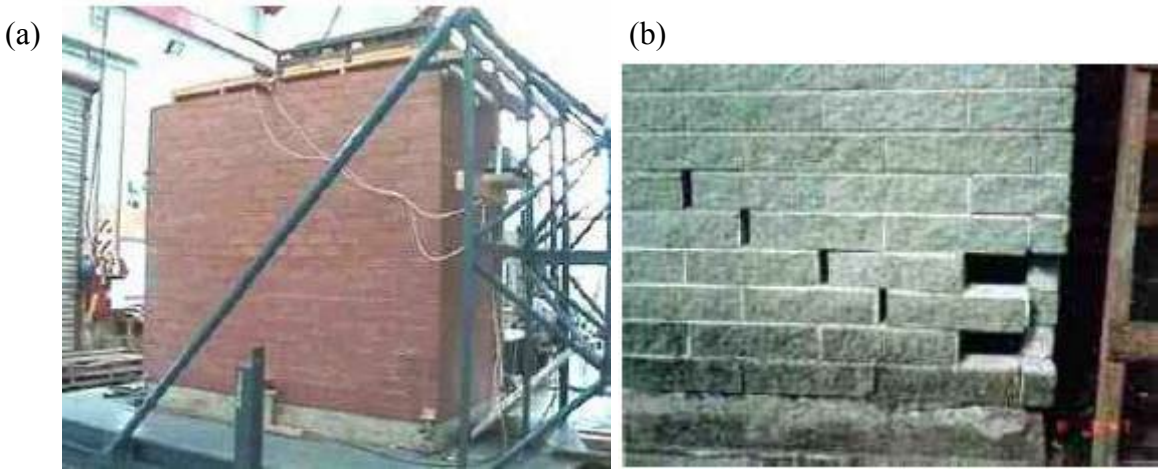

Figure 2.13 – Experimental test setup and brick veneer corner failure observations by Beattie (2004).

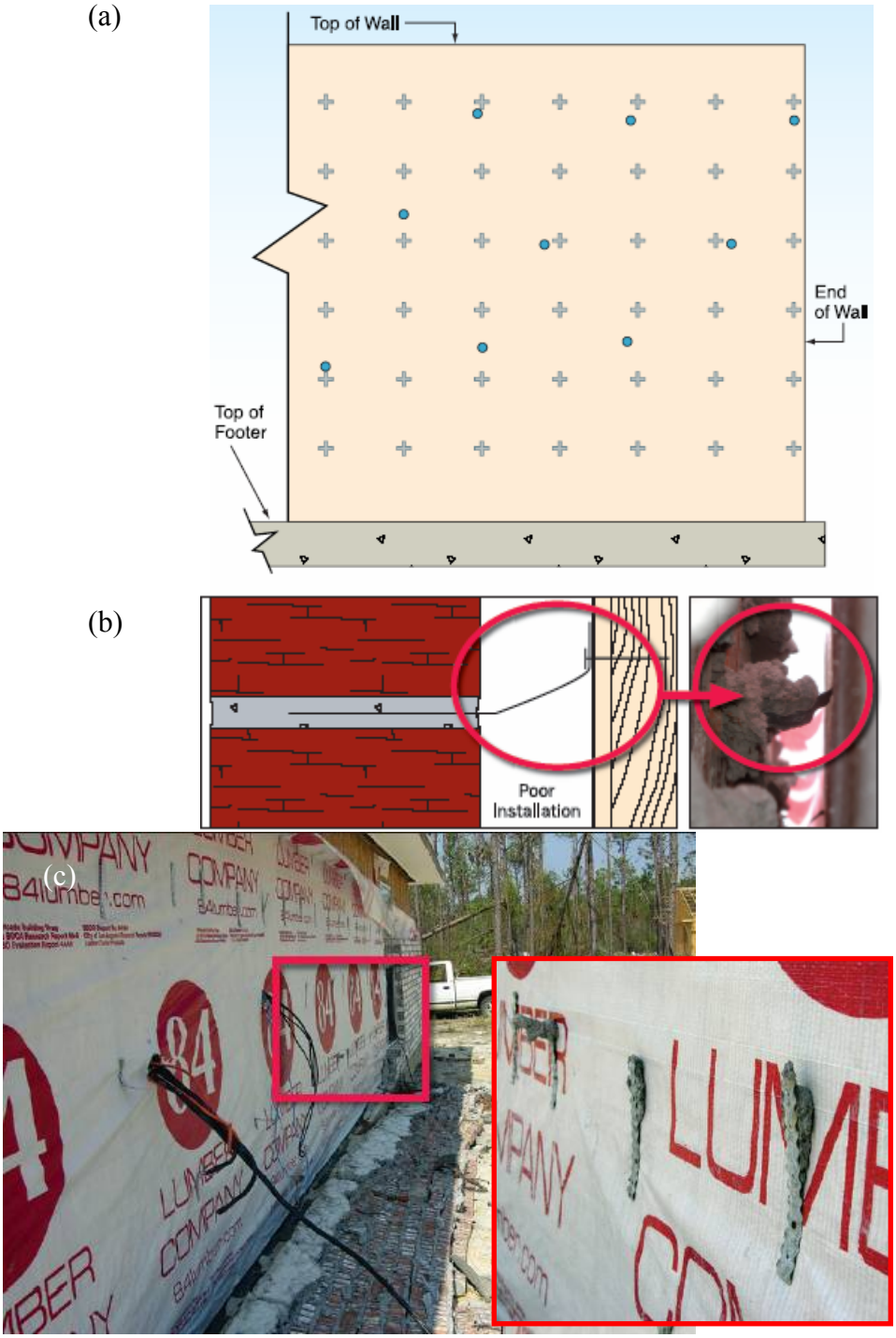

Figure 2.14 – Examples of poor workmanship in construction of brick veneer walls revealed following Hurricane Katrina (FEMA 2006): (a) collapsed wall with an inadequate number of ties (+'s indicate required ties, o's indicate ties provided), (b) poor alignment of ties with mortar joint, and (c) a collapsed wall where ties were never embedded in mortar joints.

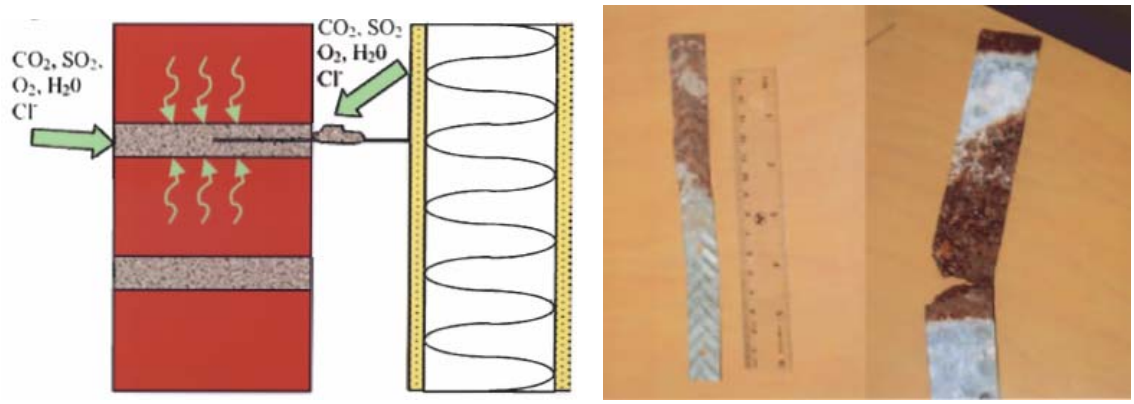

Figure 2.15 – (a) Process of tie corrosion in a brick veneer wall, and (b) corroded ties (Hagel et al. 2007).

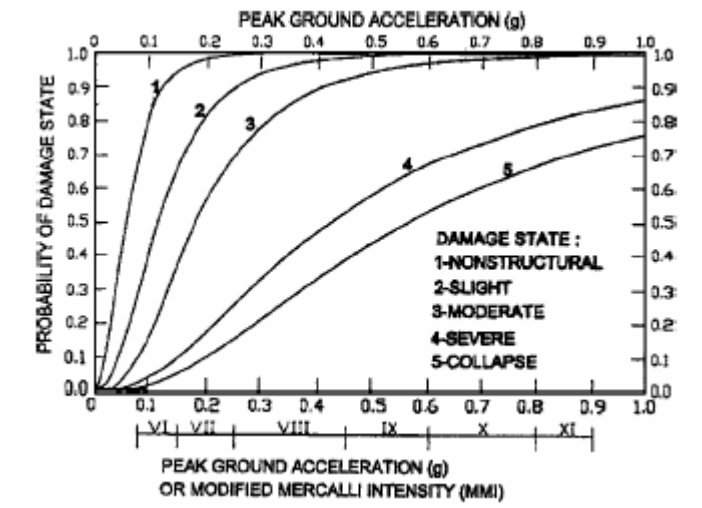

Figure 2.16 – Fragility curves for low-rise unreinforced masonry buildings (FEMA 1985).

EXPERIMENTAL TESTING OF TIE CONNECTIONS

Laboratory testing was conducted on brick-tie-wood connection subassemblies representing residential anchored brick veneer construction, to explore the effects of tie thickness, tie attachment method, tie eccentricity, and tie embedment length on the strength and stiffness of typical brick veneer corrugated sheet metal tie connections. This experimental study was started by Choi and LaFave (2004) on approximately 210 tie connection subassemblies, which were subjected to monotonic and cyclic in-plane and out-of-plane loads (tension, compression, and shear), permitting an evaluation of the stiffness, strength, and failure modes for a local portion of a veneer wall system, rather than just of a single tie by itself. An additional 35 subassembly tests have been conducted to further explore tie connection behavior, primarily when loaded in tension, for various code compliant and non-compliant tie installation methods (selected in part by consideration of the reports of inadequate attachment to the wood frame backup, as described back in Chapter 2). Detailed descriptions of the types of tie connection test specimens, test setups, and testing procedures used, as well as a summary of the most important experimental results, are presented in the sections that follow. Experimental results from this study have then been used in analytical models of brick veneer wall panels to assess the effects of different tie connection installation procedures on wall system performance, as described later in Chapter 5.

3.1 Tie Connection Subassembly Testing Program

3.1.1 Tie Connection Test Specimens

Sets of tie connection subassemblies were tested to evaluate the strength and stiffness behavior of corrugated sheet metal brick veneer ties of different thicknesses, installed in various ways representing common residential construction practice. The tests described herein were conducted under monotonic tension and cyclic tension-compression loading. This chapter emphasizes tie connection tensile strength and stiffness results gleaned from approximately 130 monotonic tension and cyclic tests, which include approximately 95 such tests conducted earlier by Choi and LaFave (2004). Results for 45 tie connection monotonic compression tests from that earlier study have also been briefly summarized.

To completely characterize the local connection behavior of a brick veneer wall system consisting of exterior brick masonry attached to wood studs by a series of corrugated sheet metal ties, brick-tie-wood subassemblies were used (rather than simply just testing the ties). The subassemblies typically consisted of two standard bricks connected to a wood stud with a corrugated sheet metal tie (see Figure 3.1). This type of test specimen (as well as the testing method) differs from that specified by American Society for Testing and Materials (ASTM) standard test method E 754 (ASTM 1998). The ASTM E 754 method is applicable only for (tension) pullout resistance of ties embedded in mortar

joints, whereas the tests reported herein include tension, compression, and cyclic loading, and can capture tie connection failure modes other than just by tie pullout.

The bricks used were 3-1/2 in. x 7-5/8 in. x 2-1/4 in. (89 mm x 194 mm x 57 mm) standard modular three-hole "Colonial Reds" joined together by professional masons using Type N mortar (cement : lime : sand = 1 : 1 : 6). In each subassembly, one end of a bent corrugated sheet metal tie was embedded into the mortar joint (a minimum distance of approximately 2-1/2 in. (64 mm)), while the other end was attached by a nail (or screw) fastener to a short length of 2x4 wood stud (Standard Grade Spruce-Pine-Fir), typically through a strip of 7/16 in. (11 mm) thick oriented strand board (OSB) APA Rated 24/16 wall sheathing (Figure 3.1(b)). Eight different groups of brick-tie-wood connection subassemblies were constructed and tested. Construction variables for the subassemblies included tie thickness, tie attachment method (to the wood stud), and tie eccentricity (at the connection to the wood stud).

Three tie thicknesses were studied: 22 ga. (0.031 in. [0.79 mm]), 28 ga. (0.013 in. [0.33 mm]), and 16 ga. (0.062 in. [1.57 mm]). Details of the 22 ga. and 28 ga. ties are shown in Figure 3.1(c). In accordance with typical prescriptive design recommendations and code requirements for brick veneer on wood backup framing, 22 ga. ties should be used (MSJC 2008; ICC 2003), so they were employed in the majority of the subassemblies. Thinner 28 ga. ties are quite often used in actual residential construction practice, which warranted their study as well, whereas 16 ga. ties are seldom used in residential construction, so they were simply included to explore what the effect would be of using ties exceeding the minimum specifications.

Nails and wood screws were each investigated as methods for attaching corrugated veneer ties to the wood backup, representing the variability in workmanship during installation of the ties. Galvanized 8d nails (2-1/2 in. [64 mm] long, with a diameter of 0.131 in. [3.3 mm]) were used in the bulk of the subassemblies, per typical prescriptive code requirements (MSJC 2008). Galvanized roofing nails of two different lengths (2-1/2 in. [64 mm] and 1-1/2 in. [38 mm], with a diameter of 0.113 in. [2.9 mm]) were also studied since such fasteners (in lengths even as short as 1-1/4 in. [38 mm]) are often "substituted" for 8d nails in practice. A few subassemblies (including all of those with 16 ga. ties) were constructed using #8 x 2-1/2 in. bugle head galvanized deck screws instead of nails.

Most of the subassemblies were constructed with the corrugated sheet metal tie bent 90-degrees right over the head of the nail or screw fastener, which represents the "best-case" installation situation from the standpoint of (minimum) tie eccentricity at the bend (with respect to the centerline of the fastener). For specimens with 8d nails or wood screws, this resulted in a small eccentricity (see Figure 3.1(b)) of approximately 5/32 in. (4 mm); in the cases where roofing nails were used, this resulted in a slightly larger eccentricity of approximately 1/4 in. (6 mm), due to the larger nail head. To investigate the effect of variability in tie eccentricity (possibly due to sloppy tie installation and/or poor tie alignment with the brick veneer mortar joint), some specimens were tested with a greater

eccentricity at the bend of 1/2 in. (13 mm), as shown in the Figure 3.1(b) inset, which is the maximum eccentricity permitted by the MSJC (2008).

A listing of the eight different types of brick-tie-wood connection subassemblies constructed and tested (per the construction variables described above) is provided in the first column of Table 3.1 (where the number of test specimens, as well as summary average tensile strength and stiffness data, is also presented for all groups of regular subassemblies subjected to either monotonic tension or cyclic loading). The shorthand notation used to designate the categories of test specimens is of the form: F(f)##e, where "F(f)" represents the type and size of fastener [Nail (8d or 2.5 in. roofing or 1.5 in. roofing) vs. Screw (–)], "##" represents the thickness of the tie (22 ga. vs. 28 ga. vs. 16 ga.), and "e" represents the eccentricity of the tie at the bend from the fastener centerline (minimum eccentricity vs. 1/2 in. eccentricity). This notation has also been described in Figure 3.1(d).

The first two categories of tie connections (N(8d)22min and N(8d)22ecc) both meet the minimum code-specified installation requirements described above. The next four categories of tie connections (N(8d)28min, N(8d)28ecc, N(2.5)22min, and N(1.5)22min) all fail to meet the minimum code-prescribed installation requirements with respect to either tie thickness or fastener type/length. Finally, the last two categories of tie connections (S(–)22ecc and S(–)16min) each exceed the minimum code-specified installation requirements for tie thickness and/or fastener type.

As part of the tie connection monotonic and cyclic tension tests reported in Table 3.1, eighteen additional tests were conducted on eccentric subassemblies where a relative offset displacement was introduced between the bricks and the wood stud at the onset of testing. This different type of test, which was conducted on subassemblies representing just three of the specimen types, is briefly described further in the next section regarding the test setup and testing procedures. There were also 35 regular and 10 offset specimens tested in monotonic compression by Choi and LaFave (2004), representing six of the eight different specimen types described above. Finally, in order to simply evaluate the relationship between tie connection tension pullout strength vs. tie embedment length, 30 brick-tie specimens (without wood studs) were prepared and tested in tension (10 sets of specimens in triplicate) with different tie embedment lengths into the mortar joint. The 22 ga. and 28 ga. ties were evaluated for embedment lengths of 1-1/2 in. (38 mm), 2 in. (51 mm), 2-1/2 in. (64 mm), and 3 in. (76 mm), while the 16 ga. ties were only tested with embedment lengths of 1-1/2 in. and 2 in. (which was almost the maximum possible embedment for this type of "pre-bent" tie, accounting for the presence of the minimum air cavity between the tie and the bricks). A 1-1/2 in. tie embedment length into the mortar joint represents the minimum embedment permitted by the MSJC (2008), while 3 in. would be about the maximum practical embedment length (for the size of bricks used in this study) in keeping with the MSJC (2008) minimum mortar cover requirement beyond the end of a tie.

3.1.2 Test Setup and Testing Procedure

Experiments on the brick-tie-wood connection subassemblies were conducted at Illinois using a universal testing machine in the Newmark Structural Engineering Laboratory, as shown in the test setup indicated on Figure 3.2. High-strength gypsum was applied to the bottom of the bricks to level the surface where they contacted the testing machine bed, thereby avoiding shear loads on the mortar joint. Steel plates and C-clamps held the bricks to the testing machine bed, with rubber sheets installed between the plates and the bricks to ensure a tight fit. C-clamps were also used to grip the wood stud in the upper part of the testing machine. All tests were performed at least 28 days after specimen fabrication

An Instron 8500 Plus controller, a 20 k MTS Systems Universal Testing Frame, and a PowerMac computer with National Instruments analog-to-digital acquisition board and custom written *LabView* software were used to control the tests and to collect the data. A small load cell in the testing frame was connected to the computer via the controller to allow for both measuring and controlling the load and overall (actuator) displacement. Two LVDTs were attached directly onto every test specimen (one on each side of the wood stud) to measure just the displacement occurring from the face of the bricks to the face of the wood stud; these LVDTs were also connected to the computer via the controller. All data were simultaneously recorded every 0.5 sec.

The monotonic tension and compression tests to failure were actuator displacement controlled at a rate of 0.1 in./min (2.5 mm/min). The cyclic tests were also controlled by actuator displacement, with a total of 24 intended cycles as shown in Figure 3.3. (The repeat same amplitude cycles and the small displacement cycles were included to explore strength and stiffness degradation.) Cyclic displacements were applied at the rate of 1 cycle/min.; after 24 cycles, additional displacement cycles were occasionally applied in increments of 0.05 in. (1.3 mm), as needed to produce subassembly failure.

To simulate possible vertical differential wall movement across the cavity (from long-term moisture and temperature effects), a few additional eccentric subassemblies were tested monotonically and cyclically after being given a substantial initial 1/4 in. (6 mm) relative offset displacement (perpendicular to the face of the tie) between the bricks and the wood stud. Such offset tests were only conducted for three of the eight different types of tie connection subassemblies (and typically in sets of only three specimens), so those results in tension are not tabulated in Table 3.1. Detailed results for the monotonic and cyclic offset tests are provided elsewhere (Choi and LaFave 2004); general behavior trends from the offset tests will be noted below whenever they are significant in comparison with the rest of the reported tie connection subassembly test data. Additionally, the brick-tie embedment specimens were all tested in monotonic tension up to pullout failure, using a slightly modified version of the apparatus described above. The test setup and testing procedure were similar to those specified by ASTM E 754, except that the ties were directly grasped by custom-made screw grips in the testing machine.

3.2 Subassembly Tension Test Results

Table 3.1 lists the number of test specimens, along with average tensile strength and stiffness data, for all groups of regular tie connection subassemblies subjected to monotonic tension or cyclic loading. An example of one set of monotonic tension force-displacement curves and one cyclic tension-compression curve, for the N(2.5)22min subassemblies, is shown in Figure 3.4. The tensile strength for each subassembly is simply defined as the maximum tension load achieved during testing. (The coefficient-of-variation for the average tensile strengths of the different groups of test specimens was typically between 10% and 20%.) The tensile stiffness for a subassembly is defined as the secant stiffness of the load vs. average LVDT displacement curve up to a tension load of 100 lbs (445 N) (or up to an opening displacement of 0.05 in. [1.27 mm] in the rare case when a particular specimen never reached a tensile load of 100 lbs). (Examples of the average tensile secant stiffnesses for the N(2.5)22min type of tie connection are also shown in Figure 3.4.) Computing the stiffness to a load of 100 lbs was in part selected because this load represents approximately two-thirds of the average maximum tension load achieved in subassembly types just meeting minimum code-specified installation requirements. Furthermore, using the secant stiffness to 100 lbs allows for easy comparison with the BIA Technical Note recommendation that a minimum tie connection load of 100 lbs should be achieved at a deflection of 0.05 in. (BIA 2003), which corresponds to a secant stiffness of 2000 lbs/in. (350 N/mm).

3.2.1 Tie Connection Tensile Strength

With respect to average tie connection subassembly tensile strength, the effect of cyclic loading vs. monotonic loading was generally negligible; the maximum reduction in average tensile strength when subjected to cyclic loading for any of the eight types of tie connections tested was only about 10%. (In some cases, there was a more significant cyclic loading effect on the connection failure modes and/or on the tie connection average tensile stiffness, as will be described in more detail later.) Furthermore, different tie eccentricities were found to typically only affect tie connection average subassembly tensile strength by about 15% or less for otherwise identical groups of test specimens (although additional movements on the order of about 0.1 to 0.2 in. [2.5 to 5.1 mm] were usually required to develop the equivalent tensile strength in the eccentric tie connections). Therefore, to best summarize the detailed average monotonic and cyclic tensile strengths presented in Table 3.1, certain aggregate values (as a function of only tie thickness and fastener type) can be computed and compared, as follows.

For all tie connection subassemblies with 8d nails and meeting the other minimum prescriptive installation specifications, the average tie connection tensile strength was 153 lbs (681 N), from 43 total tests, whereas for otherwise similar tie installations that used thinner (28 ga.) ties, the average tie connection tensile strength was 158 lbs (703 N), from 18 total tests. This indicates that using a thinner tie does not necessarily compromise the strength of a typical brick-tie-wood connection (assuming that no tie deterioration has occurred). However, when 8d nails were replaced with similar length (2-1/2 in.) roofing nails in subassemblies with 22 ga. ties, the average tie connection tensile strength was 99 lbs (441 N), from 11 total tests; the average tie connection tensile

strength was only 76 lbs (338 N) when 1-1/2 in. roofing nails were used (also from 11 total tests). (For reference, a tie connection tensile strength of 76 lbs would correspond to an ultimate uniform local wall suction pressure of about 28.5 psf [1.35 kPa] applied over a wall area of 2.67 ft^2 [0.25 m^2].) This indicates that using short roofing nails (instead of 8d nails) to attach veneer ties to the wood backup can result in as much as a 50% or more reduction in tie connection tensile strength.

The predominant tie connection failure mode observed in the monotonic tension tests of nailed subassemblies was nail pullout from the wood stud, which helps to explain why tie thickness had no effect on average tie connection tensile strength for these specimens, while nail type had a significant effect. During cyclic testing of subassemblies with nails, various failure modes were observed (see Figure 3.5), including nail pullout, tie fracture, yield around the tie hole (permitting the head of the nail to pass through), and tie pullout from the mortar joint. Finally, the maximum effect of an initial offset displacement on average tensile strength of tie connections with nail fasteners was found to be only about a 15% reduction in strength.

When 2-1/2 in. long wood screws were used to replace 8d nails in subassemblies with 22 ga. ties (or as the principal fastener in subassemblies with 16 ga. ties), the average tie connection tensile strength was 409 lbs (1820 N), from 25 total tests, an increase of more than 150% over the average strength of tie connection subassemblies just meeting the minimum prescriptive installation requirements. The predominant tie connection failure mode observed in both monotonic and cyclic tension tests of subassemblies with screw fasteners was tie pullout from the mortar joint, with a few occurrences of either yield around the tie hole (permitting the screw head to pass through) or tie fracture. The deleterious effect of initial offset displacement on the tensile strength of tie connections with screw fasteners was more pronounced than in subassemblies with nails, but the strength of connections with wood screws subjected to initial offset was still always much higher than that of any category of tie connection using nails.

3.2.2 Tie Connection Tensile Stiffness

With respect to average tie connection subassembly tensile stiffness, the effect of cyclic loading vs. monotonic loading was more apparent than it was for tensile strength, but the reduction in average tensile stiffness when subjected to cyclic loading for most types of tie connections was still typically less than about 15%. However, variation in tie eccentricity was consistently found to have a considerable effect on tie connection average subassembly tensile stiffness, while fastener type also had an effect.

In terms of overall average tensile stiffness (for the monotonic tests plus the cyclic tests), all but one group of tie connections that were constructed with the minimum possible tie eccentricity from the fastener at the tie bend had average tensile stiffness values close to or in excess of 2000 lbs/in. (350 N/mm) – 3560 lbs/in. (624 N/mm) for N(8d)22min (from 13 total tests), 2230 lbs/in. (391 N/mm) for N(8d)28min (from 9 total tests), 2400 lbs/in. (420 N/mm) for N(2.5)22min (from 11 total tests), and 1980 lbs/in. (347 N/mm) for S(–)16min (from 10 total tests). The one exception to this was tie connection subassembly group N(1.5)22min, which had a somewhat lower overall average tensile

stiffness of 1240 lbs/in. (217 N/mm), from 11 total tests, due to the relatively early onset of nail pullout contributions to connection flexibility since very short roofing nails were used.

On the other hand, all three groups of tie connections that were constructed and tested with the larger 1/2 in. tie eccentricity from the fastener at the tie bend had overall average connection tensile stiffness values of only about one-third or less of 2000 lbs/in. (350 N/mm) – 600 lbs/in. (105 N/mm) for N(8d)22ecc (from 30 total tests), 690 lbs/in. (121 N/mm) for S(–)22ecc (from 15 total tests), and 260 lbs/in. (46 N/mm) for N(8d)28ecc (from 9 total tests). When monotonic and cyclic tension tests were conducted including initial offset displacements, there was typically a small additional decrease in connection stiffness for these groups of specimens with tie eccentricity, by as much as about 20%.

As a comparative measure of the overall tension behavior (including both strength and stiffness) for the various types of brick-tie-wood connection subassemblies tested, idealized multi-linear average load-displacement curves have been prepared and plotted together in Figure 3.6 for all specimen types. The properties of each idealized multi-linear curve have been summarized in Table A.1, which may be found in Appendix A. The idealized multi-linear curves were generated based on the actual load-displacement curves for each type of specimen, as shown in greater detail in Figures A.1 through A.8 (also in Appendix A). (This was done to provide an easy comparison between the different types of tie connection specimen behavior in an average sense, and to provide simple average stiffness data for input into analytical models of overall brick veneer wall system behavior.) For the various specimens, the first step was to locate an inflection point that separated the initial and intermediate stages of loading along the actual load-displacement curves. A line from the origin to the inflection point represented the initial stage, and the intermediate stage was represented by a line from the inflection point to the maximum load point. Point A of the ideal curves (Figures A.1 through A.8) was determined from the average stiffness of the initial stage and the average load of the inflection point. Point B was determined from the average stiffness of the intermediate stage and the average maximum load. The stiffness for the entire unloading (descending) region was simply taken as the average stiffness from the peak to a displacement of 0.6 in. (15 mm). The unloading portion of these idealized curves represented an aggregate of onset and evolution of tie connection tensile failure modes from all subassembly tests, with nail pullout from the wood stud as the dominant mode of failure.

As shown in Figure 3.7, it is also apparent that the overall average tension envelope curves from cyclic tests are typically well-matched with the idealized curves for monotonic tension loading, with the ultimate strength values within approximately 10% for most types of tie connections. Overall, because of these general similarities, the monotonic idealized curves were later implemented in FE models for brick veneer tie connection behavior. Effects of tie connection tensile strength and stiffness on overall brick veneer wall system performance will be explored in Chapters 4 and 5.

3.2.3 Tie Embedment Tests

The average maximum mortar joint tensile pullout strengths from the brick-tie connection embedment tests as a function of tie thickness and embedment length are provided in Table 3.2. For any particular embedment length, thicker ties generally had greater pullout strengths, and as would be expected, longer embedment lengths generally resulted in greater pullout strengths as well. The sets of embedment length test specimens typically exhibited higher average strengths than did the corresponding groups of brick-tie-wood subassemblies that had similar or even longer embedment lengths, because the strength of those subassemblies was usually controlled by other failure modes (at lower loads), such as pullout of the nail from the wood stud. Therefore, even if the brick-tie-wood subassemblies had been constructed with the MSJC (2008) minimum embedment length of 1-1/2 in. (38 mm), instead of the 1-3/4 to 2-1/2 in. (64 mm) that was actually used, it is unlikely that there would have been any significant changes in the average subassembly tensile strength and stiffness values presented earlier.

3.3 Summary of Subassembly Compression Test Results

All of the brick-tie-wood subassemblies that were tested in compression failed by flexural buckling of the tie, regardless of the type of test specimen, as shown in Figure 3.5(d). Idealized multi-linear compression force-displacement curves were also generated by Choi and LaFave (2004), as shown in Figure 3.8. In general, the compression load typically decreased after buckling and then increased again at very large displacements as the tie began to be crushed in the air cavity. For 22 ga. ties, the average subassembly compressive strengths at buckling typically ranged anywhere from about two-thirds to even greater than the tensile strengths for similar nailed subassemblies, while the average compressive strengths were typically only about one-fourth of the average tensile strengths for subassemblies with the thinner 28 ga. ties (and for the much thicker 16 ga. ties, subassembly compressive strengths were usually about twice their tensile strengths). Furthermore, subassembly compressive stiffness values were lowest when 28 ga. ties were used and highest when 16 ga. ties were used. This indicates that tie thickness is the main determinant for both subassembly compressive strength and stiffness, while the presence of an initial offset displacement and/or cyclic loading was also found to have a small detrimental effect on subassembly behavior in compression.

It should be understood that all of the compressive strength and stiffness values from such subassembly testing are lower bounds for actual brick veneer walls, owing to the invariable presence of some “mortar droppings” in the air cavity that effectively increase both the compressive strength and stiffness attributable to any one tie connection in the system. Approximate modeling strategies to deal with this effect, at least in terms of tie connection compressive stiffness, are summarized later in Chapter 5; relying on this effect a priori with respect to tie compressive strength and stiffness may not be advisable, however, which further points up the desirability of using at least 22 ga. ties.

3.4 Summary and Conclusions Related to the Tie Connection Tests

Residential anchored brick veneer construction, which is typically designed and built based on prescriptive code requirements, has sometimes exhibited distress resulting from moderate earthquakes and strong wind events. The damage has often been attributed to the performance of the corrugated sheet metal tie connections used to connect the brick veneer to the wood backup. Laboratory testing of brick-tie-wood connection subassemblies was conducted to explore the effects of tie thickness, tie attachment method to the wood stud, tie eccentricity at the connection to the wood stud, and tie embedment length on the strength and stiffness of veneer tie connections. Results from the tie connection tests and related brick veneer wall panel experiments have then been used in analytical models of brick veneer walls to assess the effects of different tie connection installation procedures on wall system performance, as described later in Chapter 5.

Overall, for nailed tie connections, their strength was typically governed by nail pullout from the wood stud, while their stiffness was mostly a function of the amount of tie eccentricity and the tie thickness. Nailed tie connections not meeting current minimum installation requirements exhibited reductions in strength (from using short roofing nails) and in stiffness (from using thinner gage ties and/or short roofing nails) of up to about 50% and 65%, respectively. On the other hand, tie connections with wood screws had much higher strength, but similar stiffness, when compared to nailed tie connections just meeting the minimum required installation criteria.

Table 3.1 – Brick-tie-wood connection subassembly types and average tension test results.

Specimen Type	Monotonic Tension Tests			Cyclic Tests (Tension Results)		
	(No.)	Ultimate Load (lbs)	Secant Stiffness (lbs/in.)	(No.)	Ultimate Load (lbs)	Secant Stiffness (lbs/in.)
N(8d)22min	9	118	3140	4	164	4510
N(8d)22ecc	20	164	640	10	159	500
N(8d)28min	5	168	2280	4	162	2180
N(8d)28ecc	5	155	280	4	146	230
N(2.5)22min	6	106	3240	5	91	1400
N(1.5)22min	6	80	1280	5	72	1190
S(–)22ecc	10	406	670	5	418	720
S(–)16min	5	397	1610	5	418	2350

(Note: 1 lb = 4.45 N; 1 in. = 25.4 mm)

Table 3.2 – Average pullout strengths for brick-tie embedment specimens.

Embedment Length (in.)	Average Ultimate Load (lbs)		
	28 ga.	22 ga.	16 ga.
1 1/2	174	263	384
2	174	410	470
2 1/2	243	500	-
3	285	594	-

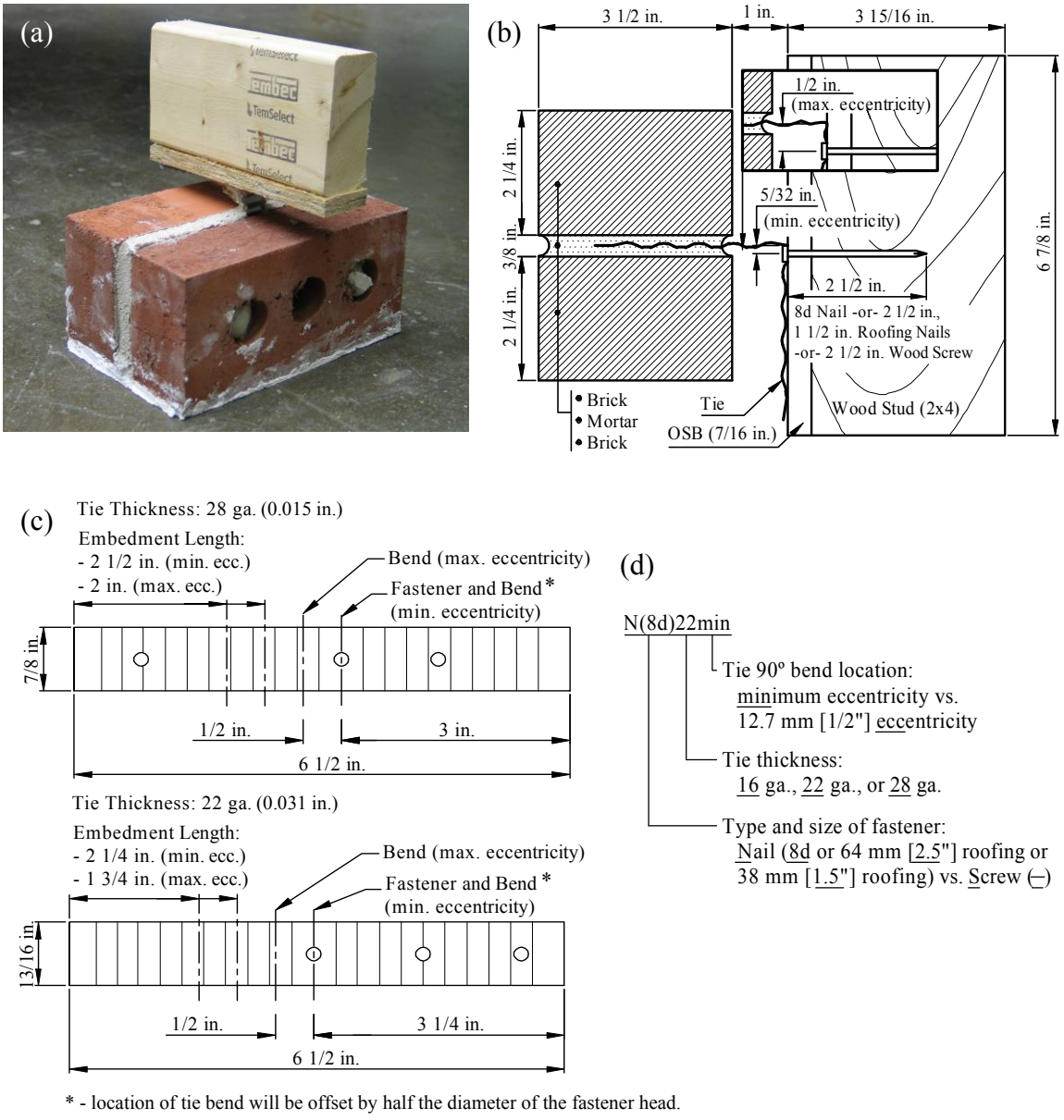

Figure 3.1 – (a) Brick-tie-wood subassembly and (b) section view of specimen; (c) dimensions of individual 28 and 22 ga. ties; (d) test specimen identification.

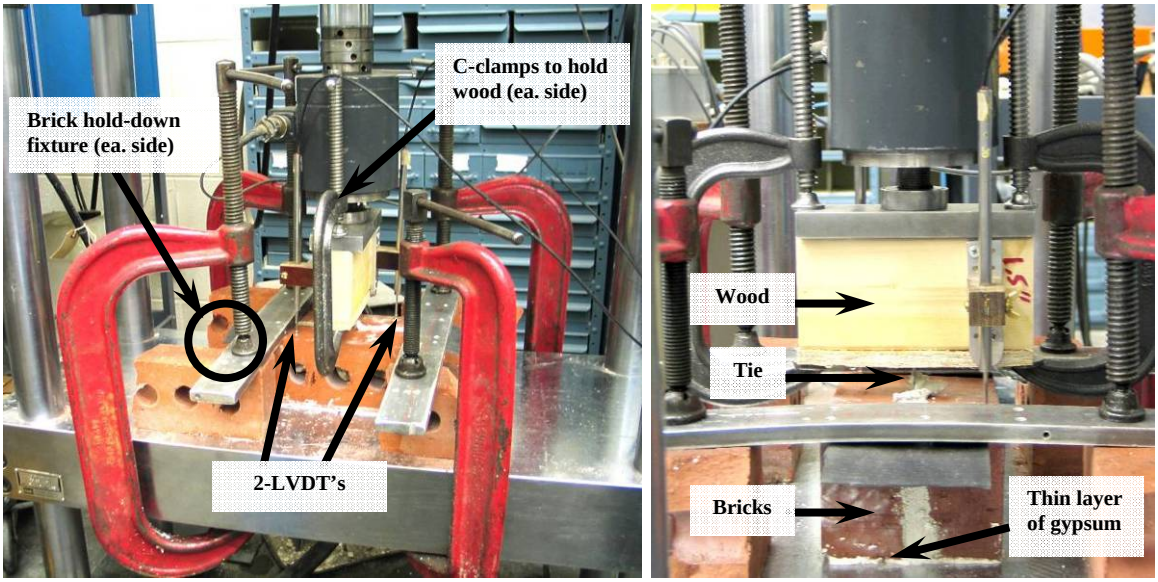

Figure 3.2 – Brick-tie-wood connection subassembly test setup.

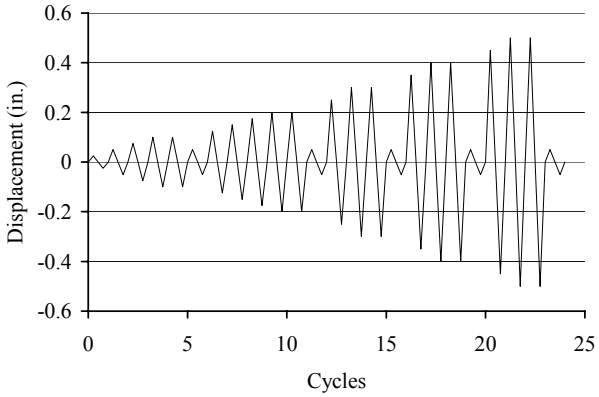

Figure 3.3 – Planned displacement history for cyclic subassembly tests.

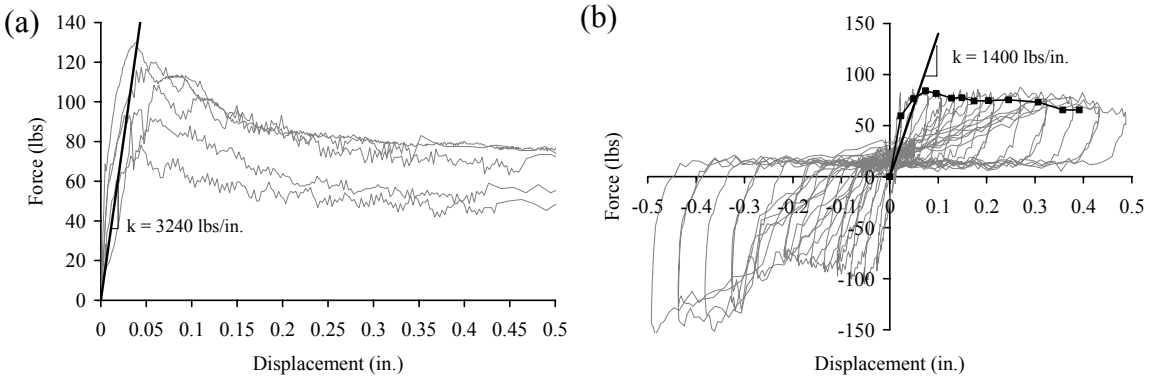

Figure 3.4 – Force-displacement curves for type N(2.5)22min subassemblies with average secant stiffnesses for (a) monotonic tension and (b) cyclic tension-compression loading, including the average envelope curve on the tension side.

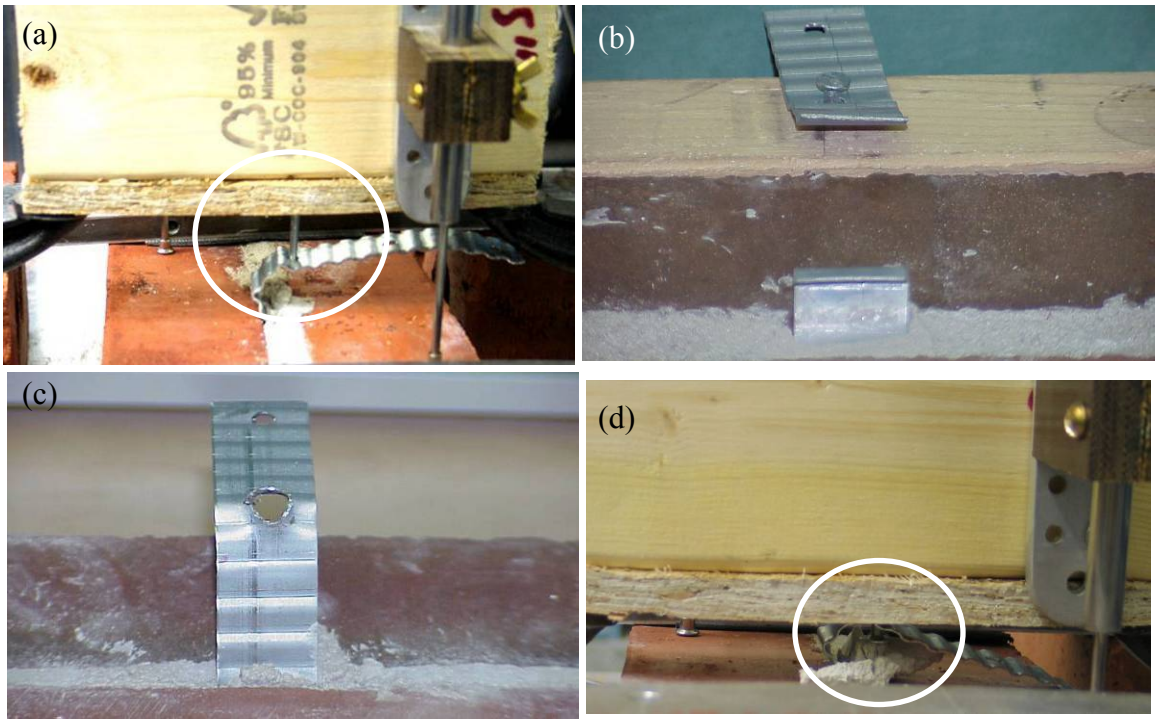

Figure 3.5 – Common tie connection failure modes: (a) nail pullout from wood stud, (b) tie fracture, (c) push through of nail or screw head, and (d) buckling of tie.

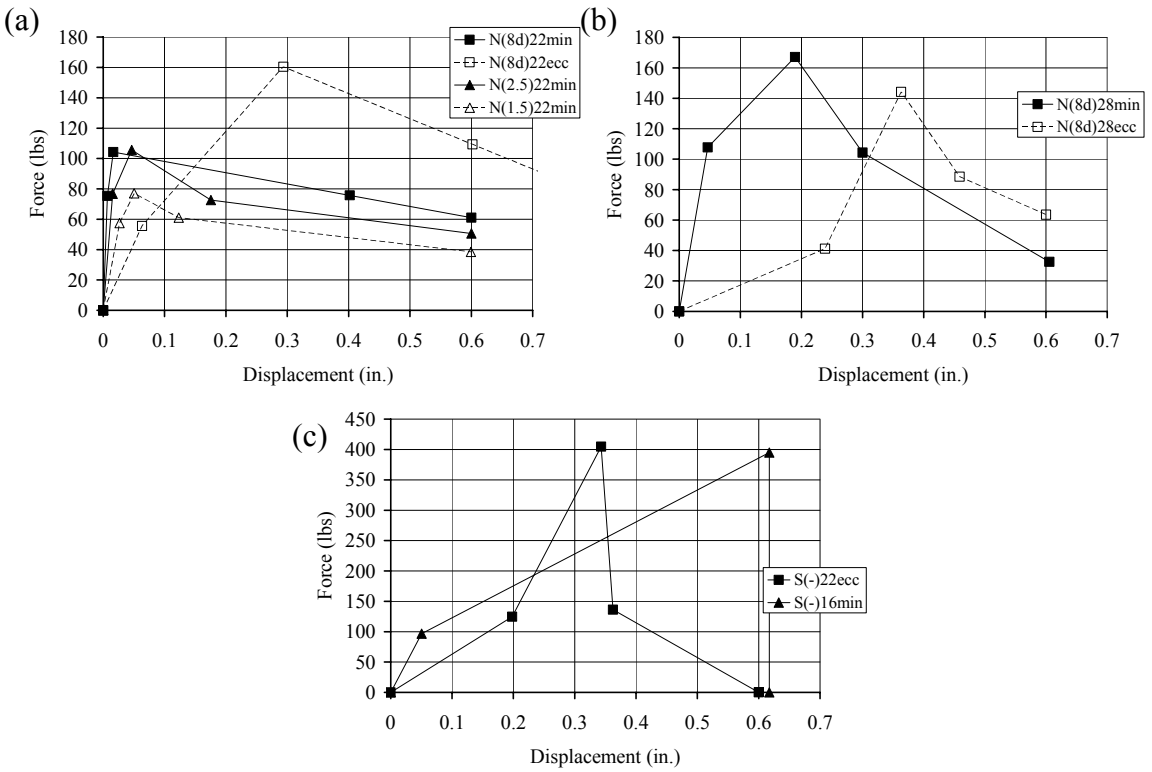

Figure 3.6 – Idealized monotonic tension force-displacement relationships for brick-tie-wood connection subassemblies: (a) 8d or roofing nail attached 22 ga., (b) 8d nail attached 28 ga., and (c) screw attached 22 ga. and 16 ga.

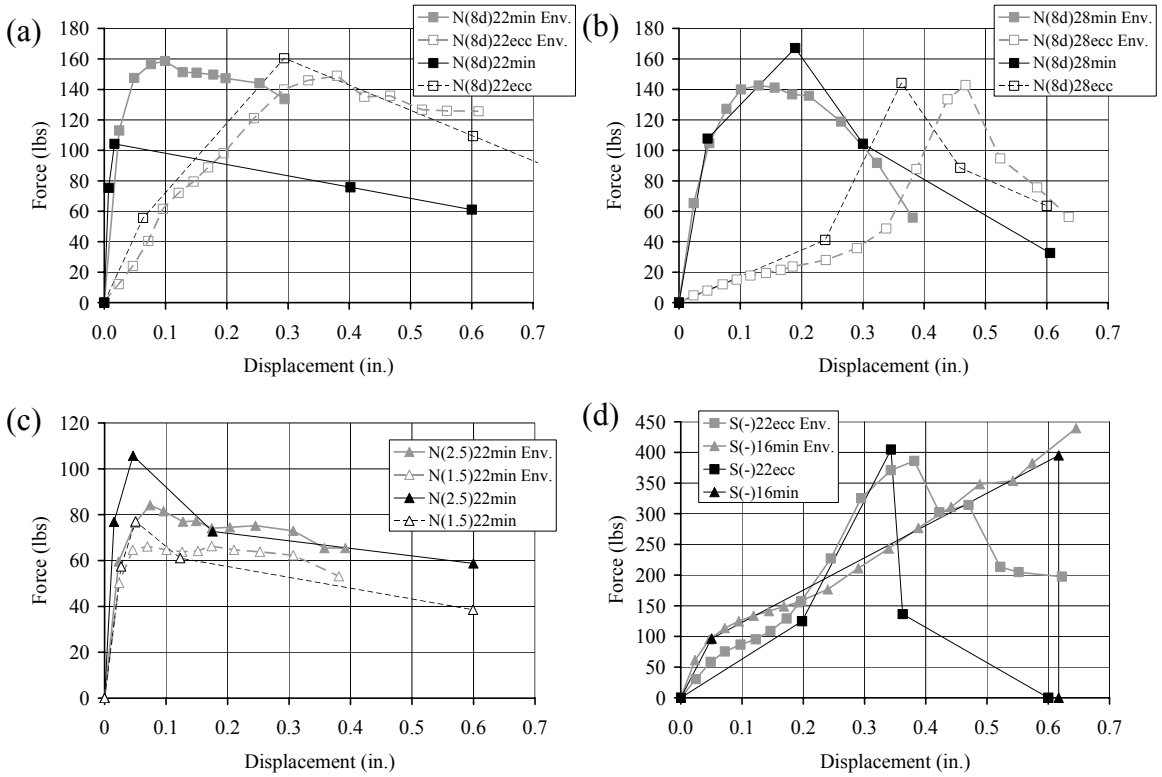

Figure 3.7 – Comparison of idealized monotonic tension force-displacement relationships with average envelopes of tensile cyclic behavior for brick-tie-wood connection subassemblies: (a) 8d nail attached 22 ga., (b) 8d nail attached 28 ga., (c) roofing nail attached 22 ga., and (d) screw attached 22 ga. and 16 ga.

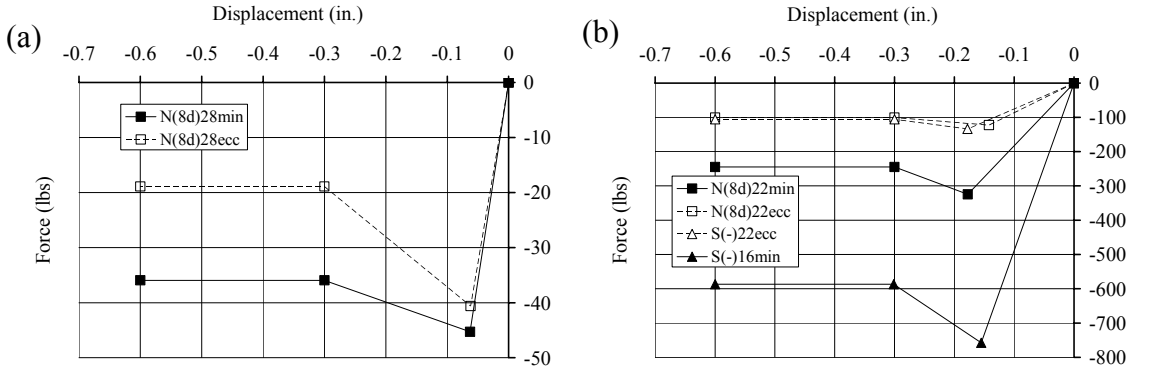

Figure 3.8 – Idealized monotonic compression force-displacement relationships for brick-tie-wood connection subassemblies: (a) 8d nail attached 28 ga., and (b) 8d nail or screw attached 22 ga. and 16 ga.

EXPERIMENTAL TESTING OF BRICK VENEER
PART I – SOLID WALL PANELS

The tie connection study led into the second phase of the project, described herein, which involved laboratory testing of full-scale brick veneer wall systems subjected to static and dynamic out-of-plane lateral loading on a shake table. This experimental study was conducted to assess the out-of-plane behavior of two single-story solid brick veneer wall specimens (Wall-1 and Wall-2) built following typical current construction practices, including effects of two different tie installation methods, as well as to test a possible retrofit strategy for enhancing the veneer-to-backup connection (Wall-2b). (Shake table tests on the first solid brick veneer wall panel specimen were performed and summarized in an interim report by Clarke (2002); those findings are also included in this chapter.) The experimental program for a third wall panel specimen (Wall-3), with a window opening and gable region, is described later in *Part II* of this chapter. Overall, the shake table tests captured the out-of-plane performance of brick veneer wall systems, including interaction and load-sharing between the brick veneer, corrugated sheet metal ties, and wood frame backup. The seismic performance of the wall panels was closely related to the individual tie connection deformation limits, especially for damage in tension. These test results have then been used to develop finite element models of brick veneer wall panels, as described in Chapter 5; parametric studies were conducted with those models to further explore the effects of different tie connection details and layouts on the seismic performance of brick veneer walls.

4.1 Description of Test Structure (Wall-1, Wall-2, and Wall-2b)

A full-scale brick veneer and wood frame test structure was designed to represent a portion of the wall system in a single-family home. The one-story wall panel and surrounding components were proportioned and constructed based on typical residential construction practices, in general conformance with Brick Industry Association (BIA) Technical Notes (2002, 2003), the Masonry Standards Joint Committee (MSJC) Code (2008), and the International Residential Code (IRC) for One- and Two-Family Dwellings (ICC 2003). Two veneer wall specimens (Wall-1 and -2) were constructed; they were anchored to a wood frame using corrugated sheet metal ties, with each wall utilizing different tie installation methods. In addition, mechanical expansion anchors were temporarily installed in the second wall specimen (Wall-2b) to test a possible repair and strengthening procedure.

4.1.1 Wall Structure Supports – Foundation and Reaction Frame

Elevation views of the complete wall test structure are shown in Figure 4.1. The brick veneer and wood frame wall structure was supported by a reinforced concrete foundation and a steel reaction frame. The 12 ft (3.66 m) long concrete foundation was designed to

represent the top portion of a typical foundation wall, directly supporting the wood framing and the brick veneer at 16 in. and 8 in. (406 mm and 203 mm), respectively, above the shake table surface. The concrete used for the foundation had a design compressive strength (f'_c) of 4.5 ksi (31 MPa); the actual f'_c was later determined to be 4.6 ksi (32 MPa) from cylinder tests.

Because of space limitations on the shake table, a steel reaction frame was designed to provide support for the wall structure in a manner similar to that found in a typical home. As seen in Figure 4.2, pinned-end steel cross beams supported the back ends of the floor and roof/ceiling framing stub joists (described below), attached by 3/4 in. (19 mm) diameter bolts. (More detailed drawings of the steel reaction frame are shown in Figures B.1 and B.2, which may be found in Appendix B.) Although the steel braces at the ends of the wall were quite stiff, the cross beams were flexible enough to permit some relative in-plane movements of the partial floor and roof/ceiling diaphragms. Therefore, the accelerations at the top backup corners and along the bottom of the wall panel were expected to be nearly equal (to each other and to the shake table input), with perhaps some modest amplification across the ceiling and roof framing at the top. (The mass and dynamic response of an entire house were not represented in this test setup.) In residential construction, exterior wood frame wall panels are usually attached to perpendicular structural walls or partitions at their edges, and to ceiling or roof framing across the top. The steel reaction frame was stronger than typical wood frame shear walls, so shake table testing was performed under the assumption that the motion intensities would not cause significant damage to the in-plane components of a typical home structure, but that they could be enough to affect the wall panels being tested in the out-of-plane direction.

4.1.2 Wood Frame Components – Wall Panel, Floor, and Roof/Ceiling

The 11.05 ft (3.37 m) length of the test structure wall panel was governed by the size of the shake table. Similar length (and longer) exterior walls without openings are often found in residential construction, particularly at garages. The wood framing in the test structure used Standard Grade Spruce-Pine-Fir; all components were connected with common type nails, in conformance with IRC requirements for nail size and spacing. An 8.1 ft (2.47 m) tall and 11.05 ft (3.37 m) long wood frame wall panel was constructed out of 2x4 (1.5 in. x 3.5 in. [38 mm x 89 mm]) lumber. The framing consisted of 92-5/8 in. (2.35 m) precut 2x4 studs spaced at 16 in. (406 mm) center-to-center on a single 2x4 sole-plate, with a double 2x4 top-plate. The exterior face of the framing was covered with 7/16 in. (11 mm) thick oriented strand board (OSB) APA Rated 24/16 wall sheathing panels. The interior face of the stud wall was covered with 1/2 in. (12 mm) thick gypsum wallboard panels, attached according to IRC specifications.

The wood wall panel rested on a partial floor frame extending back 3.41 ft (1.04 m) from the interior face of the wall to the steel reaction frame (Figure 4.1). The floor framing comprised 2x10 (1.5 in. x 9.25 in. [38 mm x 235 mm]) joists spaced at 16 in. (406 mm), attached to a 2x10 header board. The floor joists were covered with 3/4 in. (19 mm) thick OSB APA Rated Sturd-I-Floor 23/32 panels. The outer edge of the floor framing rested on a 2x6 (1.5 in. x 5.5 in. [38 mm x 235 mm]) sill-plate, attached to the concrete

foundation with one 1/2 in. (12 mm) diameter anchor bolt every 4 ft (1.22 m). A thin layer of Styrofoam sill sealer was installed between the foundation surface and the sill-plate.

The top of the wood wall panel supported the outer edge of the partial roof/ceiling diaphragm, which in turn laterally braced the top of the wall across its length. The diaphragm framing was constructed of 2x6 joists spaced at 16 in. (406 mm), extending back to the steel reaction frame in a similar fashion as the floor framing did (Figure 4.1). The roof/ceiling joists were covered with 3/4 in. (19 mm) thick OSB Sturd-I-Floor panels, and they were attached to the wall frame top-plate (exterior face) with one-sided rafter ties, using 8d nails. At each of the outermost joists, two one-sided (on the exterior face) and one double-sided (on the interior face) rafter ties were installed to provide additional strength and stiffness at the corner connections of the wood wall panel. The IRC specifies that roof/ceiling joist connections to an exterior wall top-plate should include toe nailing plus rafter ties spaced no more than 4 ft (1.2 m) on-center along the length of the wall (with more rafter ties added as needed for higher design wind uplift resistance). The test structure employed rafter ties at each connection to ensure sufficient durability for carrying repeated loads from the dynamic tests of a couple of veneer walls, while also maintaining a connection stiffness comparable to toe nailing.

A simple pre-compression system was installed to include the effect of roof/ceiling dead load on wall behavior; however, the mass of this dead load was not represented. The system consisted of four 1/2 in. (12 mm) diameter threaded rods. These rods were threaded into the shake table and ran up through small holes in the subflooring, roof/ceiling sheathing, and a 2x4 laid flat across the top of the sheathing (Figure 4.1). Each rod was equipped with a 1 kip (4.5 kN) capacity tension load cell; a nut at the top of the rod was adjusted to provide 600 lbs (2.7 kN) of tension. The tension in the rods was transferred to the stud wall as a compressive force of approximately 180 lbs (0.8 kN) per stud (accounting for the portion of the load shared by the steel reaction frame). This pre-compression load was chosen based on an evaluation of typical design dead loads for residential construction, in conjunction with detailed material quantity take-offs for residential home roof structures. (The mass and dynamic response of an entire house were not represented in this test setup.)

4.1.3 Brick Masonry Veneer

The 9.42 ft (2.87 m) tall and 11.05 ft (3.37 m) long brick veneer walls of the test structure were constructed by professional masons. The test specimen veneer walls had free edges (open ends), similar to those found in residential construction with “front face” veneer walls only (where the masonry is terminated at a corner and some other siding material is used on perpendicular exterior walls). Veneer wall separation at edges is also common in practice at corners with control joints and near large window and door openings, which permit individual sections of veneer to move independently of one another (Lapish 1988). The bricks used were 3-1/2 in. x 7-5/8 in. x 2-1/4 in. (89 mm x 194 mm x 57 mm) standard modular “Colonial Reds” with three holes, joined by type N mortar (cement : lime : sand = 1 : 1 : 6) in running bond. (The brick masonry materials in the wall panels matched the materials used in tie subassembly testing.) Mortar for the first course of

bricks was placed on flashing material, which had little or no bond to the top of the foundation surface. (Flashing, though not always used in residential construction, is mandated by building codes to collect condensation at foundation wall surfaces and around openings.) The test specimen employed 0.017 in. (0.43 mm) thick vinyl flashing, in addition to cotton weep ropes spaced at 24 in. (610 mm). The flashing was suspended from the topmost vertical surface of the foundation, attached with polyurethane sealant; then, it extended down to and across the lower horizontal surface of the foundation (under the brick veneer), held in place by the veneer weight, estimated to be 360 lb/ft (5.3 kN/m).

An air space of 1 in. (25 mm) was maintained between the outside face of the wood frame sheathing and the inside face of the brick veneer. While laying the brick, the masons formed concave type mortar joints by scraping off excess mortar on the exterior face of the veneer. On the interior face, however, any excess mortar seeped out into the air space; at a few locations, mortar even landed on the corrugated sheet metal ties and locally filled in the space between the veneer and the sheathing. (Small amounts of excess mortar cannot be avoided, but recommended practice is to limit such "mortar droppings" into the air space as much as possible, as they may provide a conduit for moisture movement across the cavity, while at the same time impairing the proper movement of moisture (drainage) out of the cavity.)

A series of tests were conducted to determine the material properties of the brick masonry veneer, following standardized ASTM testing procedures. During construction of the brick veneer walls, identical materials were used to prepare brick prism and mortar cube specimens, which were allowed to cure for 28 days. For the solid wall panels, brick prism tests determined the masonry compressive strength (f'_m) to be 3.4 ksi (23.5 MPa), the modulus of elasticity (E_m) to be 2,020 ksi (13.9 GPa), and the modulus of rupture (f_r) to be 86.5 psi (596 kPa). Tests on mortar cubes established the mortar compressive strength (f_u) to be 0.93 ksi (6.4 MPa). (More detailed results from the masonry material tests have been summarized in Table B.1, which may be found in Appendix B.) These material properties are consistent with the MSJC (2008) specifications for brick masonry using type N mortar.

4.1.4 Veneer Ties and Anchors

As part of masonry installation, brick veneer was attached to the wood frame wall panel test structure using corrugated sheet metal ties. With the exception of the brick veneer resting atop the foundation, these ties provided the only positive connection between the brick and the backup system. The use of at least 22 ga. (0.031 in. [0.79 mm] thick) ties is required by the MSJC (2008) and ICC (2003); however, for the wall test specimens, typical residential construction practice was followed by using thinner 28 ga. (0.013 in. [0.33 mm] thick) ties, as shown in Figure 4.3(a). Tie spacing was also based on typical construction practice, namely 16 in. (406 mm) horizontally and 24 in. (610 mm) vertically, which is in general conformance with various specifications, as described earlier in Chapter 2.

Before laying the masonry, the ties were attached to the wood frame studs (through the OSB sheathing) with galvanized 8d nails (one per tie), ensuring proper alignment with the mortar joints. Later, each tie was bent and then embedded into the mortar joint by more than the specified minimum of 1.5 in. (38.1 mm) (Figure 4.3(a)), while at the same time leaving at least 5/8 in. (15.9 mm) mortar cover to the outside face of the veneer, meeting MSJC requirements. A total of 45 ties were installed in the wall specimens, arranged in nine columns (numbered 1 through 9, starting at the south edge) and five rows, as shown in Figure 4.4. The bottom row of ties was located 14 in. (356 mm), or 5 courses, above the base, and the uppermost row of ties was 1 course from the top of the veneer wall.

For the first series of tests (Wall-1), all of the ties were installed following a typical "best-case" construction practice, where the 90-degree bend was located at the nail, as shown in Figure 4.3(b), with just a small eccentricity of the bend due to the head of the nail (N(8d)28min type of tie connections, as indicated in Chapter 3). This wall specimen was subjected to static and dynamic tests up until partial collapse of the veneer (including destruction of the top two rows of ties), as will be described in more detail later. The wood frame backup and the remaining veneer did not sustain visible damage during the first set of tests, so they were kept in place for a second series of tests (Wall-2). For Wall-2, the collapsed portion of the veneer from Wall-1 was rebuilt with new brick masonry, attached using the same type of ties. However, the 90-degree bend in these ties was located 1/2 in. (12.7 mm) above the nail (N(8d)28ecc type of tie connections), also shown in Figure 4.3(b); this eccentricity of the bend is the maximum permitted by the MSJC (2008). (Analysis of test results from Wall-1 showed that ties in the upper rows dominated the wall's behavior, so the rebuilt specimen was intended to fully explore the influence of a different tie installation method, even though the bottom portion of the veneer wall system from the first series of tests was reused.)

The average structural behavior of a single 28 ga. tie under monotonic tensile and compressive loading is shown in Figure 4.5 for both installation techniques, based on previous tests of brick-tie-wood subassemblies. (Test results of 22 ga. ties for both installation methods exhibited somewhat higher initial stiffness and compressive strength; however, the ultimate tensile strength was similar to that of the 28 ga. ties.) As described earlier in Chapter 3, cyclic tension-compression tie subassembly test results showed that the average envelope curves for cyclic behavior were similar to the companion monotonic test results. Subassemblies under monotonic tensile loading past the ultimate capacity exhibited various failure modes, including: yielding at the tie hole followed by partial tearing of the tie adjacent to the hole, nail pullout from the wood stud, and tie pullout from the mortar joint. During cyclic loading, the most common failure mode (also in tension) was tie fracture; yielding at the tie hole leading to push-through of the nail was also observed. The typical failure mode of subassemblies in compression was by buckling of the tie, with the ultimate compression capacity much less than that in tension. However, subassembly compressive strength and stiffness results should be considered as lower bounds for actual veneer walls because of mortar in the air space, as described above, which can help transmit compressive forces and reduce the compression demand on the ties. Specifications for horizontal and vertical spacing at installation of

the ties limit the strength demands placed on them; the BIA also recommends a minimum initial stiffness of 2,000 lbs/in. (0.35 kN/mm) (in both tension and compression) (BIA 2003), which was only satisfied in subassembly tension tests for ties with the bend at the nail.

After several Wall-2 tests, it was apparent that the veneer-to-backup connection was much more flexible than in Wall-1. To increase the connection stiffness and explore a possible retrofit strategy, mechanical expansion anchors, shown in Figure 4.3(c), were installed for another series of tests (Wall-2b). As part of the anchor installation process, pilot holes (1/2 in. [13 mm] diameter) were drilled in the masonry veneer mortar joints, lining up with the wood studs. At one end, the anchor was self-tapping and self-threading into the wood stud; at the other end, as torque was applied to activate (expand) the anchor, a radial preload was established in the masonry. As specified by the manufacturer, the installed anchor capacity, which depends on the veneer and back-up materials, should have an average ultimate tension value of 900 lbs (4.0 kN), limited by pullout from the wood stud (Dur-O-Wal 1998). For the Wall-2b tests, four of these anchors (designated as A through D) were installed between the top two rows of ties, at the locations shown in Figure 4.1. The overall strength of the top two rows of ties (18 total) in tension, estimated from the single tie subassembly tests, was approximately 3.0 kips (13 kN) and 2.8 kips (12 kN) for the first and second tie installation methods, respectively. In effect, then, the four mechanical anchors were intended to be able to completely replace the top two rows of ties, with a capacity of 3.6 kips (16 kN). The anchors were removed after their effects on wall performance were understood, and the wall specimen (Wall-2) was then subjected to additional dynamic testing until collapse.

4.2 Shake Table Testing Program (Wall-1, Wall-2, and Wall-2b)

4.2.1 Shake Table Test Setup

The test structure was constructed on a shake table in the Newmark Structural Engineering Laboratory. The shake table had a 12 ft x 12 ft (3.66 m x 3.66 m) surface and a uniaxial, servo-controlled, hydraulic actuator having a total available piston stroke of ±2 in. (±50 mm) (Figure 4.2). The test structure foundation and reaction frame were attached to the shake table with 1/2 in. (12 mm) diameter bolts every 6 in. (305 mm). The foundation also rested on a thin bed of high strength gypsum, ensuring that it was well-coupled to the shake table surface. The wall panel was positioned on the shake table to be excited in the out-of-plane direction.

4.2.2 Specimen Instrumentation

Displacements and accelerations were measured at various locations on the wall specimens, as shown in Figure 4.4. Cable extension displacement transducers ("yo-yo" gages) were located on stationary reference frames (off the shake table) and linked to the wall panels by extension cables, on both the brick veneer and the wood frame sides (Figure 4.2). Veneer and backup displacements were measured along the vertical centerline and at the top south corner of the walls, at tie locations (except for Wall-1, where displacements were not measured at the top corner of the wood frame). Shake

table "input" displacements were recorded by a transducer located in the actuator piston. Accelerometers were placed at five locations on the wall specimens and one on the shake table. Out-of-plane accelerations were measured with three accelerometers along the centerline of the veneer and one at the top center of the wood frame, while in-plane accelerations were monitored at the top south corner of the veneer wall. During testing, data were recorded every 0.005 seconds using a PC with *LabView* software. All tests were recorded with a video camera; still photographs were also taken between dynamic tests to document observed damage.

4.2.3 Static Loading

Preliminary static displacement and free vibration tests were performed to evaluate the variation in lateral stiffness of the wall structure from before to after construction of the brick veneer, as well as any variation resulting from different veneer-to-backup connections. The static displacement tests were performed by applying horizontal point (pull) loads directly to the bare wood frame wall panel (before veneer construction) and then later to the brick veneer itself (before any damage had occurred due to subsequent dynamic testing). Free vibration tests were performed by suddenly releasing a point load applied to the brick veneer. For these purposes, a steel frame was constructed on the laboratory testing floor, facing the wall structure (Figure 4.2), with an attached pulley aligned with the centerline of the wall (and adjusted for desired vertical location). Weights ranging from 250 to 400 lbs (1.1 to 1.8 kN) were suspended on a steel cable, running through the pulley and linked to points on the wall, for static testing, and then released as needed for free vibration testing.

4.2.4 Input Motions

Three scaled earthquake records were used during shake table testing (as well as sine-sweep inputs to characterize the dynamic properties). The earthquake records included two synthetic motions and one recorded ground motion, chosen to be representative of intra-plate earthquakes found in the central and eastern U.S. The synthetic motions were from a Mid-America Earthquake Center project that, among other things, developed records to represent seismic hazard levels in Memphis, Tennessee, with probabilities of exceedance of 10% and 2% in 50 years (Wen and Wu 2001). The two synthetic records used (labeled as m10_01s (M10) and m02_03s (M02)) were selected from sets of ten available at each hazard level; the specific records were chosen in part because they had the smoothest spectral accelerations in the low period range. The recorded ground motion used was from the Nahanni earthquake of December 23, 1985 (Site-1, component 010) (USGS 2005). The sine-sweep input, used to evaluate the dynamic properties, had a frequency range of 1 to 10 Hz and was scaled to very low peak ground accelerations (PGA) of approximately 0.02 to 0.04g.

Acceleration histories and response spectra for the three earthquake records are presented in Figure 4.6. (The program *Utility Software for Earthquake Engineering* (USEE), also developed through the MAE Center, was used to generate the response spectra (Inel et al. 2001). This program also contains a library of the synthetic ground motions described above.) The M10 record was based on an earthquake with a moment magnitude of 6.7, an epicentral distance of 85.7 mi (138 km), and a focal depth of 12.1 mi (19.5 km). The

M02 record was based on an earthquake with a moment magnitude of 8.0, an epicentral distance of 101 mi (163 km), and a focal depth of 16.5 mi (26.5 km). The historic Nahanni record had a magnitude of 6.9, an epicentral distance of 5 mi (8 km), and a focal depth of 3.7 mi (6 km). For the shake table tests, all three records were normalized (scaled) with respect to PGA. Throughout dynamic testing, the input PGA intensities were progressively increased (starting from very low values) by increments of approximately 0.04 to 0.06g. The PC for recording data was also used to scale and send the earthquake record signals to the shake table actuator controller.

4.3 Experimental Results (Wall-1, Wall-2, and Wall-2b)

Static and dynamic shake table tests were conducted on the wall specimens following the procedures described above. The most important experimental results are summarized in Table 4.1 and explained in greater detail below.

4.3.1 Preliminary Tests – Static Displacements and Dynamic Properties

Static load tests revealed some of the differences in the out-of-plane lateral stiffness of the wall structures. Point (pull) loads of 300 lbs (1.3 kN) and 400 lbs (1.8 kN) were applied to the bare wood wall panel directly at the top-plate and at 16 in. (0.4 m) below it, respectively (locations "a" and "b" indicated on Figure 4.4). Overall, the measured out-of-plane displacements along the centerline and at the top-south corner, shown in Figure 4.7(a), portray the variation in stiffness throughout the wood wall panel. The top corner of the wall panel did not move when the wall was subjected to small point loads at the center because of the flexibility of the wood frame wall (and the higher stiffness rafter ties at the top corners). Displacements at the top middle of the wall panel indicate that the rafter ties were, in general, flexible enough to allow significant deformations across the wall panel-to-roof/ceiling joist connections.

Point loads were also applied to the veneer of Wall-1 (300 lbs [1.3 kN]), and of Walls-2 and -2b (250 lbs [1.1 kN]), at 40 in. (1.2 m) and 16 in. (0.4 m) below the top of the veneer, respectively. The elastic displacements, shown in Figure 4.7(b-d), portray the effects of the different veneer-to-backup connections on overall wall deformations. (An example set of static displacement results are shown in Figure B.4(a-b), which can be found in Appendix B.) As seen in Figure 4.7(e), the highest relative displacements (tie elongations) between the veneer and the backup along the wall centerline were measured in Wall-2; however, after installing the mechanical anchors (Wall-2b), the tie elongations resembled those measured in Wall-1. Also, the total displacements were significantly lower for the (undamaged) walls with veneer compared to the bare wood frame wall panel, which shows that the presence of the brick veneer enhanced the out-of-plane stiffness of the system. The brick veneer displaced almost as a rigid body, which in effect spread the applied point load to the tie and/or anchor connections that then more uniformly distributed the load to the wood frame backup, resulting in smaller overall displacements. (These qualitative observations about the measured static displacements are true regardless of the small variations in the magnitude and location of the point loads applied to the walls.)

The free vibration period was evaluated before testing, and then again after certain dynamic tests of the wall specimens; it was an indicator of the variation in specimen stiffness for different veneer-to-backup connections, and as damage occurred in the specimens. Upon suddenly releasing a static load applied to the veneer, the resulting free vibration displacements of the wall were recorded. (An example of this is shown in Figure B.5, in Appendix B.) The period of vibration was the average time required to complete a full cycle. Furthermore, by performing forced vibration tests (using the sine-sweep record described above), the natural period of vibration could also be determined from the excitation frequency that caused a resonant response in the wall specimens (as shown in Figure B.6). Throughout wall testing, each method produced similar period results, which are listed in Table 4.1.

Specific tests to evaluate the viscous damping ratio were not performed for the solid wall specimens; however, it was possible to estimate the damping ratio from the results of the free vibration, sine-sweep, and some dynamic tests. After select tests, the data clearly exhibited the decay of displacement and acceleration vibration amplitude over time (see Figure B.5). For wall specimens early in the dynamic testing sequence (before any visible damage), the damping ratios were computed as approximately 3% and 5% for Walls-1 and -2, respectively, by applying the logarithmic decrement method (Chopra 2001).

4.3.2 Dynamic Tests

Dynamic shake table tests were conducted to evaluate the overall performance of brick veneer walls under distributed (inertial) loads. For each wall specimen, sets of the most important dynamic test results are listed in Table 4.1. For Walls-1 and -2, the results correspond to three levels of specimen response and damage, which can be described as: *elastic* (no visible damage), *intermediate* (onset of tie and veneer damage), and *ultimate* (accumulation of tie and veneer damage sufficient to lead to collapse).

In dynamic testing, it is important that the shake table acceleration output captures the scaled input earthquake ground motions. Throughout wall panel testing, recorded shake table acceleration output was generally well in-phase with the input earthquake ground motion drive signal; however, the amplitude of the shake table accelerations was somewhat higher than the targeted scaled input, for example as shown in Figure 4.8(a). In particular, recorded spikes in the shake table acceleration output indicated spurious maximum PGAs, which did not necessarily represent overall upward scaling values across the entire period range of the original earthquake ground motion, as seen in Figure 4.8(b). Therefore, for analysis of experimental results and for later FE model calibration, nominal scaled PGA values were computed, capturing the overall intensity and damage potential of the recorded shake table acceleration output per the original earthquake record input, by matching key engineering characteristics of the motions, including Arias intensity, Fourier spectra, and response spectra. (Such engineering characteristics and scaling methods of earthquake ground motions are discussed in more detail by Bozorgnia and Campbell (2004).) For example, Figure 4.8(c) shows the response spectra of the recorded M10 earthquake record with a PGA of 0.23g, with an overlapped original M10 earthquake record scaled to match the intensity of the experimental test at a nominal PGA

of 0.18g. During solid wall panel testing, the computed nominal scaled PGA values were typically within 20% of the target PGA values for the M10 earthquake record, whereas the nominal and target PGA values were nearly equal for the M02 and Nahanni earthquake records. Both measured and nominal scaled PGA values for each earthquake record are presented in Table 4.1 and in the dynamic testing summary below.

In general, the maximum response of the test specimens, corresponding to the peak measured accelerations and displacements, occurred right after the PGA of the earthquake input records. The peak acceleration values were collected from the acceleration traces measured on the wall specimens. The maximum positive displacements (veneer deflecting away from the backup) of the brick veneer and of the wood backup, as well as the peak positive tie deformations (elongations) were also of particular interest. The brick and wood displacements were evaluated as the difference between the wall and shake table displacements (i.e., they were the displacements relative to the shake table). Tie deformations were evaluated as the relative displacements between the brick veneer and the wood frame backup (except for at the top south corner of Wall-1, where wood backup displacements were not measured, so tie elongations were (over)estimated as the total brick displacement relative to the shake table). (An example set of shake table and wall panel accelerations, as well as total and relative displacements, are shown in Figures B.7 through B.9 (see Appendix B) for Wall-2 during M10-0.23[0.18]g testing.) For a particular dynamic test, maximum brick and wood displacements at all of the measurement locations took place at the same time; however, the various peak tie elongations did not always occur at exactly the same time and did not necessarily correspond to the same instant as the maximum brick and wood displacements.

Listed in Table 4.1 are: names of the input earthquake records with the measured and nominal scaled PGAs; peak measured accelerations and displacements at the top-center of the brick veneer; period of vibration (evaluated after certain dynamic tests); tie elongations at the upper three rows along the wall centerline, and also at the top south corner; and descriptions of any tie and veneer wall damage (as appropriate). Dynamic test results, including the progression of wall system damage up through failure, are described for each wall in detail here below.

Wall-1 The initial period of vibration for Wall-1 was evaluated to be 0.10 sec.; by the end of the *elastic* tests, following the M10-0.37[0.29]g run, the period of vibration had increased somewhat. By this point, cracks were also noticed at the mortar-to-concrete foundation interface. During the M10-0.58[0.43]g record, the top south corner tie (at grid A/1, per Figure 4.4) suffered a straight-line fracture, causing the period to further increase. The *ultimate* dynamic test before collapse (M10-0.66[0.47]g) caused the most tie damage in the upper wall region, with the common types of tie distress shown in Figure 4.9(a-b).

After the M10-0.66[0.47]g run, another test using the M10 record with a nominal scaled PGA of 0.54g was begun. However, the upper portion of the Wall-1 brick veneer collapsed early in this run (immediately following a recorded input acceleration of

0.64g), with the collapse shown in Figure 4.10(a). The collapsed veneer pivoted about a crack at the horizontal mortar joint above the 27th course of bricks, midway between the second and third rows of ties (from the top). All previously unbroken ties in the upper two rows, as well as the entire upper portion of the wall, were now completely damaged. Most of the tie failure modes noted in the veneer wall collapse matched those observed in the individual tie subassembly study. The dominant tie failure mode in the top row was a straight-line (brittle) fracture, similar to that shown in Figure 4.11(a). The majority of ties in the second row experienced fracture and tearing at the nail hole (which typically also involved nail push-through at the tie hole, after some ductile nail pullout from the wood framing), as shown in Figure 4.11(b). Other less common tie failure modes included complete nail pullout from the wood backup, tie pullout from the mortar joint, and yielding at the tie hole resulting in push-through of the nail (Figure 4.11(c)).

Wall-2 The initial period of vibration for Wall-2 was evaluated to be 0.17 sec., higher than for Wall-1 because of the more flexible ties in the top two rows. After the *elastic* tests (following the M10-0.23[0.18]g run) the period of vibration had increased to 0.23 sec. Immediately thereafter, the mechanical expansion anchors were installed for Wall-2b testing (as described below). After the anchors were removed, testing resumed by approximately repeating the pre-anchor runs of M02-0.19[0.18]g and M10-0.23[0.18]g for Wall-2, which exhibited a similar response as before the retrofit and Wall-2b testing. (These results indicate that the overall wall structure did not sustain any significant damage during the Wall-2b tests.) However, during the M10-0.22[0.18]g record, the top corner tie (at grid A/1) did fracture (Figure 4.9(a)). *Intermediate* and *ultimate* tests (M02-0.24[0.24]g through M10-0.41[0.39]g) resulted in further tie and veneer damage, causing nail pullout at one tie (Figure 4.9(b)), several partial tie fractures (Figure 4.9(c)), and horizontal cracking of the veneer through the mortar joint at mid-height, below the third row of ties (Figure 4.9(d)).

During the M10-0.49[0.36]g record, the upper half of the Wall-2 brick veneer collapsed about the horizontal crack (immediately after the PGA), as shown in Figure 4.10(b). Any remaining unbroken ties in the top three rows were broken as the veneer collapsed. Similar to in Wall-1, the dominant tie failure modes were straight-line fracture in the upper row of failed ties (Figure 4.11(a)) and fracture and tearing at the nail hole in the lower (third) row of failed ties (Figure 4.11(b)). In the middle row of failed ties (the second row from the top), the dominant tie failure mode was yielding at the tie hole, resulting in push-through of the nail (Figure 4.11(c)). A few of the other tie failure modes described above for Wall-1 were also seen in Wall-2.

Wall-2b The initial period of vibration for Wall-2b (Wall-2 with the mechanical expansion anchors installed) was evaluated to be 0.14 sec., indicating an increase in the veneer-to-backup connection stiffness over Wall-2. During the M10-0.59[0.42]g test, anchor-A began to slip, resulting in a slight increase in the period of vibration of the wall panel. (The part of the anchor that expands and grips the masonry overcame the preload friction, which is expected to occur after about half the ultimate tension capacity is reached (Dur-O-Wal 1998).) Even though the relative displacements increased, and therefore more demand was placed on the ties, this anchor was still effective. Shaking

was increased up to M10-0.80[0.54]g, exceeding the collapse loading of Wall-1, after which there was no damage noted in the Wall-2b veneer or ties, except for slight nail pullout from the wood wall panel at one of the top corner rafter ties. A modest increase in the period of vibration was noted, however, mainly due to anchor-A continuing to slip.

4.4 Analysis of Experimental Results (Wall-1, Wall-2, and Wall-2b)

Veneer wall performance and damage observed throughout dynamic testing correlated well with the measured displacement data. The *elastic* tests characterized the dynamic response of brick veneer wall systems, and showed the effects of different tie installation methods (and post-installed anchors), without structural damage. Walls-1 and -2 showed similar overall displacements at the onset of tie damage (*intermediate* tests) and during collapse of the upper regions of the veneer (*ultimate* tests), while being subjected to quite different dynamic loads. When subjected to the highest dynamic input, Wall-2b reacted without any damage, exceeding the strength of the walls with corrugated sheet metal tie connections only.

4.4.1 *Elastic* – Initial Response of the Veneer Walls

As the walls were subjected to dynamic inputs, the mass of the brick veneer produced inertial forces that were transferred through the ties into the wood frame backup. The different tie installation methods (and the post-installed anchors) affected the peak dynamic response of the wall specimens, as shown in Figure 4.12 for one particular example of input loading. The brick veneer essentially displayed rigid body rotation about its base, as recognized from the almost linear veneer displacements measured along the centerline (in conjunction with the cracked mortar beneath the first course of bricks). The displaced shape of the wood frame backup depended on both the backup stiffness and the stiffness of the ties and/or anchors through which the veneer forces were transferred to the backup. During dynamic loading, maximum accelerations were measured at the top of the brick veneer, subjecting the ties in the top row to the highest inertial forces, which led to the highest peak tie elongations in the wall (Figure 4.12(b)). In the top row, the corner ties experienced higher elongations than at the center, mainly due to variation in backup stiffness. Measurements along the wall centerline showed that the lower three rows of ties experienced relatively small peak elongations, typically comparable to or less than the third row peak elongations listed in Table 4.1. The total and relative displacements shown in Figure 4.12 indicate that the stiffer ties in Wall-1 caused the movement of the brick veneer to be closely coupled to that of the backup system, whereas the more flexible ties in Wall-2 resulted in greater relative movement between the veneer and the backup. The post-installed anchors in Wall-2b successfully coupled the upper portion of the veneer to the backup, resulting in relative displacements comparable to those seen in Wall-1.

The M10 earthquake measured test PGAs, along with their corresponding maximum displacement responses of the brick veneer, wood backup, and tie connections, are shown in Figure 4.13 for both inward and outward movement of all solid wall panels. (The M10 input record is presented here because it generally caused greater overall dynamic response of the wall panel specimen compared to the M02 and Nahanni inputs.) In the

elastic range of wall behavior, the displacement and tie elongation responses at all of the measured locations generally exhibited a linear relationship with respect to PGA. (Throughout the *elastic* and into the *intermediate* ranges of wall behavior, the modest measured tie deformations could be somewhat inaccurate due to the relative amount of instrumentation noise in the displacement data compared to the actual tie deformations; however, this was only true for fairly small deformations, of approximately 0.04 in. (1 mm) or less, and the noise was insignificant for higher input tests.)

Towards the end of the *elastic* tests for Walls-1 and -2, the period of vibration increased due to some stiffness loss in the brick veneer-to-wood backup connections. Excess mortar in the air gap initially constrained some of the ties, protecting them from buckling, as well as increasing the initial tension stiffness. The excess mortar also ensured that the 1 in. (25 mm) air gap could not close up very much in compression. (No buckled ties were observed after any of the dynamic tests; however, some results during testing did show relative displacements for the top row of ties in the negative direction in excess of the "tie buckling" displacements given in Figure 4.5 from the previous subassembly tests.) The initial tension stiffness of this type of tie is typically governed by straightening of the corrugations (for ties with the bend at the nail) and by opening of the 90-degree bend (for ties with the bend at an eccentricity). These types of tensile deformations were initially limited by the presence of excess mortar from wall construction. As some of the excess mortar cracked loose from the ties, the constraint was reduced and the ties became more flexible in both tension and compression, which had a greater relative effect on the eccentric ties in Wall-2. At this point of specimen testing (end of the *elastic* range), tie elongations across the top row were just reaching the second stiffness slope on the idealized tension strength and stiffness curves (Figure 4.5).

4.4.2 *Intermediate* – Onset of Veneer System Damage

First structural damage in the veneer wall systems (both Walls-1 and -2) occurred at the top south corner tie (A/1). For Walls-1 and -2, Figure 4.14 shows the peak displacements and tie elongations during the dynamic tests before testing which caused tie damage. (The onset of tie connection damage in a brick veneer wall system can also be characterized as the Immediate Occupancy performance level for architectural components per ASCE 41-06.) The brick veneer and wood frame displacements were relatively similar in both walls, even though the dynamic loading intensities were quite different. The relative displacements (tie elongations), however, were different, with the veneer more closely coupled to the backup in Wall-1. During tests when the first tie failures occurred, the peak tie elongation at the top corner in Wall-1 was estimated to be approximately 0.19 in. (5 mm) (because of missing data for the M10-0.58[0.43]g run, the peak veneer displacements at the top corner were considered from similar dynamic tests, and a peak wood backup corner displacement was estimated from similar Wall-2b tests); the peak tie elongation at the top corner in Wall-2 was measured as 0.3 in. (7.5 mm), during the M10-0.22[0.18]g run. Thus, the top corner tie elongation at first tie fracture in Wall-1 was directly at, and in Wall-2 was slightly less than, the opening displacements (elongations) at ultimate tensile loading determined from the tie subassembly (monotonic tension) tests. Figure 4.13(b,d) further shows that as the corner tie connection (A/1) elongations exceeded their ultimate tensile load displacements of 0.19 in. (5 mm) and

0.36 in. (9.1 mm) in Walls-1 and -2, respectively, the top center tie connections (A/5) still exhibited displacements below those at ultimate loading. The failure modes of the top corner ties (which were comparable to some failures seen in the tie subassembly cyclic load tests) suggest that low-cycle fatigue may have contributed to their fracture. During these dynamic tests, it was noted that, prior to tie tensile damage, peak tie deformations in compression were typically on the order of one-fourth to one-half of their peak tensile elongations.

The variation in stiffness along the backup system resulted in certain ties being more highly loaded than others. The smallest centerline tie elongations (lowest loading) occurred halfway up the wall, where the wood frame wall panel deflected the most (especially at the third row of ties). Near the topmost tie connections, the top edge of the wood wall panel was limited from deflecting as much, especially at the top corners where the rafter connections were stiffer, resulting in larger tie elongations. Ties in the bottom row also experienced significant elongations starting in the *intermediate* range of dynamic loading (Figure 4.14(b)); however, these ties did not play a critical role in the ultimate stability of the veneer. The ties in the bottom row were nailed to the header board of the floor framing, which had negligible deflection relative to the shake table during dynamic loading. In general, then, ties anchored near (or directly at) stiffer regions of the wood backup frame had to absorb the highest loads generated by movement of the brick veneer, whereas other ties had much less demand placed upon them. (Experiments on a full-scale brick veneer home structure subjected to static lateral face loads (representing wind pressure) exhibited similar results for ties at different vertical locations (DeVekey 1987).)

In Wall-2, a crack formed in the mortar bed joints across the mid-height of the brick veneer because of the more flexible veneer-to-backup connections (Figure 4.9(d)). Walls-1 and -2b did not exhibit any veneer cracking after being subjected to more than twice the scaled dynamic input that caused the veneer to crack in Wall-2 (mainly because the veneer was more closely coupled to the backup in those walls). In Wall-2, the large brick mass had more freedom to move independently from the backup, developing high enough inertial forces to bend and crack the veneer, without complete tie failure and collapse, at the upper region of the veneer during the M10-0.30[0.24]g input run. Test results for that run, presented in Figure 4.15, show higher curvature in the veneer at the region of cracking than for earlier runs, specifically when the veneer traveled backward towards the wood frame (at an instant when the veneer was not at maximum displacement in either direction). In general, then, the type of veneer-to-backup connection appeared to affect brick flexure and eventual rupture. (For anchored veneer crack control, BIA (2003) and MSJC (2008) only specify *backup* deflection limits, based primarily on studies with metal stud framing where a relationship between backup deflection and veneer flexural cracking has been established.) Overall, the wood frame backup stiffness was preserved during the veneer wall tests, except for minor softening at the nail connections from repeated loading; therefore, backup flexibility was not a controlling factor for cracking of the veneer in these tests.

4.4.3 *Ultimate* – Collapse of the Brick Veneer

As tie damage progressed in the upper region of Walls-1 and -2, the distribution of inertial forces along the height of the wall placed a greater demand on the remaining ties. Peak measured displacements from the most severe dynamic tests before veneer collapse (M10-0.66[0.47]g and M10-0.41[0.30]g for Walls-1 and -2, respectively) are shown in Figure 4.16 (which also includes the final test of Wall-2b for comparison). (This level of response and damage in a brick veneer wall system can be characterized as the Life Safety performance level for architectural components per ASCE 41-06.) Veneer and backup displacements were similar in shape and magnitude for Walls-1 and -2 (Figure 4.16(a)); the relative displacements were also quite similar for both walls at this higher stage of damage (Figure 4.16(b)). After these tests on Walls-1 and -2, all of the ties along the centerline were still intact; however, the top center tie in Wall-1 had been subjected to significant elongations, reaching deformations up to 0.33 in. (8.4 mm), well beyond the displacement corresponding to ultimate tensile loading in the tie subassembly tests (Figure 4.5). (High deformations of this tie in Wall-1 were ultimately explained after the veneer collapsed; this tie was one of three in the top row to undergo a failure involving tearing, fracture, and nail push-through at the nail hole, after some ductile pullout from the wood framing.) During the most severe dynamic tests before collapse of Wall-2, the center tie reached a peak elongation of 0.32 in. (8.2 mm), slightly below the elongation corresponding to ultimate tensile loading in the tie subassembly tests. Furthermore, the equivalent resultant seismic forces imposed on these tie connections, as computed from the peak measured accelerations at the top center of the brick veneer and the mass of the tributary wall area supported by the ties, were generally comparable to the ultimate tensile strengths of these tie connections. Finally in Figure 4.16, the measured displacements in Wall-2b at much higher dynamic loading (M10-0.80[0.54]g) demonstrate that the mechanical anchors were very effective at transferring a major part of the inertial forces. (Similarly, another study showed that the performance of older (turn of the 20th century) veneer construction could be improved by post-installing anchors (Paquette et al. 2001).) Figure 4.13 further shows the relationship between the M10 input PGAs vs. peak overall displacements and tie deformations for these wall panels, with the response of Wall-2b exhibiting a nearly linear relationship between the input PGAs and the displacements.

In Walls-1 and -2, during their last dynamic tests (resulting in collapse), the top of the veneer could already move somewhat freely, due to damage in the wall system. For these tests, Figure 4.17 shows traces of relative displacement (along the wall centerline) between the brick veneer and the wood backup, leading up to and during veneer collapse. The displacement traces not only identify the deformations of the ties, but also the events of damage across entire rows of ties. Generally, for both walls in Figure 4.17, the topmost trace (row-1) exhibits several displacement cycles up to about 0.3 in. (8 mm), approximately the peak displacement reached at the top center during the previous runs described above. As shaking intensified, row-1 displacements rapidly jumped up to and beyond 0.4 in. (10 mm), coinciding with the instant when all ties in the top row were damaged; thereafter, row-2 displacements increased to 0.3 in. (8 mm). By this time in the test of Wall-1, the veneer had already cracked below the second row of ties (from the top). In Wall-2, there was a pre-existing crack across the veneer below the third row of ties, and after a short time, the second row of ties was fully damaged as peak separations

(row-2) jumped from 0.4 to 0.8 in. (10 to 20 mm), while row-3 elongations increased to 0.2 in. (5 mm) (Figure 4.17(b)). At this stage, the free-standing portions of the veneer walls briefly rocked about the horizontal cracks; following higher peaks in the shaking input, these portions collapsed, destroying most of the ties in the lowest corresponding row (the second and third row from the top in Walls-1 and -2, respectively) only as the veneer toppled. Overall, final collapse of the brick veneer walls resembled a "zipper" effect – initial tie damage occurred across the upper rows, immediately placing more demand on the next row of ties below, which also experienced damage, and so on. For both specimens, displacement traces below the collapsed region did not exhibit any significant deformations, even as portions of the veneer collapsed. (Collapse and instability of brick veneer walls can be associated with the Hazards Reduced performance level for architectural components per ASCE 41-06.)

4.5 Summary and Conclusions (Wall-1, Wall-2, and Wall-2b)

Performance of solid brick veneer walls on a wood frame backup (typical of residential construction) was experimentally investigated under static and dynamic out-of-plane lateral loading on a shake table. The test specimens, representing common construction practice, comprised full-scale brick veneer walls attached to a wood frame backup with 28 ga. corrugated sheet metal ties (utilizing two different installation methods), as well as with post-installed mechanical "retrofit" anchors. With respect to overall wall behavior and the effect of different veneer-to-backup connections, the most important results and conclusions may be summarized as follows:

- Preliminary static tests showed that brick veneer enhanced the out-of-plane stiffness of the wall system, compared to the stiffness of the bare wood frame wall panel. The free vibration period of the veneer walls varied in relation to the initial stiffness of the veneer-to-backup connections; furthermore, changes in period of vibration were a good measure of the progression of damage in the wall system.
- The brick veneer rotated as a rigid body about its base when subjected to dynamic input, producing inertial forces transferred through the ties into the wood frame backup. As a result, the ties in the upper rows controlled the veneer wall system performance because they were subjected to the highest displacements (elongations).
- "Mortar droppings" in the air space between the veneer and the backup increased the initial stiffness of some ties (by providing constraint) and also reduced the demand on ties in compression (by locally filling the air space).
- Ties anchored at or near stiff regions of the wood frame backup (floor or roof/ceiling framing) were more highly loaded than ties anchored near more flexible regions (half-way up the wall panel), where the wood frame backup could deflect together with the veneer; these results were similar to those from other studies for ties at different vertical locations in veneer walls subjected to wind loads.
- Overall wall deformations depended on the stiffness of the ties, particularly in tension. With stiffer ties, the veneer was more closely coupled to the backup than in walls with more flexible ties, which allowed the veneer to move somewhat

independently from the backup. This made the brick veneer more susceptible to cracking in the case of flexible tie connections.

- Post-installed mechanical anchors were able to improve the performance of the brick veneer wall system, compared to using corrugated sheet metal ties only. The anchors effectively transferred a large portion of the inertial loads, while securing the veneer closely to the backup.
- Initial tie damage always occurred near the top corners of the veneer walls. As tie damage spread, gradually reducing the stiffness and strength of the veneer-to-backup connections, a portion of the veneer became unstable and eventually collapsed. The majority of ties near the top of the walls experienced brittle fracture at collapse, whereas ties near the lower rows of the collapsed veneer region often underwent more ductile tearing damage. Tie failure modes noted in the veneer wall collapses matched well with those observed in the study on individual tie behavior.
- For veneer walls subjected to dynamic input, lower inertial loads were produced by the veneer when stiffer ties were used. The veneer wall with a "best-case" installation method of 28 ga. ties (bent at the nail) was able to sustain dynamic input up to the M10-0.58[0.43]g record without any tie damage, and up through the M10-0.66[0.47]g record before collapse of the brick veneer. On the other hand, the veneer wall with a worse installation method of 28 ga. ties (bent at an eccentricity from the nail) could only sustain dynamic input up to the M10-0.22[0.18]g record without tie damage, and up through the M10-0.41[0.30]g record before collapse of the brick veneer. Finally, the veneer wall with mechanical expansion anchors was able to sustain dynamic input up to and including the M10-0.80[0.54]g record without any veneer system damage. These results emphasize the importance of both stiffness and strength in veneer-to-backup connections.
- As has already been described, the wall specimens utilized 28 ga. ties even though 22 ga. ties are the minimum specified. Subassembly tests have shown that the ultimate tensile strength is similar for both types of ties, while the initial stiffness is slightly higher for the 22 ga. ties (for each installation method); therefore, a veneer wall with 22 ga. ties may perform only slightly better than the walls tested with 28 ga. ties. The specific effects of different types (thicknesses) of ties, different tie installation methods (with or without eccentricity; nail vs. screw attached), and different tie spacings on overall wall behavior have been investigated analytically, as described in Chapter 5.

Table 4.1 – Summary of experimental results.

	Ground Motion Properties:		Top center of brick veneer:			Peak tie elongations (centerline):			(corner):	
	Input Type	Measured [Nominal Scaled] PGA (g)	Acc. (g)	Displ. (in.)	Period* (sec.)	C/5 (in.)	B/5 (in.)	A/5 (in.)	A/1** (in.)	Damage:
Wall-1					**0.10**					
Elastic	M02	0.19[0.17]	-0.38	0.04		0.02	0.02	0.03	0.04	
	M10	0.22[0.17]	-0.47	0.06		0.02	0.02	0.03	0.06	
	M10	0.37[0.29]	0.84	0.15	0.12	0.02	0.02	0.05	0.14	Cracks at mortar-to-concrete foundation interface
Intermediate	M10	0.51[0.38]	1.09	0.29		0.02	0.03	0.08	0.26	
	M10	0.58[0.43]	n/a	n/a	0.15	n/a	n/a	n/a	n/a	Fracture at tie: A/1
	Nahanni	0.30[0.30]	1.39	0.30		0.02	0.04	0.12	0.33	Fracture at tie: A/9
Ultimate	M10	0.66[0.47]	2.19	0.69	0.22	0.03	0.11	0.33	0.73	Fracture at ties: A/8 and B/1. Nail pullout (~0.25 in.) at ties: A/3 and B/9.
	M10	0.64[0.54]	-5.01	1.69		0.10	0.60	1.69	1.71	Veneer collapse
Wall-2					**0.17**					
Elastic	M02	0.19[0.18]	0.79	0.28		0.03	0.10	0.19	0.27	
	M10	0.23[0.18]	1.52	0.37	0.23	0.03	0.11	0.24	0.29	
Intermediate	M02	0.20[0.18]	0.68	0.25		0.03	0.08	0.18	0.26	
	M10	0.22[0.18]	-0.91	0.31		0.03	0.08	0.20	0.30	Fracture at tie: A/1
	M02	0.24[0.24]	0.75	0.31		0.04	0.08	0.19	0.33	Fracture and nail pullout at tie: C/1
	M10	0.30[0.24]	1.07	0.45	0.21	0.04	0.09	0.24	0.42	Crack across veneer
	M02	0.30[0.30]	0.95	0.38		0.03	0.09	0.22	0.37	Partial fracture at tie: A/9
Ultimate	M10	0.41[0.30]	1.63	0.52		0.03	0.11	0.28	0.44	Partial fracture at tie: A/4. Fracture at tie: A/6.
	M02	0.31[0.31]	1.23	0.47		0.03	0.15	0.32	0.45	Nail pullout (~0.125 in.) at tie: A/5.
	M10	0.49[0.36]	-2.98	1.85		0.20	0.93	1.73	1.91	Veneer collapse
Wall-2b					**0.14**					
Elastic	M02	0.18[0.18]	0.41	0.10		0.03	0.03	0.04	0.09	
	M10	0.22[0.18]	0.53	0.15	0.14	0.03	0.03	0.05	0.12	
	Nahanni	0.35[0.35]	1.78	0.32		0.03	0.03	0.08	0.19	
	M10	0.59[0.42]	1.74	0.44	0.15	0.04	0.03	0.07	0.24	Slipping at anchor-A
	M10	0.67[0.48]	2.00	0.51	0.16	0.05	0.03	0.09	0.27	
	M10	0.80[0.54]	-3.00	0.53	0.17	0.04	0.06	0.11	0.30	

* - Dynamic properties evaluated *after* the tests listed in each row.
** - Top-south corner elongations for Wall-1 are estimates, computed by B6-piston.

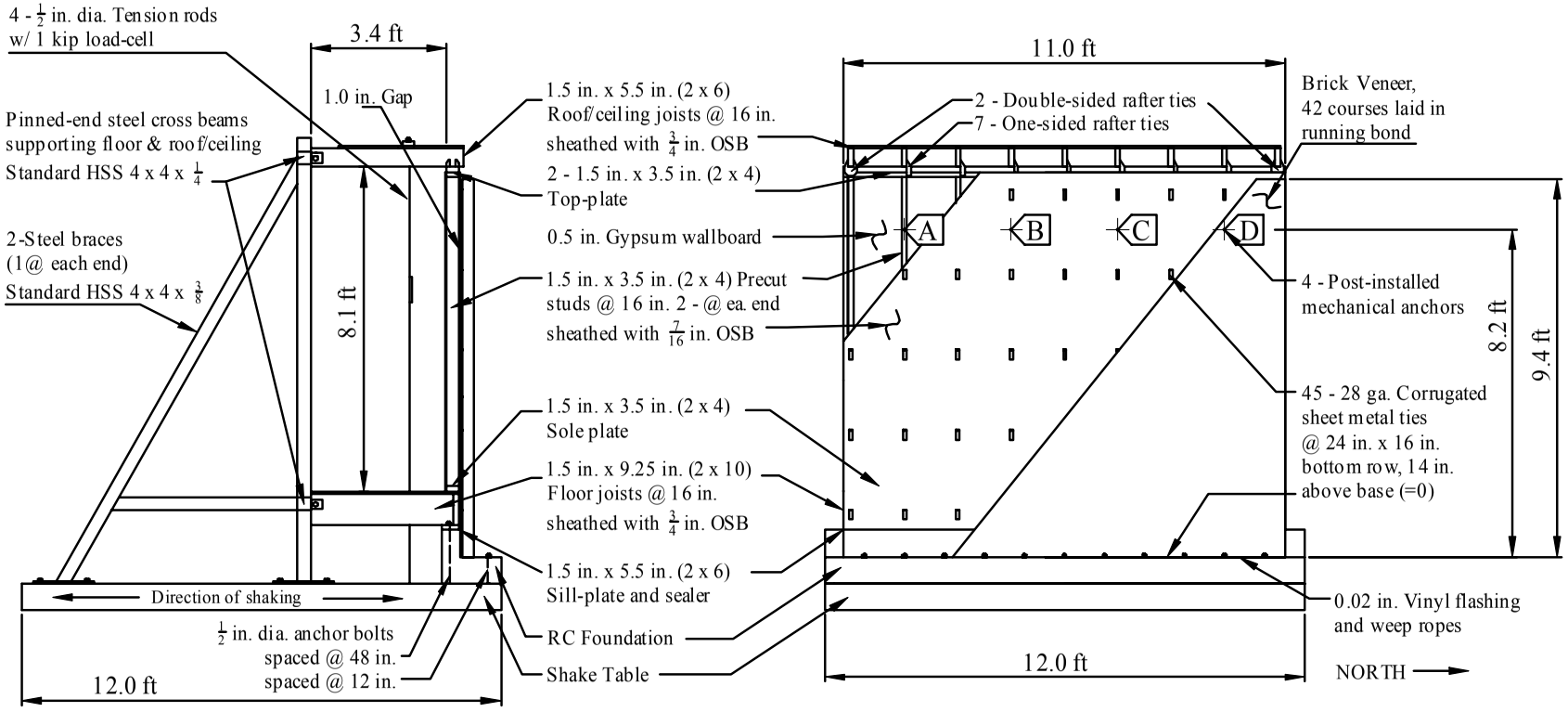

Figure 4.1 – Elevation views of the wall test structure.

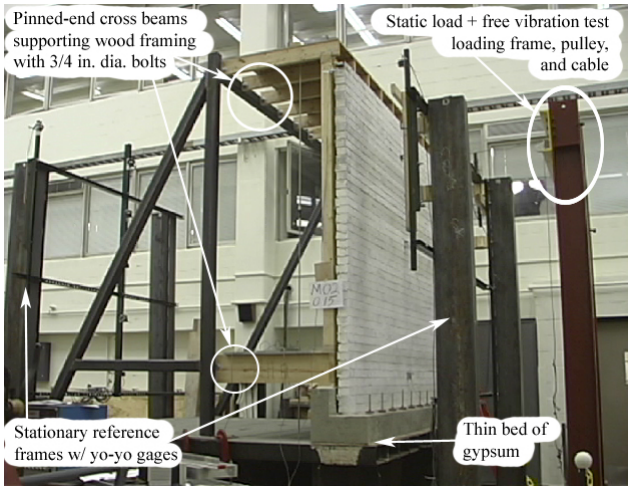

Figure 4.2 – Wall test structure setup on the shake table.

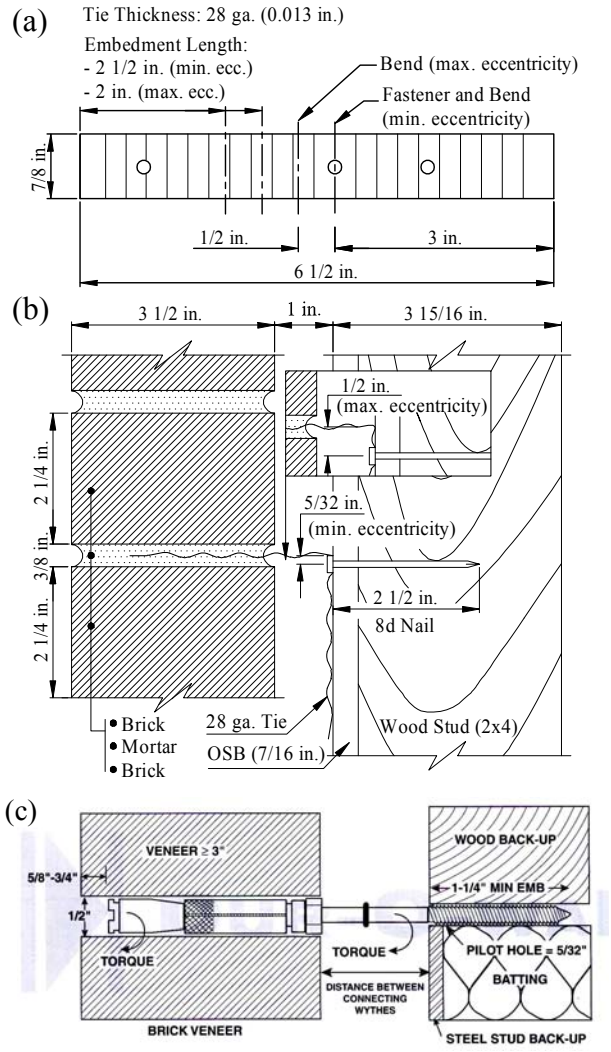

Figure 4.3 – Corrugated sheet metal tie (28 ga.) (a) overall dimensions and (b) section view of installation with 90-degree bend located at the nail and at an eccentricity above the nail. (c) Post-installed Series 5300 Dur-O-Wal mechanical anchors for Wall-2b (Dur-O-Wal 1998).

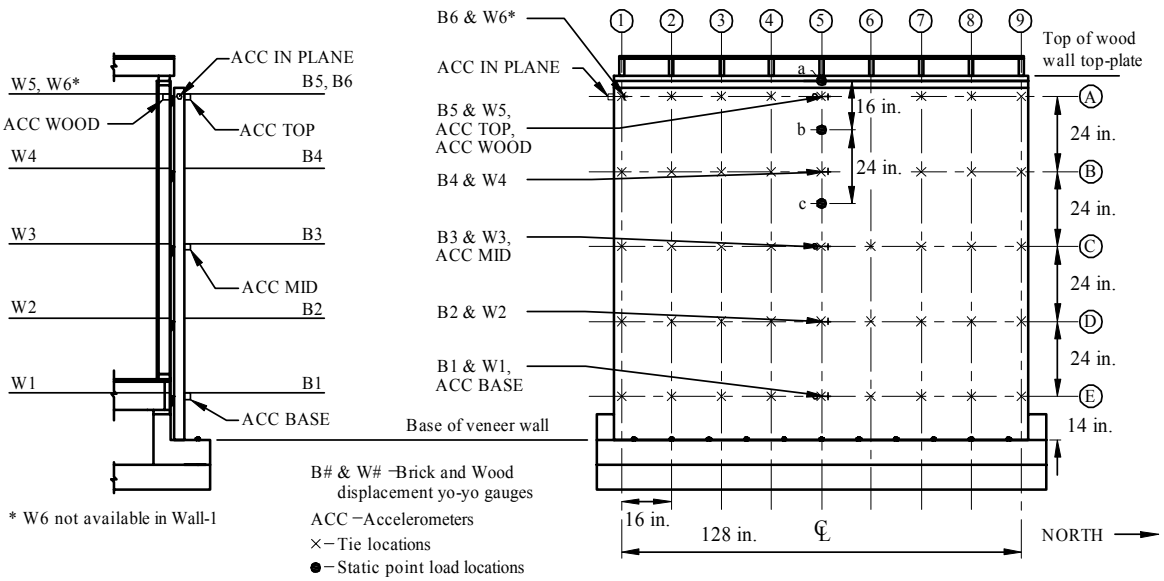

Figure 4.4 – Wall-1, -2, and -2b specimen instrumentation, static point load location, and tie grid layout.

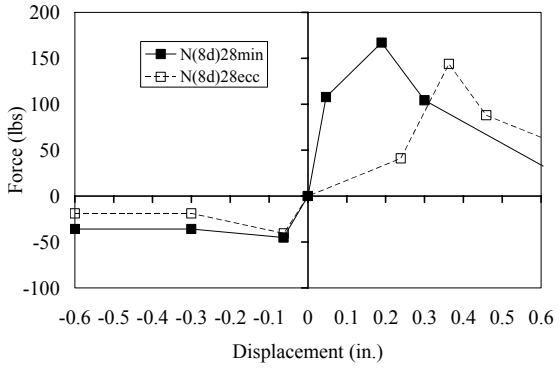

Figure 4.5 – Behavior of 28 ga. ties under tension and compression (from subassembly tests).

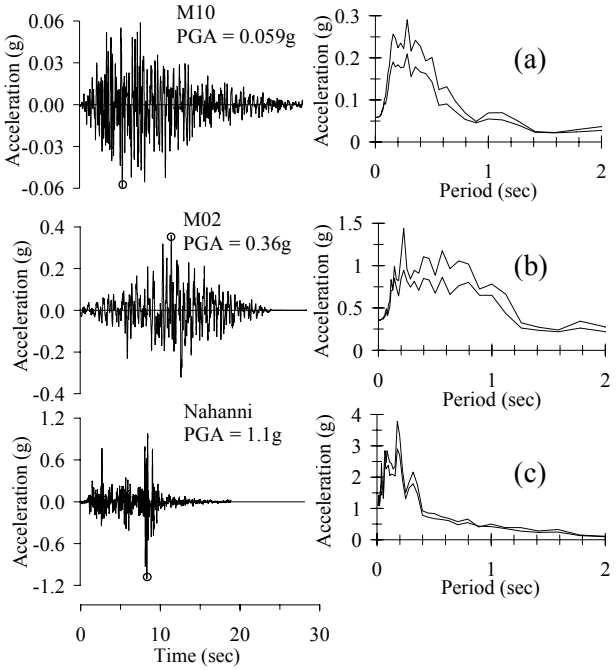

Figure 4.6 – Acceleration time histories and response spectra (3% and 6% damping) for (a) M10, (b) M02, and (c) Nahanni earthquakes.

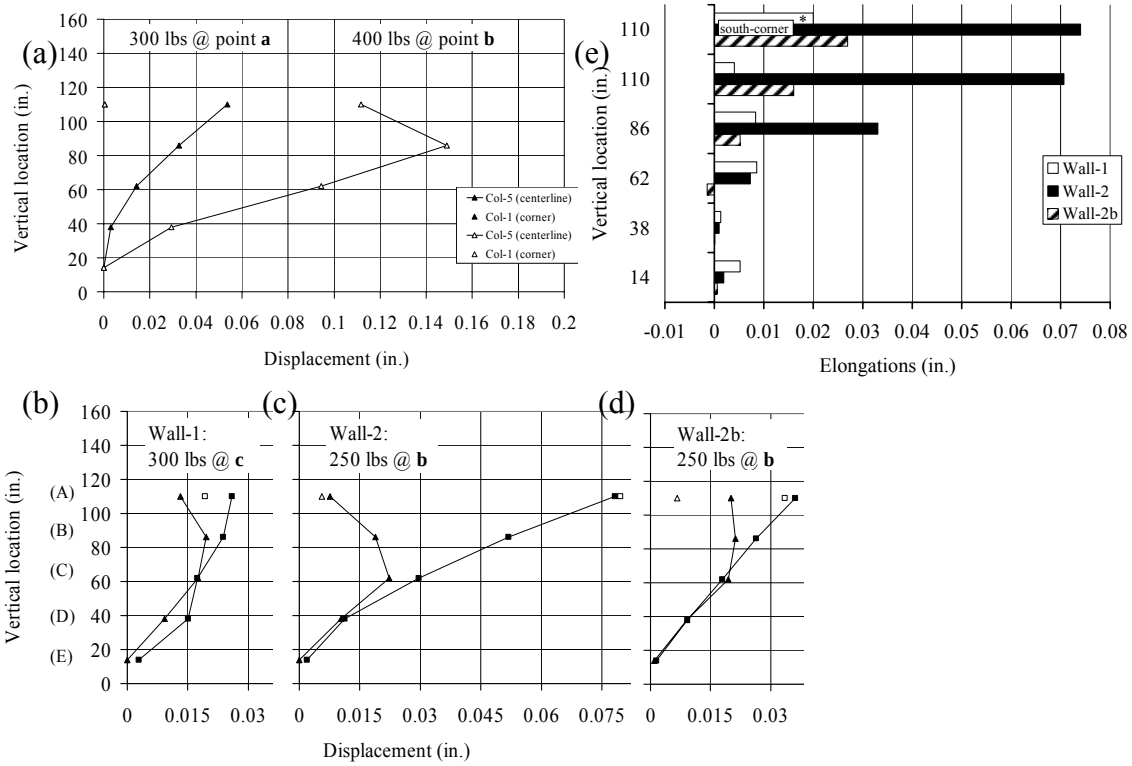

Figure 4.7 – Results from static load tests. (a) Bare wood frame backup displacements w.r.t. the shake table. Brick veneer and wood frame backup displacements w.r.t. the shake table for (b) Wall-1, (c) Wall-2, and (d) Wall-2b. (e) Relative displacements between the veneer and the wood frame backup (* – net brick displacement).

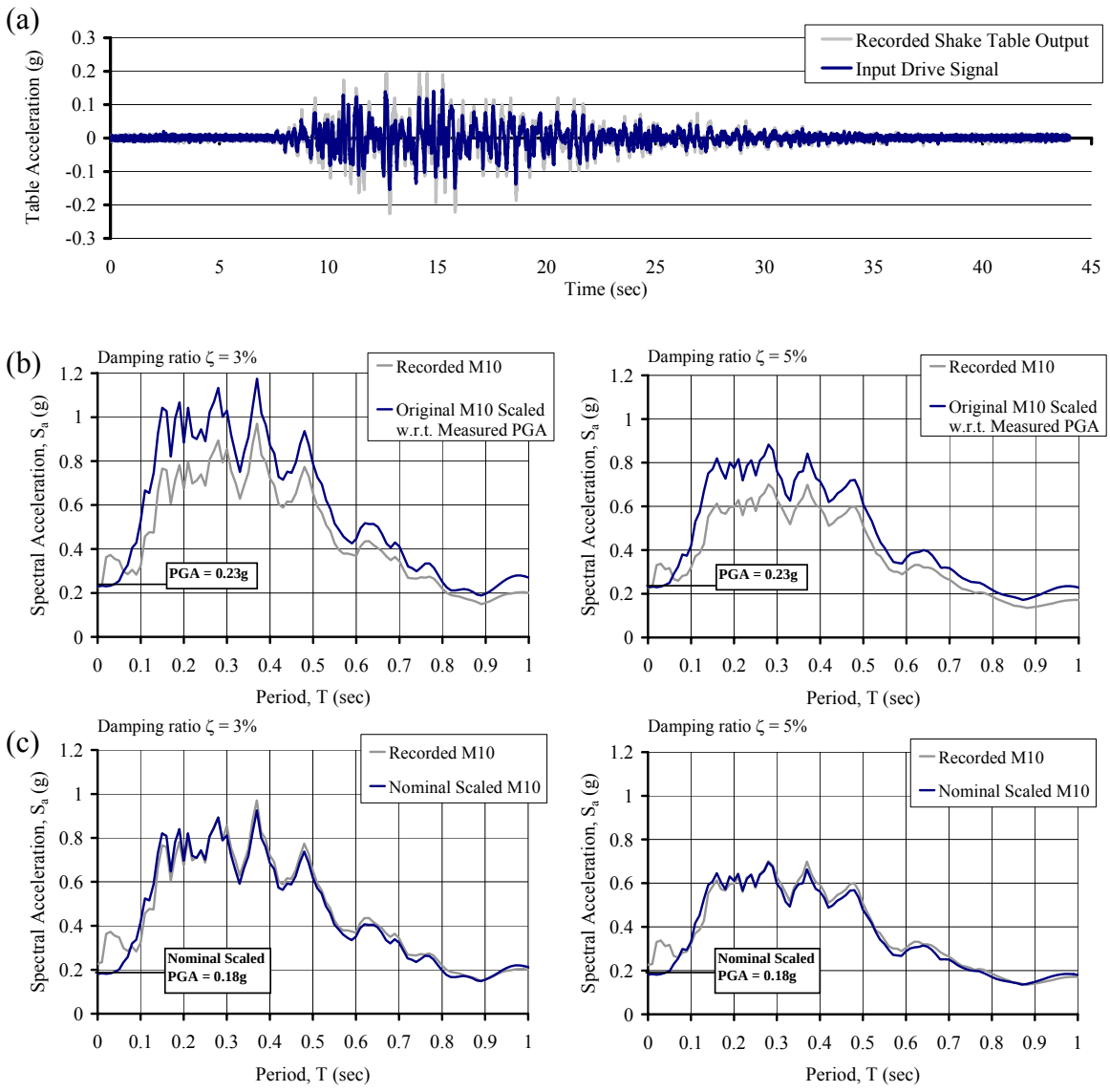

Figure 4.8 – (a) Recorded shake table output vs. input drive signal accelerations for M10-0.23[0.18]g test of Wall-2. (b) Response spectra for measured M10 earthquake with a PGA of 0.23g vs. original M10 earthquake record scaled to 0.23g. (c) Response spectra for measured and original nominal scaled M10 acceleration histories.

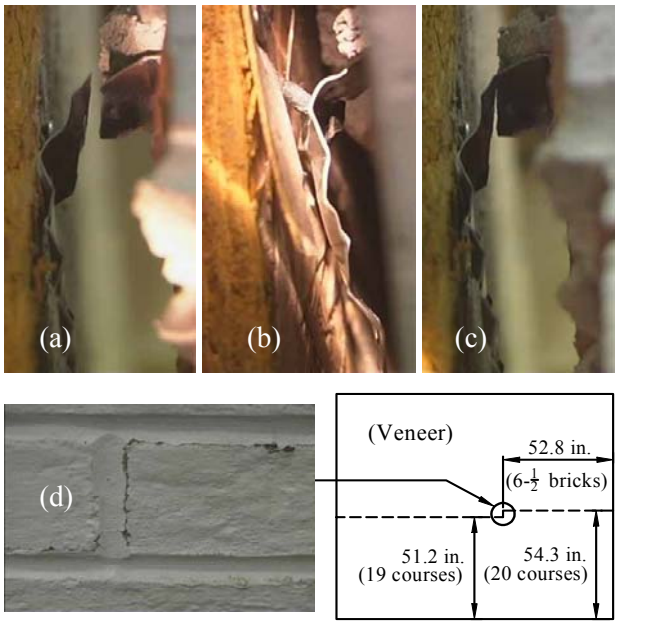

Figure 4.9 – Veneer wall damage before collapse in both Walls-1 and -2: (a) tie fracture and (b) nail pullout. In Wall-2 only: (c) partial tie fracture and (d) cracks in the brick veneer bed joints.

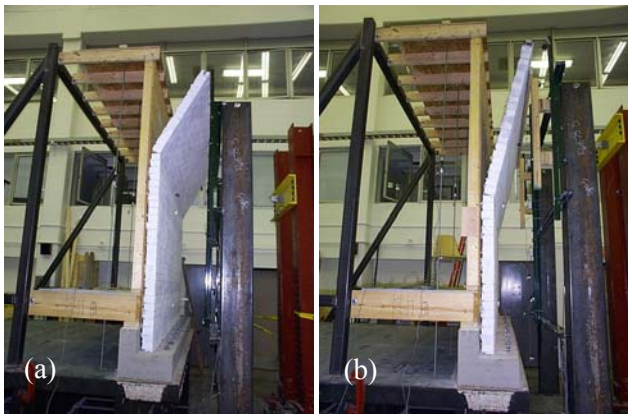

Figure 4.10 – Collapse of the brick veneer in (a) Wall-1 and (b) Wall-2.

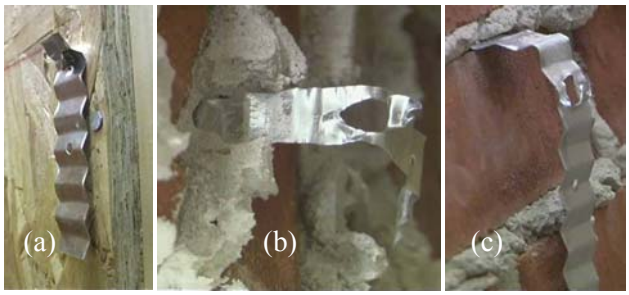

Figure 4.11 – Common tie failure modes noted after collapse of the veneer.

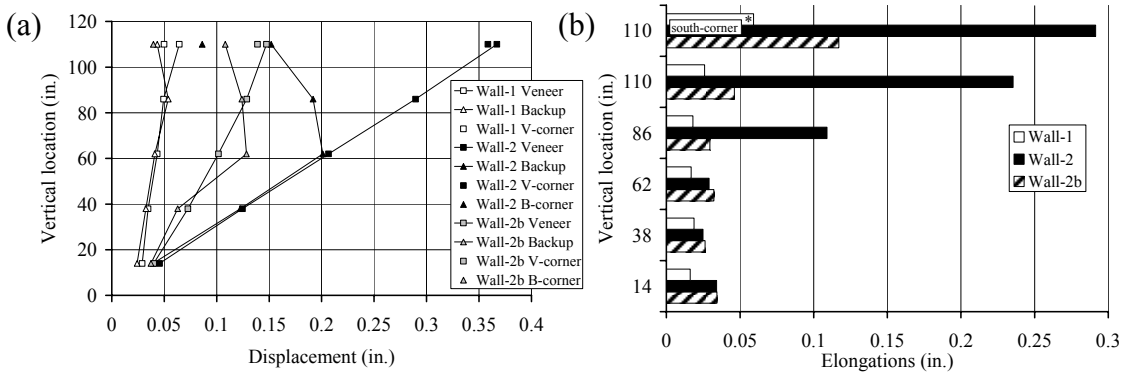

Figure 4.12 – (a) Peak positive displacements in all walls during the M10-0.22/0.23g tests; and (b) peak tie elongations for those same tests (* – net brick displacement).

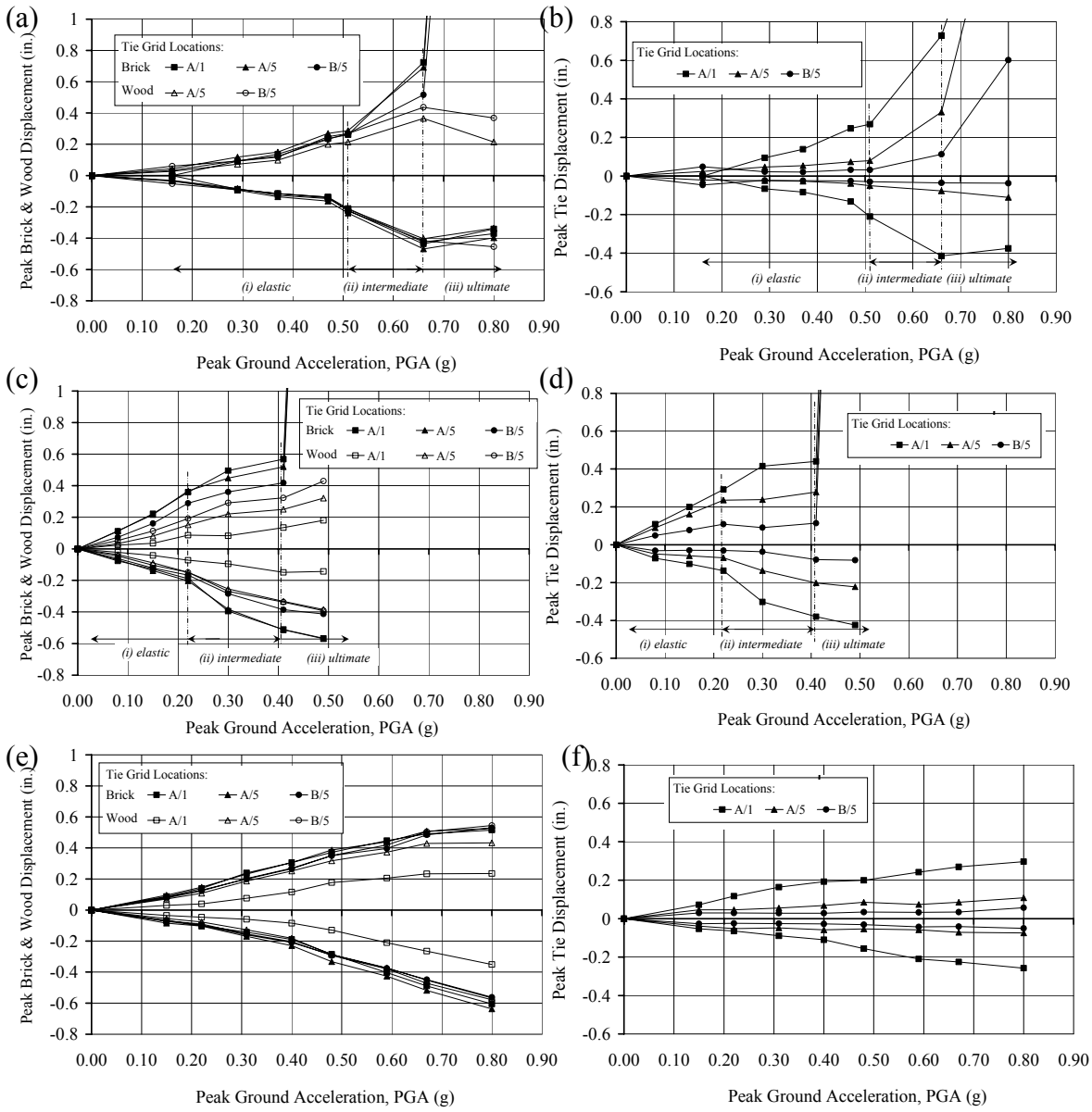

Figure 4.13 – Peak negative and positive wall and tie displacement response plots, during M10 input tests for: (a-b) Wall-1, (c-d) Wall-2, and (e-f) Wall-2b.

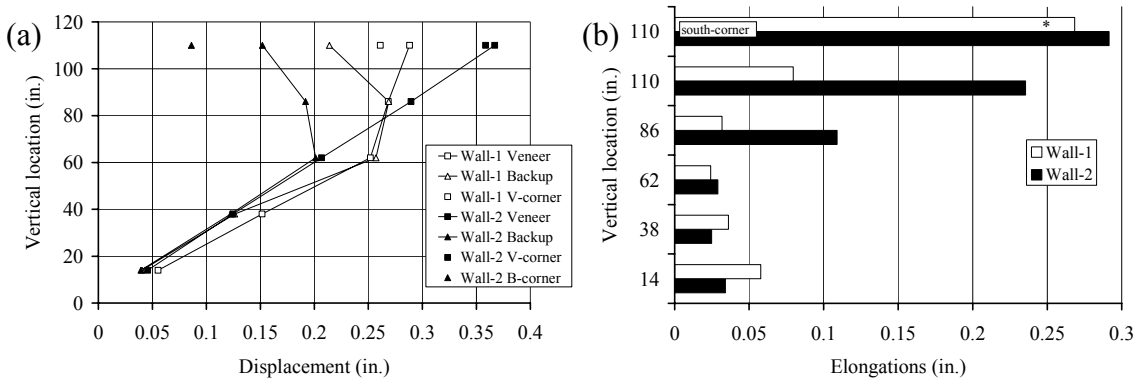

Figure 4.14 – (a) Peak positive displacements right before tie damage in Walls-1 and -2 during the M10-0.51g and M10-0.23g tests, respectively; and (b) peak tie elongations for those same tests (* – net brick displacement).

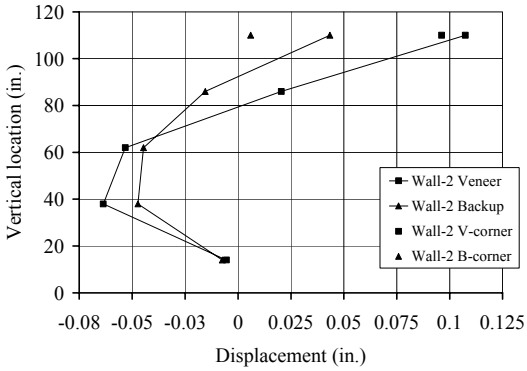

Figure 4.15 – High curvature in the veneer of Wall-2 at the onset of cracking, during the M10-0.30[0.24]g test.

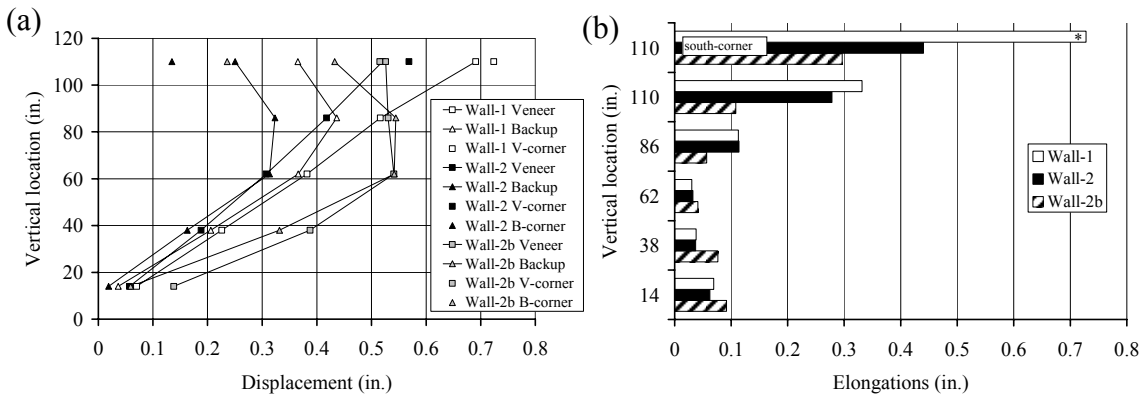

Figure 4.16 – (a) Peak positive displacements in Walls-1 and -2 during the highest dynamic runs prior to collapse (M10-0.66g and M10-0.41g, respectively), and in Wall-2b during the maximum dynamic test (M10-0.80g); and (b) peak relative displacements for those same tests (* – net brick displacement).

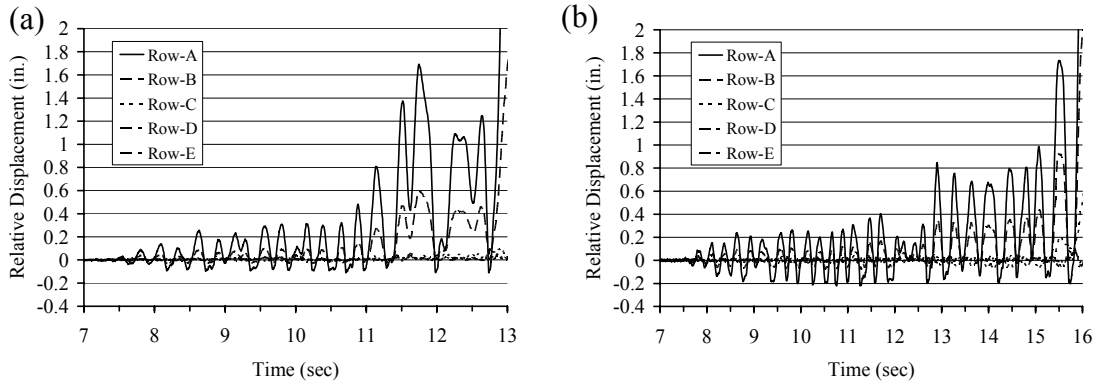

Figure 4.17 – Relative displacement traces along the centerline during the collapse runs of (a) Wall-1 and (b) Wall-2.

PART II – WALL PANEL WITH GEOMETRIC VARIATIONS

A third wall specimen (Wall-3) was tested to evaluate the effects on the out-of-plane earthquake performance of brick veneer walls from architectural variations and construction detailing, as a complement to the experimental findings described in *Part I* of this chapter. As reported below, out-of-plane static and dynamic load tests were conducted on a full-scale brick veneer wall specimen, with a window opening, representing the gable-end wall of a typical residential home structure. The test results have then been used to develop FE models of the wall panel, as described in Chapter 5, to further explore the effects on structural behavior of brick veneer walls due to geometric variations in wall construction, as well as from different brick veneer tie connection layouts and details.

4.6 Description of Test Structure (Wall-3)

A full-scale, one-and-a-half story brick masonry veneer and wood frame backup wall panel (12.8 ft [3.90 m] tall by 11.1 ft [3.38 m] long) was designed and constructed to represent a typical gable-end wall, with a window opening, in a single-family home structure, as shown in Figures 4.18 and 4.19. Design and construction of the wall specimen was based on typical practices for residential structures, in general conformance with the prescriptive requirements of BIA Technical Notes (2002, 2003), the MSJC (2008), and the IRC (ICC 2003).

4.6.1 Wall Structure Supports and Wood Frame Components

The brick veneer with 2x4 wood stud backup wall panel was set up to be excited in the out-of-plane direction on a uniaxial shake, in a similar fashion as the solid brick veneer wall specimens described earlier in *Part I* of this chapter. A reinforced concrete foundation pad, representing the upper portion of a typical home foundation wall, was constructed for support of the wood frame and brick veneer wall panel. In residential construction, exterior wood frame walls are generally attached to perpendicular structural walls or partitions at their edges, and to ceiling or roof framing across the top; therefore, the wood frame backup was constructed containing partial floor, sidewall, ceiling, and roof components, to provide representative boundary conditions for the 2x4 stud wall panel being tested (see Figures 4.18 and 4.19). The wood framing in the test structure comprised Standard Grade Spruce-Pine-Fir lumber, assembled in conformance with IRC (ICC 2003) requirements for nail size and spacing. The outside face of the wood frame wall was covered with 7/16 in. (11 mm) thick oriented strand board (OSB) sheathing panels, and the interior face with 1/2 in. (12 mm) thick gypsum wallboard. A simple pre-compression system was installed onto the wood frame backup (Figure 4.18), by means of four tension rods each adjusted to a 600 lbs (2.7 kN) force, capturing the overall compressive effects of attic and roof dead loads on the wood wall panel and backup framing (based on representative residential construction and occupancy loads).

Due to the limitations of shake table size and loading capacity, a steel reaction frame was utilized to represent the "rest of the house", providing gravity and lateral load support along the rear of the wood frame backup components. (The steel reaction frame utilized during solid wall panel testing was adjusted to accommodate this third brick veneer wall panel and backup, including the wood frame sidewalls and gable region, as shown in greater detail in Figures B.1 through B.3, which may be found in Appendix B.) The partial floor, sidewalls, ceiling, and roof were all connected back to the steel reaction frame with 3/4 in. (19 mm) diameter bolts. In general, the steel braces at each end of the wall panel (Figure 4.18) were relatively stiff, whereas the pin-ended cross beams were flexible enough to permit some relative in-plane movement at the floor, ceiling, and roof framing. Therefore, the accelerations at the top backup corners and along the bottom of the wall panel were expected to be nearly equal (to each other and to the shake table input), with perhaps some modest amplification across the ceiling and roof framing at the top. (The mass and dynamic response of an entire house were not represented in this test setup.) Furthermore, the steel reaction frame was stronger than typical wood frame construction, so the dynamic tests were conducted under an assumption that the motion intensities would not cause significant damage to the in-plane components of a typical wood frame home structure, but that they could be enough to affect the wall panel being tested in the out-of-plane direction.

4.6.2 Brick Masonry Veneer and Tie Connections

The brick masonry veneer wall was constructed by professional masons, with free edges (open ends) similar to those found in residential construction with "front face" veneer walls only, where the masonry is terminated at a corner and some other siding material is used on the perpendicular return walls. (In brick veneer construction, it is also common to have veneer wall terminations at vertical expansion joints and openings, which permit individual sections of veneer to move independently of one another.) The bricks used in the veneer wall were 3-1/2 in. x 7-5/8 in. x 2-1/4 in. (89 mm x 194 mm x 57 mm) standard modular "Colonial Reds" with three holes, joined by type N mortar (cement : lime : sand = 1 : 1 : 6) in running bond. A set of prisms and mortar cubes were tested to confirm that the strength properties generally agreed with this type of masonry (and those test results have been summarized in Table B.1, which may be found in Appendix B). Mortar for the first course of bricks was placed on flashing material, which had little bond to the top of the foundation surface; flashing was also installed under the brick window sill and over the steel angle lintel that spanned the window opening (see Figure 4.18). (Flashing, though not always used in residential construction, is mandated by building codes to collect and discharge condensation at foundation wall surfaces and around openings.)

As part of masonry installation, the brick veneer was attached to the wood frame wall panel using corrugated sheet metal tie connections generally complying with the prescriptive requirements for tie installation per the BIA (2003), IRC (ICC 2003), and MSJC (2008). Individual brick veneer tie connection stiffness and strength properties are typically controlled by the type of tie, the kind of fastener, and the extent of tie bend eccentricity; the loading on tie connections in a veneer wall is then governed by their stiffness and their location within the wall system, as well as by their horizontal and

vertical spacing (i.e., supported wall area per tie). As shown in Figure 4.20(a), the 22 ga. (0.031 in. [0.79 mm] thick) by 0.88 in. (22 mm) wide ties in the wall specimen were fastened to the wood backup studs with 2-1/2 in. (64 mm) long smooth-shank (roofing) nails. These nails are practically equivalent to 8d nails, which are the minimum prescribed form of attachment for corrugated sheet metal ties to a wood backup – they are equal in length, with a diameter approximately 10% less than that of an 8d nail. The ties were bent as close as possible to the nail head, resulting in a small bend eccentricity of approximately 1/4 in. (6 mm) (from the line of the tie to the center of the fastener); the maximum allowable bend eccentricity is 1/2 in. (12.7 mm), as specified by the MSJC (2008) and BIA (2002). During construction, an air space of approximately 1 in. (25 mm) was maintained between the outside face of the wood frame sheathing and the inside face of the brick veneer, though at some locations it narrowed a bit as a result of the wood wall being slightly out-of-plumb. At a few locations, excess mortar seeped out into the air space, landing on the corrugated sheet metal ties and locally filling the space. (Small amounts of excess mortar cannot be avoided, but recommended practice is to limit such "mortar droppings" into the air space as much as possible, as they may provide a conduit for moisture intrusion across the cavity and could impair the passage of moisture out of it.) A general tie grid spacing of 406 mm horizontally and 610 mm vertically was employed, as shown in Figure 4.21, with additional ties provided within 8 in. (203 mm) of open edges, such as below the window opening and along the roof edge, as recommended by BIA (2003). The tie layout also satisfied the IRC maximum tie spacing limit of 36 in. (914 mm) around the window opening perimeter.

Static and cyclic force-displacement tests were conducted on brick-tie-wood subassemblies representing the type of tie connection used in this wall specimen, as described earlier in Chapter 3. Force-displacement behaviors for tie connection specimens with a 22 ga. tie and a 2-1/2 in. (64 mm) roofing nail (labeled as N(2.5)22min) under monotonic tensile loading, as well as the average idealized multi-linear monotonic tension behavior, are shown in Figure 4.20(b). Then, the cyclic tension behavior for one example specimen of this type, along with the corresponding average envelope curve (based on five cyclic subassembly tests) are shown in Figure 4.20(c). Tensile performance of these tie connections was governed by nail pullout from the wood stud, and their overall average ultimate tensile capacity was found to be 95 lbs (0.42 kN), with a coefficient-of-variation of 0.17, at an average opening displacement of approximately 0.06 in. (1.5 mm). (The average measured tensile capacities of tie connection subassemblies controlled by nail pullout from the wood stud were typically in the range of 50-70% of computed direct nail withdrawal strength values (without a factor of safety) per the NDS (2001).) On the other hand, the usual failure mode of subassemblies in compression was by buckling of the tie; however, subassembly compressive strength and stiffness results should be considered as only lower bounds for actual veneer walls because of the excess mortar at some places in the wall air space, as described above, which can help transmit compressive forces and reduce the compression demand on the ties. As mentioned earlier, BIA (2003) recommends that brick veneer tie connections should provide a minimum initial stiffness of 2,000 lbs/in. (0.35 kN/mm) in both directions. In compression, this stiffness would clearly be satisfied by the combined resistance of the 22 ga. tie itself plus some excess mortar in the wall cavity; in tension,

the combined effect of tie deformation and prying on the nail also still satisfies this requirement, with an average secant stiffness of 2,400 lbs/in. (0.42 kN/mm) determined from subassembly tests. These tie connection properties have been utilized for analysis of the experimental results, as well as for later FE modeling of the tie connections (described in Chapter 5).

4.7 Shake Table Testing Program (Wall-3)

Shake table testing was carried out in multiple stages: a) preliminary out-of-plane static point load tests were performed on the wall specimen, both before and after construction of the masonry veneer; b) dynamic tests were conducted by subjecting the wall specimen to different scaled earthquake acceleration records; and c) dynamic properties, including period of vibration and damping ratio, were evaluated by regularly subjecting the wall specimen to free vibration and harmonic excitations.

4.7.1 Static and Dynamic Loading

Preliminary static displacement tests were performed to evaluate the variation in lateral stiffness of the wall structure from before to after construction of the brick veneer. Point (pull) loads of 200-450 lbs (1-2 kN) were applied to the wall panel by means of a steel cable running through a pulley, attached to a loading frame facing the wall panel (see Figure 4.19). The period of vibration and viscous damping ratio of the wall specimen were evaluated before and then again after certain dynamic tests. To evaluate the period of vibration, a sine-sweep with a frequency range of 1-20 Hz was employed, scaled to very low peak ground accelerations (PGAs) of approximately 0.02-0.04g. Free vibration tests were also conducted, by suddenly releasing the static point loads applied to the wall panel and then measuring the subsequent dynamic response. And finally, the wall specimen was occasionally subjected to gradually increasing short-duration harmonic (H) inputs, corresponding to the approximate period of the wall structure (at low to moderate PGAs); at the end of this input, the table was stopped abruptly to measure the wall panel free vibration response, with the damping ratio then evaluated by the logarithmic-decrement method.

Dynamic tests were conducted to evaluate the overall performance of the brick veneer wall panel under distributed (inertial) loads. The earthquake records employed in these tests included two synthetic motions and one recorded ground motion, as shown earlier in Figure 4.6, chosen to be representative of intra-plate earthquakes found in the central and eastern U.S. All of the records were normalized (scaled) with respect to PGA, and then progressively increased by increments of approximately 0.05-0.10g throughout testing (starting from fairly low values). At higher levels of shaking, the lower frequency components of the earthquake records (within the range of 0-1 Hz) were filtered out with *Seismosignal* (Seismosoft 2006), to avoid exceeding the maximum stroke ±2 in. (±50 mm) capacity of the shake table actuator piston.

4.7.2 Specimen Instrumentation

Out-of-plane displacements of the brick veneer and of the wood frame backup were measured at eleven tie locations using cable extension displacement transducers, as follows (per Figure 4.21): two along each end of the wall (rows B & E; columns 1 & 9), four along the vertical centerline (rows O, B, D.6, & F; column 5), and three along the north vertical edge of the window opening (rows B, C, & D; column 7). As part of dynamic testing, shake table "input" displacements were recorded by a transducer located in the actuator piston. Additionally, accelerometers were placed at key locations along the wall centerline (rows O, B, D.6, & F; column 5), and at the top corner of the wall (row B; column 9), as well as on the shake table itself. During dynamic testing, maximum response of the wall panel (peak measured accelerations and displacements) typically occurred shortly after the PGA of the earthquake input records. As in the solid wall panel tests, maximum positive displacements of the brick veneer and the wood backup (outward deflections of the wall panel), as well as peak positive tie deformations (elongations), were of particular interest. Brick and wood displacements were evaluated as the difference between the wall and shake table values (i.e., they were the displacements relative to the shake table). Tie deformations at a particular location were evaluated as the relative movement between the brick veneer and the wood frame backup.

4.8 Experimental Results and Analysis (Wall-3)

Static and dynamic shake table tests were conducted on the Wall-3 specimen following the procedures described above. Preliminary tests were used to evaluate wall panel stiffness and dynamic properties in general, as well as overall performance of the shake table. Dynamic tests were then conducted to evaluate the seismic performance of the brick veneer wall panel under distributed (inertial) loads. Key dynamic test results and observations are listed in Table 4.2, including: name of the input earthquake record, with measured and nominal scaled PGAs (as described further below); peak accelerations on the brick veneer; dynamic properties; and descriptions of observed tie connection and veneer wall damage (as appropriate). The wall panel behavior corresponded to three levels of response and damage, as also seen during earlier solid wall tests, which can be described as: *(i) elastic* (no visible damage), *(ii) intermediate* (onset of tie and veneer damage), and *(iii) ultimate* (accumulation of tie and veneer damage sufficient to lead to collapse). The experimental results and performance of the brick veneer wall panel specimen are further described below.

4.8.1 Preliminary Tests – Static Displacements and Dynamic Properties

Static load tests provided useful overall force vs. displacement results, displaying the relative effects from the window opening and the partial wood backup frame supports (floor, ceiling, sidewalls, and roof) both before and after construction of the brick veneer. The static load test results were especially useful later for calibration of FE models, as described in greater detail later in Chapter 5. The period of vibration and damping ratio were then also evaluated between certain dynamic tests, as listed in Table 4.2. The period of vibration at the start of dynamic testing was 0.09 sec, with the average damping ratio being approximately 4% of critical (based on an initial set of harmonic load tests); these values gradually increased during testing, as the wall specimen experienced

changes in stiffness due to damage. (Recall that during the solid brick veneer wall panel tests, the period of vibration was also an indicator of the variation in wall stiffness from one wall to another with different veneer-to-backup connections.)

As discussed in *Part I* of this chapter, it is important that the shake table acceleration output captures the scaled input earthquake ground motions during dynamic testing. Because of recorded spikes in the shake table acceleration output, nominal scaled PGA values were computed, to capture the overall intensity and damage potential of the recorded shake table acceleration output per the original earthquake record input. The computed nominal scaled PGA values were typically within 10% of the target PGA values for the M10 earthquake record, whereas the nominal and target PGA values were nearly equal for the M02 and Nahanni earthquake records. Measured and nominal scaled PGA values for each earthquake record are presented in Table 4.2 and in the dynamic testing summary below.

4.8.2 *Elastic* Dynamic Tests

Throughout the *elastic* range of testing, the overall dynamic response (mode shape) of the wall panel was identified, without it undergoing any visible damage. As the wall specimen was subjected to dynamic inputs, the mass of the brick veneer produced inertial forces that were transferred through the tie connections into the wood frame backup. For example, overall peak displacements relative to the shake table during the M10-0.38[0.29]g input test are shown in Figure 4.22. The brick veneer essentially displayed rigid body rotation about its base, where the mortar cracked across the bottom of the wall (during early testing), as seen from the almost linear veneer displacement measurements along the centerline and edges of the wall panel (starting from the base). Some flexural deformations were visible in the brick veneer directly above the window opening, corresponding to the location of the partial ceiling support at the wood wall backup. Therefore, the first mode of vibration of the wall panel was simply noted as out-of-plane swaying of the entire brick veneer and wood frame wall system.

The M10 earthquake measured test PGAs with their corresponding maximum displacement responses of the brick veneer, wood backup, and tie connections are shown in Figure 4.23, for both inward and outward movement of the wall panel. (The M10 input record is presented here because it generally caused greater overall dynamic response of the wall panel specimen compared to the M02 and Nahanni inputs.) In the *elastic* range of wall behavior, the displacement and tie elongation responses at all of the measured locations generally exhibited a linear relationship with respect to PGA. (Throughout the *elastic* and into the *intermediate* ranges of wall behavior, the modest measured tie deformations were somewhat inaccurate due to the relative amount of instrumentation noise in the displacement data compared to the actual tie deformations; however, this was only true for fairly small deformations, of approximately 0.04 in. (1 mm) or less, and the noise was insignificant for higher input tests.) Toward the end of this range of testing, the brick veneer continued to be closely coupled to the wood frame backup along the wall centerline, but there were signs of the veneer pulling further away from the backup at both of the wall ends (Figure 4.22(a) and Figure 4.23(b)), subjecting the tie connections at those locations to higher loads.

4.8.3 *Intermediate* Dynamic Tests

At the start of the *intermediate* range of testing, the first signs of tie connection damage were noted at the two top corners of the wall panel; onset of nail pullout was visible at these tie connections, as shown in Figure 4.24(a), and their measured elongations exceeded the 0.06 in. (1.5 mm) opening displacement at the average ultimate tensile load for these ties, per Figure 4.20(c). In general, the greatest demands were experienced by: i) tie connections at the upper region of the wall panel (where the acceleration response was highest, as listed in Table 4.2), and ii) those ties anchored directly to or near the stiffer regions of the wood backup (sidewall, ceiling, roof, and/or floor framing locations). On the other hand, where ties were anchored near the relatively flexible vertical edge of the window opening, the brick veneer generally moved closely together with the backup wall, and therefore those tie elongations were typically lower. Similar observations were made during the dynamic tests of solid brick veneer walls, and in previous experiments by De Vekey (1987) on a full-scale brick veneer home structure subjected to static lateral face loads (representing wind loads).

As testing progressed into the *intermediate* range of wall behavior, the wood frame backup underwent minor softening. Even though no physical damage was observed, this softening was identified from the slightly greater rate of increase in peak wood backup displacements, deviating somewhat from the initial linear relationship with input PGA (Figure 4.23(a,c)). Despite this modest shift in wood displacement response, the wood backup behavior remained mostly linear, even up through the highest levels of shaking.

Horizontal veneer cracks first started to form along the base of the masonry gable (initiating from the upper corners of the window opening), as indicated in Figure 4.24(d), during the M10-0.63[0.49]g test. Throughout this and later tests, cracking of the brick veneer was closely related to tie connection damage and loss of stiffness; as tie connections became less effective, the large mass of the veneer had more freedom to move independently from the backup, developing high enough inertial forces to bend and crack the veneer. Furthermore, as tie connection damage and related strength and stiffness loss progressed, inertial forces were then distributed to adjacent ties that were still well-engaged, placing a greater force demand on them, resembling a “zipper” effect. Collected data and visual observations indicate that tie damage in this wall panel typically spread horizontally, starting from stiffer backup regions (wall edges), toward the more flexible center region; tie damage then also extended vertically, starting at the ceiling framing elevation, up into the gable region and down toward the base of the wall panel. The overall wall panel behavior was most closely related to the tie connection deformation limits and damage in tension, whereas tie deformations in compression continued to be quite low (Figure 4.23(b,d)) at all levels of testing, primarily due to restraint from mortar droppings bridging the wall cavity, thereby increasing their effective stiffness. During these dynamic tests, it was noted that, prior to tie tensile damage, peak tie deformations in compression were typically on the order of one-fourth to one-half of their peak tensile elongations; a higher effective tie compressive stiffness due to excess mortar (vs. their deformation in tension) was also noted during earlier solid wall tests.

4.8.4 *Ultimate* Dynamic Tests

The beginning of the *ultimate* range of wall testing was defined by the M10-0.98[0.68]g test, which caused tie connection damage to even spread to the top center of the window opening and the peak of the gable (see B/5 and O/5 in Figure 4.23(b)). Based on tie displacement measurements, it appears that all ties within the gable region suffered some damage at this point in testing. Tie connections at the upper wall region generally experienced the highest inertial loads; however, ties at the peak of the gable experienced somewhat lower loads than the row of ties right above the window opening (Figure 4.23(b)) because a much smaller area of masonry was supported per tie at the gable peak (in part as a result of strictly adhering to tie installation recommendations per BIA (2003)). Maximum brick veneer accelerations were also a bit lower at the gable peak than at the top center of the window opening (see Table 4.2). Additionally, brick veneer cracking and hinging along the base of the gable eventually allowed the masonry panel to bend and somewhat assume the shape of the wood backup, further reducing demand on the topmost ties.

A bit farther into the *ultimate* range of wall testing, there was even more tie damage (Figure 4.24(b-c)) and brick veneer cracking at approximately mid-height of the wall on each side of the window opening (Figure 4.24(d)). Even though many of the tie connections had been loaded far beyond their ultimate capacities (with significant nail pullout, as seen in Figure 4.24(c)), they continued to provide modest strength to at least prevent the wall from toppling over, as a result of some residual nail pullout resistance. The vinyl flashing, which was properly glued to the wood backup and tucked under the brick masonry at the window sill and lintel, also provided some unexpected modest additional restraint for the brick veneer during these later tests. Even though the wall panel bricks did not topple over during any particular test, the accumulation of damage throughout the masonry and tie connections was enough to essentially make it unstable during the M10-1.15[0.75]g test, when all measured tie elongations within the gable region and along the vertical side of the window opening (down to D/7) were well above the displacements at their average ultimate load capacity (Figure 4.23(b,d)), with severe diagonal cracking in the masonry also starting from near the corners of the window opening. (Horizontal cracks typically indicated one-way bending damage of the brick masonry; whereas, diagonal cracks starting at or near the window opening corners were a result of two-way bending. Such diagonal cracking at window opening corners is common, as also observed by Griffith et al. (2007) during cyclic out-of-plane tests of structural brick masonry walls.) A relationship between tie connection damage and subsequent cracking (as well as collapse) of brick veneer walls was also noted during the solid wall panel tests.

Taken as a whole, these Wall-3 test results and observations present useful information on the seismic performance of a brick veneer wall system with a window opening and gable, containing a "best-case" installation detail for the 22 ga. ties. The overall performance of the brick veneer wall was closely related to the local performance at the tie connections. These experimental results and observations have been used to develop detailed FE models of brick veneer walls, which are described in Chapter 5. Parametric

studies have then been conducted with those models, evaluating the effects on structural behavior of brick veneer walls due to geometric variations in veneer wall construction, as well as from a variety of tie connection details (by applying structural properties of the different types of tie connections established from earlier subassembly tests). The three levels of brick veneer wall response and damage (*elastic*, *intermediate*, and *ultimate*) defined during wall testing are used to assess the FE wall models throughout those parametric studies.

4.9 Summary and Conclusions (Wall-3)

The performance of a full-scale brick veneer wall on wood frame backup with a window opening and a gable region was investigated under static and dynamic out-of-plane loading on a shake table. The test specimen was designed and constructed based on typical practices for residential structures, and in general conformance with prescriptive recommendations and requirements for brick veneer construction per BIA Technical Notes (2002, 2003), the MSJC (2008), and the IRC (ICC 2003). The tests provide useful information on overall performance of the brick veneer wall system, including interaction and load-sharing between the brick veneer, corrugated sheet metal ties, and wood frame backup. Key findings from this part of the experimental study can be summarized as follows:

- Residential brick veneer construction built in general conformance with current recommendations and code requirements, containing a "best-case" installation detail with 22 ga. ties, exhibited satisfactory performance by withstanding seismic inputs up through a PGA of 0.54[0.39]g without damage, and until a PGA of 1.15[0.75]g without enough tie connection and masonry damage to cause out-of-plane collapse.
- Brick veneer wall system performance was closely related to the tensile properties of the tie connections. At onset of tie damage during dynamic veneer wall tests, tie connection deformations in tension were typically similar to the opening displacements at ultimate tensile loading determined from subassembly (monotonic tension and cyclic) tests. Tie connections anchored at or near stiffer regions of the wood frame backup experienced the highest loads and therefore exhibited the first signs of damage; as a result, tie damage spread throughout the wall panel, starting from the stiffer and upper regions of the wood backup, to more flexible backup regions. Loss in tie stiffness and strength then made the brick veneer more susceptible to cracking.
- Horizontal cracking and hinging eventually formed in the brick veneer along the base of the gable, making that portion of the wall panel more vulnerable to damage and collapse. However, the gable portion maintained its stability up through the highest levels of shaking, in part as a result of the additional tie connections installed within 8 in. (203 mm) of all wall edges (per BIA (2003) recommendations).
- Presence of a window opening resulted in greater wood backup flexibility, causing the wood framing to closely follow the masonry wall (when subjected to inertial loads) along the vertical edges of the opening, in turn resulting in lower load

demands on tie connections at those locations. The brick veneer wall panel experienced two-way bending deformations and subsequent diagonal cracking originating from the corners of the opening.

Table 4.2 – Summary of experimental results.

	Ground Motion Properties:		Peak Accelerations of Veneer (g):			Dynamic Properties*:		NOTES:
	Input Type	Measured [Nominal Scaled] PGA (g)	Wndw bot center (D.6/5)	Wndw top center (B/5)	Top center (O/5)	Period (sec)	Damping Ratio (%)	
Elastic	Nahanni	0.21[0.25]	0.51	0.78	0.80	0.09	3.00	
	M10	0.28[0.23]	0.52	0.46	0.50	0.10	4.38	
	M02	0.37[0.37]	-0.52	-0.59	0.71	0.10		Hairline cracks in brick veneer at top corners of window opening and below window sill
	M10	0.38[0.29]	-0.60	0.65	0.69	0.11	4.60	
	M02	0.51[0.42]	0.83	1.00	0.93	0.11	5.30	
	M10	0.54[0.39]	-0.92	-0.91	0.93	0.11		
Intermediate	H-9Hz	0.54	1.72	2.29	1.92	0.12	8.04	Visible nail pullout at ties: B/9 and C/9
	M10	0.63[0.49]	1.30	1.67	1.63	0.13		Horizontal cracks in brick veneer across top of window opening; visible nail pullout at ties: B/1, C/1, D/1, and D/9
	M10	0.74[0.55]	-	2.33	1.72	0.13		Increase in nail pullout at ties listed above
	M10	0.83[0.62]	-	-	-	0.14		Visible nail pullout at ties: E/1, E/9; broken nail head at tie B/9
	M10	0.89[0.65]	2.65	3.02	2.79			
Ultimate	M10	0.98[0.68]	2.40	3.21	2.74	0.17		Horizontal cracks in brick veneer at mid-height, on each side of window
	M10	1.15[0.75]	5.67	4.41	4.07			Significant nail pullout at majority of tie connections; diagonal cracks in brick veneer originating at window corners and horizontal cracks at gable; brick veneer unstable

* - Dynamic properties evaluated *after* the tests listed in each row.

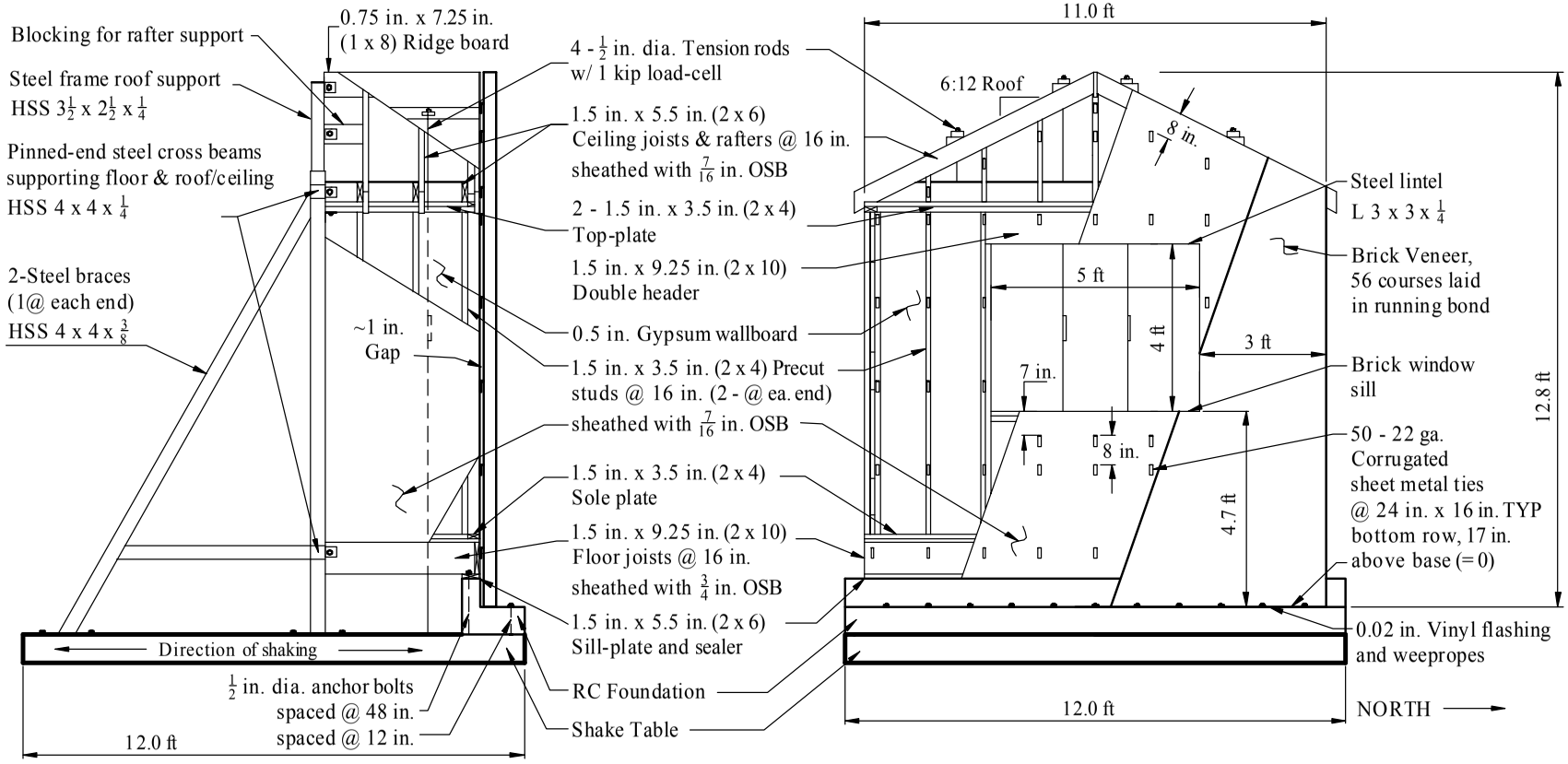

Figure 4.18 – Elevation views of the Wall-3 test structure.

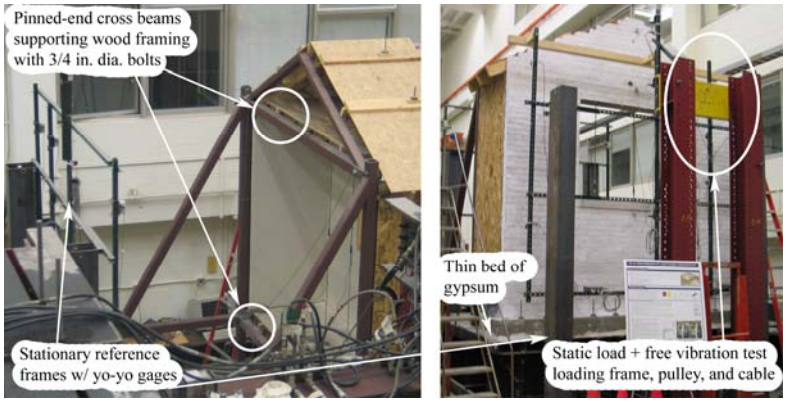

Figure 4.19 – Wall-3 test structure setup on the shake table.

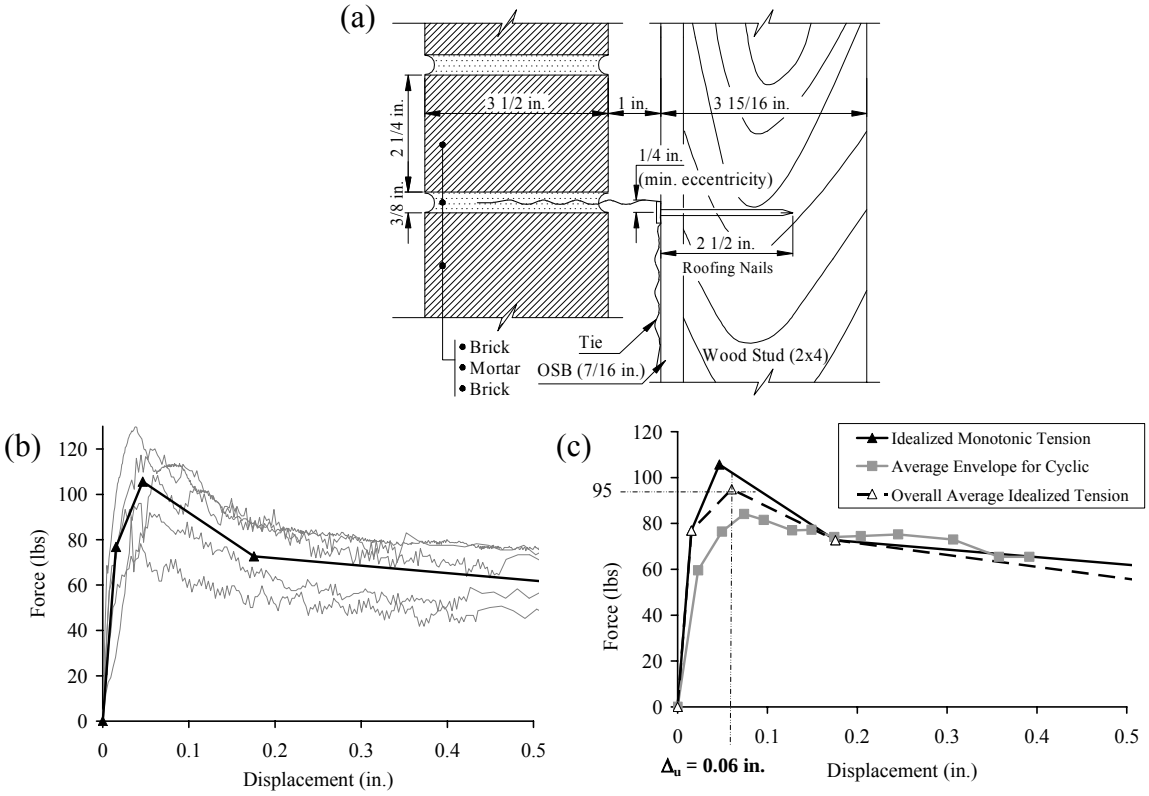

Figure 4.20 – Wall-3 tie connection details: (a) section view of installation; force-displacement behavior under (b) monotonic tension loading, and (c) monotonic tension and cyclic loading.

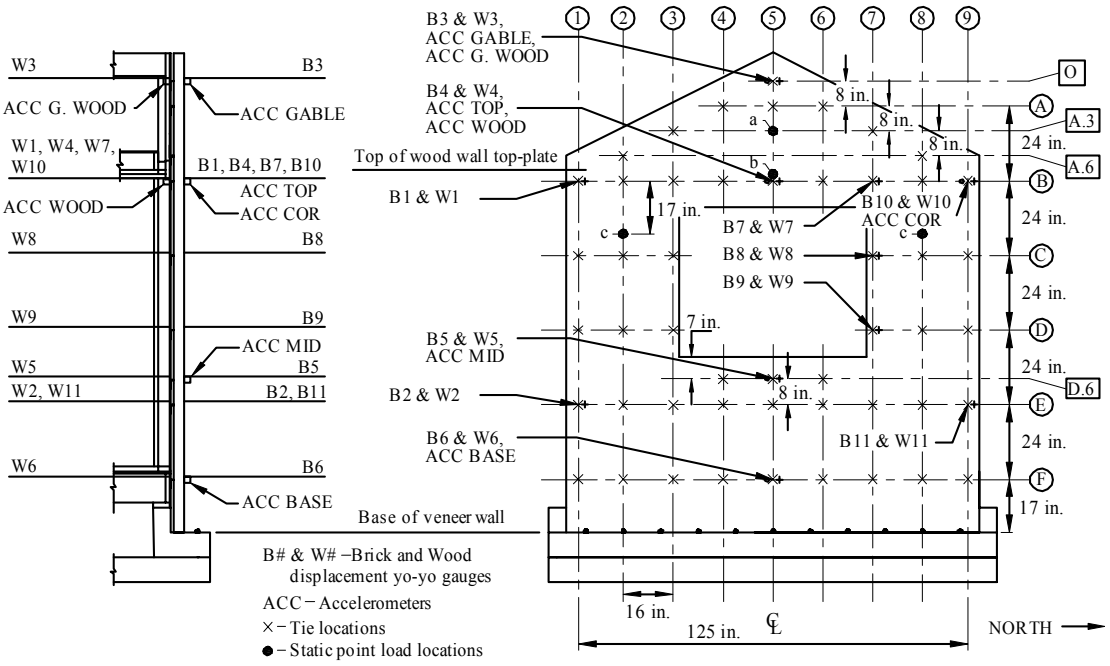

Figure 4.21 – Wall-3 specimen instrumentation, static point load location, and tie grid layout.

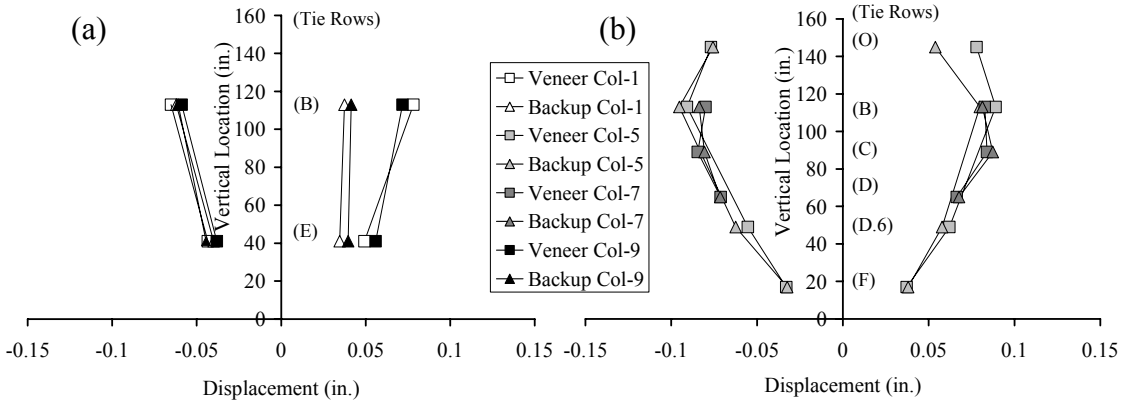

Figure 4.22 – Wall-3 peak negative and positive displacements during the M10-0.38[0.29]g test along wall (a) vertical edges, and (b) centerline and vertical window edge.

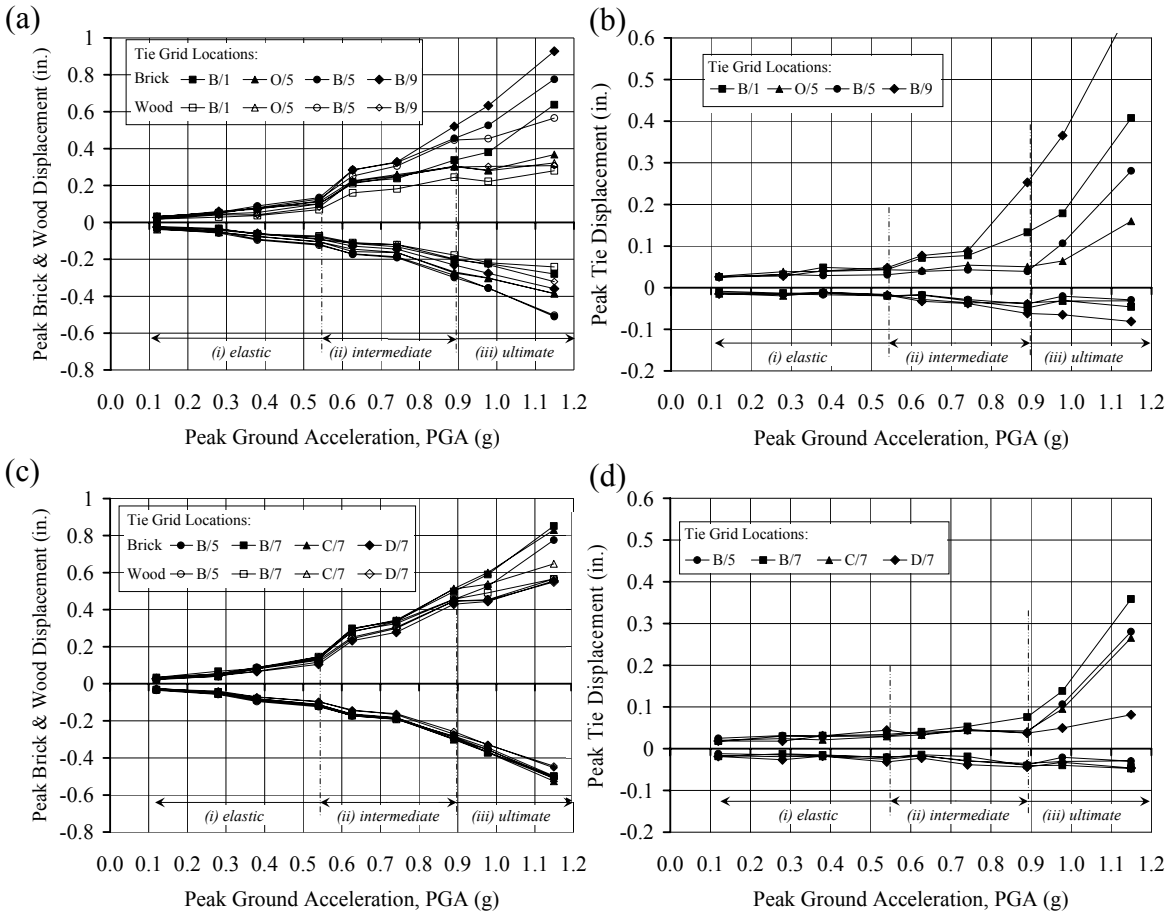

Figure 4.23 – Wall-3 peak negative and positive displacement response plots, during M10 input tests: gable (a) displacements and (b) tie elongations; window edge (c) displacements and (d) tie elongations.

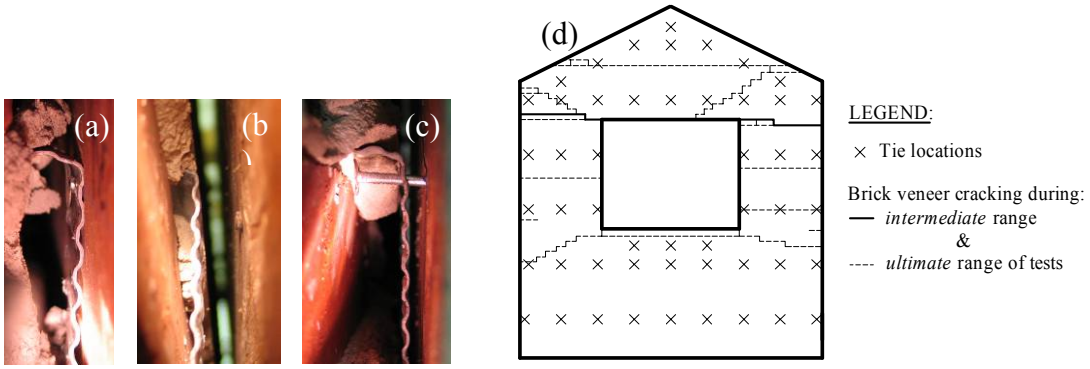

Figure 4.24 – Typical damage at the tie connections, including: (a) onset of nail pullout, (b) broken nail head, and (c) major nail pullout. (d) Observed cracking patterns in the brick masonry veneer.

FINITE ELEMENT ANALYSIS OF BRICK VENEER
PART I – SOLID WALL PANELS

Modern residential brick masonry veneer construction has been investigated by separate laboratory testing of corrugated sheet metal tie connections and full-scale solid brick veneer wall panels, as described in Chapters 3 and 4. Based on these experiments, detailed three-dimensional finite element (FE) models were developed, representing the single-story solid full-scale brick veneer wall panel specimens (Walls-1 and -2), including nonlinear inelastic properties for the tie connections. Upon calibration, the FE wall panel models effectively captured the static and dynamic experimental brick veneer wall behaviors at different response levels (up to and including tie damage and even collapse). Parametric studies were then carried out using the solid FE wall panel models to evaluate the effects of certain combinations of tie connections and layouts on the out-of-plane performance of brick veneer walls, subjected to static and dynamic loading. Results from these analytical studies provide important information on the performance limits of residential brick veneer wall construction for various tie connection and loading conditions.

5.1 Wall Structure Model

The analysis software *ABAQUS* (Abaqus Inc. 2006) and the pre- / post-processor software *MSC.Patran* (MSC 2005) were used to develop the FE brick veneer wall panel models. The models consisted of the wood frame wall panel, the brick veneer, and the corrugated sheet metal tie connections; other surrounding "boundary" components of the (experimental) test structure were implemented as spring support conditions. The wood backup spring supports, as well as the wood frame and brick veneer masonry material properties, were assumed to be linear elastic (primarily based on the observed experimental behavior). Nonlinear elastic spring supports were implemented along the base of the brick veneer wall panel, representing a rigid body rocking behavior. Nonlinear inelastic models for the tie connections were developed and implemented in the FE wall models, to capture key features of the absolute and relative performance of different types of ties and tie installation methods, as observed in both the tie subassembly tests and the wall panel tests. Analyses were performed by subjecting the FE wall models to out-of-plane static and dynamic loads, as was done in the shake table tests.

5.1.1 Wood Frame Wall Panel

The wood frame wall panel (2x4 studs and exterior OSB sheathing) was modeled as a linear elastic composite frame, as shown in Figure 5.1. Nail slip was neglected because, even after partial collapse of the veneer walls, no splitting of the wood-frame components was visible, and the nail connections remained tight. (Some small undetectable nail slip

could have occurred during testing, having an overall softening effect, but the out-of-plane response of the wood frame wall panel was mostly controlled by the (elastic) flexibility of the wood material.)

The 2x4 stud and exterior OSB sheathing composite wall panel was represented by joined 3-D beam and shell elements. These elements, while neglecting shear deformations, effectively capture the out-of-plane flexibility of the wood frame wall panel. As shown in Figure 5.1(b), the studs (beam elements for which a local axis offset *d* can be specified) were implemented as stiffeners to the exterior OSB sheathing (shell elements), where both elements shared the same nodes; as a result, the shell mid-surface axis was the reference plane of the assembled wood frame FE model. The material properties for the wood components, listed in Table 5.1, were based on the wood material grade used in the wall specimens. The interior gypsum wallboard was not explicitly modeled because its effect on out-of-plane flexure was negligible; however, its weight was indirectly accounted for as part of the OSB density specification in the model. The wood frame components were assigned the actual section dimensions from the physical model, as described earlier in Chapter 4.

5.1.2 Brick Veneer and Tie Connections

The experimental brick veneer walls generally exhibited more rigid body rotation (rocking about their base) than bending when subjected to out-of-plane static and moderate dynamic loading. However, as the level of shaking increased, the veneer showed more noticeable flexural deformations, and Wall-2 did eventually crack at mid-height prior to collapse. Overall though, experimental results indicated that wall response, up to and including ultimate cracking and collapse of the veneer, was most closely associated with the performance of the tie connections. (A few preliminary FE analyses were also carried out actually including brick veneer cracking, though.) Therefore, the brick veneer was assumed to be linear elastic and was modeled using shell elements (with their reference plane at the shell mid-surface) assigned the same section dimensions as in the test structure. The brick masonry elastic properties and density are listed in Table 5.1.

The brick veneer and wood frame backup FE models were linked together with axial bar elements representing the tie connections. The experimental load vs. displacement behaviors of the tie connections, evaluated both during tie subassembly and also brick veneer wall panel testing, were implemented in unique nonlinear material constitutive models for these axial elements, as described in more detail below.

5.1.3 Assembled Wall Model

The assembled wall model geometry is shown in Figure 5.1. The tie layout and the distance between the physical model section centerlines (of the wood frame and the brick veneer) defined the entire FE model geometry. The model was 128 in. (3.25 m) long (spanning 9 columns of ties, spaced at 16 in. [406 mm]) and 120 in. (3.05 m) tall (from the supports at the base of the brick veneer to the supports at the top of the wood frame backup). The wood frame stud wall model extended to a height of 112 in. (2.84 m) from its bottom supports at the top of the foundation to the centerline of the roof/ceiling joists

in the test structure. The brick veneer model, supported 8 in. (203 mm) below the wood frame, reached a height of 110 in. (2.79 m), terminating at the top row of ties. The small overhangs of approximately 3 in. (76 mm) of masonry beyond the edge ties of the test specimens were not explicitly modeled; however, lumped mass was added to the edge nodes of the veneer shell model based on the tributary area of these overhangs. The 3 in. (76 mm) distance between the reference planes of the brick veneer and the wood frame models (which included the 1 in. [25 mm] air space) defined the length of the tie connection elements.

Initially, coarse meshes were generated for the wood frame backup and brick masonry model elements, based on the geometry of the tie layout (a grid of 24 in. x 16 in. [610 mm x 406 mm], with masonry and wood frame element nodes aligned at tie connection locations). In a mesh refinement study, the wood frame model (subjected to a lateral point load) and the masonry veneer model (subjected to an edge moment) exhibited convergent displacement results for the element meshes shown in Figure 5.1(a), so these meshes (and more refined ones, when tie connection layouts were varied) were used for all subsequent FE modeling.

5.2 Model Support Conditions

The wood frame backup and brick veneer wall FE model support conditions were based on the test structure setup, as well as on certain key aspects of the observed experimental behavior, as explained here.

5.2.1 Wood Frame Supports

As the wall test structure was subjected to out-of-plane loads, the wood frame wall panel exhibited rotation across the bottom, as well as combined rotation and horizontal translation across the top (relative to the shake table). Because the physical supports (concrete foundation and steel reaction frame) and the surrounding wood backup components (floor and roof/ceiling framing, including rafter ties and other nail connections to the wall frame) were not explicitly modeled, their cumulative effects were incorporated into linear elastic spring supports at the top and bottom of the wall panel FE model.

Across the top of the wood frame wall panel in the test structure, direct lateral restraint was provided by the rafter ties in conjunction with the preload friction from the tension rods; rotational resistance was relatively low at these connections. Furthermore, the upper portion of the backup system (the cross beam of the steel reaction frame and the partial roof/ceiling diaphragm) was able to deflect somewhat during dynamic testing, thereby indirectly contributing additional top-of-wall flexibility. (Any diaphragm flexibility contribution to acceleration amplification during testing was somewhat limited by the relatively short length of the wall.) In order to represent these combined resistance and deformation effects, the top of the wood frame wall panel FE model was laterally supported at the end of each stud by axial (translational) spring supports, as shown in Figure 5.1(c).

As described in Chapter 4, the physical wood frame wall panel rested on top of a partial floor frame, which was in turn supported by the foundation. The OSB sheathing panels covering the exterior face of the wood frame stud wall extended down over and were connected to the much stiffer floor framing header board and sill-plate; as a result, the overlapped sheathing limited rotation of the stud wall at its base. Furthermore, the header board (which also supported the bottom row of veneer ties) exhibited small horizontal deformations relative to the shake table during dynamic loading. To account for these two behaviors, the wood frame wall panel FE model was extended down to the level of the foundation surface (below the bottom row of ties), and rotational spring elements were implemented at the wood frame wall model bottom simple supports, as shown in Figure 5.1(c). The rotational springs accounted for the restraint generated by the overlapping sheathing panels and the stiff floor framing, while the downward extension of the framing in the wall model permitted some horizontal movement of the wood frame at the level of the bottom row of ties, representing small wood frame translations that actually occurred at this location.

Overall, then, spring supports were located at the ends of each vertical beam (stud), resulting in nine translational springs across the top and nine more rotational springs across the bottom of the wood frame wall panel FE model. Preliminary analyses (presented below) were performed to calibrate the model spring stiffnesses, using static and dynamic experimental test results.

5.2.2 Brick Veneer Supports

In the experimental setup, the brick masonry veneer wall had little bond to the foundation surface because of the flashing material. The foundation did however provide lateral and vertical support (without slipping of the veneer) throughout testing, and the brick veneer wall pivoted about its base when subjected to out-of-plane loads. Therefore, pin supports with nonlinear elastic rotational springs were implemented across the base of the brick veneer wall model. As shown in Figure 5.1(d), a rigid body rocking response of the brick veneer wall was represented by these springs, which were assigned bilinear force-displacement behavior defined by the masonry wall weight and geometric properties, as explained in earlier analytical studies by Doherty et al. (2002) and Simsir (2004). In the FE model (as in the experimental structure), only the tie connections back to the wood frame provided lateral stability to the brick veneer wall.

5.3 Tie Connection Properties

The axial (tension-compression) tie connection elements were assigned nonlinear inelastic "material" properties, representing the behavior observed in the tie subassembly and brick veneer wall panel tests. Dynamic veneer wall tests showed that different levels of wall specimen response (*elastic, intermediate,* and *ultimate*) were closely related to certain key tie connection deformation limits in tension. Tensile behavior of brick veneer tie connections is generally controlled by a combination of deformation modes, such as: straightening of the tie bend eccentricity and/or of the tie corrugations, prying on the nail or screw head, nail pullout from the wood stud, yielding and tearing of the tie at the nail hole, and/or tie pullout from the mortar joint. Furthermore, at the onset of tie damage

during the dynamic veneer wall tests, measured tie connection deformations were typically similar to the opening displacements at ultimate tensile loading determined from the subassembly (monotonic tension and cyclic) tests. On the other hand, the compressive behavior of tie connections in brick veneer walls is mainly controlled by deformation of the tie itself (perhaps as also affected by eccentricity) and any beneficial restraint provided by excess mortar within the wall cavity. Therefore, the overall tie connection model was assigned nonlinear inelastic "material" properties in tension (based on subassembly test results) and linear elastic in compression (based on both subassembly and wall test results), to combine the effects of the ties and excess mortar within the wall cavity. This overall tie connection "material" model was implemented in a user subroutine (*UMAT* written in *FORTRAN90* code), to be executed outside of *ABAQUS*.

5.3.1 Tie Tensile Behavior

The average force-displacement behavior for monotonic tension, as well as the average envelope curves for the tension portion of cyclic (tension-compression) loading (plus one set of cyclic test results), are shown in Figure 5.2 for subassemblies with 28 ga. and 22 ga. ties, respectively, bent at an eccentricity from the nail. These and other tie subassembly test results indicate that the average envelope curves for cyclic (tension-compression) behavior were very similar to the companion monotonic test results, as described in more detail in Chapter 3. Because of this, the idealized (multi-linear) monotonic tension behavior from the tie subassembly tests, shown in Figure 5.3 for different tie thickness and installation configurations, was used as a simple estimate of the backbone curve for the tie connection "material" hysteresis rule in tension. For certain tie connections where the ultimate tensile strength during cyclic testing differed by more than 10% from the monotonic test results, an average of both sets of test results was used. (To apply all these experimental results into "material" models, the force-displacement responses were converted into equivalent stress-strain relations, considering the axial connection model element cross-sectional area and length.)

When loaded in tension, the tie connection subassemblies exhibited two distinct behaviors, which involved transitions from either lower-to-higher stiffness or from higher-to-lower stiffness, corresponding to combinations of various deformation modes (tie bending, straightening of the corrugations, nail pullout, yielding at the tie hole, etc.) in the connection components. The hysteresis rules representing these "material" model tensile behaviors are shown in Figure 5.4. The backbone curves are defined by the path *O-A-B-C-D*, with the envelope slopes E_1 through E_4 assigned to be the converted idealized monotonic tension behavior properties (from Figure 5.3). The unloading slope (E_5) was estimated from cyclic test results to be constant at all stages of deformation; after the unloading path reaches zero stress (*a-b*), the path maintains zero stress (*b-O*) until compression or reloading occurs. The reloading paths (E_r) were estimated to be linear (*O-a*) from the point where reloading begins to the load reversal point on the backbone curve (at the highest previously imposed strain), a reasonable approximation of the tie subassembly cyclic test results. For one range of reloading in the low-to-high stiffness hysteresis rule (Figure 5.4(a)), slightly different paths are followed – if the highest previously imposed strains along the backbone curve are between points *A* and *C*,

and if reloading begins at a strain below point *A*, the path first follows along a line parallel to E_1; after passing the strain *A*, it then aims at the load reversal point on the backbone curve, as in (*c*-*d*-*e*).

5.3.2 Tie Compressive Behavior

As stated above, wall tie connection behavior in compression was generalized as linear elastic (E_6), as shown in Figure 5.4. Compressive strength and stiffness values from subassembly testing were found to be lower bounds for actual brick veneer walls, owing to the invariable presence of some "mortar droppings" in the air cavity that effectively increased both the compressive strength and stiffness of the tie connections. To determine the effect of excess mortar on tie compression stiffness, experimental veneer wall dynamic test results were studied to relate peak tie deformations in tension to those in compression for *elastic* and early *intermediate* levels of wall response, where the peak tie elongations were generally in the initial tie stiffness region. From this, it was noted that peak deformations in tension were approximately two to four times those in compression. As described below, then, preliminary time history analyses were performed (in conjunction with calibration of the spring support properties) to determine an appropriate multiplier for idealizing the tie connection compressive stiffness as a function of the initial tensile stiffness found from the tie subassembly tests.

5.3.3 User Subroutine

The idealized behavior (including hysteresis) of a single tie connection (nonlinear inelastic in tension and linear elastic in compression) was too difficult to represent with standard available constitutive models; thus, a user subroutine (*UMAT*) was written in *FORTRAN90* code to be executed outside *ABAQUS*. During nonlinear FE analysis, the subroutine is called at all material calculation points and produces updates for the axial (one-dimensional) stress at the end of each increment, by following the hysteresis rules in tension and the linear elastic rule in compression, as described above. Hysteretic curve properties presented in Figure 5.4 (stress-strain pairs at points *A* through *D*, and slopes (moduli) E_n for $n = 1$ through 6) were specified as part of the wall model input. The subroutine updated the solution-dependent state variables (highest imposed strain and corresponding stress on the backbone curve) to determine the reloading paths (E_r), as needed. (As shown in Appendix C.1, the subroutine was driven by a state table.) Presented in Figure 5.5, then, are examples of the force-displacement behaviors for the tie connection models (28 and 22 ga. ties bent at an eccentricity) cycled at gradually increasing displacements (representative of the experimental cyclic behaviors in Figure 5.2); tie connection model force-displacement "repeat" cycles not reaching the backbone curves were also verified to be representative of experimental behavior.

5.4 FE Model Setup and Analysis Procedure

FE models representing the experimental specimens (Walls-1 and -2) were developed and calibrated per experimental observations. The FE wall models were then validated to capture the experimental specimen behaviors at different static and dynamic load levels.

Finally, parametric studies were carried out with the wall models under static and dynamic loads, by varying the tie connection types and the tie connection layouts.

During calibration, the FE wall model was subjected to static and dynamic loading as in the experimental study; the model was then verified to capture different levels of experimental specimen dynamic response. Preliminary linear elastic calibration analyses were performed with static point loads applied to the FE wall models at the same locations and of equal magnitudes as in certain experimental tests. Time history analyses were then conduced by using the electronic earthquake records from the shake table testing program, which were labeled as the M10, M02, and Nahanni earthquakes, as shown in Figure 5.6. These electronic earthquake records were normalized and scaled with respect to peak ground acceleration (PGA). Throughout calibration and validation of the FE wall model, analytical wall panel response and scaled electronic earthquake record PGA values were compared with experimental wall response and corresponding electronic earthquake record "nominal scaled" PGA values. (As described in Chapter 4, measured shake table PGA values were identified to be somewhat spurious maximums because they did not represent scaling values across the entire frequency range of the applied earthquake records; therefore, "nominal scaled" PGA values were computed to better match the intensities of input earthquake records to those of actual measured shake table acceleration histories.)

The earthquake records were applied to the FE wall model wood frame backup and brick veneer supports. Time history analyses were executed in *ABAQUS* using the direct integration method. The maximum time step was specified as 0.01 sec (roughly $1/10^{th}$ of the wall models' natural periods of vibration), and the minimum as 1E-15 sec. Automatic time incrementation was used during the analyses to control the accuracy of the solutions, by specifying the half-step residual tolerance. The residual, a fraction of the estimated total horizontal reaction in the model (from taking into account the tie connection capacities), was assigned as 2 kips (9 kN) to provide adequate solutions in the analyses. From shake table testing, the experimental viscous damping ratios were approximated to be 3% and 5% of critical for Walls-1 and -2, respectively; as a result, an average of these experimental values (4%) was used in the FE models. This damping was implemented in the model material properties with Rayleigh damping coefficients (mass and stiffness proportional damping). To evaluate these coefficients, eigen-frequency analyses were performed on the wall models to evaluate the first and second mode frequencies, with the tie connections modeled as linear springs (using the average initial tension/compression stiffness).

During shake table testing (described in Chapter 4), displacement measurements were used to evaluate different levels of wall specimen behavior. The displacements were measured at key tie locations throughout the wall specimens and on the shake table, thereby providing veneer and backup displacements relative to the shake table and also differential displacements between the veneer and backup (tie deformations). The experimental peak displacement response of the wall specimens was noted in the positive (outward; veneer deflecting away from the backup) and negative (inward) directions; likewise, peak experimental tie deformations were measured in both directions for each

particular test. (The maximum positive displacements of the brick veneer and of the wood backup, as well as the peak positive tie deformations, were of particular interest because these results were closely related to different levels of experimental specimen response and damage.) Similarly, for the FE wall models, computed displacements (at the same tie locations as in the experimental specimens) were used to first verify and then further identify the model response when subjected to out-of-plane loading (i.e., peak brick veneer and wood backup model displacements relative to the supports, as well as peak relative displacements between the veneer and the backup models). Key analytical and experimental results are presented below to establish the validity of this "calibrated" model, followed by parametric studies and overall FE analysis findings.

5.5 Preliminary FE Analyses

Preliminary static and time history analyses were performed to establish reasonable linear elastic properties for the spring supports and for the tie connections in compression, from comparing analytical and experimental results. The effect of brick masonry veneer cracking on overall wall performance was also evaluated.

5.5.1 Spring Support Properties

Static FE analyses were performed on a model of the bare wood frame wall panel (without brick veneer in front), subjecting it to static out-of-plane point (pull) loads at the top-plate and at 16 in. (0.4 m) below it, as was done during preliminary experimental testing (Figure 4.4). Then, time history analyses were performed using complete (wood frame plus brick veneer) FE models of Walls-1 and -2, applying acceleration traces scaled to levels that produced *elastic* to *intermediate* amounts of response in the experimental brick veneer wall panel specimens.

In these preliminary analyses, computed displacements of the wood frame backup were compared to those measured during the experiments. Based on the results, each of the nine rotational springs across the bottom of the wood frame panel FE model was assigned a stiffness of 1,000 k-in./rad (110 kN-m/rad). Across the top of the wood frame panel model, the seven "interior" lateral translational springs (in between the corners) were each assigned a stiffness of 0.8 k/in. (140 kN/m), while the two corner springs were assigned four times that stiffness (3.2 k/in. [560 kN/m]), to represent the higher stiffness at the top corner connections of the wood frame wall panel to the reaction frame due to the additional hurricane ties.

5.5.2 Tie Connection Compression Properties

While calibrating the support springs, time history analysis results were also used to approximate the multiplier (of initial tension stiffness) appropriate for the tie connection linear elastic compression properties. These linear elastic properties were estimated to represent the compressive strength and stiffness of tie connections influenced by excess mortar in the wall cavity. During the FE analyses, peak tie deformations, as well as the overall veneer wall model displacement response, were compared to the experimental results. The linear elastic tie compression properties were approximated as $E_6 = 3.5 \times E_1$

(Figure 5.4), with an upper stiffness limit of 8.5 k/in. (1,500 kN/m). This same multiplier and limit were also used later to estimate the adjusted compression properties for tie connection models representing other tie types that were not implemented in the veneer wall tests (but that were part of the tie subassembly testing program), in order to permit FE model analyses of various tie scenarios. As presented later in Section 5.7, the out-of-plane performance of brick veneer walls was also evaluated as a function of the nonlinear inelastic properties in compression for the tie connections, as evaluated from tie subassembly tests without capturing the effect of excess mortar in the wall cavity (Figure 3.8). The out-of-plane capacities of brick veneer walls subjected to inward pressures (governed by the compressive properties of ties) were then compared to the capacities of walls subjected to outward pressures (as governed by the tensile properties).

5.5.3 Cracking in the Brick Masonry Veneer

As seen from the experiments, the brick masonry veneer under out-of-plane loading eventually experienced some cracking during testing due to flexural deformations. Cracking in the brick veneer generally took place along clearly defined linear patterns, primarily along the mortar joints. Brick masonry veneer cracking has sometimes been represented with a discrete crack model by introducing hinges between wall element nodes, as shown by Arumala (1991) and Junyi et al. (2003). Casolo et al. (2000) demonstrated that a classic plasticity model is also effective at capturing the pre- and post-cracked flexural behavior of masonry. The effects of cracking on the performance of the current brick veneer wall panel models were investigated by introducing hinges with elastic-plastic rotational resistance between the brick veneer shell element nodes, as described in greater detail in Appendix C.2. This type of a cracking model was effective at capturing the performance of the wall panels leading up to and including cracking. Overall, however, cracking was not represented in the final analytical program, in order to simplify the wall panel models for various parametric studies, and also because the most important features of brick veneer wall performance were effectively represented through utilizing detailed nonlinear inelastic FE models for the tie connections.

5.6 FE Model Validation

During the calibration process (discussed above), the FE wall models were subjected to static and dynamic loading as in the experimental study; the models were then verified to capture different levels of the experimental specimen response. Some key analytical and experimental results are presented here to establish the validity of these "calibrated" models.

5.6.1 Static and *Elastic* Dynamic Loading

As described in Chapter 4, the wall test specimens were subjected to modest static point loads, to evaluate the relative stiffness of the walls resulting from different veneer to backup connections. These static point (pull) loads were applied to the veneer of Wall-1 (300 lbs [1.3 kN]) and Wall-2 (250 lbs [1.1 kN]) at 40 in. and 16 in. (1.0 m and 0.4 m) below the top of the veneer, respectively; FE wall models representing the specimens were subjected to these same loads. As shown in Figure 5.7, the FE models of Walls-1

and -2 captured the overall trends in outward displacements (of veneer and backup) relative to the supports, as well as the tie elongations, when compared with the experimental results for these relatively low loads.

Some small disparities are present in these analysis results. The FE models of the wood frame backup deflect a bit more than the experimental specimens (while the veneer deflects by almost the same amount in the model and in the experiment); as a result, the tie elongations are somewhat smaller for the FE models than in the experiments. The main explanation for these differences is probably the low magnitude of the applied loads, for which the wall specimen behavior was disproportionately affected by factors not represented in the models, like friction. To evaluate more significant response of the wall models, scaled earthquake records were applied. The models were verified to capture the response of the experimental specimens (Walls-1 and -2) at different stages of behavior, first by subjecting the FE models to scaled input records that produced specimen response at the end of the *elastic* level (tests that caused significant excitation of the specimens without tie damage). Later, the wall FE models were also subjected to input records that produced *intermediate* and *ultimate* response levels of the test specimens, sufficient to cause tie and brick veneer wall damage.

The FE wall model first elastic period of vibration was computed to be 0.12 sec for Wall-1 and 0.17 sec for Wall-2, which were similar to the experimental wall panel periods (at onset of testing). Models of Walls-1 and -2 were subjected to the M10 input record scaled to 0.51[0.38]g and 0.23[0.18]g, respectively, to verify the model response at the end of the *elastic* level (these scaled inputs caused similar levels of total response in their respective specimens). FE and experimental peak displacements of the brick veneer and the wood backup in the positive and negative directions, as well as peak tie deformations (in each direction), are compared in Figure 5.8 for Walls-1 and -2. The FE wall specimen models effectively captured overall wall displacements and key tie deformations in both directions. The end of *elastic* response of the experimental wall specimens (similar to that in Figure 5.8) was also captured by the FE models for the other earthquake records (M02 and Nahanni) used during the testing program. For the M02 input record, the analytical response of the Wall-1 model was higher, and the response of the Wall-2 model was lower, than the experimental response; this may have been an effect of some sharper changes in the M02 response spectra near the wall specimen and model periods of vibration. (An example set of analysis and experimental results are shown in Figures C.6 and C.7 (Appendix C.3), respectively, for Walls-1 and -2 subjected to these records.)

The M10 (nominal) earthquake test and FE analysis PGAs with their corresponding maximum displacement responses of the brick veneer, the wood backup, and the tie connections (at key tie grid locations) are shown in Figures 5.9 and 5.10, respectively, for Walls-1 and -2 (for both inward and outward movement). Overall displacement vs. dynamic input PGA analysis results exhibit a linear relationship in the *elastic* range of behavior, with FE analysis results closely matching the experimental response. The FE models also effectively captured higher tie forces in the upper regions of the wall panels, and at those ties anchored to stiffer backup regions (near the supports). For lower magnitude dynamic loading (early *elastic*), the FE wall model of Wall-1 slightly

overestimated overall experimental displacement results, and the computed tie deformations appear to be a bit off from experimental values. (Measured experimental tie deformations were less accurate during early dynamic tests due to the level of instrumentation noise in the displacement data compared to the actual tie deformations; however, this was only true for relatively small deformations, of approximately 0.04 in. [1 mm] or less, while the noise was insignificant for higher input tests.) For Wall-2, peak wood frame backup displacements computed with the FE models in both directions are somewhat lower than in the experiments; however, the displacements of the brick veneer as well as tie deformations in both directions are close to the experimental results. Overall, the FE models have mainly been used to evaluate veneer wall response at much higher loads, where these modest discrepancies present at lower levels of loading did not play a critical role.

5.6.2 *Intermediate* and *Ultimate* Dynamic Loading

During the experimental study, it was noted that the overall veneer wall response (at *elastic, intermediate,* and *ultimate* levels) depended primarily on the performance of the tie connections. Veneer wall damage started off at certain tie connections; as damage spread, the brick veneer walls became more unstable (and susceptible to cracking), and they each eventually collapsed. At the onset of tie damage during dynamic wall testing, peak measured tie elongations were found to be closely related to elongations determined for ultimate loading during the tie subassembly tests. First tie failures occurred at the top of the walls, near stiffer regions of the wood backup (at the corners). As the shaking increased, damage spread to adjacent ties across the top row and then to lower rows, ultimately leading to collapse. Based on these experimental results and observations, the occurrences and sequences of tie damage were assessed with the FE models. Tie connection damage in the FE models was determined from the maximum computed tie elongations. At a stage when these elongations exceeded the ultimate load capacity opening displacements found from the tie subassembly tests (approximately 0.19 in. [4.8 mm] for the ties used in Wall-1 and 0.36 in. [9.1 mm] for the ties in Wall-2 (Figure 5.3(c)), the tie connections in the FE models were considered to be damaged. Three damage limit states were then identified for these FE wall panel models, based on the onset of tie failures at key tie locations in the model (per the tie grids shown in Figure 5.1(a)), which were related to the experimental wall behavior and damage, as follows (FE analysis – *experiment*):

(i) first tie failure at top corners (at grids A/1 & A/9) – *same [end of elastic range]*;
(ii) tie failures across entire top row (across row A) – *highest input before collapse, accumulation of tie damage [end of intermediate range]*;
(iii) tie failures across second row (across row B) – *instability/collapse [end of ultimate range]*.

Three distinct levels of tie connection and brick veneer damage that were found experimentally were effectively represented with the three associated levels of tie damage (initiation and accumulation) in the FE wall models, as presented in Table 5.2 for the M10 input record. (During the experimental study, the greatest response of the specimens for any particular PGA value typically occurred for the scaled M10 input record.) First, the onset of tie damage at the top corners of Wall-1 was computed with the FE models to occur at a similar PGA as during the related test; analysis results for

Wall-2 predicted initial tie failure at a somewhat higher level of shaking, probably because the Wall-2 experiment was slightly affected by a set of tests (Wall-2b) with post-installed anchors, which may have contributed some fatigue damage at the top corner ties.

The second and third levels of damage were assessed with the FE models at higher PGAs than measured experimentally because the test specimens had experienced a number of complete tie failures (by fracturing) which were not represented in the FE models. Therefore, another set of analyses were conducted using the FE models without the tie connections at the locations where complete failure had been noted in the experiments. After accounting for tie damage, the analytical PGA values were significantly closer to the experimental results (Table 5.3). Both sets of analytical displacement results are compared to the experimental values in Figures 5.9 and 5.10. Overall, the FE wall panel models effectively captured the experimental wall behavior and ultimate dynamic load capacity by representing the key nonlinear inelastic behavior of the tie connections, closely matching their force-displacement response (up to their peak and even post-peak capacities). The FE wall panel models also consistently exhibited a close match to experimental wall response in the negative (inward) direction (Figures 5.9 and 5.10). Overall, these three levels of tie connection and brick veneer wall damage can also be associated with the seismic performance levels assigned for architectural components per ASCE 41-06 respectively as Immediate Occupancy, Life Safety, and Hazards Reduced.

The same levels of damage were also evaluated with the M02 and Nahanni earthquake inputs from the experimental program, as shown in Table 5.3. These earthquake records were normalized with respect to PGA and then scaled at 0.05g increments, showing that the M02 and Nahanni earthquakes had to be elevated to higher PGAs than the M10 record to cause the three damage limit states. The variation between the earthquake inputs resulted in a somewhat different response of the wall model, indicating that the M10 earthquake had relatively the most damage potential, so it was therefore selected for the parameter studies described below. These criteria for different stages of veneer wall damage were then also implemented to assess the ultimate performance of other veneer walls with different types and layouts of ties, as presented here below.

5.7 FE Wall Model Parametric Studies

5.7.1 Brick Veneer Wall Panel Parameters

Parametric studies were conducted to explore effects on out-of-plane seismic performance of brick veneer walls due to different brick veneer tie connection details. FE wall panel models were generated to represent veneer walls built in accordance with prescriptive construction and design requirements (per MSJC (2008), IRC (ICC 2003), and BIA Technical Notes (2002, 2003)), as well as per methods employed in actual construction practice (which do not always meet the prescribed requirements). As described in greater detail in Chapter 2, for brick veneer built over a wood-frame backup, codes require that the corrugated sheet metal ties should be at least 22 ga. (0.031 in. [0.8 mm]) thick, embedded at least 1.5 in. (38.1 mm) into the brick veneer mortar joint (with at least 0.625 in. [15.9 mm] mortar cover to the outside face), attached to the wood

backup studs with at least 8d nails, and installed with a maximum bend eccentricity of 0.5 in. (12.7 mm) (with the exception of the IRC, which does not specify tie bend eccentricity or embedment length limitations). The air cavity between the brick veneer and wood backup should be 1 in. (25.4 mm). Furthermore, the maximum wall area supported by a tie is limited to 2.67 ft^2 (0.25 m^2) for construction in seismic design categories C and below, which is reduced to 2.0 ft^2 (0.19 m^2) in higher seismic design categories (among several other requirements for those design categories, such as installation of horizontal joint reinforcement); respectively, these wall areas correspond to tie grid spacings of 24 in. x 16 in. (610 mm x 406 mm), and 16 in. x 16 in. (406 mm x 406 mm), in actual construction. Furthermore, the MSJC (2008) and IRC (ICC 2003) require that ties be provided within 12 in. (305 mm) of wall edges near openings; this is reduced to 8 in. (203 mm) in BIA (2003), with this maximum edge distance recommended for tie placement near openings, as well as at other discontinuities in brick veneer walls (such as at wall edges, expansion joints, or shelf angles). The IRC also specifies a maximum tie spacing limit of 36 in. (914 mm) around wall opening perimeters. The test specimen configuration, shown in Figure 5.1(a), represents a wall panel built in general conformance with most of the prescriptive code requirements for tie installation in seismic design category C, and also included ties within 8 in. (203 mm) of all edges of the wall panel.

In actual construction practice, tie installation in brick veneer walls frequently deviates from these requirements. As outlined in greater detail in Chapter 2, brick veneer wall damage from fairly recent moderate earthquakes and strong wind events has revealed various deficiencies in construction practice, particularly in tie connection installation details. Ties are often spaced further apart than permitted by codes, and thinner 28 ga. ties are widely used, attached either with 6d or 1.25 in. (32 mm) long roofing nails. Recent visits to local construction sites around central and northern Illinois further confirm the common use of 28 ga. ties (often at fairly large eccentricities) with 1.25 in. (32 mm) roofing nails; however, it was also noted that reduced tie spacings (such as 16 in. x 16 in. [406 mm x 406 mm]) have sometimes been adopted. Overall, it appears that residential brick veneer walls are typically constructed without inspection, and therefore tie connections are frequently installed by the preferred methods of the masons. Variability in workmanship during tie installation was represented analytically by implementing the different tie connection properties established from subassembly tests, as shown in Figure 5.3(a).

After calibration and validation of the FE brick veneer wall model, the test specimen configuration was analytically adjusted to represent various combinations of tie connection layouts, as shown in Figure 5.11. General tie grids of 24 in. x 16 in. (610 mm x 406 mm) and 16 in. x 16 in. (406 mm x 406 mm) were employed; the tie grid of 24 in. x 16 in. was also varied as a function of location of the bottom row of ties from the base of the wall panel, resulting in approximately 12 in. (305 mm) of brickwork above the top row of tie connections. The tie layout was also staggered into a “checkerboard” pattern, resulting in a 12 in. x 32 in. (305 mm x 813 mm) spacing. (These geometric and tie layout variations did not require significant adjustments to the FE model of the test specimen configuration; the boundary conditions were unchanged, with the exception of

some necessary rearrangement of the wood backup frame and shell elements to match the tie layout geometries.)

The various wall panel models are labeled as "Tie Layout / Tie Properties" per the following: Tie Layout is identified as grid A through D, and in some cases including (5) or (9) extra ties between the top two rows (Figure 5.11(a)); and, Tie Properties is identified by attachment type, thickness, and bend eccentricity (Figure 5.3(a)). For example, the Wall-1 specimen configuration is labeled as "A/N(8d)28min"; then, a wall labeled as "A (5)/N(8d)28min" would have the same properties as the test configuration, with 5 extra ties added between the top two rows of ties, and so on. During these analytical studies, the earthquake record labeled as M10 was utilized, which was normalized with respect to PGA, and then scaled up in PGA increments of 0.10-0.20g for loading in the elastic range of wall behavior, and at reduced increments of 0.05g when estimating wall panel damage limit states. The criteria set earlier to evaluate the three levels of veneer wall model damage during the validation analyses were also used here; during a particular analysis, peak tie elongations exceeding the elongations at ultimate load (from the subassembly tests) at key locations in the wall models were used to evaluate the levels of veneer damage. Additionally, static pushover analyses were performed on the FE wall models subjected to uniform suction pressures, to determine the performance of veneer walls with different types of tie connections and tie layouts. A total of twenty five wall panels were examined.

5.7.2 Parametric Study Results and Discussion

Dynamic FE analysis results (in the form of dynamic pushover plots) are grouped and summarized in Figure 5.12, showing the M10 PGAs vs. peak outward brick displacements evaluated at the top center of the wall panels (at grid location A/5 per Figure 5.1 (a)). PGA values to cause the three key damage limit states for brick veneer wall panels with various tie connection properties are also summarized in Table 5.4 (with an example set of PGA vs. key tie elongation results shown in Figure C.9 in Appendix C.4). In general, analysis results indicate that the PGA at ultimate response (instability/collapse) of the veneer walls was relatively close to the PGA at the onset of tie failures (at wall corners). As mentioned earlier, wall displacement response at certain locations for higher PGA values might be somewhat arbitrary because wall cracking and other factors were not represented analytically; however, wall model outward displacement up to the peak load points accurately reflected the key effects of tie connection tensile deformations.

As seen from Figure 5.12(a) and Table 5.4, tie connection strength and stiffness properties had a major influence on the out-of-plane seismic performance of brick veneer walls. The relative out-of-plane stiffness of the veneer walls is closely related to the initial tension stiffness for the type of tie connections used. At onset of the second damage limit state (defined by tie failure across the entire top row), wall panel models with high-to-low stiffness ties experienced significant out-of-plane softening (down to below 50% of their initial out-of-plane stiffness); walls with low-to-high stiffness ties typically first underwent out-of-plane hardening, as wall damage progressed. For most types of tie connections, ultimate capacities of the walls were proportional to tie

connection tensile capacities, except for the wall with the most flexible tie connections (28 ga. nailed with maximum allowable eccentricity), which performed worse even though these tie connections were not necessarily any "weaker" than the others. Walls utilizing 22 ga. ties and one with a best case installation of 28 ga. ties, attached with larger nails (8d or similar) or screws, sustained much higher loading than walls utilizing short roofing nails and/or 28 ga. ties with the maximum allowable bend eccentricity. The out-of-plane dynamic load capacity of brick veneer walls with poorly installed tie connections, such as those utilizing short roofing nails (sometimes as short as 1.25 in. [32 mm], as commonly seen used in practice), will be reduced to 50% or lower of the capacity attainable with code-compliant installation and the use of 8d (or similar) nails.

Grid spacings also played a major role in overall wall performance, as seen in Figure 5.12(b-c). The location of the first row of ties at 8 in. (203 mm) below the original layout, which equals to three courses of brick masonry in real construction, determined the location of the top row of ties and therefore the ultimate behavior of the wall panels. As shown in Figure 5.12(b-c), brick veneer wall response and ultimate behavior was sensitive to the supported brick veneer wall areas and mass at the top of the wall panels. Walls with the top row of ties located approximately 12 in. (305 mm) below the top of the wall panel (tie grid B), resulted in a 15% to 30% reduction in overall strength compared to those with ties located at the very top (tie grid A). Staggering the tie connections in a "checkerboard" pattern (tie grid C), also resulted in a noticeable reduction in overall stiffness and strength, even though the total supported wall area per tie was generally unchanged. Furthermore, the test structure configuration with a tie grid of 16 in. x 16 in. (406 mm x 406 mm) (tie grid D), prescribed for wall construction in seismic design category D and above, sustained approximately 25% higher intensity shaking than the same walls with a tie grid of 24 in. x 16 in. With reduced tie spacing, even a wall panel comprising ties attached with short roofing nails resulted in an out-of-plane dynamic capacity comparable to walls designed and built for seismic design category C. The addition of only a few tie connections can be just as effective at increasing the total strength of the walls as reducing the spacing altogether, as seen in Figure 5.12(d). For walls with tie grids of 24 in. x 16 in. (610 mm x 406 mm), adding five or nine extra ties to the top of the wall panel (respectively, a 10% or 20% increase in the total number of ties), resulted in a significant increase in wall capacity (by up to 25-40%). In general, these results emphasize that the tie connections in the upper portions of veneer walls play a critical role in overall wall performance in response to dynamic horizontal out-of-plane loading.

5.7.3 Static Pushover Analysis

Static pushover analyses were performed by subjecting the veneer wall FE model outer shell elements to uniformly distributed pull (outward) loads (representing a wind "suction" pressure load), and also to push (inward) pressure loads. As mentioned previously, residential veneer wall damage often occurs due to excessive wind suction pressures, placing a high demand on the tensile performance of the tie connections. For comparison, inward pressure analyses were conducted to evaluate the brick veneer wall capacity as a function of tie compressive properties based on tie subassembly test results

(as shown earlier in Figure 3.8), where the positive effect of mortar droppings in the wall cavity were not represented.

Uniform suction pressure load vs. displacement responses of the FE wall models are shown in Figure 5.13(a-b). The effects of the different types of tie connections are clearly visible in these results. The relative stiffness of the veneer walls is closely related to the initial tension stiffness for the type of tie connections used (Figure 5.3). As also seen from the dynamic test results, for most types of tie connections the ultimate capacities of the walls were similar, except for the wall with the most flexible tie connections (28 ga. nailed with eccentricity), which performed worse even though these tie connections were not necessarily any "weaker" than the others. Overall, the wall panels with tie connections fastened using 1.5 in. (38 mm) roofing nails were the weakest ones. The wall model with a 24 in. x 16 in. tie spacing exhibited a uniform capacity below 30 psf (1.5 kPa). This capacity is less than the minimum design unfactored leeward wind pressure (suction) often used for wall components and cladding of typical residential structures for exposures in the coastal regions of the U.S.; even in non-coastal regions, this capacity can be less than the appropriate factored design wind suction pressure.

FE analysis results for brick veneer wall models subjected to uniform inward pressures are shown in Figure 5.13(c). Brick veneer walls with 28 ga. ties exhibited ultimate uniform pressure capacities of approximately 20 psf (1.0 kPa). On the other hand, brick veneer anchored with 22 ga. ties resulted in a peak inward wall pressure capacity comparable to its peak outward pressure capacity. As mentioned earlier, the tie connection compressive properties from subassembly tests were only seen as lower bounds because the effect of mortar droppings in the wall cavity was not represented by those experiments. However, the peak inward pressure analysis results further prove the desirability of using at least 22 ga. ties because relying on the positive effect of mortar droppings on the 28 ga. ties a priori may not be advisable. Overall, the displacement ranges for all of these static pushover curves going well past the wall ultimate load points and into the unloading range could be viewed as somewhat arbitrary because masonry veneer cracking (not represented by these models) can occur at such higher displacements (after the onset of tie damage). The wall model load-displacement curves up to the peak load points, however, do accurately reflect the effects of individual tie unloading (post-peak) behavior.

5.8 Summary and Conclusions (Solid Wall Panels)

Three-dimensional FE models were developed to represent one-story, residential brick veneer on wood frame construction wall panels, based on full-scale experimental brick veneer wall specimen and brick-tie-wood subassembly test results. The FE wall model wood frame backup, brick veneer, and support conditions were modeled as linear elastic; the corrugated sheet metal tie connections were modeled as nonlinear inelastic, to specifically capture different tie connection features (as a function of tie thickness and installation method). The FE wall models were calibrated and validated per experimental results to capture the veneer wall behavior at different static and dynamic load levels.

Then, parametric studies were performed using the FE wall models, by varying the tie types, installation methods, and layouts. With respect to the overall modeling procedure and the parametric studies, the most important results and conclusions may be summarized as follows:

- The brick veneer FE wall models developed were able to effectively capture static and dynamic performance of the experimental test specimens at different levels of loading. Various degrees of brick veneer wall damage observed experimentally (onset of tie failure, spread of tie failures across the top row, and ultimately collapse) could be captured by considering whether tie connections at key locations in the models exceeded their ultimate load (and/or displacement) capacities.
- For the various FE wall models with different tie connections subjected to out-of-plane dynamic loading, the scaled dynamic PGA inputs necessary to cause first tie damage and to cause complete collapse were often not much different from one another.
- Static and dynamic analyses of the FE brick veneer wall models provided relative out-of-plane strength capacities of brick veneer wall systems as a function of the tie connection properties. The walls containing 28 ga. ties without an eccentricity from the nail at the tie bend typically exhibited capacities similar to (or even above) those with 22 ga. ties; however, walls having 28 ga. ties with an eccentricity of the bend performed very poorly, compared to the other cases. The use of wood screws to attach ties to the wood backup resulted in a significant increase in overall out-of-plane strength of the brick veneer walls, whereas the wall panels with tie connections fastened using short roofing nails were the weakest ones. In general, stiffer tie connections, and not necessarily stronger ones, improved the overall strength of the veneer walls modeled (Figures 5.12(a) and 5.13).
- The top row of ties in the brick veneer walls played a critical role in the overall strength of the wall panel FE models, which was also demonstrated in the experimental studies. The location of the bottom row of ties determined the resulting tie layout, and therefore the extent of brick masonry beyond the top row of ties. Relatively small variations in the masonry wall dimensions beyond the top row (edge) ties played a significant effect on the ultimate performance of the brick veneer walls. Rearrangement of the tie layout into a checkerboard pattern, resulting in removal of top row ties at every other stud, still satisfied many of the prescriptive code requirements, but it reduced the overall wall panel strength. The out-of-plane strength of brick veneer walls improved significantly when a reduced tie spacing was employed (Figure 5.12(b,c)).
- The addition of ties at every stud or every other stud between the top two rows of ties significantly improved the overall strength of the veneer walls (Figure 5.12(d)).
- For some of the tie connections investigated, the ultimate uniform pressures that could be sustained by the veneer walls did not compare favorably to typical design wind suction pressure loads for different geographic regions where residential brick veneer construction is widespread. This is another indicator of

how “sub-standard” tie connection behavior can impact overall brick veneer wall performance at the systems level during extreme loading events.

Table 5.1 – FE wall model material properties.

Material	Modulus of Elasticity, E (ksi)	Poisson's Ratio, ν	Density, ρ (pcf)
Wood Studs[a]	1,200	0.4	26.2
OSB Sheathing[a]	930	0.4	31.2
Gypsum Wallboard	-	-	41.2[b]
Brick Masonry	2,000[c]	0.2	115[b]

[a] Modulus of elasticity and density from NDS (2001).

[b] Density from wall specimen material weight.

[c] Modulus of elasticity determined from masonry prism tests.

Table 5.2 – Damage limit state PGAs for solid wall panels subjected to the M10 earthquake, experiments vs. analysis.

Damage State	Wall-1			Wall-2		
	Experiment Nominal Scaled PGA (g)	FE Scaled PGA (g)	FE* Scaled PGA (g)	Experiment Nominal Scaled PGA (g)	FE Scaled PGA (g)	FE* Scaled PGA (g)
(i)	0.43	**0.43**	-	0.18	**0.27**	-
(ii)	0.47	0.54	**0.45**	0.30	0.37	**0.32**
(iii)	0.54	0.64	**0.52**	0.36	0.48	**0.44**

* - Tie connections were removed in the FE models at the locations where complete tie failure was noted during experimental testing leading up to damage states *(ii)* and *(iii)*.

Table 5.3 – Damage limit state PGAs for solid FE wall models subjected to M02 and Nahanni earthquakes.

Damage State	Wall-1		Wall-2	
	M02 Earthquake PGA (g)	Nahanni Earthquake PGA (g)	M02 Earthquake PGA (g)	Nahanni Earthquake PGA (g)
(i)	0.70	0.80	0.50	0.35
(ii)	0.80	1.00	0.60	0.40
(iii)	0.95	1.20	0.80	0.55

Table 5.4 – FE wall model parameters with damage states and M10 earthquake input PGAs.

Tie Grid / Tie Properties	Damage States		
	(i)	*(ii)*	*(iii)*
A/N(2.5)22min	0.25	0.35	0.40
A/N(1.5)22min	0.15	0.25	0.35
A/N(8d)22min	0.30	0.40	0.50
A/N(8d)22ecc	0.45	0.50	0.65
A/N(8d)28min	0.45	0.55	0.65
A/N(8d)28ecc	0.30	0.35	0.45
A/S(-)22ecc	0.60	0.70	0.85
A/S(-)16min	1.10	1.30	1.30
B/N(8d)28min	0.30	0.40	0.55
C/N(8d)28min	0.35	0.45	0.60
D/N(8d)28min	0.55	0.65	0.80
B/N(8d)28ecc	0.20	0.25	0.35
C/N(8d)28ecc	0.25	0.30	0.35
D/N(8d)28ecc	0.35	0.40	0.55
B/N(1.5)22min	0.10	0.15	0.25
C/N(1.5)22min	0.15	0.15	0.25
D/N(1.5)22min	0.20	0.25	0.40
A(5)/N(8d)28min	0.55	0.65	0.80
A(9)/N(8d)28min	0.60	0.75	0.90
A(5)/N(8d)28ecc	0.35	0.40	0.50
A(5)/N(1.5)22min	0.20	0.25	0.40

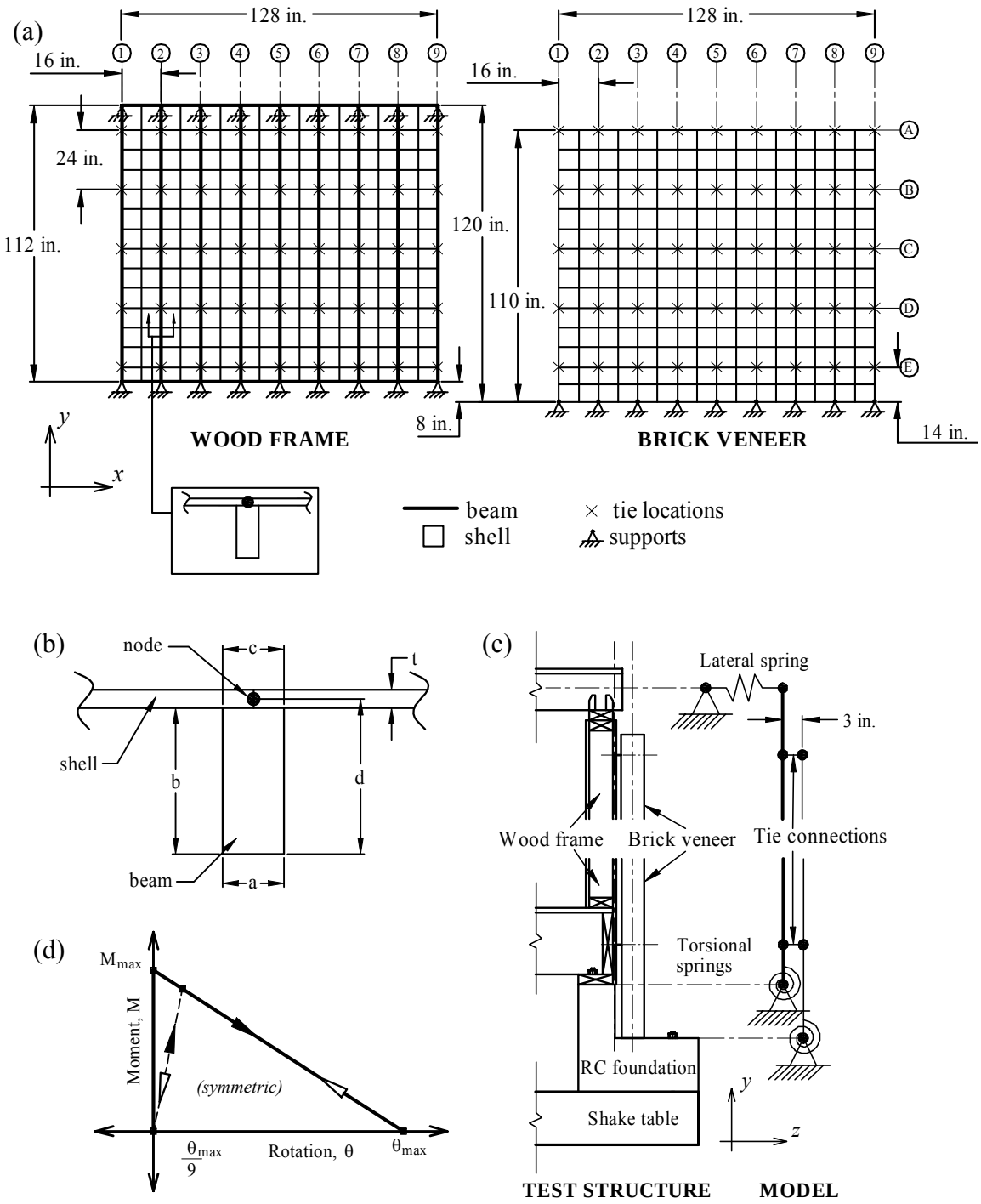

Figure 5.1 – (a) FE wall model geometry elevation views, (b) stiffened shell model (OSB sheathing with stud), (c) wall support details, and (d) bi-linear elastic brick masonry rocking behavior model.

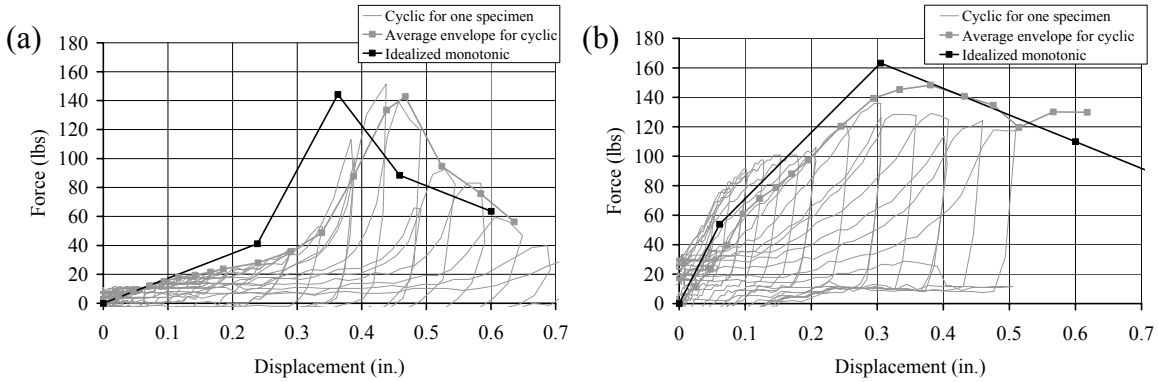

Figure 5.2 – Cyclic and monotonic tension behaviors for subassemblies with (a) N(8d)28ecc and (b) N(8d)22ecc types of tie connections.

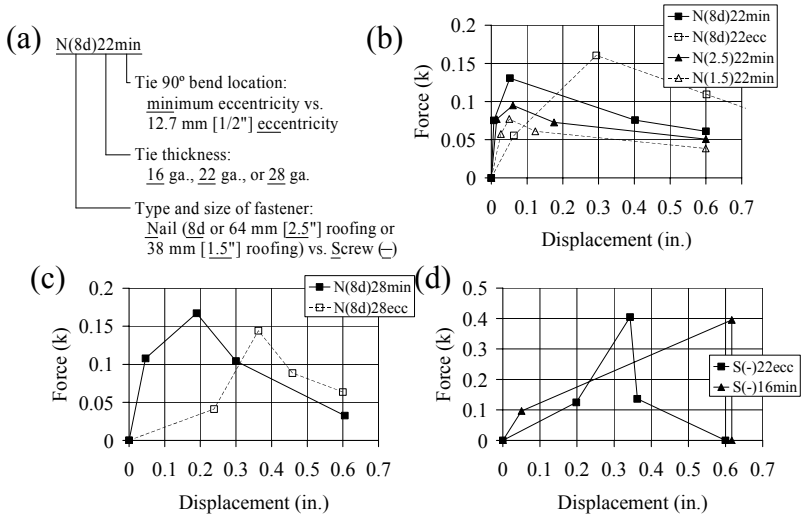

Figure 5.3 – (a) Outline of tie connection IDs. (b-d) Average idealized tensile force-displacement behaviors of various tie connections.

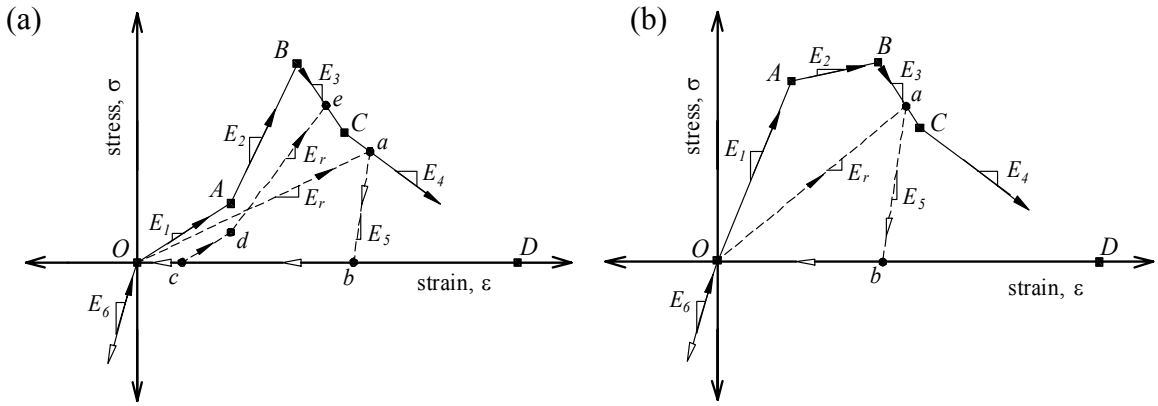

Figure 5.4 – Tie connection "material" model idealized hysteretic rules and properties for (a) low-to-high stiffness and (b) high-to-low stiffness backbone curves.

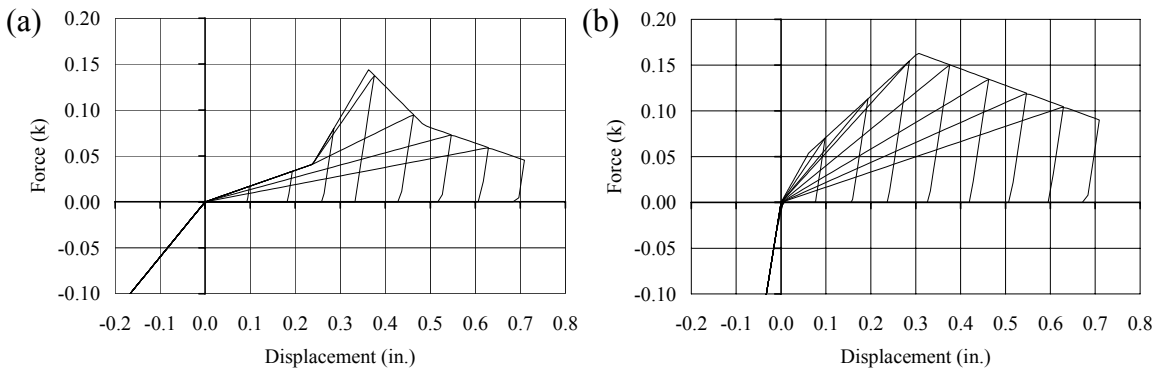

Figure 5.5 – Tie connection model cycled at increasing displacements for (a) N(8d)28ecc and (b) N(8d)22ecc types of tie connections.

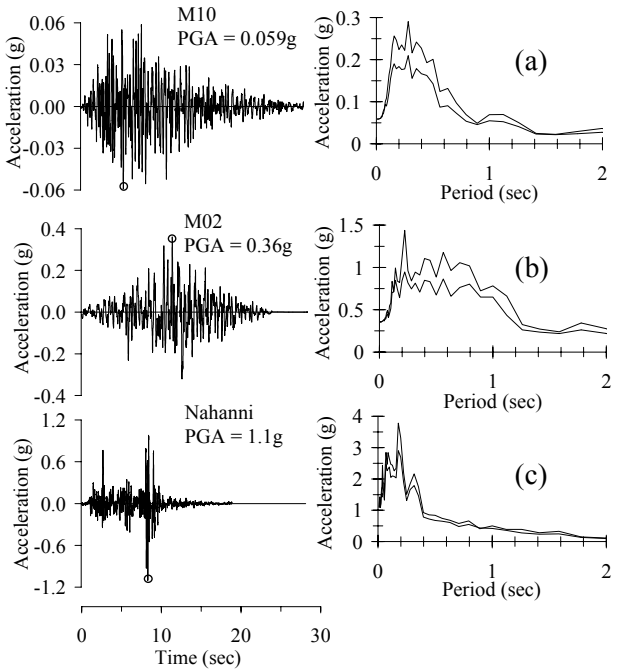

Figure 5.6 –Acceleration time histories and response spectra (3% and 6% damping) for (a) M10, (b) M02, and (c) Nahanni earthquakes.

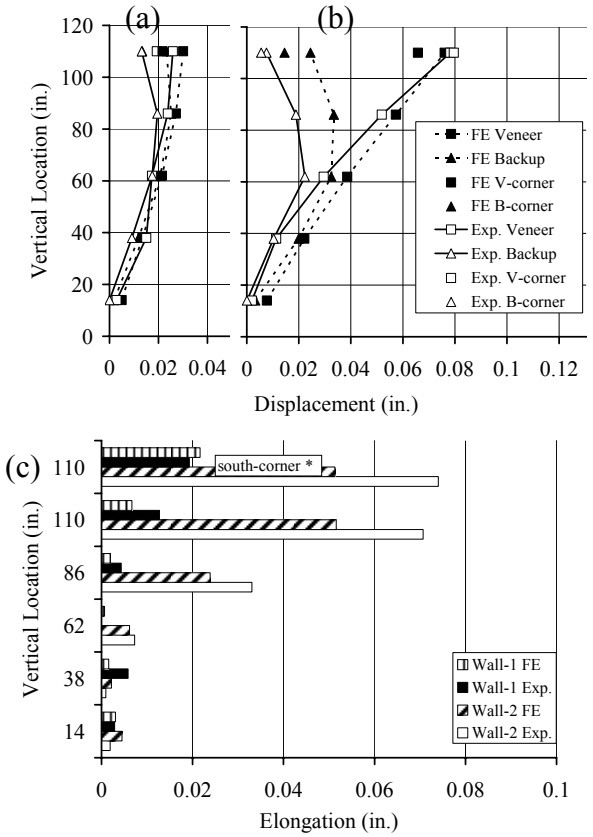

Figure 5.7 – Static load test displacements relative to the supports for (a) Wall-1, (b) Wall-2; and (c) tie elongations for both (* - net brick displacement for Wall-1).

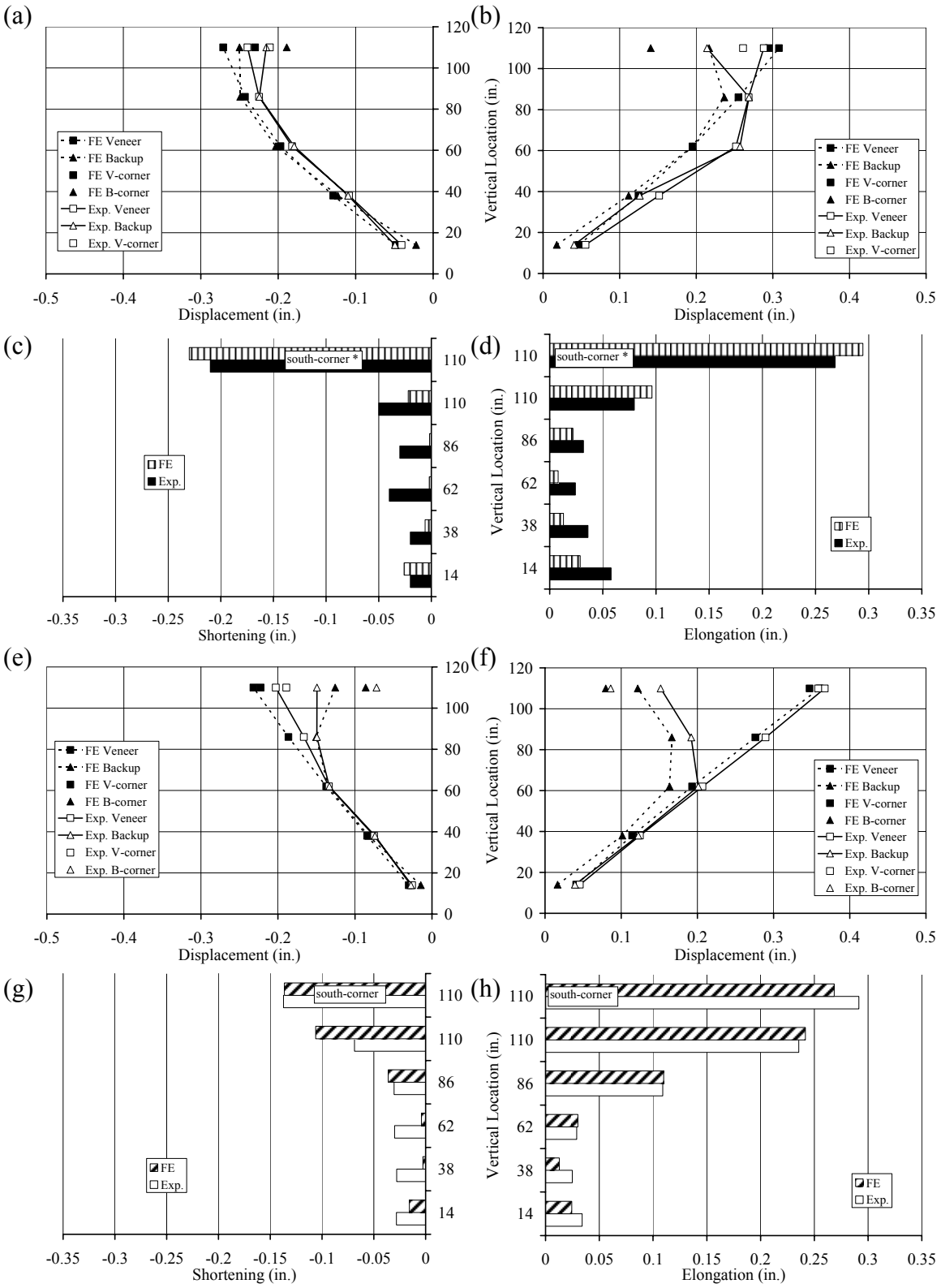

Figure 5.8 – Peak displacements and tie deformations in the negative (inward) and positive (outward) directions for (a-d) Wall-1 during M10-0.51[0.38]g; (e-h) Wall-2 during M10-0.23[0.18]g record (* - net brick displacement).

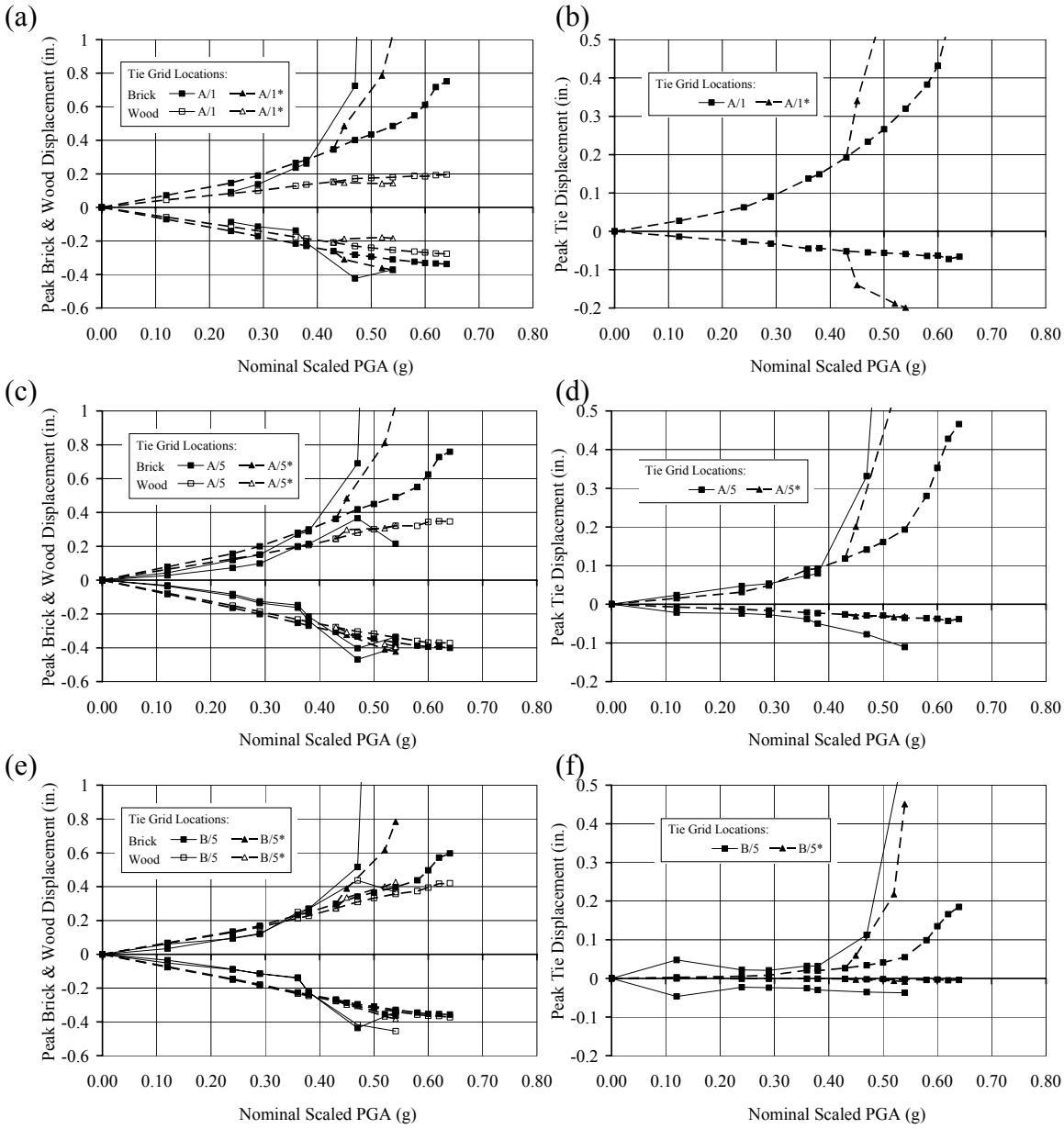

Figure 5.9 – Peak negative and positive displacement response plots, during M10 input tests and FE analysis for Wall-1: top corner (a) displacements and (b) tie deformations; top center (c) displacements and (d) tie deformations; and, second row center (e) displacements and (f) tie deformations. (Experimental results – solid curves; FE results – dashed curves). (* - failed tie connections leading to this point in testing were removed in the FE model)

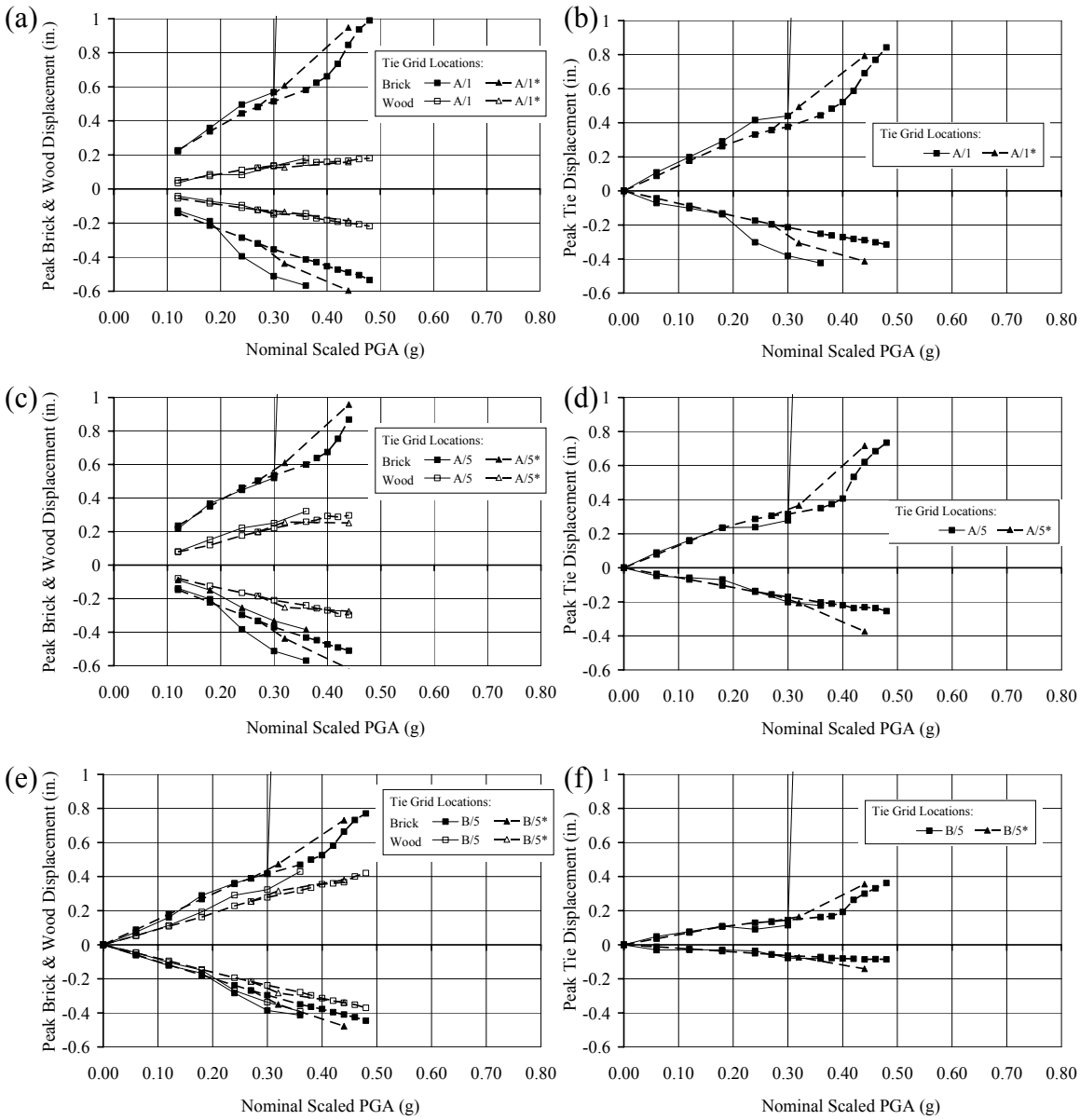

Figure 5.10 – Peak negative and positive displacement response plots, during M10 input tests and FE analysis for Wall-2: top corner (a) displacements and (b) tie deformations; top center (c) displacements and (d) tie deformations; and, second row center (e) displacements and (f) tie deformations. (Experimental results – solid curves; FE results – dashed curves). (* - failed tie connections leading to this point in testing were removed in the FE model)

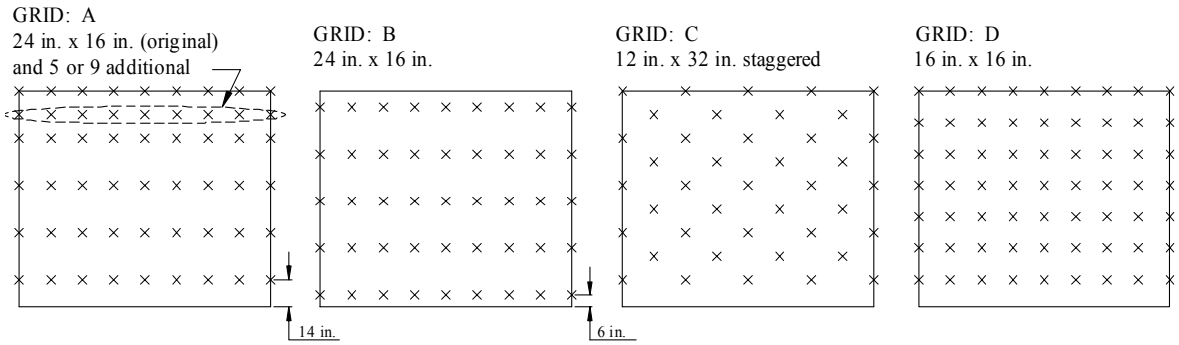

Figure 5.11 – FE wall panel parameters and IDs.

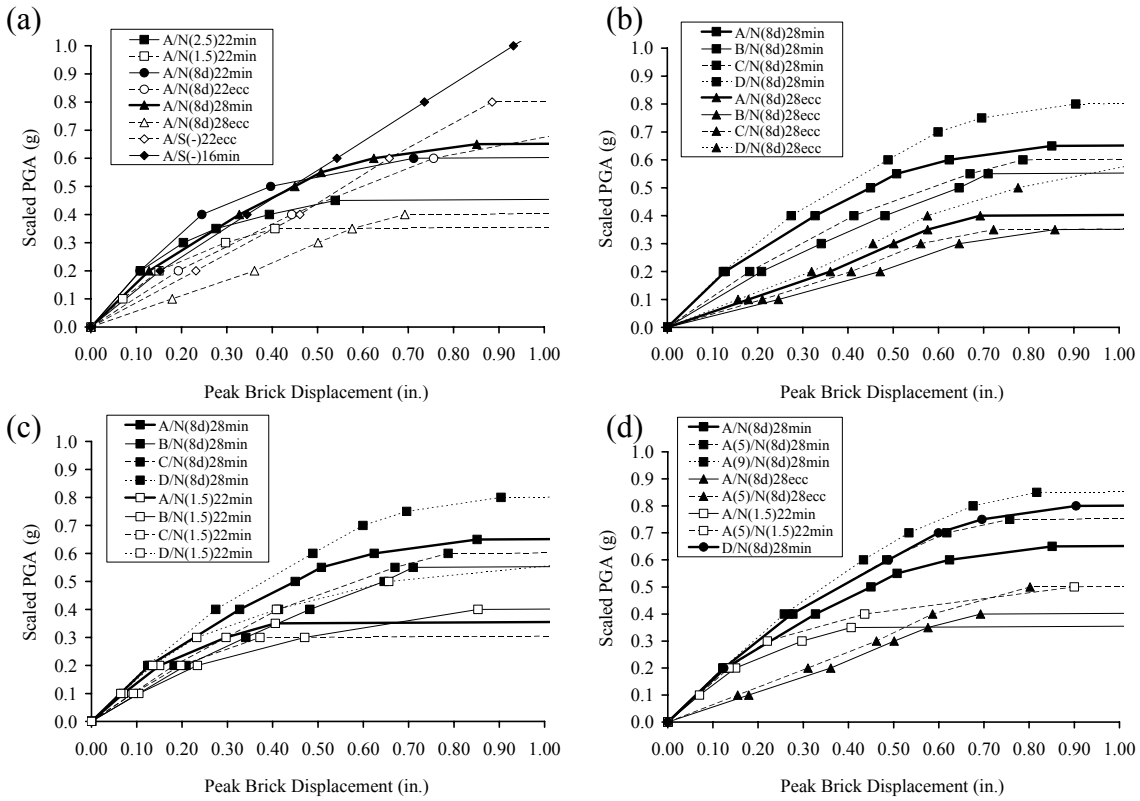

Figure 5.12 – FE dynamic pushover results, for various parameters: (a) tie connection properties, (b-c) tie layouts, (d) typical tie layouts with five or nine additional ties.

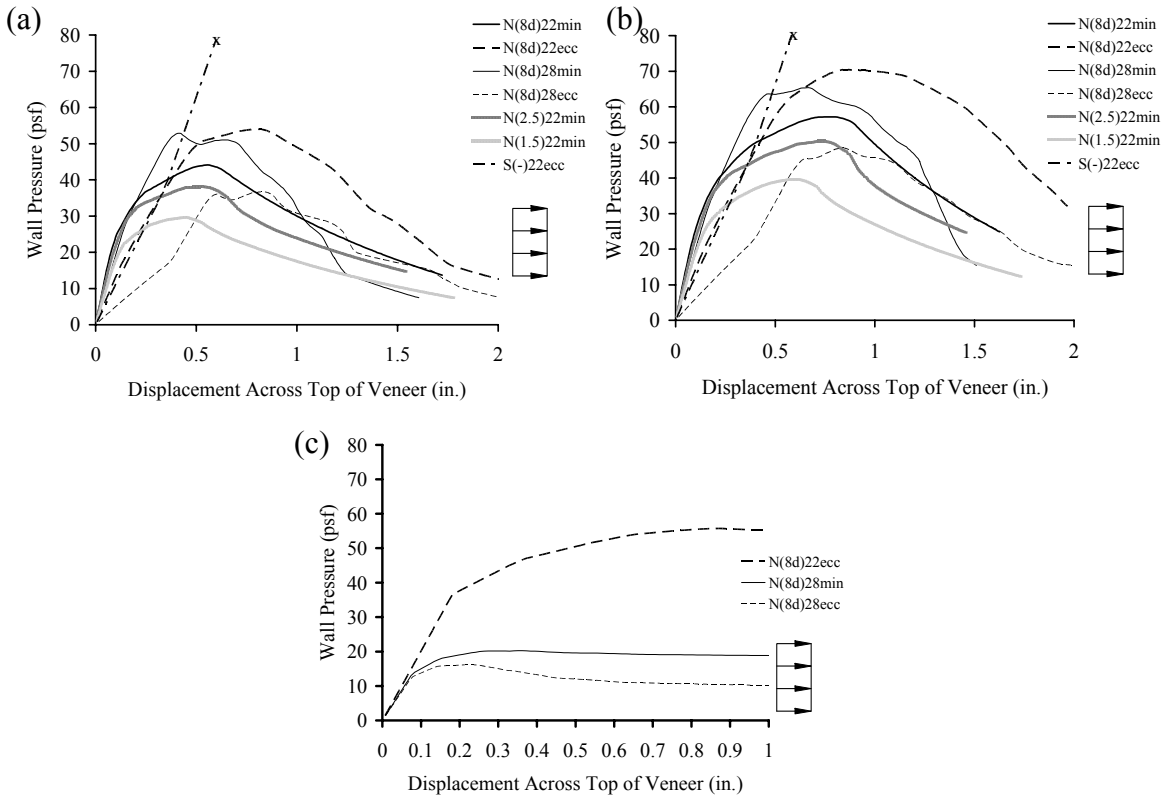

Figure 5.13 – FE wall model uniform suction (outward) pressure pushover curves for tie layout (a) 5 rows and 9 columns (24 in. x 16 in.) and (b) 7 rows and 9 columns (16 in. x 16 in.); (c) uniform push (inward) pressure curves for select tie properties with a 24 in. x 16 in. tie layout.

PART II – WALL PANELS WITH GEOMETRIC VARIATIONS

Detailed three-dimensional finite element (FE) models were developed to represent the one-and-a-half story gable-end wall specimen with a window opening (Wall-3). A similar analysis approach was used for this brick veneer wall panel as that described in *Part I* of this chapter. After calibration based on the test results, the FE wall panel model effectively captured static and dynamic experimental brick veneer wall behavior at different response levels (up to and including tie damage and even instability/collapse of the wall panel). Parametric studies were then carried out using FE wall panel models to evaluate the effects of certain types and layouts of tie connections, as well as geometric variations in brick veneer wall construction.

5.9 Wall Structure Model

5.9.1 Wood Frame Wall Panel and Backup Supports

As for the solid wall panels, the analysis software *ABAQUS* (Abaqus Inc. 2006) and pre- / post-processor software *MSC.Patran* (MSC 2005) were used throughout this part of the study. The 2x4 stud and oriented strand board (OSB) exterior sheathing composite wood frame wall panel was represented by joined 3-D beam and shell elements, as shown in Figure 5.14(a), which were assigned the actual section dimensions from the physical test structure described in *Part II* of Chapter 4. The interior gypsum wallboard was not explicitly modeled because its effect on out-of-plane flexure was negligible; however, its mass was indirectly accounted for as part of the model's OSB density specification. The wood-frame components were assigned linear elastic material properties, as listed earlier in Table 5.1, based on the wood material species and grade used in the wall test specimen. Softening and nail slip in the wood-frame components were not explicitly modeled because, even after instability of the veneer wall, no splitting of the wood-frame wall components was visible, the nail connections appeared to be tight, and the out-of-plane response of the wood-frame wall panel was mostly controlled by the (elastic) flexibility of the wood material.

The wood-frame backup support conditions were based on the test structure setup, as well as on certain key aspects of observed experimental behavior (similar to what was done for solid wall panel models developed earlier in *Part I* of this chapter). As the wall test structure was subjected to out-of-plane loads, the wood frame wall panel exhibited rotation across the bottom and translation at the ceiling framing, as well as combined rotation and horizontal translation at the sidewalls and roof framing (relative to the shake table and the steel reaction frame). Because the physical supports (concrete foundation and steel reaction frame) and the surrounding wood backup components (floor, sidewalls, ceiling, and roof), including nail connections to the wall frame, were not explicitly modeled, their cumulative effects were incorporated into linear elastic spring supports for the wood wall model base, sidewalls, ceiling, and roof, as shown in Figure 5.14(a-b). Support spring stiffness constants were calibrated per the experimental results, by conducting preliminary static and dynamic load FE analyses, to be as follows: K_{base} =

1,000 k-in./rad (110 kN-m/rad), $K_{sidewall}$ = 1.1 k/in. (195 kN/m), $K_{ceiling}$ = 0.4 k/in. (70 kN/m), and K_{roof} = 0.65 k/in. (115 kN/m). Static load test results were used to qualitatively assess the relative stiffnesses of the various wood backup supports, whereas dynamic test results toward the end of the *elastic* range of experimental wall behavior (which caused significant excitation of the specimen without tie or wall system damage) were then used to quantitatively optimize these support properties. The spring supports also reflected any diaphragm (ceiling and roof) or steel frame backup flexibility in terms of their contribution to acceleration amplification during dynamic testing.

5.9.2 Brick Masonry Veneer

Experimental brick veneer wall response was dominated much more by rigid body rotation (rocking about its base) than by bending when subjected to out-of-plane static and moderate dynamic loading. However, as the level of shaking increased, the veneer showed more noticeable flexural deformations, and the wall did eventually crack at the base of the gable, at the corners of the window opening, and at its mid-height. Overall though, experimental results presented in Chapter 4 indicate that wall response, up to and including ultimate cracking and instability of the veneer, was most closely associated with the performance of the tie connections. Therefore, the brick veneer was assumed to be continuous and linear elastic; it was modeled using shell elements (with their reference plane at the shell mid-surface) assigned the same section dimensions as in the test structure, with the material properties listed in Table 5.1. (Cracking in brick masonry veneer walls was briefly explored analytically, as has been summarized in Appendix C.2.) Overall, brick veneer cracking was not represented in this analytical program, in order to simplify the wall panel models for various parameter studies, and also because brick veneer wall performance was effectively represented by utilizing detailed nonlinear inelastic FE models for the tie connections, as described below.

In the experimental setup, the brick masonry veneer wall had little bond to the foundation surface because of the flashing material. The foundation did however provide lateral and vertical support (without slipping of the veneer) throughout testing, with the brick veneer wall pivoting about its base when subjected to out-of-plane loads. Therefore, pin supports with nonlinear elastic rotational springs were implemented across the base of the brick veneer wall model, labeled as $K_{rocking}$ in Figure 5.14(a). As shown in Figure 5.14(c), a rigid body rocking response of the brick veneer wall was represented by these springs, which were assigned bilinear force-displacement behavior defined by the masonry wall weight and geometric properties, as explained in earlier analytical studies by Doherty et al. (2002) and Simsir (2004). In the FE model (as in the experimental structure), only the tie connections back to the wood frame provided lateral stability to the brick veneer wall. (The FE models did not represent the modest unintended added restraint from the vinyl flashing along the window sill and lintel.)

5.9.3 Tie Connections

Dynamic brick veneer wall tests showed that different levels of wall specimen response (*elastic, intermediate,* and *ultimate*) were closely related to certain key tie connection deformation limits in tension. As described in greater detail in *Part I* of this chapter, the overall tie connection model was assigned nonlinear inelastic "material" properties in

tension (based on subassembly monotonic tension test results) and linear elastic in compression (based on both subassembly and wall test results), to combine the effects of the ties and excess mortar within the wall cavity. The tie connection models were developed to capture two distinct tensile behaviors, which involved transitions from either lower-to-higher stiffness or from higher-to-lower stiffness. (The tie connections in the FE model of the Wall-3 experimental specimen are labeled as N(2.5)22min back in Figure 5.3(b).)

5.10 FE Model Setup and Analysis Procedure

The tie layout grid and the distance between the physical model section centerlines (of the wood frame and brick veneer) defined the overall FE model geometry, as seen in Figure 5.14(a-b). The distance between the reference planes of the brick veneer and wood frame models (which included the 1 in. [25 mm] air space) defined the length of the analytical tie connection elements. Small overhangs of masonry beyond the edge ties of the test specimen were not explicitly modeled; however, their lumped mass was added to edge nodes of the veneer shell model based on tributary area. From shake table testing, the viscous damping ratio was determined to be approximately 4% of critical, which was implemented in the FE model in terms of Rayleigh damping coefficients (mass and stiffness proportional damping, in the first and second elastic modes of vibration).

Calibration of this FE wall panel model was similar to that of the solid FE wall panel models, as described earlier. The FE wall model was subjected to static and dynamic loading as in the experimental study; the model was then verified to capture different levels of experimental specimen dynamic response. Preliminary linear elastic calibration analyses were performed with static point loads applied to the FE wall models at the same locations and of equal magnitudes as in certain experimental tests. Time history analyses were then conducted by using the electronic earthquake records from the shake table testing program, which were labeled as the M10, M02, and Nahanni earthquakes. These electronic earthquake records were normalized and scaled with respect to peak ground acceleration (PGA). The earthquake records were applied to the FE wall model wood frame backup and brick veneer supports, and time history analyses were executed in *ABAQUS* using the direct integration method, with automatic time incrementation. Throughout calibration and validation of the FE wall model, analytical wall panel response and scaled electronic earthquake record PGA values were compared with experimental wall response and corresponding electronic earthquake record "nominal scaled" PGA values. (As described in Chapter 4, measured shake table PGA values were identified to be somewhat spurious maximums because they were not representative scaling values across the entire frequency range of the applied earthquake records; therefore, "nominal scaled" PGA values were computed to better match the intensities of input earthquake records to those of actual measured shake table acceleration histories.)

Displacement measurements were used to evaluate different levels of wall specimen behavior during shake table testing. Displacements were measured at key tie locations throughout the wall specimen and on the shake table, thereby providing veneer and

backup displacements relative to the shake table, as well as differential displacements between the veneer and backup (tie deformations). The experimental peak displacement response of the wall specimen was noted in the positive (outward – veneer deflecting away from the backup) and negative (inward) directions; likewise, peak experimental tie deformations were measured in both directions for each particular test. (Maximum positive displacements of the brick veneer and of the wood backup, as well as peak positive tie deformations, were of particular interest because these were closely related to different levels of experimental specimen response and damage.) So, similarly in the FE wall models, computed displacements (at the same tie locations as in the experimental specimen) were used to first verify and then further identify model response when subjected to out-of-plane loading (i.e., peak brick veneer and wood backup model displacements relative to the supports, as well as peak relative tie displacements between the veneer and backup models). Key analytical and experimental results are presented below to establish the validity of this "calibrated" model, followed by parametric studies and overall FE analysis findings.

5.11 FE Model Validation

5.11.1 Static and *Elastic* Dynamic Loading

The FE model representing the wall specimen was calibrated with the load vs. displacement results from static point (pull) tests, as well as with scaled earthquake (dynamic) tests toward the end of the *elastic* range of experimental wall behavior. For example, shown in Figure 5.15 are calibrated FE wall model and experimental displacement results for the wood frame backup subjected to static point loads, while in Figure 5.16 are results for the complete brick veneer wall panel subjected to the dynamic M10-0.54[0.39]g input. For static point loads, the FE model generally captured the overall trends of wood backup displacements, despite certain differences. At some locations the analytical displacements are a bit high, probably due to the relatively low magnitude of applied static loads, for which the experimental wall specimen behavior was disproportionately affected by factors not represented in the model (like friction); at locations where the FE displacement results are lower, experimental wood backup deformations were most likely affected by nail slip (which was not captured by the FE model) rather than just flexure of the wood elements. Nevertheless, the complete FE wall specimen model quite effectively captured overall wall displacements in both the positive and negative directions under distributed dynamic loads (Figure 5.16). The FE wall model elastic period of vibration was computed to be 0.10 sec, which was only about 10% higher than the experimental wall period (at the onset of testing).

The M10 (nominal) earthquake test and FE analysis PGAs with their corresponding maximum displacement responses of the brick veneer, the wood backup, and the tie connections (at key tie grid locations) are shown in Figure 5.17, for both inward and outward movement of the wall. Overall displacement vs. dynamic input PGA analysis results exhibit a linear relationship in the *elastic* range of behavior, with FE analysis results closely matching the experimental response (Figure 5.17(a,c)). The FE model also effectively captured higher tie forces in the upper regions of the wall panel, and at those ties anchored to stiffer backup regions (near the supports). For lower magnitude

dynamic loading (early *elastic*), the FE wall specimen model slightly overestimated overall experimental wall displacement results, and the computed tie deformations appear to be a bit off from experimental values. (Measured experimental tie deformations were less accurate during early dynamic tests due to the level of instrumentation noise in the displacement data compared to the actual tie deformations; however, this was only true for relatively small deformations, of approximately 0.04 in. [1 mm] or less, while the noise was insignificant for higher input tests.) The FE model has mainly been used to evaluate veneer wall response at much higher loads, where these modest discrepancies present at lower levels of loading did not play a critical role.

Throughout experimental testing, the greatest response of the specimen for any particular PGA value typically occurred for the scaled M10 input record, compared to the M02 and Nahanni inputs; however, the FE wall model was also shown to effectively capture the response of the experimental wall specimen for these two additional earthquake records (see Figure C.8 in Appendix C.3). For the Nahanni input record, analytical response was a bit higher than the experimental response, which may have been an effect of some sharper changes in the Nahanni response spectrum near the wall specimen and model periods of vibration. All three of these earthquake records were further utilized to evaluate the wall panel damage limit states, as described below.

5.11.2 *Intermediate* and *Ultimate* Dynamic Loading

During the experimental study, it was noted that overall brick veneer wall response (from *elastic* on into *intermediate*, and even up to *ultimate* levels) depended primarily on the performance of the tie connections. Ties anchored to or near stiffer regions of the wood backup, and those at the upper region of the wall panel, experienced the highest loads and therefore showed the first signs of damage (partial nail pullout for these particular tie connections); at higher load levels, tie damage spread out to more flexible (backup) and lower regions of the wall panel. At the onset of tie damage during dynamic wall testing, peak measured tie elongations were found to be closely related to the elongations determined for ultimate loading during the tie subassembly tests. Therefore, tie connection damage in the FE model was determined from the maximum computed tie elongations, at a stage when those elongations exceeded the opening displacements at ultimate tensile load capacity (approximately 0.06 in. [1.5 mm] for the ties used in the Wall-3 test specimen, as seen in Figure 5.3(b)).

Three damage limit states were then identified for this FE wall panel model, based on onset of tie failures at key tie locations in the model (per the tie grids shown in Figure 5.14(a)), which were related to the experimental wall behavior and damage, as follows (FE analysis – *experiment*):

(i) first tie failure at top corners (at grids B/1 & B/9) – *same [end of elastic range]*;

(ii) tie failures in entire gable region (across rows O through B) – *highest input before collapse, accumulation of tie damage [end of intermediate range]*;

(iii) tie failures across third row from base (across row D) – *instability/collapse [end of ultimate range]*.

The three distinct levels of tie connection and brick veneer damage found experimentally were effectively represented with the three associated levels of tie damage in the FE wall model subjected to the M10 earthquake, as seen from the tie deformation response plots

presented in Figure 5.17(b,d) (for key tie locations), with the load intensities summarized in Table 5.5. (Similarly, FE models of solid single-story wall specimens developed earlier in *Part I* of this chapter were also effective at capturing experimental wall behavior. Additionally, these three levels of tie connection and brick veneer wall damage can also be associated with the seismic performance levels assigned for architectural components per ASCE 41-06 respectively as Immediate Occupancy, Life Safety, and Hazards Reduced.) Damage limit states were well captured by the FE wall model with dynamic M10 loading, scaled to within approximately 10% of the nominal scaled experimental PGA values. The same levels of damage were also evaluated with the M02 and Nahanni earthquake inputs from the experimental program; for comparison, the 1994 Northridge earthquake ground motions from Canoga Park and Rinaldi recording stations (PEER 2008) were also employed. All of these other earthquake records were normalized with respect to PGA and then scaled at 0.05g increments (Table 5.5), showing that the M02, Nahanni, and Northridge earthquakes had to be scaled to higher PGAs than the M10 record to cause the three damage limit states. The variation between the earthquake inputs resulted in a somewhat different response of the wall model, indicating that the M10 earthquake had relatively the most damage potential, so it was therefore selected for the parameter studies described below.

Overall, the FE model was somewhat conservative at estimating experimental wall panel damage in the *intermediate* and *ultimate* ranges of behavior, most likely due to three aspects of the experimental wall structure behavior which were not explicitly represented in the model. The experimental wood backup structure experienced some modest softening, and therefore overall peak outward displacements of the experimental wall panel were a bit higher than the computed displacements (Figure 5.17(a,c)). Additionally, the topmost tie connections in the gable region experienced less loading than predicted analytically, in part due to the eventual occurrence of cracking in the brick veneer during testing, permitting it to bend and more closely assume the shape of the wood backup, thereby reducing the demand on the topmost ties (Figure 5.17(b,d)). (Accumulation of tie damage leading into the second and third damage states was not accounted for in this FE wall model. During experimental testing, damage of these tie connections was mainly dominated by onset of nail pullout, and the tie connections maintained their tensile strength even after onset of nail pullout was noted.) The presence of flashing above and below the window opening in the test structure also provided some modest added restraint to the brick veneer. Nevertheless, the FE wall panel model effectively captured the experimental wall behavior and ultimate dynamic load capacity by representing the key nonlinear inelastic behavior of the tie connections, closely matching their force-displacement response (up to their peak and even post-peak capacities). Therefore, in the range of wall panel behavior leading to brick veneer outward instability/collapse, experimental displacement vs. PGA response appears to be fairly gradual, whereas the corresponding analytical response appears to be a bit more abrupt. The FE wall panel model also consistently exhibited a close match to experimental wall response in the negative (inward) direction (Figure 5.17). Finally, then, the criteria described above for different stages of veneer wall damage (as a function of tie failure) have also been implemented throughout the parametric studies, as described below.

5.12 FE Wall Model Parametric Studies

5.12.1 Brick Veneer Wall Panel Parameters

The prescriptive design and construction requirements for brick veneer walls have been described in detail in *Part I* of this chapter, as well as in Chapter 2. The test specimen configuration, shown in Figure 5.14(a), represented a wall panel built in general conformance with the prescriptive code requirements for tie installation in seismic design category C, and also included ties within 8 in. (203 mm) of all edges of the wall panel. In actual construction practice, tie installation in brick veneer walls frequently deviates from the established requirements. After calibration and validation of the FE brick veneer wall model, the test specimen configuration with a window opening and gable was analytically adjusted to represent various combinations of a number of wall geometries and tie connection layouts, as shown in Figure 5.18. Different sized wall openings were investigated, along with two different masonry edge dimensions along the wall gable. Then, general tie grids of 24 in. x 16 in. (610 mm x 406 mm) and 16 in. x 16 in. (406 mm x 406 mm) were employed, with and without ties along the wall opening and edges; the tie grid of 24 in. x 16 in. (610 mm x 406 mm) was also varied as a function of location of the first row of ties at the base of the wall panel, which determined the tie layout above and below the window opening, as well as in the gable region. (These geometric and tie layout variations did not require significant adjustments to the FE model of the test specimen configuration; the boundary conditions were unchanged, with the exception of some necessary rearrangement of the wood backup frame and shell elements to match wall opening and tie layout geometries.)

The various wall panel models are labeled as "Wall Type – Tie Layout / Tie Properties" per the following: Wall Type is identified as I through IV, including Case (b) where the gable masonry edge dimension was increased from 8 in. (203 mm) to 12 in. (305 mm) (Figure 5.18(a)); Tie Layout is identified as grid A through D, where Y = with (and N = without) minimum required ties at wall gable and opening edges, and in some cases including (3) or (6) extra ties in the gable region (Figure 5.18(b)); and, Tie Properties is identified by tie attachment type, thickness, and bend eccentricity (Figure 5.3(a)). For example, the test specimen wall configuration is labeled as "I-AY/N(2.5)22min"; then, a wall labeled as "I-AY(3)/N(2.5)22min" would have the same properties as the test configuration, only with 3 extra ties added in the gable region, and so on. During these analytical studies, the earthquake record labeled as M10 was utilized, which was normalized with respect to PGA, and then scaled up at PGA increments of 0.10g to 0.20g for loading in the elastic range of wall behavior, and at reduced increments of 0.05g when estimating wall panel damage limit states. A total of forty wall panels were examined.

5.12.2 Parametric Study Results and Discussion

Dynamic FE analysis results (in the form of dynamic pushover plots) are grouped and summarized in Figure 5.19, showing the M10 PGAs vs. peak outward brick displacements evaluated at the middle of the wall panels, directly above the window opening (at grid location B/5 per Figure 5.14(a)). PGA values to cause the three key

damage limit states for certain groups of brick veneer wall panels are also summarized in Table 5.6. (An example set of PGA vs. key tie displacement results used to evaluate the damage limit states are shown in Figure C.10, in Appendix C.4.) In general, analysis results indicate that the expected PGA at ultimate response (instability/collapse) of the veneer walls was relatively close to the analytically predicted PGA at the onset of tie failures (at wall corners). As mentioned earlier, wall displacement response at certain locations for higher PGA values might be somewhat arbitrary because wall cracking and other factors were not represented analytically; however, wall model outward displacement up to the peak load points accurately reflected the key effects of tie connection tensile deformations.

As seen from Figure 5.19(a) and Table 5.6, tie connection strength and stiffness properties had a major influence on the out-of-plane seismic performance of brick veneer walls. The relative out-of-plane stiffness of the veneer walls is closely related to the initial tension stiffness for the type of tie connections used. At onset of the second damage limit state (defined by tie failure throughout the entire gable region of the wall panels), wall panel models with high-to-low stiffness ties experienced significant out-of-plane softening (down to below 50% of their initial out-of-plane stiffness); walls with low-to-high stiffness ties typically first underwent out-of-plane hardening, as wall damage progressed. For most types of tie connections, ultimate capacities of the walls were proportional to tie connection tensile capacities, except for the wall with the most flexible tie connections (28 ga. nailed with maximum allowable eccentricity), which performed worse even though these tie connections were not necessarily any "weaker" than the others. Walls utilizing 22 ga. ties, and one with a best case installation of 28 ga. ties, attached with larger nails (8d or similar) or screws, sustained much higher loading than walls utilizing short roofing nails and/or 28 ga. ties with the maximum allowable bend eccentricity. The out-of-plane dynamic load capacity of brick veneer walls with poorly installed tie connections, such as those utilizing short roofing nails (sometimes as short as 1.25 in. [32 mm], as seen commonly used in practice), will be reduced to 40% or lower of the capacity attainable with code-compliant installation and the use of 8d (or similar) nails.

Tie grid spacings and tie installation at wall edges also played a major role in overall wall performance, as seen in Figure 5.19(b). For walls with tie grids of 24 in. x 16 in. (610 mm x 406 mm), adding three or six extra ties to the top of the wall panel (respectively, a 5% or 10% increase in the total number of ties), resulted in a significant increase in wall capacity (by up to 20-30%). On the other hand, removing the minimum edge ties resulted in a significant reduction in wall panel capacity (by up to 50%, as a result of 20% fewer ties). The location of the first row of ties (at nominal 8 in. [203 mm] increments, which generally equals three courses of brick masonry in real construction (Figure 5.18(b)), played a role in the resulting tie connection layout (in the upper region of the wall panel) and also on ultimate behavior of these wall panels. Furthermore, the test structure model configuration with a tie grid of 16 in. x 16 in. (406 mm x 406 mm), prescribed for wall construction in seismic design category D and above, sustained 50% higher intensity shaking than the same walls with a tie grid of 24 in. x 16 in. (610 mm x 406 mm). With reduced tie spacing, even a wall panel comprising ties attached with

short roofing nails resulted in an out-of-plane dynamic capacity comparable to walls designed and built for seismic design category C.

As shown in Figure 5.19(c), brick veneer wall response and ultimate behavior was sensitive to the supported brick veneer wall areas, particularly for the wall mass at the top of the wall panels. A relatively small increase in the supported masonry area, by extending gable edges beyond the ties by approximately an additional 4 in. (100 mm) (less than a 5% increase in total wall area), appeared to reduce the wall dynamic capacity by approximately 10%. An increase in total wall area near its center of mass, by infilling the window opening (roughly 20% more wall area), resulted in a directly proportional reduction in wall capacity (by 20%), when compared to the test structure configuration for all types of tie connections (Table 5.7). Increasing the wall opening size, by extending it downward, resulted in a relatively small change in overall capacity, whereas wall panels with a wider opening were able to sustain much higher intensity shaking. Walls with a large opening were very sensitive to the tie connection properties, their placement, and total masonry wall area in the gable region (Figure 5.19(d)). Removing only five ties from the edges of the gable (roughly a 13% reduction in the total number of ties), resulted in a nearly 40% drop in wall capacity; a 4 in. (100 mm) increase in the gable edge dimensions (6% increase in total wall area), resulted in a reduction in out-of-plane capacity by up to 25%.

5.13 Summary and Conclusions (Wall Panels with Geometric Variations)

FE models of brick veneer wall panels were developed based on shake table experiments and results for the case with a gable and window opening. Parameter studies were then conducted to evaluate the effects on out-of-plane seismic performance of brick veneer walls due to various combinations of tie connection types and layouts, as well as geometric changes in wall construction. The most important results and observations may be summarized as follows:

- Tie connection strength and stiffness properties had a major influence on the out-of-plane seismic performance of brick veneer walls (Figure 5.19(a)).
- Behavior of brick veneer walls was controlled by the overall grid spacing of tie connections, and particularly by tie installation along the edges and in the upper regions of the walls (Figure 5.19(b)). A relatively small increase in the gable edge distance of brick masonry, from 8 in. (203 mm) to 12 in. (305 mm), caused a significant decrease in the overall dynamic capacity of brick veneer walls. Therefore, it is recommended that codes incorporate specific requirements for tie connection installation along all brick veneer wall edges, such as a maximum wall edge distance of 8 in. (203 mm) (as prescribed by BIA (2003)).
- Three wall panels comprising tie grids of 24 in. x 16 in. (610 mm x 406 mm), with the minimum required ties along wall edges, exhibited similar overall behavior; the ultimate strength of those walls shifted noticeably after adding extra ties to the gable region, or after removing ties from wall edges. Out-of-plane strength of brick veneer walls improved significantly when a reduced tie spacing of 16 in. x 16 in. (406 mm x 406 mm) was employed.

- The total area of brick masonry veneer wall panels determined their overall inertial response, and the resulting forces that were then transferred through the tie connections into the wood-frame backup (Figure 5.19(c)). Brick veneer walls without openings, and those with slightly larger wall edges at the gable, needed significantly lower dynamic loads to cause damage, when compared to walls with larger window openings and less masonry at the gable.
- Behavior of wall panels with a relatively large opening was mainly governed by the brick veneer mass and the tie connections within the gable region (Figure 5.19(d)).

Table 5.5 – Physical test specimen configuration subjected to various earthquake records with damage states and earthquake input PGAs.

Earthquake Record	Damage States		
	(i)	*(ii)*	*(iii)*
Experiment (Nominal Scaled PGAs):			
M10	0.49	0.68	0.75
Analysis (Scaled PGAs):			
M10	0.45	0.60	0.66
M02	0.70	0.90	1.05
Nahanni	0.45	0.60	1.05
Canoga Park	0.60	0.85	1.15
Rinaldi	0.85	1.05	1.20

Table 5.6 – FE wall model parameters with damage states and M10 earthquake input PGAs.

Wall Type - Tie Grid / Tie Properties	Damage States		
	(i)	*(ii)*	*(iii)*
I-AY/N(2.5)22min	0.45	0.60	0.66
I-AY/N(1.5)22min	0.35	0.50	0.55
I-AY/N(8d)22min	0.55	0.80	0.90
I-AY/N(8d)22ecc	0.80	1.00	1.05
I-AY/N(8d)28min	0.80	1.00	1.00
I-AY/N(8d)28ecc	0.35	0.50	0.60
I-AY/S(-)22ecc	1.25	1.60	1.60
I-AY/S(-)16min	1.85	2.10	2.10
IV-AY/N(2.5)22min	0.35	0.50	0.60
IV-AY/N(1.5)22min	0.30	0.40	0.50
IV-AY/N(8d)22min	0.35	0.60	0.75
IV-AY/N(8d)22ecc	0.65	0.80	0.85
IV-AY/N(8d)28min	0.65	0.80	0.85
IV-AY/N(8d)28ecc	0.30	0.45	0.50
IV-AY/S(-)22ecc	0.85	1.10	1.10
IV-AY/S(-)16min	1.40	1.65	1.65

Wall Type - Tie Grid / Tie Properties	Damage States		
	(i)	*(ii)*	*(iii)*
I-AN/N(2.5)22min	0.35	0.45	0.55
I-AN/N(1.5)22min	0.25	0.35	0.45
I-AN/N(8d)28ecc	0.30	0.35	0.45
I-AY(3)/N(2.5)22min	0.45	0.70	0.75
I-AY(6)/N(2.5)22min	0.45	0.80	0.85
I-BY/N(2.5)22min	0.45	0.65	0.70
I-BN/N(2.5)22min	0.25	0.35	0.50
I-CY/N(2.5)22min	0.50	0.65	0.75
I-CN/N(2.5)22min	0.30	0.35	0.50
I-DY/N(2.5)22min	0.70	0.90	1.05
I-DY/N(1.5)22min	0.55	0.70	0.80
I(b)-AY/N(2.5)22min	0.40	0.55	0.65
II-AY/N(2.5)22min	0.50	0.65	0.70
IV(b)-AY/N(2.5)22min	0.35	0.45	0.55
IV-AN/N(2.5)22min	0.25	0.35	0.50
IV-AN/N(1.5)22min	0.20	0.25	0.40
IV-AN/N(8d)28ecc	0.20	0.30	0.40
III-AY/N(2.5)22min	0.70	0.80	0.85
III(b)-AY/N(2.5)22min	0.50	0.60	0.70
III-AN/N(2.5)22min	0.35	0.50	0.60
III-AY/N(1.5)22min	0.45	0.55	0.65
III-AY/N(8d)28ecc	0.45	0.55	0.65
III-AN/N(1.5)22min	0.25	0.35	0.40
III-AN/N(8d)28ecc	0.25	0.35	0.45

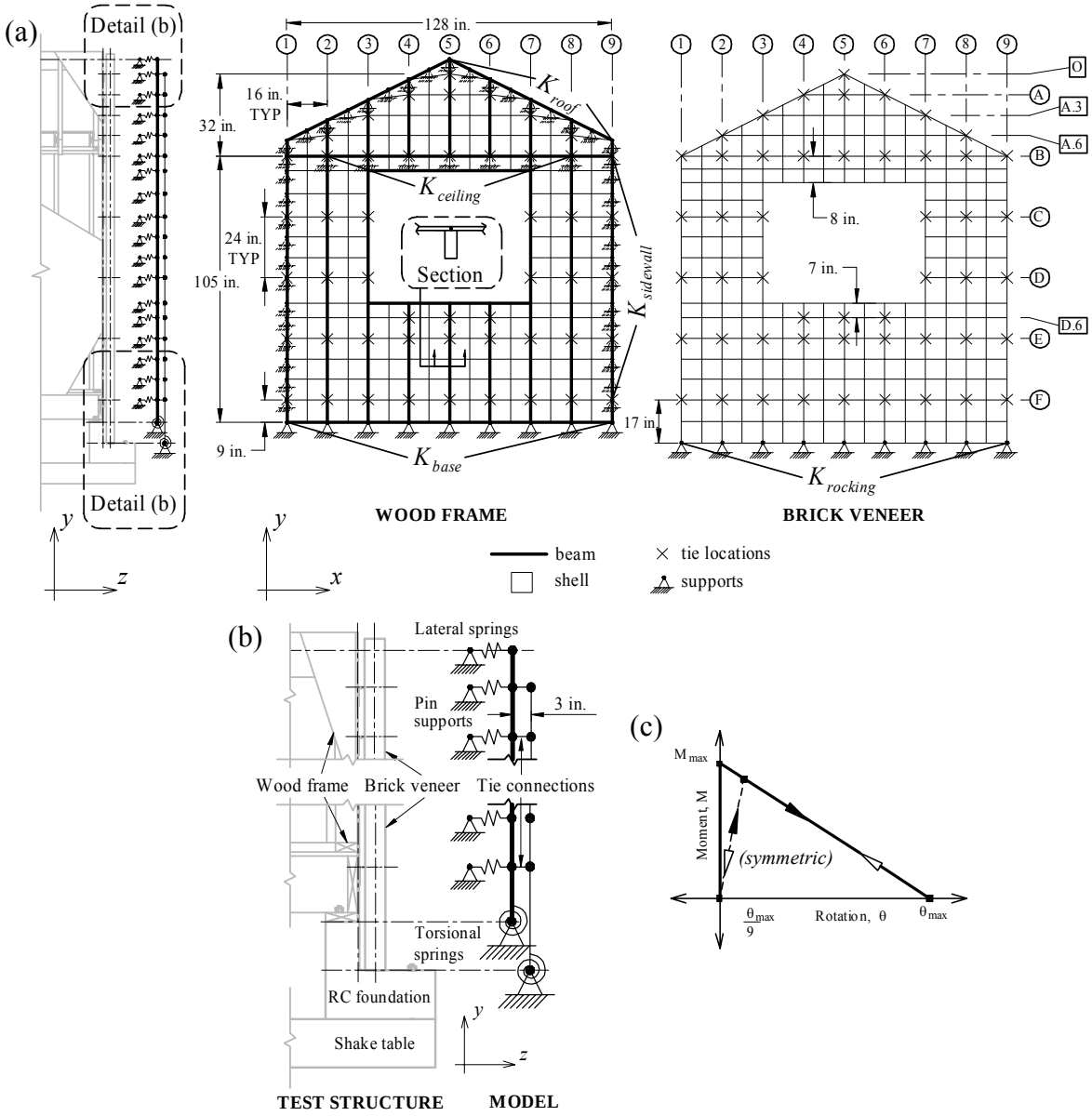

Figure 5.14 – (a-b) FE wall model geometry and support details, and (c) bi-linear elastic brick masonry rocking behavior model.

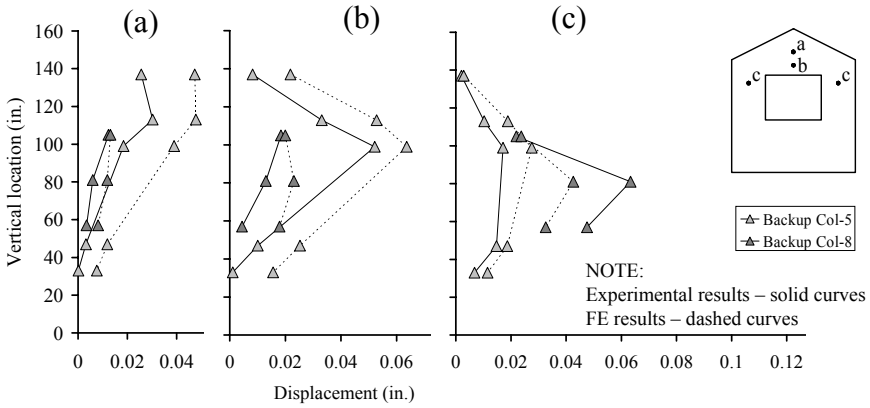

Figure 5.15 – Static load test and FE analysis displacements of bare wood backup, for point loads at (a) wall gable, (b) top-plate, and (c) both sides of window opening.

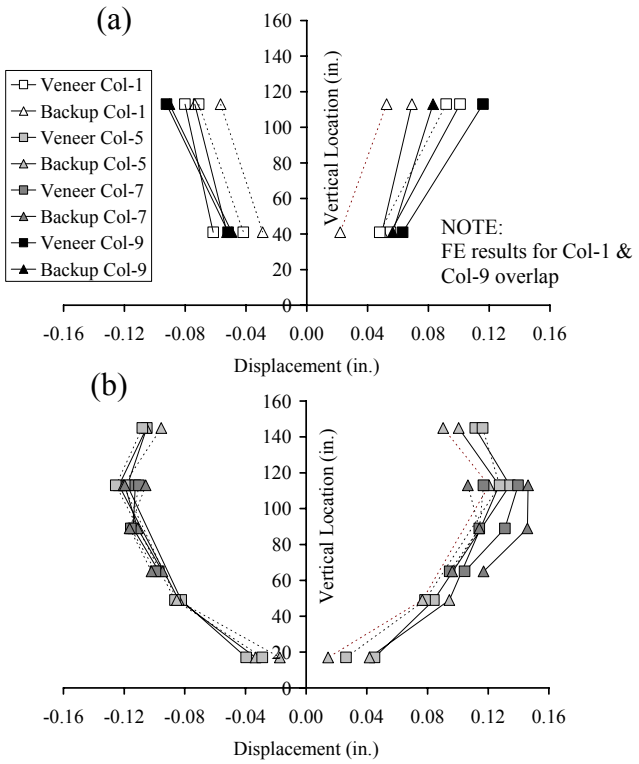

Figure 5.16 – Peak negative and positive displacements during dynamic M10-0.54[0.39]g experimental test (solid lines) and FE analysis (dashed lines) along (a) vertical edges, and (b) centerline and vertical window edge.

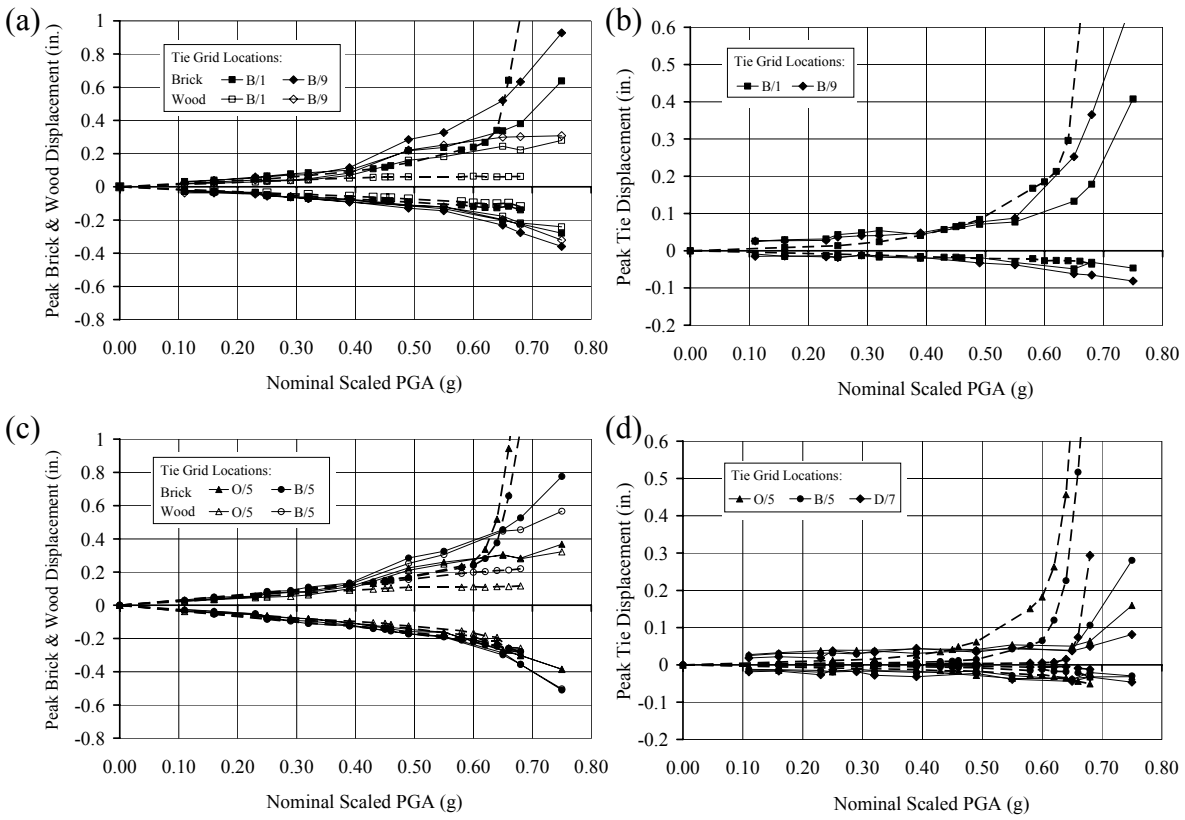

Figure 5.17 – Peak negative and positive displacement response plots, during M10 input tests and FE analysis: top corner (a) displacements and (b) tie deformations; (c) gable displacements and (d) gable and window tie deformations. (Experimental results – solid curves; FE results – dashed curves)

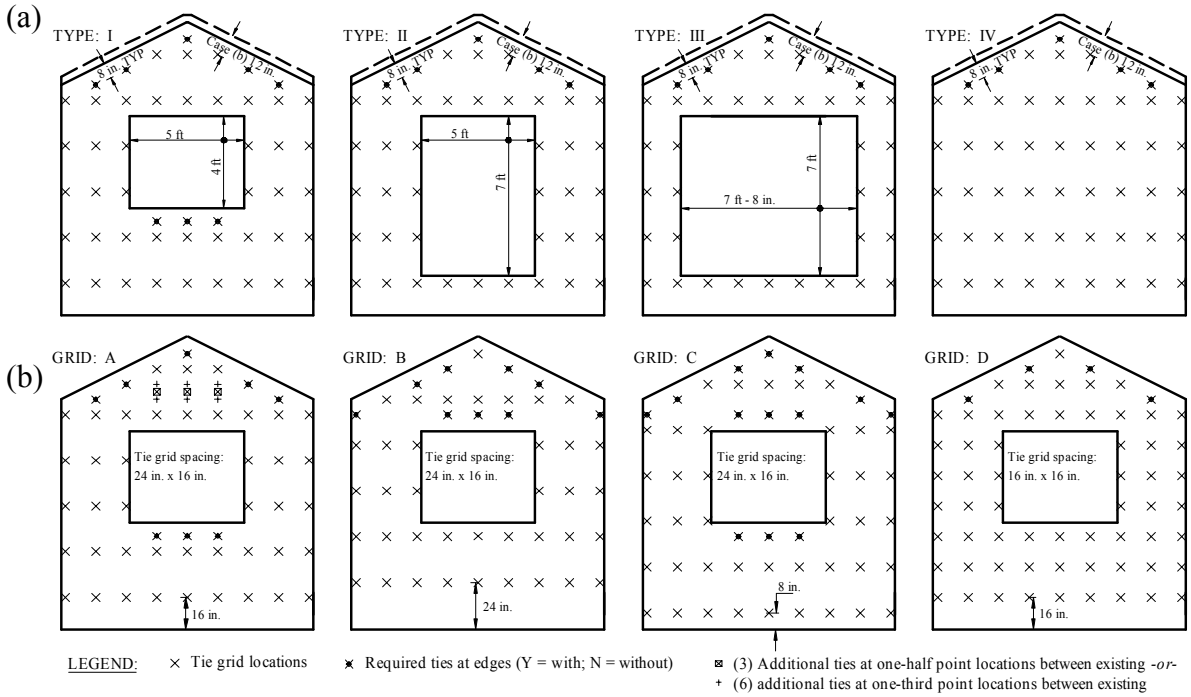

Figure 5.18 – FE model parameters and IDs: (a) wall panel geometries, and (b) tie connection grids and overall layouts.

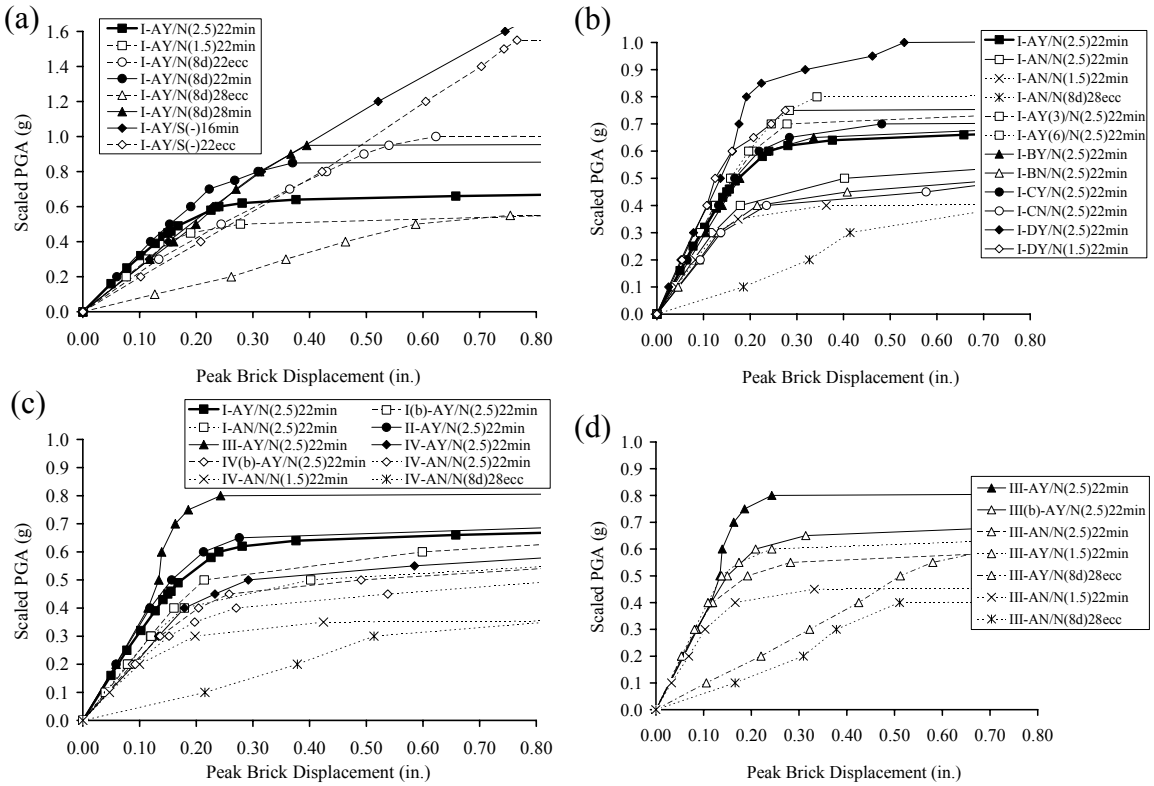

Figure 5.19 – FE dynamic pushover results, for various parameters: (a) tie connection properties, (b) tie layouts, (c) wall panel geometries, and (d) tie connection properties and layouts in gable region of a wall with a large opening.

FRAGILITY ASSESSMENT OF BRICK VENEER

The out-of-plane seismic fragilities of brick veneer walls built over a wood frame backup were evaluated analytically. Three-dimensional FE brick veneer wall panel models, developed and validated earlier in Chapter 5, were first simplified to functionally similar 2-D wall strip models. Nonlinear time history analyses were then carried out by subjecting the FE models to synthetic earthquake ground motion records, selected to represent the seismic characteristics of the central and eastern U.S. Onset of damage at key tie connection locations was used to evaluate the damage limit states of brick veneer walls; the two damage limit states evaluated in this fragility study were onset/accumulation of wall tie damage (described as repairable damage), and brick veneer wall instability/collapse. Throughout the analytical fragility study, the brick veneer wall panel component properties were assumed to be deterministic, therefore mainly focusing on wall damage uncertainty due to seismic loads only. The sensitivity of wall damage probabilities to variability in the ultimate capacities of the tie connections was reviewed afterwards. Three types of tie connection properties and two distinct tie layouts were represented in the FE wall models. Additionally, the influence of typical wood frame house backup properties on the out-of-plane seismic performance of brick veneer walls was also reviewed. Finally, the computed seismic fragility functions were used to compute the seismic hazard of brick veneer wall construction for key U.S. locations. Both current design standards and common practice for residential brick veneer construction have been evaluated.

6.1 Seismic Fragility Model

The seismic fragility of a structure and its components is generally identified as the failure probability of meeting their strength and/or serviceability performance objectives, as a function of seismic demand. To evaluate the fragility, a structural and/or component damage analysis has to be conducted, with the earthquake intensity measure as the input, and the damage limit state as the output. The damage limit state can be described by a system response variable D_j exceeding a deterministic threshold d. Therefore, a fragility function is the probability of exceeding a damage limit state at a given excitation intensity measure X, as follows:

$$F_R(x) \equiv P[D_j \geq d \,|\, X = x]. \tag{6.1}$$

This relationship has been idealized by a lognormal distribution as

$$F_R(x) = \Phi\left(\frac{\ln(x/m_R)}{\beta}\right), \tag{6.2}$$

where Φ denotes the standard normal (Gaussian) cumulative distribution function, m_R is the median value of the distribution, and β is the logarithmic standard deviation. The evaluation of these lognormal distribution parameters, the definition of damage limit states for brick veneer walls, and the selection of synthetic earthquake ground motions for

this fragility study are all described in this section. The FE brick veneer wall models and the fragility analysis method are then described in the subsequent sections.

6.1.1 Evaluation of Lognormal Distribution Parameters

Aleatory and epistemic sources of uncertainty have to be considered during seismic hazard analysis of structures (Wen 2004). Aleatory uncertainty has been identified as the inherent randomness, generally characterized by uncertainty in seismic demand and structural capacity. The seismic excitation uncertainty usually dominates the vulnerability of structures because the uncertainty in seismic excitation is typically much larger than that of the structural capacity (Wen and Ellingwood 2005). Therefore, in the current study, all of the brick veneer wall system components were simply assumed to be deterministic, and they were assigned average material properties based on experimental observations and standard published values. On the other hand, epistemic or knowledge based uncertainty is generally characterized by modeling error. This type of uncertainty was not evaluated in the current study because alternate prediction models (such as different FE wall panel models and/or earthquake ground motions) were not investigated.

In general, the seismic demand uncertainty β ($=\beta_{D|X}$) and median m_R were calculated through nonlinear time history analyses, as described in more detail below. (The logarithmic standard deviation $\beta_{D|X}$ was estimated to be equal to the coefficient of variation of the analysis response data, which is an appropriate estimate if the coefficient of variation does not exceed about 0.30 (Ang and Tang 1975).) Following the time history analyses, the sensitivity of brick veneer wall damage to the variability in tie connection capacity β_C was evaluated by combining the seismic uncertainty with that of the tie connection strength, as follows:

$$\beta = \sqrt{\beta_{D|X}^2 + \beta_C^2} \,. \tag{6.3}$$

The uncertainty in brick veneer tie connection strength β_C was characterized by the coefficient of variation of their ultimate strength capacities, as determined from a statistical analysis of tie subassembly test results (which are summarized in Table A.1, in Appendix A).

6.1.2 Damage Limit States for Residential Anchored Brick Veneer

During dynamic testing of brick veneer walls, it was noted that out-of-plane damage of such wall systems was closely related to the tensile performance limits of the tie connections. At the onset of tie damage, peak measured tie elongations were found to be closely related to elongations determined for ultimate loading during the tie subassembly tests. Different ranges of brick veneer wall behavior (including *elastic*, *intermediate*, and *ultimate*) and damage limit states were then identified and evaluated by focusing on the tensile performance of key tie connections. Simplified brick veneer wall strip models were used to evaluate the seismic fragilities in terms of two damage limit states for these wall systems, including: (*i*-*ii*) onset/accumulation of wall tie damage, and (*iii*) brick veneer wall instability/collapse. The maximum computed tie elongations D_j during nonlinear time history analyses were used to identify the damage limit states, where index j denotes the key tie connection locations associated with each damage limit state. The

analysis methods for these limit states are described in greater detail in the following sections, along with development and validation results of the simplified wall strip model, and with the fragility analysis procedure.

According to the ASCE 41-06 Standard for Seismic Rehabilitation of Existing Buildings (ASCE 2006), the seismic performance objectives for buildings can be described qualitatively in terms of: the safety afforded to building occupants during and after the event; the cost and feasibility of restoring the building to its pre-earthquake condition; the length of time the building is removed from service to effect repairs; and economic, architectural, or historic impacts on the larger community. These performance characteristics are directly related to the extent of damage that would be sustained by the building. Overall, it appears that the primary objectives for the seismic performance of residential anchored brick veneer will be related to maintaining occupant safety, along with cost and feasibility of repairs.

In terms of safety objectives, ASCE 41-06 requires that anchored brick veneer wall components satisfy three performance levels, including: Immediate Occupancy (IO), Life Safety (LS), and Hazards Reduced (HR). Qualitative descriptions of these performance levels for architectural cladding components, most applicable to anchored brick veneer, are summarized in Table 6.1. As mentioned earlier, damage limit states for brick veneer walls throughout this study were identified and evaluated by focusing on the tensile performance of key tie connections, without explicitly evaluating for cracking of the brick veneer. In general, both IO and LS performance levels can therefore be related to the (*i*-*ii*) onset/accumulation of wall tie damage limit state for residential brick veneer, and the HR performance level can be related to the ultimate (*iii*) collapse/instability damage limit state.

In terms of repair costs, these two damage limit states can be generally described as (*i*-*ii*) repairable damage and (*iii*) collapse, respectively. Repairable damage will typically involve re-anchoring, as well as some tuckpointing or crack repair of the brick veneer; at the ultimate limit state, collapse will involve partial or full reconstruction of the brick veneer. A summary of average typical brick masonry veneer repair costs is provided in Table 6.2. Overall, it can be expected that "repairable damage" will result in repair costs of approximately several hundred dollars (perhaps up to a few thousand); reconstruction of collapsed walls, on the other hand, might result in a few thousand and maybe up to tens of thousands of dollars worth of repairs (a significant portion of the total cost of a single-family home). This type of information can be utilized by building owners, as well as insurance companies, to estimate probable financial losses of residential brick veneer construction during earthquakes.

6.1.3 Earthquake Ground Motion Records

The seismic vulnerability of brick veneer with wood frame backup construction was evaluated for residential buildings located in the central and eastern U.S. Few moderate earthquake ground motion records are available for this region, and almost none that correspond to large earthquakes. Therefore, for seismic performance evaluation of buildings and structures, synthetic uniform hazard ground motions have been generated

by Wen and Wu (2001). The ground motions were developed for representative soil and rock site conditions, with 10% and 2% in 50 year hazard levels, based on the latest seismicity information in and around Memphis, Tennessee, St. Louis, Missouri, and Carbondale, Illinois. These records were based on point-source, finite-fault, and quarter-wavelength models, effectively representing the seismic characteristics of the region; the body wave magnitudes of these earthquakes are approximately in the range of 5 to 8.

A total of twenty synthetic earthquake records (ten records with a hazard level of 10%, and another ten with a hazard of 2%, in 50 years) for representative soil conditions in Memphis, Tennessee, were selected for the current study. The elastic response spectra for these synthetic earthquake records are shown in Figure 6.1, and the acceleration traces are presented in Figures D.1 and D.2 (in Appendix D). (Two earthquake records, labeled as M10 and M02, were selected earlier from this set of twenty and were used during the experimental and analytical studies described in Chapters 4 and 5.)

For seismic fragility assessment of brick veneer walls, the seismic excitation intensity measure X was characterized by the earthquake input peak ground accelerations (PGAs). The intensity can also be measured by spectral accelerations, evaluated at the first natural period of the structure being analyzed and 5% or higher damping (Cornell et al. 2002). However, the PGA appeared to be the most appropriate seismic intensity measure for this problem because the dynamic properties of nonstructural components (such as brick veneer walls) and those of the supporting structure vary case by case, making it difficult to select a fixed set of dynamic properties for evaluating spectral accelerations that would effectively characterize the loading on these components. As part of the current study, the influence of wood frame home backup dynamic response on the out-of-plane seismic performance of brick veneer walls was also reviewed.

6.2 FE Wall Strip Model Setup and Validation

For analytical fragility assessment of brick veneer walls, the 3-D solid single-story brick veneer wall panel models, which were developed, calibrated, and validated per experimental wall behavior (as described in *Part I* of Chapter 5), were reduced to a 2-D wall strip. As shown in Figure 6.2(a), this wall strip was set up to be 16 in. (406 mm) wide, representing the tributary width of a wall system with a wood backup stud spacing of 16 in. on center. Preliminary time history analyses were conducted by subjecting the FE wall strip model to out-of-plane seismic loads, to validate its performance against earlier analytical and experimental results, capturing different ranges of wall behavior and key damage limit states. FE modeling of a lumped wood house backup structure, and its effects on the out-of-plane behavior of brick veneer walls, was also explored. The analysis software *ABAQUS* (Abaqus Inc. 2006) and the pre- / post-processor software *MSC.Patran* (MSC 2005) were used to develop these FE brick veneer wall strip models and to carry out the time history analyses. Development and validation of the 2-D wall strip model are described in this section.

6.2.1 Brick Veneer Wall Strip Model

As shown in Figure 6.2(a), the brick veneer wall strip model consisted of the wood frame wall, the brick veneer, and the corrugated sheet metal tie connections; other surrounding "boundary" components of the wall structure were implemented as spring support conditions. The wall strip was 16 in. (406 mm) wide (with one column of ties along its center) and 120 in. (3.05 m) tall (from the supports at the base of the brick veneer to the supports at the top of the wood frame backup). As in the 3-D solid wall panel models (described in *Part I* of Chapter 5), the wood frame stud wall model extended to a height of 112 in. (2.84 m) from its bottom supports at the top of the foundation to the centerline of the roof/ceiling joists. (To represent the behavior of taller brick veneer walls, such as the experimental setup of the gable-end wall specimen, a centerline model would have to be developed, however without the interruption of the window opening.) The brick veneer model, supported 8 in. (203 mm) below the wood frame, reached a height of 110 in. (2.79 m), terminating at the top row of ties. The small overhang (one brick) of masonry beyond the top tie, of approximately 3 in. (76 mm), was not explicitly modeled; however, lumped mass was added to the top node of the veneer shell model based on the tributary area of this overlap. The 3 in. (76 mm) distance between the reference planes of the brick veneer and the wood frame models (which includes the 1 in. [25 mm] air space) defined the length of the tie connection elements.

The vertical tie spacing of 24 in. (610 mm) and the distance between the physical model section centerlines (of the wood frame and the brick veneer) defined the entire FE model geometry (Figure 6.2(a)). The wood frame wall panel strip (2x4 stud and exterior OSB sheathing) was modeled as a linear elastic composite beam. The 2x4 stud beam was assigned dimensions of 1.5 in. x 3.5 in. (38 mm x 89 mm), and the OSB was modeled as 7/16 in. (11 mm) thick (as in the experimental brick veneer wall system described earlier in Chapter 4). The brick veneer was also assumed to be linear elastic and was modeled using shell elements, with its reference plane at the shell mid-surface, assigned a thickness of 3.5 in. (89 mm). As mentioned earlier, the material properties for wood and masonry components were assumed to be deterministic; median modulus of elasticity and density values were assigned, based on those utilized in modeling of the experimental wall specimens, as listed in Table 5.1 of Chapter 5.

In the 3-D solid wall panel models, the cumulative effects of the surrounding wood backup components (such as the concrete foundation, floor and roof/ceiling framing, including rafter ties and other nail connections to the wall frame) on the brick veneer wall system were incorporated into nine elastic torsional springs along the bottom of the wall and nine translational spring supports along the top. The spring supports were reduced to one of each in the simplified 2-D model; the torsional spring stiffness at the wall base was kept at 1,000 k-in./rad (110 kN-m/rad), and a weighted average stiffness of 1.4 k/in. (250 kN/m) was assigned to the lateral support spring at the top of the wall strip. Furthermore, a pin support with a nonlinear elastic rotational spring was implemented at the base of the brick veneer wall model, representing a rigid body rocking response (based on the self-weight and geometry of the brick veneer). As in the earlier FE models, a viscous damping ratio of 4% was assigned to the brick veneer wall strip model.

The brick veneer and wood frame backup FE models were linked along their vertical centerline by axial bar elements representing the tie connections. As discussed in Chapters 4 and 5, the experimental brick veneer walls generally exhibited more rigid body rotation (rocking about their base) than bending when subjected to out-of-plane static and moderate dynamic loading. Experimental results also indicated that wall response, up to and including ultimate cracking and collapse of the veneer, was most closely associated with the performance of the tie connections. The experimental load vs. displacement behaviors of the tie connections, evaluated both during tie subassembly and brick veneer wall panel testing (Figure 5.3), were implemented in unique nonlinear material constitutive models for these axial elements. The overall tie connection model was assigned nonlinear inelastic "material" properties in tension (based on the average idealized monotonic tension behavior from subassembly test results) and linear elastic in compression (based on both subassembly and wall test results), to combine the effects of the ties and excess mortar within the wall cavity. The effects on wall fragilities due to three distinct tie connection properties were studied, as defined in the following section. Before conducting fragility analyses with this type of brick veneer wall model, it was first validated to effectively represent the seismic performance of these wall systems evaluated earlier by 3-D modeling.

6.2.2 Validation of FE Wall Strip Model

Three wall strip models were set up for validation against the 3-D solid FE wall model behavior. Each model represented wall construction with ties spaced vertically at 24 in. (610 mm), defined earlier as wall type A in *Part I* of Chapter 5, containing tie types: N(8d)28min, N(8d)22ecc, and N(1.5)22min. The wall strip models were then subjected to the scaled M10 earthquake input record, with the computed response displacements compared to those from 3-D FE wall analyses. The performance of the 2-D brick veneer wall models was also verified for different levels of wall response (which included *elastic*, *intermediate*, and *ultimate*), as well as for key damage limit states.

As shown in Figure 6.3(a), the total outward displacements of the brick veneer and wood frame backup wall in the 2-D wall strip model with N(8d)28min type ties matched very closely with the centerline displacements in the 3-D wall model. The centerline tie elongation results were also similar, as seen in Figure 6.3(b). The peak displacements at the top of the wood frame backup in the 2-D model, however, are somewhat lower than those in the 3-D model; the topmost tie elongations are therefore a bit higher in the 2-D model. This behavior was expected because the lateral support spring at the top of the 2-D wall strip model, which represented the average of all nine support springs in the 3-D model, was somewhat stiffer than the intermediate supports in the 3-D model. Nonetheless, the average stiffness properties captured the total effect of the nine translational springs quite effectively, as shown in the total displacement response vs. M10 input PGAs for the three different wall panels in Figure 6.3(c).

During the experimental and analytical studies discussed earlier (in Chapters 4 and 5), it was noted that the overall veneer wall response depended primarily on the performance of the tie connections. Three damage limit states were then identified for the 3-D FE wall panel models, based on onset of tie failures at key tie locations in the models. In the

simplified 2-D wall strip model, however, only two comparable damage limit states were able to be evaluated because the spread of tie damage horizontally (starting at the corners, and moving toward the center) could not be represented by the 2-D model. The two damage limit states were: *(i-ii)* onset/accumulation of tie failure at top of the wall (a combination of the first two damage limit states evaluated earlier with the 3-D models) and *(iii)* tie failure at the second row from the top (representing brick veneer wall instability/collapse). Overall, the 2-D model effectively captured the key damage limit states identified earlier with 3-D models, as shown in Table 6.3. On average, the M10 input earthquake PGAs for the onset of tie failure in the 2-D models were very close to the first two damage limit state PGAs evaluated with the 3-D model; the PGAs for the third damage limit state were also very close. (An example set of PGA vs. key tie displacement results used to evaluate the damage limit states with the 2-D models are shown in Figure D.3, in Appendix D.)

6.2.3 Lumped Backup Structure Model

In general, the dynamic response of nonstructural elements, such as brick veneer walls, will depend on the response of the structure to which they are connected. Therefore, the response of elements will not only depend on the characteristics of the ground motion that excites the base of the structure, but also on the dynamic characteristics of the structure itself. It is likely that the natural frequency of the nonstructural element could be close to the natural frequency of the supporting structure, further increasing the excitation magnitude of that nonstructural element (Villaverde 2004). For example, Gad et al. (1999) showed that brick veneer walls built over a light frame steel backup structure responded out-of-plane at somewhat higher frequencies than the first mode of vibration of the backup system (as described in greater detail earlier in Chapter 2, and shown in Figure 2.9(c)), demonstrating the interaction between the brick veneer response and that of the backup structure. For dynamic analysis of nonstructural components, the floor response spectrum method is typically employed, involving analysis of components by subjecting them to the dynamic response of the supporting structure. Paquette et al. (2001) employed a similar method during shake table testing of brick veneer walls, which were extracted from the second floor of an existing two-story building; an estimated seismic acceleration response of that two-story building was used as the shake table input excitation for dynamic testing of the wall panels.

The FE brick veneer wall models employed in this fragility study were generally based on the experimental brick veneer wall specimens and their observed behavior. The experimental wall specimens effectively captured the various details of actual brick veneer wall systems, including their boundary conditions; however, due to limitations of the shake table size and capacity, the mass and dynamic response of an entire house were not represented in the test setup. Furthermore, it is difficult to estimate a fixed set of properties to characterize a typical wood frame home structure because they are highly variable. The total layout of the home, such as shown in Figure 6.4, can play a significant role on the effective mass, stiffness, and damping properties of the structure. (The home structure architectural details, including the type of exterior wall construction, number of openings, layout of interior partitions, among other details will determine its dynamic characteristics.) For example, Kharazzi and Ventura (2006) showed that the

natural period of vibration for non-engineered two-story wood frame homes can vary between 0.19 and 0.55 sec. Experimental tests conducted by Filiatrault et al. (2002) showed that the first mode period for two-story wood frame homes can fall in the range of 0.15 to 0.25 sec., depending on the wall siding materials. On the other hand, the average damping properties will generally depend on the building materials, as well as the magnitude of dynamic response (total drift) of the wood frame home structure (closely related to the amount of damage and dissipated energy). It is common to assume a viscous damping ratio as low as 2% for wood frame homes, when their total response is relatively low and mainly linear elastic. However, for higher response magnitudes, when the total building drifts enter highly nonlinear behavior of structural components, the equivalent viscous damping ratio has been shown to be as high as 20% (Filiatrault et al. 2003).

To evaluate the sensitivity of the dynamic response of brick veneer walls as a function of the backup structure properties, a simple lumped backup structure model was introduced at the top support of the brick veneer wall strip model, as shown in Figure 6.2(b). A lumped weight of 32 kips (corresponding to a mass of 14,500 kg) was used, representing an estimated weight of a single-story wood frame home. A viscous damping ratio of 5% was assigned to the lumped backup structure model, assuming that the backup response would primarily be dominated by linear behavior. Then, the stiffness properties of the lumped backup model were varied during this sensitivity study, in relation to the first natural period of vibration of the brick veneer wall panel T_{wall}. Five different backup stiffness models were explored, which included stiffness properties defined by T_{backup}/T_{wall} equal to 0.0, 0.5, 1.0, 1.5, and 2.0 (e.g., a ratio of 0.0 represents a wall strip with a rigid backup). In this sensitivity study, the wall strip models were assigned N(8d)22ecc types of ties, resulting in a T_{wall} equal to 0.139 sec (Table 6.1). Each model was then subjected to all twenty Memphis, Tennessee, earthquake ground motion records normalized and scaled to PGAs of 0.5g.

The average peak tie elongation response was computed for each group of models, as shown in Figure 6.5. As expected, the highest computed tie elongations at the top two tie connections were for a wall strip with T_{backup}/T_{wall} equal to 1.0; however, a significant increase in response was also seen for a T_{backup}/T_{wall} equal to 1.5. A lumped backup with a period of vibration set to half or twice that of the wall panel, resulted in little to no amplification in tie displacement response, with the results being similar to those evaluated for a wall with a rigid backup. (Note that a backup structure with a higher period of vibration will generally result in higher total drifts, which could play another detrimental role on the out-of-plane performance of brick veneer walls, by imposing high in-plane shear deformations on the tie connections.) Overall, it appeared that the experimental test setup (where $T_{backup}/T_{wall} = 0.0$, without representing a house backup structure) was an effective upper bound for evaluating the out-of-plane dynamic performance of brick veneer walls, capturing the minimal amplification effects of both very rigid and flexible backups. On the other hand, a brick veneer wall model supported by a backup structure assigned dynamic properties similar to those of the wall panel ($T_{backup}/T_{wall} = 1.0$) presented a conservative lower bound. Therefore, the seismic fragility

of brick veneer walls was analyzed by employing these two types of backup support models.

6.3 Fragility Analysis Setup and Procedure

6.3.1 Brick Veneer Wall Parameters

A total of eight FE brick veneer wall strip models were developed for seismic fragility analysis of this form of construction. FE wall strip models were generated to represent walls built in accordance with prescriptive construction and design requirements per MSJC (2008), IRC (ICC 2003), and BIA (2003), as well as per methods employed in actual construction practice (which do not always meet the prescribed requirements). The seismic performance and damage of brick veneer walls has been attributed to the performance of corrugated sheet metal tie connections; therefore, brick veneer wall fragilities were evaluated as a function of three representative types of tie connections, capturing the effects of different tie thickness, tie bend eccentricity, and tie attachment method to the wood stud. The three tie connection properties explored were: (1) the code compliant 22 ga. ties with 1/2 in. maximum bend eccentricity, attached to the wood stud by an 8d nail (N(8d)22ecc); (2) the thinner 28 ga. ties without a bend eccentricity, also attached by an 8d nail (N(8d)28min, which is the same type of tie connection used in experimental Wall-1); and (3) the 22 ga. ties without a bend eccentricity, attached by a 1.5 in. roofing nail (N(1.5)22min), representing poor workmanship during tie installation. Current design standards and common practice for residential brick veneer construction were evaluated by focusing on these tie connections with two distinct layouts. A vertical tie spacing of 24 in. (610 mm), labeled as wall type A (earlier in Chapter 5), was employed for walls with all three types of tie connections, representing the maximum supported brick veneer wall area (per tie) requirement with seismic design category C or lower per MSJC (2008). Two types of lumped backup models were represented for each of these walls, with dynamic properties defined by T_{backup}/T_{wall} equal to 0.0 and 1.0. Then, two additional wall models were studied, with N(8d)22ecc and N(1.5)22min types of ties, with a vertical spacing of 16 in. (406 mm), labeled as wall type D (per Chapter 5), representing a maximum supported wall area requirement for seismic design category D or higher. These two models were studied for the worst-case scenario backup properties only, with T_{backup}/T_{wall} equal to 1.0.

6.3.2 Analysis Procedure

The fragility of brick veneer walls was evaluated by conducting nonlinear time history analyses with the FE wall strip models defined above. The FE wall strip models were subjected to twenty synthetic earthquake ground motions, normalized and scaled with respect to PGA at 0.1g increments. The peak tie elongation response D_j was recorded for each wall panel model. As discussed earlier, the occurrences and sequences of tie damage were assessed with the FE models to evaluate key damage limit states of brick veneer walls. Tie connection damage in the FE models was determined from the maximum computed tie elongations D_j; at a stage when these elongations exceeded the opening displacements at ultimate load capacity (d) found from the tie subassembly tests, the tie connections in the FE models were considered to be damaged. As mentioned earlier, the seismic fragilities of brick veneer walls were evaluated for two damage limit

states, including: *(i-ii)* onset/accumulation of tie failure at the top of the wall (with $D_A \geq d$) and *(iii)* instability/collapse as defined by tie failure at the second row from the top in walls with a vertical spacing of 24 in. (610 mm) (with $D_B \geq d$), or by tie failure at the third row from top in walls with a vertical spacing of 16 in. (406 mm) (with $D_C \geq d$).

As depicted in Figure 6.6, the likelihood of damage was then computed for the known earthquake excitation intensities. The probability of wall damage was computed at each PGA increment by

$$P_f = \frac{m+1}{M+1}, \tag{6.4}$$

where m is the number of walls which experienced damage, and M is the total number of analyses (equal to twenty in this study). This probability function, as presented by Porter et al. (2007), generally provides a conservative estimate of the failure probability, when a relatively small sample is available; an alternate function m / (M + 1) can also be employed for computing the failure probability, but was not utilized in the current study. (According to Porter et al. (2007), good quality fragility functions can be obtained by conducting at least twenty analyses per PGA increment.) Lognormal distribution parameters were then computed based on the damage probabilities and the natural logarithm of the input PGAs. The analysis results and fragility functions are presented below.

6.4 Fragility Analysis Results

Nonlinear time history analyses were conducted with the simplified wall strip models, to evaluate the seismic fragility of brick veneer walls by following the methods and procedures described above. The out-of-plane response of brick veneer wall strip models subjected to synthetic earthquake records (Figure 6.1) was computed for selected PGA magnitudes, at 0.1g increments. Damage limit state probabilities were then evaluated at each PGA increment, as seen in the example set of results in Tables 6.4 and 6.5, for a wall strip with a rigid backup, containing N(8d)22ecc type tie connections, spaced vertically at 24 in. (610 mm). The number of walls which experienced damage (m) at each PGA increment was computed from the sum of indexes, taken as 0 or 1 for each set of analysis results (where 0 implies no failure of key tie connections, and 1 implies failure). As seen from these tables, time history analyses were not necessary for all cases because certain of these indexes could be assigned by inspection.

Lognormal distribution parameters for the two damage limit states were then computed by constructing lognormal "probability paper" plots for each brick veneer wall type. The inverse of the damage limit state probabilities was graphed along the x-axis, and the natural logarithm of the earthquake input PGAs along the y-axis of these plots, as shown in Figure 6.7 (for the same example wall strip discussed above). (All of the "probability paper" plots and parameter calculations are shown in Figure D.4 in Appendix D, for all eight wall panel types studied herein.) Overall, the plotted data exhibited a nearly linear trend, indicating that a lognormal distribution was generally a good fit to the analysis data. The y-intercept of the best fit line to the plotted data represented the lognormal

distribution median m_R, and the slope was the standard deviation $\beta_{D|X}$ (Ang and Tang 1975). Lognormal distribution parameters for all brick veneer wall panels have been summarized in Table 6.6.

Finally, the fragility curves based on these analysis results are shown in Figure 6.8 for the six walls with a vertical tie spacing of 24 in. (610 mm), and in Figure 6.9 for the two walls with a tie spacing of 16 in. (406 mm). In addition to brick veneer wall fragilities based on the lognormal parameters from Table 6.6, a set of curves was also evaluated to show the sensitivity of the fragilities to variability in the ultimate capacities of the tie connections (β_C), per Equation 6.3. (From Table A.1, the coefficients of variation for the ultimate strength of the tie connections studied were 0.36, 0.13, and 0.17, respectively for N(8d)22ecc, N(8d)28min, and N(1.5)22min types of ties.) A detailed discussion of these results and an evaluation of the seismic hazard for this type of construction are presented below.

6.5 Discussion of Fragility Analysis Results

6.5.1 Fragility Functions for Brick Veneer Walls

The seismic fragilities of brick veneer walls were evaluated for a number of different wall construction parameters. As seen from Figure 6.8, the two wall panels with ties attached by 8d nails exhibited similar fragilities at both damage limit states, and walls with ties attached by short roofing nails experienced damage at significantly lower PGAs (with fragility curves shifted noticeably to the left of those developed for walls with stronger tie connections). For walls with reduced tie spacings (Figure 6.9), the fragility curves exhibited a slight shift to the right, as compared to the curves for walls with larger tie spacings. Damage to brick veneer walls was also affected by the amplification of the lumped backup structure model, with the damage limit state PGAs nearly two times lower for walls with the worst-case backup stiffness defined by T_{backup}/T_{wall} equal to 1.0. (Overall, these fragility functions developed analytically provide a more accurate estimate of brick veneer wall seismic vulnerabilities, compared to the expert opinion based fragilities for unreinforced masonry buildings, which may only act as a baseline case for fragility assessment of brick veneer construction (Figure 2.16).)

The sensitivity of brick veneer wall fragilities to uncertainty in tie connection strength β_C is also presented in Figures 6.8 and 6.9. Overall, increasing the lognormal standard deviation reduced the slope of the fragility curves, which appear to rotate about the mean damage PGAs. (The probability of brick veneer wall failure computed with consideration of uncertainty in tie connection strength was generally higher for earthquake excitation PGAs on the left side of the mean damage PGA, and the probability of failure was lower on the right side of the mean.) The fragilities for walls containing N(8d)22ecc type tie connections experienced the largest change in their slope because these tie connections had a somewhat high β_C, whereas the other two types of walls showed minor variations.

6.5.2 Seismic Hazard of Brick Veneer Wall Construction

The seismic fragility functions for brick veneer walls were used to compute the seismic hazard of this form of construction built in selected regions of the central and eastern U.S. Peak ground accelerations for 10% and 2% in 50 year earthquake hazards were obtained from the USGS website (http://gldims.cr.usgs.gov/) for Urbana, Illinois, Memphis, Tennessee, Atlanta, Georgia, and Charleston, South Carolina. The cities in Illinois and Georgia were selected to represent regions with low to moderate seismicity, whereas those in Tennessee and South Carolina represented regions with higher seismicity. The probabilities of brick veneer damage for all locations and earthquake hazard PGAs were then evaluated and listed in Table 6.7. These failure probabilities were computed without considering variability in tie connection strength (i.e., $\beta = \beta_{D|X}$).

The performance of anchored residential brick veneer presented in Table 6.7, along with Figures 6.8 and 6.9, can be compared with the acceptable seismic performance levels established in ASCE 41-06. The Basic Safety Objective (BSO) for the seismic performance of buildings requires that the Life Safety (LS) performance objective is met for a 10% in 50 year earthquake hazard level, and that the Collapse Prevention (CP) objective is met for a 2% in 50 year hazard. In general, the BSO for residential anchored brick veneer can be achieved when damage limit state (*i-ii*) onset/accumulation of wall tie damage (similar to the IO and LS performance objectives) is met for the 10% in 50 year earthquake hazard, and damage limit state (*iii*) wall instability/collapse (similar to the Hazards Reduced (HR) performance objective) is met for the 2% in 50 year hazard. (These performance levels and associated damage for nonstructural architectural cladding components were summarized earlier in Table 6.1.)

From Table 6.7, it appears that brick veneer walls built according to the minimum design and construction requirements (by utilizing N(8d)22ecc types of ties) will generally perform well in low to moderate seismicity regions; even with non-compliant construction methods, where ties are attached to the backup with short roofing nails (N(1.5)22min types of ties), the repairable damage and collapse probabilities are very low, respectively, for 10% and 2% in 50 year earthquake hazard levels. The probabilities of the first damage state for the 2% in 50 year earthquake hazard level are also somewhat high for the worst-case scenario brick veneer construction with ties utilizing short roofing nails. On the other hand, in higher seismicity regions, brick veneer walls with non-compliant construction methods and the worst-case scenario backup properties, exhibit greater than 90% probabilities for the first damage state during a 10% in 50 year event, and approximately 100% probability of collapse during a 2% in 50 year event; probability of onset of damage for the 2% in 50 year hazard is also high for all wall types. Overall, brick veneer walls anchored by tie connections utilizing short roofing nails will not meet the minimum seismic safety objectives for these earthquake hazards, and brick veneer wall construction of this type would also result in significant repair and/or replacement costs. Walls built in accordance with the minimum code requirements (with N(8d)22ecc types of ties) will result in approximately 2% or lower probabilities of exceeding the first damage state during a 10% in 50 year earthquake hazard; however, brick veneer walls with the same types of tie connections, and with the worst-case scenario backup properties, will result in relatively high probabilities of collapse for the

2% in 50 year hazard, indicating that the BSO per ASCE 41-06 will generally not be met by this form of construction in regions of higher seismicity. In general, the 2% in 50 year earthquake hazard PGAs appeared to govern the seismic performance of residential brick veneer construction in these regions.

Finally, brick veneer wall fragility functions were used to compute damage limit state PGAs at failure probabilities of 5% and 95%, for walls with the worst-case scenario backup properties, and those PGA values were summarized in Table 6.8. In general, these results can be implemented to identify geographic locations in the central and eastern U.S. where anchored brick veneer construction would be viable, by utilizing USGS seismic hazard maps shown in Figure 6.10. The results imply that the minimum code requirements should be followed for anchored brick veneer construction throughout low to moderate seismicity regions; 22 ga. ties with a maximum bend eccentricity of 1/2 in. (12.7 mm) should be attached to the backup by 8d nails with a vertical spacing of 24 in. (610 mm), resulting in a supported wall area per tie of 2.67 ft^2 [0.25 m^2] (i.e., the maximum wall area for construction with seismic design category C or lower per MSJC (2008)), in regions with 2% in 50 year earthquake hazard PGAs of up to 0.26g. Then, a vertical spacing of 16 in. (406 mm), a supported wall area per tie of 1.78 ft^2 [0.17 m^2], should be employed in regions with 2% in 50 year hazard PGAs of up to 0.36g. Standard methods of construction are not recommended in higher seismicity regions, where 2% in 50 year PGAs exceed 0.36g; in such regions, improved methods for connecting the brick veneer to the wood frame backup should be employed.

6.6 Summary and Conclusions

The out-of-plane seismic fragilities of brick veneer walls built over a wood frame backup were evaluated analytically. FE models of brick veneer walls were developed with three types of tie connection properties and two distinct tie layouts. Additionally, a lumped model representing wood frame house backup properties was also implemented. Nonlinear time history analyses were then carried out by subjecting FE brick veneer wall models to synthetic earthquake ground motion records, selected to represent the seismic characteristics of the central and eastern U.S. Onset of damage at key tie connection locations was used to evaluate the damage limit states of brick veneer walls. Both current design standards and common practice for residential brick veneer construction have been evaluated. Key findings from this study can be summarized as follows:

- The two damage limit states evaluated in this fragility study were (*i*-*ii*) onset/accumulation of wall tie damage, and (*iii*) brick veneer wall instability/collapse. These damage limit states were then assessed in terms of approximate safety objectives and repair costs. In terms of safety objectives, the first damage limit state (*i*-*ii*) was related to Immediate Occupancy (IO) and Life Safety (LS) performance levels, and the second limit state (*iii*) was related to Hazards Reduced (HR) performance level, as established in ASCE 41-06. In terms of repair costs, these two damage limit states were generally described as (*i*-*ii*) repairable damage (involving possible re-anchoring of the brick veneer and tuckpointing or crack repair) and (*iii*) collapse (which would involve partial or full reconstruction of the brick veneer).

- Two-dimensional FE brick veneer wall strip models were developed, and they were shown to effectively capture the seismic performance and key damage limit states for brick veneer walls. A lumped backup structure model was then introduced at the top support of the wall strip models, to represent the influence of typical wood frame house backup properties on the out-of-plane seismic performance of brick veneer walls (assuming that the backup response would primarily be dominated by linear behavior). In the fragility study, two stiffness properties were assigned to the lumped backup model, in relation to the first natural period of vibration of the brick veneer wall panel T_{wall}, including: T_{backup}/T_{wall} = 0.0 (an effective upper bound for evaluating the out-of-plane dynamic performance of brick veneer walls, capturing the minimal amplification effects of both very rigid and flexible backups), and T_{backup}/T_{wall} = 1.0 (an effective conservative lower bound, representing the worst-case scenario backup properties).
- The seismic fragilities for residential brick veneer wall construction were evaluated as a function of earthquake excitation peak ground accelerations (PGAs). On average, brick veneer walls with 22 ga. and 28 ga. ties attached by 8d nails exhibited similar fragilities at both damage limit states, and walls with 22 ga. ties attached by short roofing nails (representing poor workmanship during tie installation) experienced damage at significantly lower PGAs. For walls with reduced tie spacings, the fragility curves exhibited a slight shift to the right, as compared to the curves for walls with larger tie spacings. Damage to brick veneer walls was also affected by the amplification of the lumped backup structure model, with the damage limit state PGAs nearly two times lower for walls with the worst-case backup stiffness defined by T_{backup}/T_{wall} equal to 1.0.
- The uncertainty in seismic loading dominated the vulnerability of brick veneer walls; however, brick veneer walls utilizing tie connections with higher variability in their ultimate strength resulted in a noticeable effect on the fragility curves. By increasing the lognormal standard deviation, the slope of the fragility curves was reduced, generally causing them to rotate about the mean damage PGAs. Brick veneer walls with N(8d)22ecc type tie connections exhibited the largest variation.
- Damage limit state probabilities for residential anchored brick veneer were computed for 10% and 2% in 50 year earthquake hazard PGAs, for selected regions of the central and eastern U.S. Results showed that brick veneer walls, built following code compliant and non-compliant construction methods, will generally meet the safety performance objectives in low seismicity regions, with minimal repair or replacement costs. On the other hand, in regions of moderate to high seismicity, brick veneer walls utilizing tie connections with short roofing nails will generally not meet the minimum seismic safety objectives, as well as result in significant repair and replacement costs. Furthermore, brick veneer walls built in accordance with the minimum code requirements, utilizing 22 ga. ties attached by 8d nails, will result in very low probabilities of exceeding the onset/accumulation of wall tie damage during a 10% in 50 year hazard in those same higher seismicity regions. However, these brick veneer walls with the worst-case scenario wood frame backup properties will result in high probabilities of collapse for the 2% in 50 year earthquake hazard.

- Overall, the 2% in 50 year earthquake hazard PGA values and the collapse limit state governed the seismic performance of residential brick veneer wall systems built throughout the central and eastern U.S. In low to moderate seismicity regions, the minimum design and construction requirements for brick veneer walls should be followed, including the use of 22 ga. ties installed with a maximum bend eccentricity of 1/2 in. (12.7 mm) and attached to the backup by 8d nails. Based on FE models with the worst-case scenario backup properties, wall construction employing ties with a vertical spacing of 24 in. (610 mm), resulting in a supported wall area per tie of 2.67 ft^2 [0.25 m^2] (i.e., the maximum wall area for construction with seismic design category C or lower per MSJC (2008)), is generally acceptable throughout regions with 2% in 50 year earthquake hazard PGAs of up to 0.26g. Then, a vertical spacing of 16 in. (406 mm), a supported wall area per tie of 1.78 ft^2 [0.17 m^2], should be employed in regions with 2% in 50 year hazard PGAs of up to 0.36g. Standard methods of construction are not recommended in higher seismicity regions, where 2% in 50 year PGAs exceed 0.36g; in such regions, improved methods for connecting the brick veneer to the wood frame backup should be employed.

Table 6.1 – Performance levels and damage for architectural cladding components per ASCE 41-06.

Immediate Occupancy (IO)	Life Safety (LS)	Hazards Reduced (HR)
Connections yield; minor cracks (< 1/16 in. width) or bending in cladding.	Severe distortion in connections. Distributed cracking, bending, crushing, and spalling of cladding components. Some fracturing of cladding, but panels do not fall.	Severe distortion in connections. Distributed cracking, bending, crushing, and spalling of cladding components. Some fracturing of cladding, but panels do not fall in areas of public assembly.

Table 6.2 – Summary of brick veneer wall repair costs.

Repair Type*	Approximate Cost (Year 2008-2009)
Installation of Repair Anchors	\$10 - \$20 per anchor
Crack Repair - Tuckpointing	\$5 - \$10 per linear ft
Reconstruction of Brick Masonry	\$15 - \$20 per square ft

* Includes materials and labor.

Table 6.3 – Solid FE wall model parameters with damage states and M10 earthquake input PGAs.

Wall Panel Type (Tie Grid / Tie Properties)	Wall Natural Period of Vibration, T_{wall} (sec)	Damage States *(i)*	*(ii)*	*(iii)*
A/N(8d)28min	0.126	0.45	0.55	0.65
A/N(8d)28min – 16 in. wide strip		0.50		0.65
A/N(8d)22ecc	0.139	0.45	0.50	0.65
A/N(8d)22ecc – 16 in. wide strip		0.45		0.65
A/N(1.5)22min	0.127	0.15	0.25	0.35
A/N(1.5)22min – 16 in. wide strip		0.20		0.30

Table 6.4 – Computed tie displacements from nonlinear time history analyses and calculations of damage limit state (*i*-*ii*) probabilities, for a wall strip with N(8d)22ecc type tie connections.

Earthquake Input\PGA (g)	Tie Elongations, D_A (in.) [d = 0.29 in.]											
	0.4		0.5		0.6		0.7		0.8		0.9	
m10_01s*	0.272	0	0.386	1	0.547	1	0.972	1		1		1
m10_02s		0	0.244	0	0.318	1	0.416	1	0.621	1		1
m10_03s	0.296	1	0.431	1	0.652	1	0.939	1	1.012	1		1
m10_04s		0	0.256	0	0.317	1	0.494	1	0.953	1		1
m10_05s		0	0.223	0	0.271	0	0.323	1	0.404	1		1
m10_06s		0	0.271	0	0.361	1	0.538	1	0.719	1		1
m10_07s		0	0.250	0	0.311	1	0.582	1	0.960	1		1
m10_08s		0	0.218	0	0.282	0	0.357	1	0.404	1		1
m10_09s		0	0.200	0	0.246	0	0.310	1	0.404	1		1
m10_10s		0	0.328	1	0.495	1	0.786	1		1		1
m02_01s		0	0.160	0	0.197	0	0.269	0	0.331	1		1
m02_02s		0	0.271	0	0.366	1	0.635	1	0.987	1		1
m02_03s*		0	0.158	0	0.197	0	0.240	0	0.290	1		1
m02_04s		0	0.184	0	0.239	0	0.283	0	0.348	1		1
m02_05s		0	0.183	0	0.230	0	0.290	1	0.350	1		1
m02_06s		0	0.261	0	0.324	1	0.449	1	0.701	1		1
m02_07s		0	0.181	0	0.230	0	0.290	1	0.360	1		1
m02_08s		0	0.204	0	0.263	0	0.310	1	0.440	1		1
m02_09s		0	0.219	0	0.275	0	0.337	1	0.456	1		1
m02_10s		0	0.148	0	0.190	0	0.236	0	0.284	0		1
Probability of Damage, $P_f\left(\frac{m+1}{M+1}\right)$		0.10		0.19		0.48		0.81		0.95		0.99
Inverse of Probability, s $\Phi^{-1}(P_f)$		-1.31		-0.88		-0.06		0.88		1.67		2.33
ln(PGA), y		-0.92		-0.69		-0.51		-0.36		-0.22		-0.11

* Earthquake records used earlier during shake table testing and FE analyses, respectively labeled as M10 and M02.

Table 6.5 – Computed tie displacements from nonlinear time history analyses and calculations of damage limit state (*iii*) probabilities, for a wall strip with N(8d)22ecc type tie connections.

Earthquake Input\PGA (g)	Tie Elongations, D_B (in.) [d = 0.29 in.]											
	0.6		0.7		0.8		0.9		1.0		1.1	
m10_01s*	0.280	0	0.584	1		1		1		1		1
m10_02s	0.143	0	0.207	0	0.321	1		1		1		1
m10_03s	0.344	1	0.560	1	0.602	1		1		1		1
m10_04s	0.150	0	0.241	0	0.577	1		1		1		1
m10_05s	0.119	0	0.147	0	0.194	0	0.242	0		1		1
m10_06s	0.170	0	0.279	0	0.394	1		1		1		1
m10_07s	0.146	0	0.296	1	0.570	1		1		1		1
m10_08s	0.124	0	0.165	0	0.201	0	0.550	1		1		1
m10_09s	0.106	0	0.138	0	0.189	0	0.278	0		1		1
m10_10s	0.242	0	0.438	1		1		1		1		1
m02_01s	0.083	0	0.126	0	0.153	0	0.217	0	0.383	1		1
m02_02s	0.171	0	0.322	1	0.584	1		1		1		1
m02_03s*	0.083	0	0.120	0	0.130	0	0.160	0	0.220	0	0.294	1
m02_04s	0.110	0	0.134	0	0.162	0	0.207	0	0.275	0		1
m02_05s	0.110	0	0.140	0	0.170	0	0.290	1		1		1
m02_06s	0.146	0	0.214	0	0.374	1		1		1		1
m02_07s	0.110	0	0.130	0	0.170	0	0.300	1		1		1
m02_08s	0.130	0	0.150	0	0.220	0	0.400	1		1		1
m02_09s	0.121	0	0.149	0	0.220	0	0.312	1		1		1
m02_10s	0.085	0	0.104	0	0.129	0		0	0.270	0		1
Probability of Damage, $P_f\left(\frac{m+1}{M+1}\right)$		0.10		0.29		0.48		0.71		0.86		0.99
Inverse of Probability, s $\Phi^{-1}(P_f)$		-1.31		-0.57		-0.06		0.57		1.07		2.33
ln(PGA), y		-0.51		-0.36		-0.22		-0.11		0.00		0.10

* Earthquake records used earlier during shake table testing and FE analyses, respectively labeled as M10 and M02.

Table 6.6 – Summary of lognormal distribution parameters.

Wall Type	Wall Natural Period of Vibration, T_{wall} (sec)	Properties of Lumped Backup Structure, T_{backup}/T_{wall}	Damage Limit States			
			Repairable Damage (*i-ii*)		Collapse (*iii*)	
			Mean, m_R	St. Dev., $\beta_{D\|X}$	Mean, m_R	St. Dev., $\beta_{D\|X}$
A/N(8d)22ecc	0.139	0.0	-0.558	0.207	-0.242	0.172
		1.0	-1.328	0.264	-0.910	0.267
A/N(8d)28min	0.126	0.0	-0.470	0.170	-0.213	0.132
		1.0	-1.298	0.247	-0.803	0.190
A/N(1.5)22min	0.127	0.0	-1.386	0.184	-1.029	0.150
		1.0	-2.460	0.366	-1.851	0.301
D/N(8d)22ecc	0.138	1.0	-1.242	0.255	-0.573	0.267
D/N(1.5)22min	0.126	1.0	-2.321	0.306	-1.363	0.208

Table 6.7 – Probability of exceeding key damage limit states for residential brick veneer construction located in Urbana, Illinois, and Memphis, Tennessee.

Wall Type	Wall Natural Period of Vibration, T_{wall} (sec)	Properties of Lumped Backup Structure, T_{backup}/T_{wall}	Probability of Exceeding Damage Limit States			
			Repairable Damage (*i-ii*)	Collapse (*iii*)	Repairable Damage (*i-ii*)	Collapse (*iii*)
			Seismic Hazard Level (and PGA) for Urbana, Illinois			
			10% in 50 years (0.036g)		2% in 50 years (0.086g)	
A/N(8d)22ecc	0.139	0.0	**0.000**	0.000	0.000	**0.000**
		1.0	**0.000**	0.000	0.000	**0.000**
A/N(1.5)22min	0.127	0.0	**0.000**	0.000	0.000	**0.000**
		1.0	**0.009**	0.000	0.507	**0.023**
D/N(8d)22ecc	0.138	1.0	**0.000**	0.000	0.000	**0.000**
D/N(1.5)22min	0.126	1.0	**0.001**	0.000	0.332	**0.000**
			Seismic Hazard Level (and PGA) for Memphis, Tennessee			
			10% in 50 years (0.157g)		2% in 50 years (0.526g)	
A/N(8d)22ecc	0.139	0.0	**0.000**	0.000	0.342	**0.010**
		1.0	**0.024**	0.000	0.995	**0.842**
A/N(1.5)22min	0.127	0.0	**0.006**	0.000	1.000	**0.995**
		1.0	**0.952**	0.499	1.000	**1.000**
D/N(8d)22ecc	0.138	1.0	**0.008**	0.000	0.991	**0.397**
D/N(1.5)22min	0.126	1.0	**0.938**	0.009	1.000	**1.000**
			Seismic Hazard Level (and PGA) for Atlanta, Georgia			
			10% in 50 years (0.035g)		2% in 50 years (0.085g)	
A/N(8d)22ecc	0.139	0.0	**0.000**	0.000	0.000	**0.000**
		1.0	**0.000**	0.000	0.000	**0.000**
A/N(1.5)22min	0.127	0.0	**0.000**	0.000	0.000	**0.000**
		1.0	**0.007**	0.000	0.495	**0.021**
D/N(8d)22ecc	0.138	1.0	**0.000**	0.000	0.000	**0.000**
D/N(1.5)22min	0.126	1.0	**0.000**	0.000	0.319	**0.000**
			Seismic Hazard Level (and PGA) for Charleston, South Carolina			
			10% in 50 years (0.151g)		2% in 50 years (0.718g)	
A/N(8d)22ecc	0.139	0.0	**0.000**	0.000	0.863	**0.301**
		1.0	**0.017**	0.000	1.000	**0.985**
A/N(1.5)22min	0.127	0.0	**0.003**	0.000	1.000	**1.000**
		1.0	**0.940**	0.447	1.000	**1.000**
D/N(8d)22ecc	0.138	1.0	**0.006**	0.000	1.000	**0.817**
D/N(1.5)22min	0.126	1.0	**0.920**	0.006	1.000	**1.000**

Table 6.8 – Damage limit state PGAs at $5\% \leq P_f \leq 95\%$ for selected brick veneer walls with worst-case scenario backup support properties.

Wall Type	Properties of Lumped Backup Structure, T_{backup}/T_{wall}	Damage Limit State PGAs (g) for $5\% \leq P_f \leq 95\%$	
		Repairable Damage (*i-ii*)	Collapse (*iii*)
A/N(8d)22ecc	1.0	0.17 - 0.41	0.26 - 0.63
A/N(1.5)22min	1.0	0.04 - 0.15	0.09 - 0.25
D/N(8d)22ecc	1.0	0.19 - 0.44	0.36 - 0.88
D/N(1.5)22min	1.0	0.06 - 0.16	0.18 - 0.36

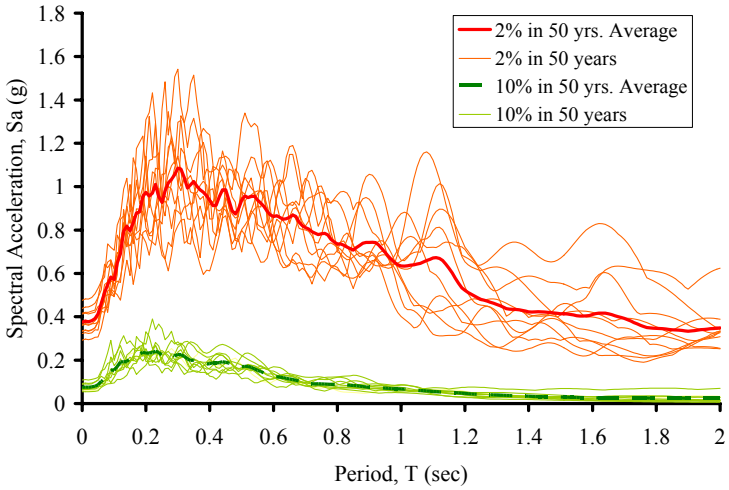

Figure 6.1 – Uniform hazard synthetic ground motion response spectra (4% damping) for Memphis, Tennessee, soil conditions (Wen and Wu 2001).

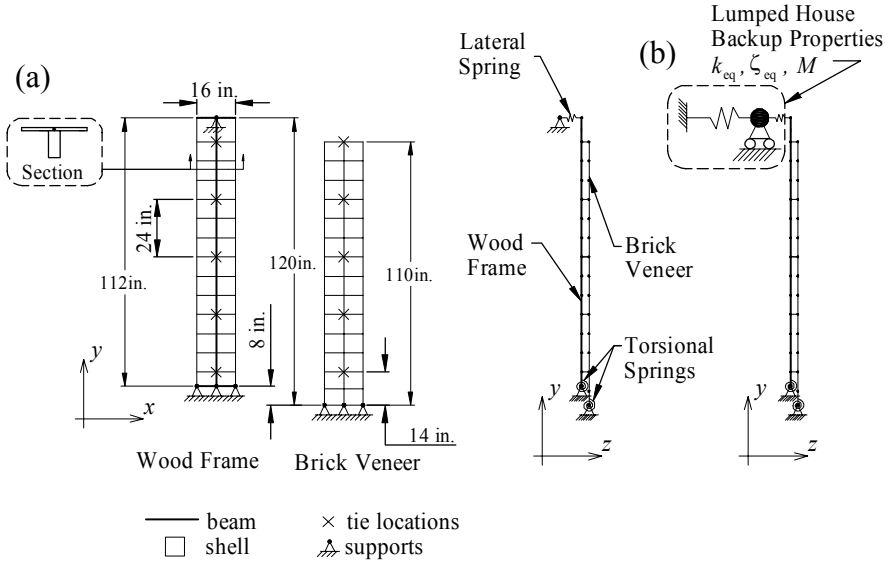

Figure 6.2 – (a) Front and side views of simplified 2-D wall strip model representing a single-story solid brick veneer wall panel. (b) Side view of wall strip with lumped properties representing a house backup structure.

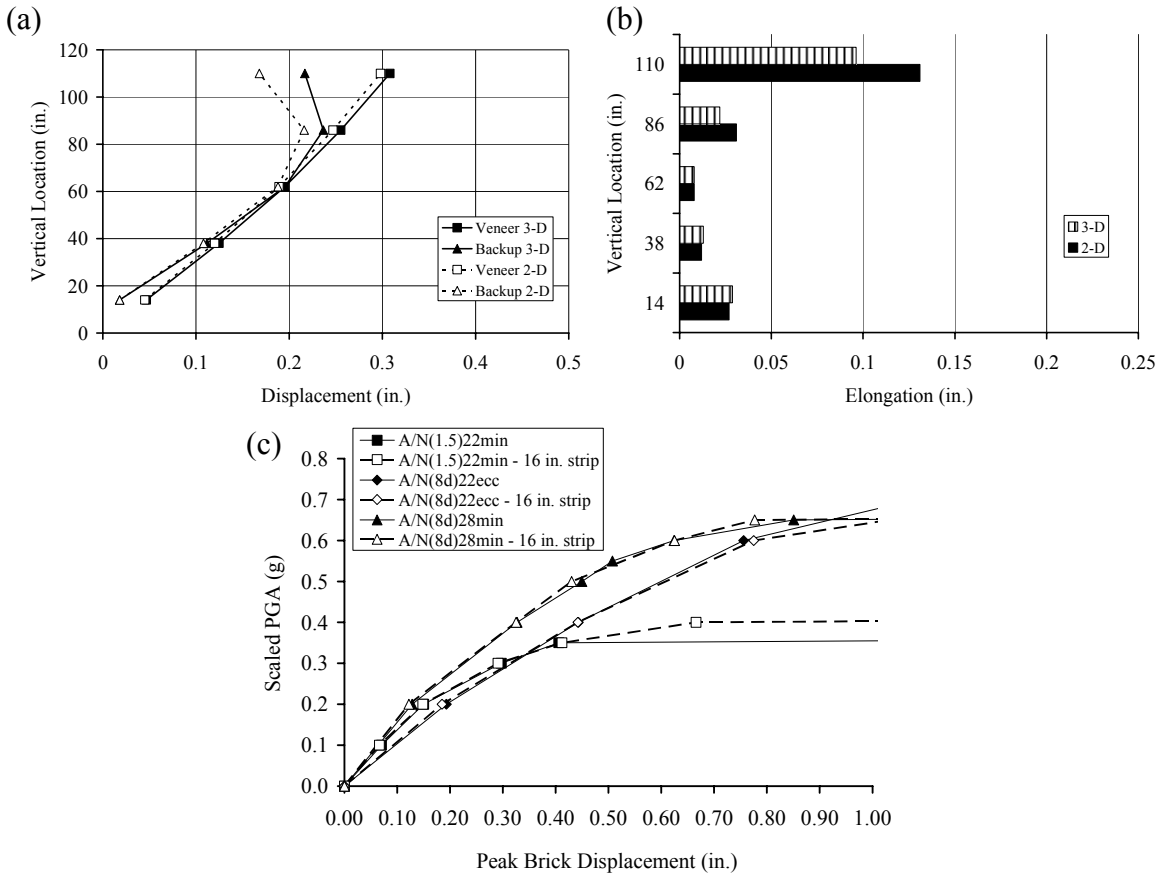

Figure 6.3 – (a) Peak outward displacements and (b) tie elongations along the centerlines of 3-D and 2-D wall panel models with N(8d)28min type ties subjected to the M10-0.38g input. (c) M10 earthquake input PGA vs. total displacements at top center of brick veneer for three different types of wall panels.

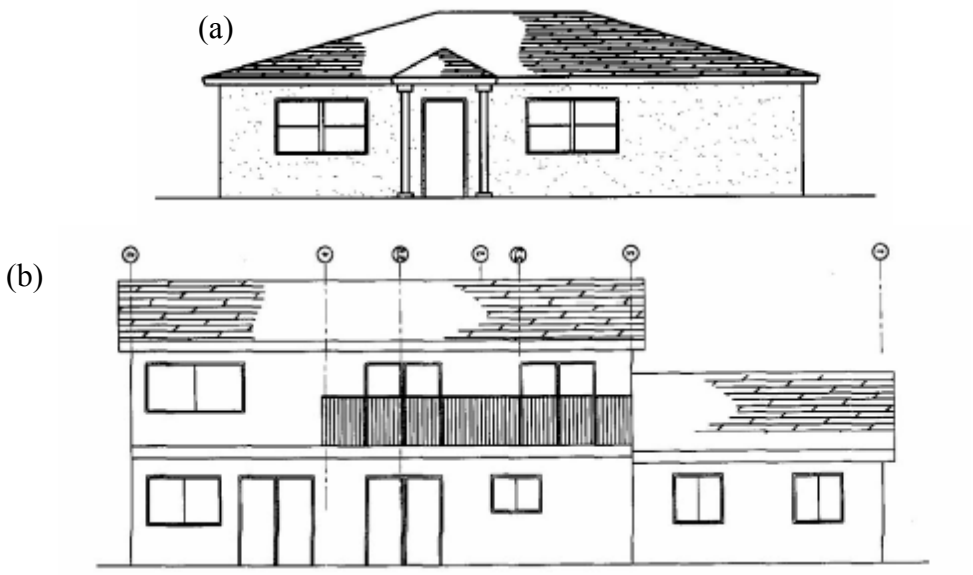

Figure 6.4 – Elevation views of (a) small and (b) large index wood frame homes (Isoda et al. 2001).

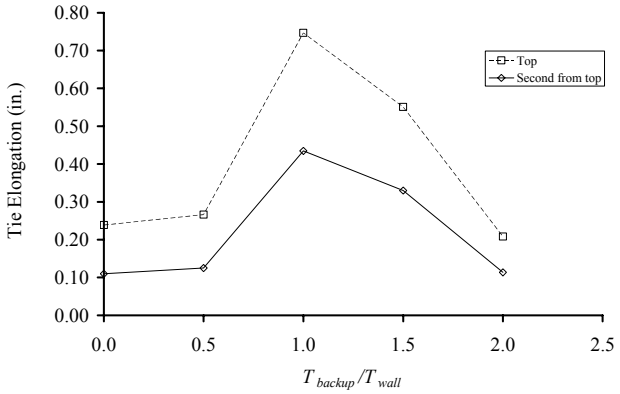

Figure 6.5 – Dynamic sensitivity study results for a wall strip with N(8d)22ecc type tie connections.

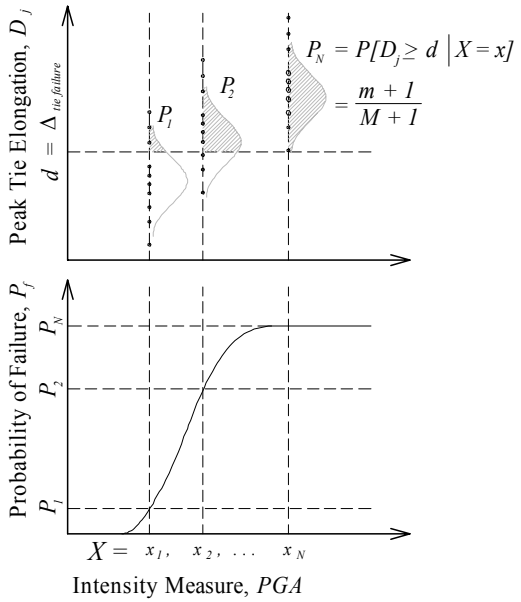

Figure 6.6 – Example of seismic fragility analysis method.

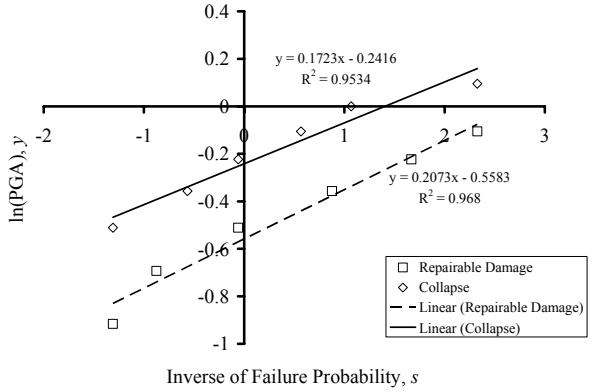

Figure 6.7 – Probability paper and lognormal parameter calculations for wall with N(8d)22ecc types of ties and T_{backup}/T_{wall} equal to 0.0.

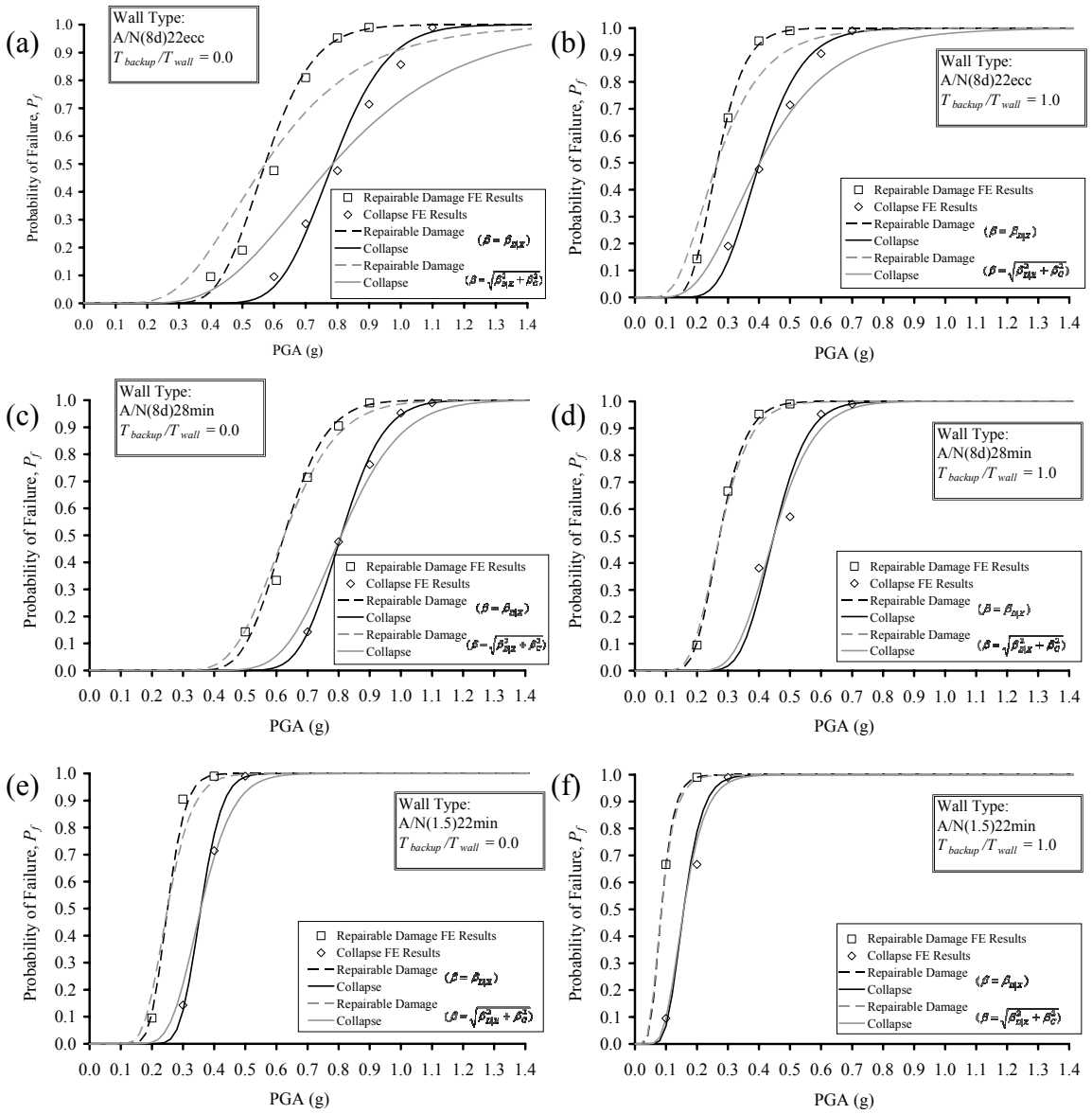

Figure 6.8 – Seismic fragility curves for brick veneer walls with (a-b) N(8d)22ecc, (c-d) N(8d)28min and (e-f) N(1.5)22min types of tie connections with a vertical spacing of 24 in.

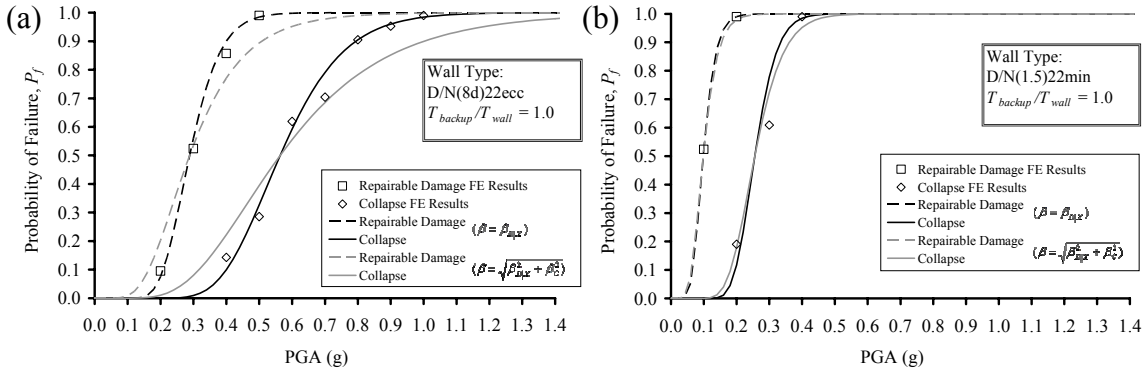

Figure 6.9 – Seismic fragility curves for brick veneer walls with (a) N(8d)22ecc and (b) N(1.5)22min types of tie connections with a vertical spacing of 16 in.

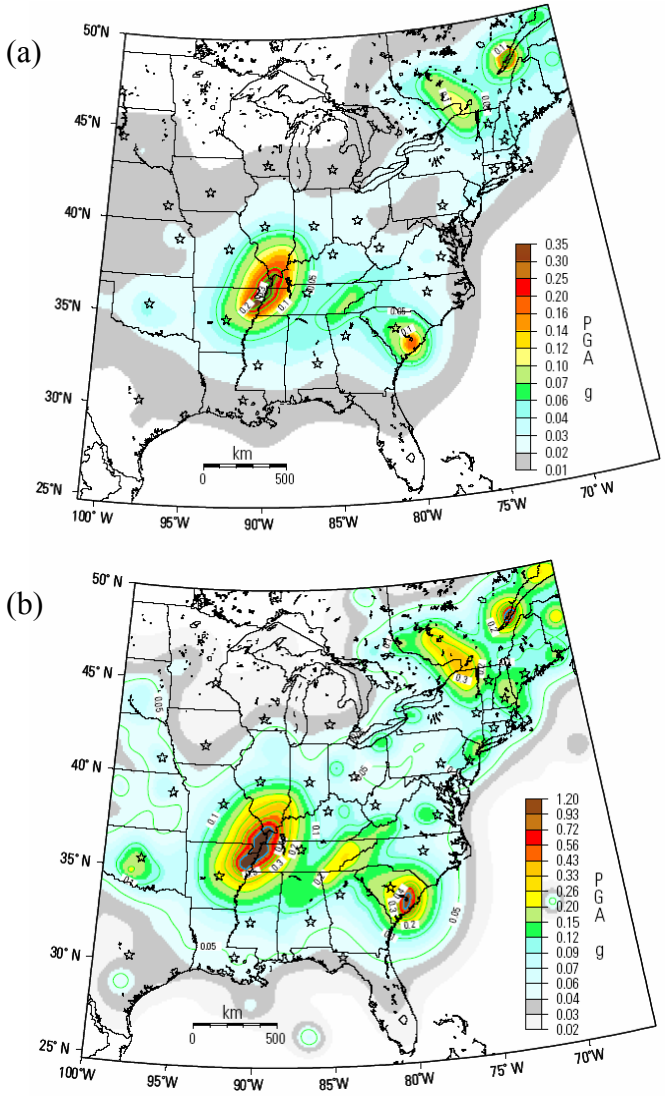

Figure 6.10 – Maps of peak ground accelerations for the central and eastern U.S. from USGS for (a) 10% in 50 year and (b) 2% in 50 year earthquake hazards.

SUMMARY AND CONCLUSIONS

7.1 Summary of the Research Project

A study was undertaken to investigate the out-of-plane seismic performance of anchored brick veneer wall systems built over wood framing, representing prescriptive design requirements and current construction practices. Prescriptive requirements for the design and construction of anchored brick veneer are currently provided by the Masonry Standards Joint Committee (MSJC) Building Code, the International Residential Code (IRC) for One- and Two-Family Dwellings, and the Brick Industry Association (BIA) Technical Notes. The research study was initiated by conducting load-displacement laboratory tests on brick-tie-wood subassemblies (consisting of two standard bricks, one 2x4 stud, and one corrugated sheet metal tie) representing a variety of brick veneer tie installation conditions, including workmanship variability. Subassembly tests were conducted to explore the effects of tie thickness, tie attachment method to the wood stud, tie eccentricity at the connection to the wood stud, and tie embedment length on the axial strength and stiffness of veneer tie connections.

Three types of tie connections evaluated in the subassembly study were later employed in separate full-scale brick veneer wall panel specimens, which were tested under static and dynamic out-of-plane loading on a shake table. Two one-story solid wall panel specimens, representing common construction practice, comprised full-scale brick veneer walls attached to a wood frame backup with 28 ga. corrugated sheet metal ties (utilizing two different installation methods), as well as with post-installed mechanical "retrofit" anchors. Another full-scale brick veneer wall panel with a window opening and a gable region was constructed with 22 ga. ties. The shake table tests captured the performance of brick veneer wall systems, including interaction and load-sharing between the brick veneer, corrugated sheet metal ties, and wood-frame backup. Overall seismic performance of brick veneer walls was closely related to the individual tie connection deformation limits and damage in tension.

The experimental test results were used to develop FE models of brick veneer walls, including nonlinear inelastic properties for the tie connections. The brick veneer FE wall models developed were able to effectively capture static and dynamic performance of the experimental test specimens at different levels of loading. Various degrees of brick veneer wall damage observed experimentally could be captured by considering whether tie connections at key locations in the models exceeded their ultimate load (and/or displacement) capacities. Parametric studies were then conducted with these models to further explore effects of certain types and layouts of tie connections, as well as geometric variations in brick veneer wall construction. Tie connection strength and stiffness properties had a major influence on the out-of-plane seismic performance of brick veneer walls. Brick veneer wall behavior was also controlled by the overall grid

spacing of tie connections, and particularly by tie installation along the edges and in the upper regions of the walls.

Finally, simplified FE wall models were developed and utilized to analyze the seismic fragility of this form of construction. Onset of damage at key tie connection locations was used to evaluate the damage limit states of brick veneer walls; the two key damage limit states evaluated in this fragility study were onset/accumulation of tie damage (described as repairable damage), as well as brick veneer wall instability/collapse. The computed seismic fragility functions were used to compute the seismic hazard of brick veneer wall construction for selected locations in the central and eastern U.S. Design guides, codes, and current construction practices have been evaluated in light of the overall findings from these experimental and analytical studies. Key findings from the overall study on the out-of-plane seismic performance of residential brick veneer construction have been summarized in the following sections, including recommendations for new design and retrofitting of brick veneer wall systems, as well as suggestions for future study.

7.2 Conclusions from Experimental and Analytical Studies

With respect to the experimental and analytical studies of anchored residential brick veneer wall systems, the most important results and conclusions may be summarized as follows:

- During tie subassembly tests, it was shown that for nailed tie connections, their tensile strength was typically governed by nail pullout from the wood stud, while their stiffness was mostly a function of the amount of tie eccentricity and the tie thickness. Nailed tie connections not meeting current minimum installation requirements exhibited reductions in strength (from using short roofing nails) and in stiffness (from using thinner gage ties or short roofing nails) of up to about 50% and 65%, respectively. On the other hand, tie connections with wood screws exhibited approximately 2.5 times higher strength, but similar stiffness, when compared to nailed tie connections just meeting the minimum required installation criteria.
- The compressive strength and stiffness results from subassembly testing were described as lower bounds for actual brick veneer walls, owing to the presence of some “mortar droppings” in the air cavity that can effectively increase both the compressive strength and stiffness attributable to any one tie connection in the system.
- In general, the dynamic out-of-plane response of residential anchored brick veneer wall panels was dominated by rigid body rotation of the brick veneer about its base, producing inertial forces transferred through the ties into the wood frame backup. The free vibration period of the veneer walls varied in relation to the initial stiffness of the veneer-to-backup connections. During testing, changes in period of vibration were a good measure of the progression of damage in the brick veneer wall systems.

- Brick veneer wall system performance was closely related to the tensile properties of the tie connections. With stiffer ties, the veneer was more closely coupled to the backup than in walls with more flexible ties, which allowed the veneer to move somewhat independently from the backup. This made the brick veneer more susceptible to cracking (as seen during the experiments) in the case of flexible tie connections. "Mortar droppings" in the air space between the veneer and the backup increased the initial stiffness of some ties (by providing constraint) and also reduced the demand on ties in compression by locally filling the air space.
- Static and dynamic analyses of the FE brick veneer wall models provided relative out-of-plane strength capacities of brick veneer wall systems as a function of the tie connection properties. The walls containing 28 ga. ties without an eccentricity from the nail at the tie bend typically exhibited capacities similar to (or even above) those with 22 ga. ties; however, walls having 28 ga. ties with an eccentricity of the bend performed very poorly, compared to the other cases. The use of wood screws to attach ties to the wood backup resulted in a significant increase in overall out-of-plane strength of the brick veneer walls, whereas the wall panels with tie connections fastened using short roofing nails were the weakest ones. In general, stiffer tie connections, and not necessarily stronger ones, improved the overall strength of the veneer walls modeled.
- As seen from experimental testing, post-installed mechanical anchors were able to significantly improve the out-of-plane performance of the brick veneer wall system, compared to using corrugated sheet metal ties only. The anchors effectively transferred a large portion of the inertial loads, while securing the veneer closely to the backup.
- Behavior of brick veneer walls was controlled by the overall grid spacing of tie connections, and particularly by tie installation along the edges and in the upper regions of the walls. Generally, the top row of ties in the brick veneer walls played a critical role in the overall strength of the wall panels. Tie connections anchored at or near stiffer regions of the wood frame backup (floor or roof/ceiling framing) experienced the highest loads and therefore exhibited the first signs of damage; as a result, tie damage spread throughout the wall panel, starting from the stiffer and upper regions of the wood backup, to more flexible backup regions. Loss in tie stiffness and strength then made the brick veneer more susceptible to cracking. A significant increase in the ultimate strength of brick veneer walls was achieved by adding a few extra ties to the upper region and/or along edges of walls.
- During experimental testing of a brick veneer wall panel with a gable and window opening, horizontal cracking and hinging eventually formed in the brick veneer along the base of the gable, making that portion of the wall panel more vulnerable to damage and collapse. However, the gable portion maintained its stability up through the highest levels of shaking, in part as a result of the additional tie connections installed within 8 in. (203 mm) of all wall edges (per BIA (2003) recommendations), which further emphasized the importance of tie installation along wall edges.
- The total area of brick masonry veneer wall panels determined their overall inertial response, and the resulting forces that were then transferred through the tie connections into the wood-frame backup; relatively small variations in the

supported brick veneer wall area, such as by extending the veneer beyond the edge ties or by introducing openings, played a significant role on overall wall behavior. Presence of wall openings resulted in greater wood backup flexibility, causing the wood framing to closely follow the masonry wall (when subjected to inertial loads) along the vertical edges of openings, in turn resulting in lower load demands on tie connections at those locations. Behavior of wall panels with larger openings will mainly be governed by the brick veneer mass and the tie connections within the upper wall regions.

- During experimental testing, the results correspond to three levels of specimen response and damage, which can be described as: *elastic* (no visible damage), *intermediate* (onset of tie and veneer damage), and *ultimate* (accumulation of tie and veneer damage sufficient to lead to collapse). At onset of tie damage during dynamic veneer wall tests, tie connection deformations in tension were typically similar to the opening displacements at ultimate tensile loading determined from subassembly (monotonic tension and cyclic) tests. As tie damage spread, gradually reducing the stiffness and strength of the overall veneer-to-backup connections, the brick veneer walls became more susceptible to cracking. Ultimately, three damage limit states were identified for the different brick veneer wall panel models, based on onset of tie failures at key tie locations in the models, which were then related to the experimental wall behavior and damage.
- Two damage limit states were evaluated in the fragility study by utilizing simplified two-dimensional brick veneer wall strip models, with a representative lumped backup structure model. The damage limit states were (*i*-*ii*) onset/accumulation of wall tie damage, and (*iii*) brick veneer wall instability/collapse. These damage limit states were then assessed in terms of approximate safety objectives and repair costs. In terms of safety objectives, the first damage limit state (*i*-*ii*) was related to Immediate Occupancy (IO) and Life Safety (LS) performance levels, and the second limit state (*iii*) was related to Hazards Reduced (HR) performance level, as established in ASCE 41-06. In terms of repair costs, these two damage limit states were generally described as (*i*-*ii*) repairable damage (involving possible re-anchoring of the brick veneer and tuckpointing or crack repair) and (*iii*) collapse (which would involve partial or full reconstruction of the brick veneer).
- The seismic fragilities for residential brick veneer wall construction were evaluated as a function of earthquake excitation peak ground accelerations (PGAs). On average, brick veneer walls with 22 ga. and 28 ga. ties attached by 8d nails exhibited similar fragilities at both damage limit states, and walls with 22 ga. ties attached by short roofing nails experienced damage at significantly lower PGAs. For walls with reduced tie spacings, the fragility curves exhibited a slight shift to the right, as compared to the curves for walls with larger tie spacings. Damage to brick veneer walls was also affected by the amplification of the lumped backup structure model, with the damage limit state PGAs nearly two times lower for walls with the worst-case backup stiffness defined by T_{backup}/T_{wall} equal to 1.0.
- The uncertainty in seismic loading dominated the vulnerability of brick veneer walls. However, brick veneer walls utilizing tie connections with higher variability in their ultimate strength resulted in a noticeable effect on the fragility curves; the

slope of the fragility curves was reduced as a function of the variability, generally causing them to rotate about the mean damage PGAs. Brick veneer walls with 22 ga. ties attached by 8d nails and a maximum bend eccentricity of 1/2 in. (12.7 mm) exhibited the largest variation.

- The 2% in 50 year earthquake hazard PGA values and the collapse limit state governed the seismic performance of residential brick veneer wall systems built throughout the central and eastern U.S. In low to moderate seismicity regions, the minimum design and construction requirements for brick veneer walls should be followed, including the use of 22 ga. ties installed with a maximum bend eccentricity of 1/2 in. (12.7 mm) and attached to the backup by 8d nails. Based on FE models with the worst-case scenario backup properties, wall construction employing ties with a vertical spacing of 24 in. (610 mm) (with a supported wall area per tie of 2.67 ft^2 [0.25 m^2]) is generally acceptable for brick veneer walls built in regions with 2% in 50 year earthquake hazard PGAs of up to 0.26g, and with a vertical spacing of 16 in. (406 mm) (with a supported wall area per tie of 1.78 ft^2 [0.17 m^2]) in regions with the same earthquake hazard PGAs of up to 0.36g. In higher seismicity regions, improved methods for connecting the brick veneer to the wood frame backup should be employed, as recommended in the following section.

7.3 Recommendations for Design and Construction of Residential Brick Veneer

Some recommendations for residential brick veneer design and construction based on the reported experimental and analytical studies are:

a) Typical prescriptive code requirements for the use of 22 ga. ties should be followed (as an absolute minimum) because the 28 ga. ties that are commonly used in construction practice can only perform as well as 22 ga. ties for their absolute "best case" installation, without any eccentricity at the bend (and thinner ties could also be more likely to have durability problems over time, although that was not a topic investigated as part of this study).
b) Thicker (and therefore stiffer) ties should be used (at least the minimum specified thickness) to ensure adequate strength (especially with respect to low-cycle fatigue) and stiffness (especially in compression for cases where the air space is free of mortar droppings).
c) Ties should be bent as close as possible to their point of attachment to obtain the highest tie and wall stiffness.
d) 8d or similar nails should be used as a minimum for attaching ties to the wood-frame backup, and galvanized wood screws should be considered as a desirable alternative to nails for securing brick veneer ties to the wood backup.
e) Tie spacings should be reduced (more ties used) at the top of veneer walls and near stiffer regions of the backup to achieve a higher veneer-to-backup connection stiffness and strength where it is most needed for resisting out-of-plane loading.
f) Variations in brick veneer wall area and geometry in the upper regions of wall panels should be closely evaluated and detailed to provide adequate out-of-plane support. It is recommended that codes incorporate specific requirements for tie

connection installation along all brick veneer wall edges, such as a maximum wall edge distance of 8 in. (203 mm) (as prescribed by BIA (2003)), and also for tie connection installation at reduced spacings in the upper regions of wall panels and near stiffer regions of the backup.

g) For older and/or damaged veneer walls (where ties may be corroded or otherwise inadequate), using post-installed anchors can be an inexpensive and effective repair technique.

7.4 Recommendations for Future Study

Based on the findings of the current study, several other topics appear to be worthy of further investigation related to seismic performance of anchored brick veneer with wood frame backup construction. The author recommends the following experimental or analytical investigations:

- According to current prescriptive recommendations and requirements, brick veneer walls should typically be limited to a height of 30 ft (9.14 m) above their support, with an additional 8 ft (2.44 m) permitted at gable ends of a home structure. In current construction practice, however, these height limits are not always met in taller engineered wood frame buildings, where brick veneer walls sometimes extend well above three stories without intermediate supports. Furthermore, the current design and construction requirements for anchored brick veneer do not specify "special" installation details for the tie connections anchored to stiffer regions of the wood frame backup, such as at the floor levels, where ties can undergo significantly higher axial loads (in wall systems subjected to out-of-plane loading). Further analytical studies should be conducted to evaluate the interaction between brick veneer walls spanning over multiple stories. Dynamic amplification of the seismic loads should also be reviewed for brick veneer built over larger scale wood frame buildings.
- For residential construction in higher seismicity regions, brick veneer built over all exterior walls of a home should be separated at the corners (i.e., the walls subjected to in-plane and out-of-plane loads should be isolated from one another). In most cases, however, the brick veneer is built as continuous around the corners. Earlier tests showed that brick veneer meeting at corners is quite vulnerable to cracking. Also, it is apparent that closed brick veneer wall corners can play an important role in the overall seismic response and performance of residential home structures. Further study is needed to evaluate the interaction of brick veneer corners, the tie connections (subjected to out-of-plane axial loads, as well as the ties under in-plane shear loads), and the wood frame backup. (Recent shake table tests on full-scale wood frame home structures with anchored brick veneer at the University of California in San Diego may reveal some useful information on the interaction between wood frame home buildings and brick veneer wall systems, as well as on the performance of walls meeting at corners.)
- It was shown that brick veneer walls constructed over gable-end regions of a wood frame building are often more susceptible to out-of-plane damage and collapse. In some wood frame buildings, the gable portion of the brick veneer can be anchored

directly to the roof framing members, which are often prefabricated wood trusses. This type of wood backup structure would result in different overall support features for the brick veneer, creating a somewhat different brick veneer wall system than that of typical wall systems with wood-frame stud wall backups. Further investigation is necessary to evaluate the performance of brick veneer wall systems anchored to wood frame trusses.

- The current study focused on the prescriptive design and construction requirements for residential anchored brick veneer wall systems. An alternative strength design approach is also available for anchored brick veneer wall systems, which involves computation of seismic and wind design forces, followed by a structural analysis and design of the brick veneer wall and its connection to the wood backup. The latest research data should be implemented to improve the design methods for brick veneer walls at the local (tie connection) and global (veneer wall system) levels.

REFERENCES

Abaqus, Inc. (2006). *ABAQUS 6.6-2,* Providence, R.I.

Allen, D. and Lapish, E.B. (1982). "The Interaction of Timber Framed Walls with a Tied Masonry Veneer Under Cyclic Racking Loads." *Proceedings of 4th Canadian Masonry Symposium,* Fredericton, Canada, 702-715.

American Concrete Institute (ACI). (2005). "Building Code Requirements for Reinforced Concrete." *ACI 318-05,* Detroit, Mich.

American Society for Testing and Materials (ASTM). (1998). "Standard Test Method for Pullout Resistance of Ties and Anchors Embedded in Masonry Mortar Joints." *ASTM E 754 – 80,* West Conshohocken, Pa.

ASTM. (2002a). "Standard Test Method for Compressive Strength of Masonry Prisms." *ASTM C 1314-02*, West Conshohocken, Pa.

ASTM. (2002b). "Standard Test Method for Young's Modulus, Tangent Modulus, and Chord Modulus." *ASTM E 111-97*, West Conshohocken, Pa.

ASTM. (2002c). "Standard Test Method for Preconstruction and Construction Evaluation of Mortars for Plain and Reinforced Unit Masonry." *ASTM C 780-00*, West Conshohocken, Pa.

ASTM. (2002d). "Standard Test Methods for Flexural Bond Strength of Masonry." *ASTM E 518-00a*, West Conshohocken, Pa.

American Society of Civil Engineers (ASCE). (2005). "Minimum Design Loads for Buildings and Structures." *ASCE 7-05,* New York, N.Y.

ASCE. (2006). "Seismic Rehabilitation of Existing Buildings." *ASCE 41-06*, New York, N.Y.

Ang, A.H.S. and Tang, W.H. (1975). *Probability Concepts in Engineering Planning and Design.* John Wiley & Sons, New York, N.Y.

Arumala, J.O. and Brown, R.H. (1982). "Performance Evaluation of Brick Veneer with Steel Stud Backup." Department of Civil Engineering, Clemson University, Clemson S.C..

Arumala, J.O. (1991). "Mathematical Modeling of Brick Veneer with Steel-Stud Backup Wall Systems." *Journal of Structural Engineering,* 117(8), 2241-2257.

Beattie, G. (2004). "Development of Damage Repair Procedures for Earthquake Damaged Buildings." *13th World Conference on Earthquake Engineering, Vancouver BC, Canada, Aug. 1-6, 2004,* Canadian Association for Earthquake Engineering, CD-ROM: paper no. 624.

Bennett, R.M. and Bryja J. (2003). "Implications of the IRC Seismic Requirements on Brick Veneer Construction in the Southeast." *Ninth North American Masonry Conference - Jun. 1-4, 2003 Clemson SC, USA,* The Masonry Society, Boulder, Colo.,

646-655.

Bozorgnia, Y. and Campbell K.W. (2004). "Engineering Characterization of Ground Motion." *Earthquake Engineering from Engineering Seismology to Performance-Based Engineering,* Edited by Bozorgnia, Y. and Bertero, V.V., CRC Press LLC, Boca Raton, Fla.

Brick Industry Association (BIA). (2002). "Technical Notes 28 - Anchored Brick Veneer, Wood Frame Construction." *Technical Notes on Brick Construction,* Reston, Va.

BIA. (2003). "Technical Notes 44B - Wall Ties for Brick Masonry." *Technical Notes on Brick Construction,* Reston, Va.

BIA. (2005). "Technical Notes 28B - Brick Veneer/Steel Stud Walls." *Technical Notes on Brick Construction,* Reston, Va.

Brown R.H. and Arumala, J.O. (1982). "Brick Veneer with Metal Stud Backup – An Experimental and Analytical Study." *Proceedings 2nd North American Masonry Conference, Aug. 1982,* The Masonry Society, Boulder, Colo., p. 13-1 to 13-20.

Bryja, J. and Bennett, R.M. (2004). "Disaster Investigation Report, Tornado and Severe Storm Damage in Tennessee November 10, 2002 – Behavior of Brick Veneer Structures." *The Masonry Society Journal,* 22(1), 111-120.

Burnett, E.F.P. and Postma, M.A. (1995). "The Pullout of Ties from Brick Veneer." *Seventh Canadian Masonry Symposium Jun. 4-7 1995,* McMaster University, Hamilton, Ontario, 1062-1073.

Casolo, S., Neumair, S., Parisi, M.A., and Petrini, V. (2000). "Analysis of Seismic Damage Patterns in Old Church Facades." *Earthquake Spectra,* 16(4), 757-773.

Catani, M.J. (1985). "Protection of Embedded Steel in Masonry." *The Construction Specifier,* January '85, 62-68.

Choi, Y.H. and LaFave, J.M. (2004). "Performance of Corrugated Metal Ties for Brick Veneer Wall Systems." *Journal of Materials in Civil Engineering,* 16(3), 202-211.

Chopra, A.K. (2001). *Dynamics of Structures: Theory and Applications to Earthquake Engineering.* 2nd Edition, Prentice Hall, New Jersey, N.J.

Chrysler, J. (1995). "Performance of Anchored Veneer on Stud Backup." *Seventh Canadian Masonry Symposium Jun. 4-7 1995,* McMaster University, Hamilton, Ontario, 630-639.

Clarke, W.M. (2002). "Seismic Performance of Brick Veneer on Wood Backup Construction." *Independent Study Report in CEE 497*, University of Illinois at Urbana-Champaign.

DeVekey, R.C. (1979). "Corrosion of Steel Wall Ties: Recognition, Assessment and Appropriate Action." *Building Research Establishment Information Paper,* IP 28/79.

De Vekey, R.C. (1987). "Timber-Framed Houses: Interaction Between Frame and Cladding Brickwork Subject to Lateral Loads." *Masonry International,* 1(1), 29-35.

De Vekey, R.C., Tarr, K., and Worthy, M. (1988). "Workmanship and the Performance

of Wall Ties: Effect of Depth of Embedment." *Masonry International,* 2(2), 43-46.

Dickson, T.J. (2007). "Investigation into Brick Masonry and Concrete Foundation Wall Distress of a Single-Family Residence." *Forensic Engineering – Proceedings of the Fourth Forensic Engineering Congress,* ASCE, v 217, 67-76.

Dodds, R.H. (2004). *CEE-490, CSE-491 Class Notes: Programming Aids,* University of Illinois at Urbana-Champaign.

Doherty, K., Griffith, C., Lam, N., and Wilson, J. (2002). "Displacement-Based Seismic Analysis for Out-of-Plane Bending of Unreinforced Masonry Walls." *Earthquake Engineering and Structural Dynamics,* 31, 833-850.

Drysdale, R.G., Hamid A.A., and Baker L.R. (1999). *Masonry Structures: Behavior and Design*, 2nd Edition, The Masonry Society, Boulder, Colo.

Dur-O-Wal (1998). "Masonry Repair Handbook – A Comprehensive Resource of Dur-O-Wal Products Applied to the Preservation and Retrofication of Our Masonry Heritage." *A Dayton Superior Company,* Aurora, Ill.

Earthquake Engineering Research Institute (EERI). (1996). "Northridge Earthquake of January 17, 1994 Reconnaissance Report, vol. 2." *Earthquake Spectra,* 11.C, 186-187.

Edgell, G.J. and De Vekey, R.C. (1983). "The Robustness of the Domestic House, Part 1: Compressive Loading Test on Walls." *British Ceramic Research Association Ltd. Technical Note 350,* 2-27.

Edgell, G.J. and De Vekey, R.C. (1985). "The Robustness of the Domestic House, Part 2: Wind Suction Tests on Gable Walls." *British Ceramic Research Association Ltd. Technical Note 364,* 3-6.

Ellingwood, B.R., Rosowsky, D.V., Li, Y., and Kim, J.H. (2004). "Fragility Assessment of Light-Frame Wood Construction Subjected to Wind and Earthquake Hazards." *Journal of Structural Engineering,* 130(12), 1921-1930.

Ellingwood, B.R., Celik, O.C., and Kinali, K. (2007). "Fragility Assessment of Building Structural Systems in Mid-America." *Journal of Earthquak Engineering and Structural Dynamics,* 36, 1935-1952.

Exponent (2001). "Nisqually Earthquake Reconnaisance." <http://www.exponent.com/practices/civilstructural/nisquallyquake.html>.

Federal Emergency Management Agency (FEMA). (1985). "An Assessment of Damage and Casualties for Six Cities in the Central United States Resulting from Earthquakes in the New Madrid Seismic Zone." *Central U.S. Earthquake Preparedness Project Rep. No. EMK-C-0057,* Wahington, D.C.

FEMA. (1999). *Midwest Tornadoes of May 3, 1999: Observations, Recommendations, and Technical Guidance, FEMA 342,* Washington, D.C.

FEMA. (2004). "Hazards: Protecting Your Home." <http://www.fema.gov/hazards/tornadoes/presskit3.shtm> (Nov. 1, 2004).

FEMA. (2003). *NEHRP Recommended Provisions for Seismic Regulations for New*

Buildings and Other Structures, FEMA 450, Washington, D.C.

FEMA. (2006). *Hurricane Katrina in the Gulf Coast: Building Performance Observations, Recommendations, and Technical Guidance, FEMA 549,* Washington, D.C.

Filiatrault, A., Fischer, D., Folz, B., and Uang, C.M. (2002). "Seismic Testing of Two-Story Woodframe House: Influence of Wall Finish Materials." *Journal of Structural Engineering,* 128(10), 1337-1345.

Filiatrault, A., Isoda, H., and Folz, B. (2003). "Hysteretic Damping of Wood Framed Buildings." *Engineering Structures,* 25, 461-471.

Gad, E.F., Duffield, C.F., Chandler, A.M., and Stark, G. (1998). "Testing of Cold-Formed Steel Framed Domestic Structures." *11th European Conference on Earthquake Engineering,* Balkema, Rotterdam.

Gad, E.F., Duffield, C.F., Hutchinson, G.L., Mansell, D.S., and Stark, G. (1999). "Lateral Performance of Cold-Formed Steel-Framed Domestic Structures." *Engineering Structures,* 21, 83-95.

Gad, E.F., Chandler, A.M., and Duffield, C.F. (2001). "Modal Analysis of Steel-Framed Residential Structures for Application to Seismic Design." *Journal of Vibration and Control,* 7, 91-111.

Gillengerten, J.D. (2001). "Engineering Characterization of Ground Motion." *The Seismic Design Handbook,* Edited by Naeim, F., Kluwer Academic Publishers, Norwell, Mass.

Griffith, M.C., Vaculik, J., Lam, N.T.K., and Lamantarna, E. (2007). "Cyclic Testing of Unreinforced Masonry Walls in Two-Way Bending." *Earthquake Engineering and Structural Dynamics,* 36, 801-821.

Grimm, C.T. (1976). "Metal Ties and Anchors for Brick Walls." *Journal of the Structural Division,* 102(ST4), 839-858.

Grimm, C.T. and Klingner, R.E. (1990). "Crack Probability in Brick Masonry Veneer over Steel Studs." *Proceedings of 5th North American Masonry Conference Urbana-Champaign (Illinois, U.S.) June 3-6, 1990,* The Masonry Society, Boulder, Colo., 1323-1333.

Grimm, C.T. (1992). "What is Wrong with Brick Masonry Veneer Over Steel Studs?" *The Masonry Society Journal,* Feb., 9-14.

Hagel, M.D., Lissel, S.L., and Sturgeon, G.R. (2007). "Comparison of Theoretical and Empirically Determined Service Lives for Wall Ties in Brick Veneer Steel Stud Wall Systems." *Canadian Journal of Civil Engineering,* 34, 1424-1432.

Hamilton, T., Thompson, J., Allen, R., and Kjorlien, B. (2001). *TMS Disaster Investigation Report: Performance of Masonry Structures in the Nisqually, Washington Earthquake of February 28, 2001. A Report by the Disaster Investigation Reconnaissance Team of TMS,* Boulder, Colo. <http://www.masonryresearch.org/Research_Reports/Nisqually.pdf>.

Hatzinikolas, M., Longworth, J., and Warwaruk, J. (1982). "Corrugated Strip Ties in Curtain Wall Construction." *Proceedings 2nd North American Masonry Conference, Aug. 1982,* The Masonry Society, Boulder, Colo., p. 14-1 to 14-14.

Heidersbach, R., Borgard, B., and Somayaji, S. (1987). "Corrosion of Metal Components in Masonry Buildings." *Proceedings of the Fourth North American Masonry Conference, August 1987,* Department of Civil Engineering, University of California, Los Angeles, Calif., 68-1 to 68-18.

Inel, M., Bretz, E.M., Black, E.F, Aschheim, M., and Abrams, D. (2001). "Utility Software for Earthquake Engineering: Program Report and Documentation." *Mid-America Earthquake Center,* CD Release 01-05.

International Code Council (ICC). (2003). *International Residential Code for One- and Two-Family Dwellings,* Falls Church, Va.

International Masonry Institute (IMI), The Brick Institute of America (BIA), The Masonry Society (TMS), and The Masonry Institute of America (MIA). (1990). *The Loma Prieta, California, Earthquake of October 17, 1989; Observations Regarding the Performance of Masonry Buildings,* Washington, D.C.

Isoda, H., Folz, B., and Filiatrault, A. (2001). *Seismic Modeling of Index Woodframe Buildings,* Report No. SSRP-2001/12, Division of Structural Engineering, University of California, San Diego.

Jalil, I., Kelm, W., and Klingner, R.E. (1993). "Performance of Masonry and Masonry Veneer Buildings in the 1989 Loma Prieta Earthquake." *The Sixth North American Masonry Conference Jun. 1993*, Philadelphia, Pa., 681-692.

Junyi, Y., Laird, D., McEwen, B., and Shrive, N.G. (2003). "Analysis of load in ties in masonry veneer walls." *Canadian Journal of Civil Engineering,* 30, 850-860.

Kelly, T., Goodson, M., Mayes, R., and Asher, J. (1990). "Analysis of the Behavior of Anchored Brick Veneer on Metal Stud Systems Subjected to Wind and Earthquake Forces." *Proceedings of 5th North American Masonry Conference, Urbana-Champaign (Illinois, U.S.), June 3-6, 1990,* The Masonry Society, Boulder, Colo., p. 1359-1370.

Kharrazi, M.H.K. and Ventura, C.E. (2006). "Vibration Frequencies of Woodframe Residential Construction." *Earthquake Spectra,* 22(4), 1015-1034.

Khudeira, S. and Mohammadi, J. (2006). "Assessment of Potential Seismic Damage to Residential Unreinforced Masonry Buildings in Northern Illinois." *Practice Periodical on Structural Design and Construction,* 11(2), 93-97.

Kjolseth, F. (2008). "Earthquake Rocks Nevada." *The Salt Lake Tribune,* <http://extras.sltrib.com/tribphoto/GalleryPhotos.asp?GID=EARTH_0221&sort=Gallery> (Feb. 21, 2008).

KPFF Consulting Engineers. (1998). "Design Guide for Anchored Brick Veneer Over Steel Stud Systems." *KPFF Consulting Engineers*, Santa Monica, Calif.

Krogstad N.B. (2003). "Troubleshooting – Different Recommendations for Corrugated Ties." *Masonry Construction,* (October), 58.

Lapish, E.B. and Allen, D. (1982). "Variability of Tie Loads in Brick Masonry Veneer Constructions." *Proceedings of 4th Canadian Masonry Symposium,* Fredericton, 716-729.

Lapish, E.B. (1988). "Aseismic Design of Brick Veneer Claddings." *Proceedings of 8th International Brick/Block Masonry Conference,* Dublin, Eire., 1579-1589.

Li, Y. and Ellingwood, B.R. (2006). "Reliability of Woodframe Residential Construction Subjected to Earthquakes." *Structural Safety,* 29, 294-307.

Liang, H. (2007). *Reliability Evaluation and Damage Reduction of Woodframe Buildings Under Seismic Loads,* Ph.D. Thesis, University of Illinois at Urbana-Champaign, Urbana, Ill.

Liaw, S. and Drysdale, R.G. (1992). "Reinforced Masonry Veneer Walls." *6th Canadian Masonry Symposium,* Department of Civil Engineering, University of Saskatchewan, Saskatoon, Canada, 35-46.

Masonry Standards Joint Committee (MSJC). (2008). *Building Code Requirements for Masonry Structures. ACI 530-08/ASCE 5-08/TMS 402-08,* ACI, Farmington Hills, Mich.; ASCE, Reston, Va.; TMS, Boulder, Colo.

McCavour, S. and Laird, D. (1995). "Masonry Veneer with Steel Stud Structural Backing." *Seventh Canadian Masonry Symposium Jun. 4-7 1995*, McMaster University, Hamilton, Ontario, 923-934.

McGinley, W.M., Warwaruk J., Longworth J., and Hatzinikolas M. (1988). "Masonry Veneer Wall Systems." Department of Civil Engineering, University of Alberta, Structural Engineering Report 156.

McGinley, W.M., Warwaruk J., Longworth J., and Hatzinikolas M. (1989). "Limit States Design of Masonry Veneer Wall Systems." *5th Canadian Masonry Symposium 5-7 Jun. 1989*, Department of Civil Engineering, University of British Columbia, Vancouver, B.C., 111-124.

McGinley, W.M., Samblanet, P., and Subasic, T. (1996). *An Investigation of the Effects of Hurricane Opal on Masonry. A Report by the TMS Disaster Investigation Team,* Boulder, Co.

McGinley, W.M. and Hamoush, S. (2008). "Seismic Masonry Veneer: Quasi-Static Testing of Wood Stud Backed Clay Masonry Veneer Walls." *ASCE Structures Congress 2008: Crossing Borders*, Vancouver, Canada.

Memari, A.M., Burnett, E.F.P., and Kozy, B.M. (2002). "Seismic response of a new type of masonry tie used in brick veneer walls." *Construction and Building Materials,* 16, 397-407.

Moore, J.F.A. (1978). "Some Preliminary Load Tests on Brick Veneer Attached to Timber Framed Panels." *Proceedings of the British Ceramic Society Symposium*.

MSC.Software Corporation (2005). *MSC Patran 2005 r2,* Santa Ana, Calif.

Naguib, E.M.F. and Suter, G.T. (1986). "Analytical Investigation of Corner Cracking in Brick Masonry Veneer." *Advances in Analysis of Structural Masonry, Edited by S.C.*

Anand, ASCE, New York, N.Y., 21-40.

National Design Specification for Wood Construction (NDS). (2001). American Forest and Paper Association, Washington, D.C.

Nelson, E.L., Ahuja, D., and Schonwetter, P. (2003). "Masonry Veneer Failure: A Case Study of Wall Tie Corrosion." *Forensic Engineering Conference Proceedings,* ASCE, 553-563.

Pacific Earthquake Engineering Research (PEER) Center (2008). PEER Center: NGA Database, <http://peer.berkeley.edu/nga/> (Aug. 28, 2008).

Page, A.W. (1991). "The Newcastle Earthquake – Behaviour of Masonry Structures." *Masonry International,* 5(1), 11-18.

Page, A.W., Kautto, J., and Kleeman, P.W. (1996). "A Design Procedure for Cavity and Veneer Wall Ties." *Masonry International,* 10(2), 55-62.

Page, A.W. (2001). "The Serviceability Design of Low-Rise Masonry Structures." *Progress in Structural Engineering and Materials,* 3, 257-267.

Paquette, J., Bruneau, M., and Filiatrault, A. (2001). "Out-of-Plane Seismic Evaluation and Retrofit of Turn-of-the-Century North American Masonry Walls." *Journal of Structural Engineering,* 127(5), 561-569.

Park, J., Towashiraporn, P., Craig, J.I., and Goodno, B.J. (2009). "Seismic Fragility Analysis of Low-Rise Unreinforced Masonry Structures." *Engineering Structures,* 31(1), 125-137.

Porter, K., Kennedy, R., and Bachman, R. (2007). "Creating Fragility Functions for Performance-Based Earthquake Engineering." *Earthquake Spectra,* 23(2), 471-489.

Priestley, M.J.N., Thorby, P.N., McLarin, M.W., and Bridgeman, D.O. (1979). "Dynamic Performance of Brick Masonry Veneer Panels." *Bulletin of the New Zealand Society for Earthquake Engineering,* 12(4), 314-323.

Rumbarger, J. and Vitullo, R.J. (2003). *Architectural Graphic Standards for Residential Construction,* Hoboken, N.J.

Seismosoft (2006). *Seismosignal Version 3.1.0.,* <www.seismosoft.com>.

Simsir, C.C. (2004). *Influence of Diaphragm Flexibility on the Out-of-Plane Dynamic Response of Unreinforced Masonry Walls,* Ph.D. Thesis, University of Illinois at Urbana-Champaign, Urbana, Ill.

Simundic, G., Page, A.W., and Neville, T.L. (1999). "The Behaviour of Wall Ties Under Cyclic Loading." *8th North American Masonry Conference, Jun. 6-9, 1999*, Austin, Tex., 753-764.

Sparks, P.R. (1986). "The Response of Low-Rise Non-Engineered Structures to Extreme Wind Conditions." *Journal of Wind Engineering and Industrial Aerodynamics,* 23(1), 181-192.

Suter, G.T. and Drysdale, R.G. (1992). "Best Design and Construction Practice for Brick Veneer Wall Systems." *6th Canadian Masonry Symposium (Jun. 1992),* Department of Civil Engineering, University of Saskatchewan, Saskatoon, Canada, 23-34.

Tawresey, J.G. (1995). "Case Studies Design & Construction of Reinforced Brick Veneer." *Seventh Canadian Masonry Symposium, Jun. 4-7 1995,* McMaster University, Hamilton, Ontario, 1062-1073.

Templeton, W., Edgell, G.J. and De Vekey, R.C. (1988). "The Robustness of the Domestic House, Part 3: Positive Wind Pressure Test on Gable Wall." *Proceedings – British Masonry Society,* 121-126.

Thomas, K. (1988). "Workmanship Defects in the Installation of Wall Ties." *Masonry International,* 2(1), 7-10.

USGS. (2005). "Digitized strong-motion accelerograms of North and Central American earthquakes 1933-1986." <http://nsmp.wr.usgs.gov/data_sets/ncae.html>.

Villaverde, R. (2004). "Seismic Analysis and Design of Nonstructural Elements." *Earthquake Engineering from Engineering Seismology to Performance-Based Engineering,* Edited by Bozorgnia, Y. and Bertero, V.V., CRC Press LLC, Boca Raton, Fla.

Wen, Y.K. and Wu, C.L. (2001). "Uniform Hazard Ground Motions for Mid-America Cities." *Earthquake Spectra,* 17(2), 359-384.

Wen, Y.K. (2004). "Probabilistic Aspects of Earthquake Engineering." *Earthquake Engineering from Engineering Seismology to Performance-Based Engineering,* Edited by Bozorgnia, Y. and Bertero, V.V., CRC Press LLC, Boca Raton, Fla.

Wilson, M.J. and Drysdale, R.G. (1990). "Structural Test Results for Full Scale BV/SS Walls." *Proceedings of 5th North American Masonry Conference Urbana-Champaign (Illinois, U.S.) June 3-6, 1990,* The Masonry Society, Boulder, Colo., 1335-1345.

Yi, J., Laird, D., McEwen, B., and Shrive, N.G. (2003). "Analysis of Load in Ties in Masonry Veneer Walls." *Canadian Journal of Civil Engineering,* 30, 850-860.

EXPERIMENTAL TESTING OF TIE CONNECTIONS

Table A.1 – Idealized multi-linear tensile behavior properties for brick veneer tie connections.

Specimen Type / Points	Average Displacement (in.)	Average Force (lbs)	*COV*	Average Stiffness (lbs/in.)
N(8d)22min /				
A	0.007	75		10,632
B	0.017	104	*0.09*	3,046
C	0.402	76		-74
D	0.600	61		-74
N(8d)22ecc /				
A	0.063	56		877
B	0.294	160	*0.36*	455
C	0.602	109		-166
N(8d)28min /				
A	0.047	108		2,311
B	0.190	167	*0.13*	415
C	0.300	104		-569
D	0.605	33		-235
N(8d)28ecc /				
A	0.239	41		181
B	0.363	144	*0.11*	811
C	0.459	88		-574
D	0.600	64		-210
N(2.5)22min /				
A	0.015	77		4,982
B	0.046	106	*0.19*	927
C	0.176	73		-255
D	0.600	51		-52
N(1.5)22min /				
A	0.027	57		2,138
B	0.050	77	*0.17*	837
C	0.123	61		-221
D	0.599	39		-47
S(-)22ecc /				
A	0.198	125		629
B	0.343	405	*0.20*	1,930
C	0.362	136		-13,876
D	0.600	0		-470
S(-)16min /				
A	0.050	97		1,914
B	0.617	395	*0.37*	527
C	0.617	0		

(Note: 1 lb = 4.45 N; 1 in. = 25.4 mm)

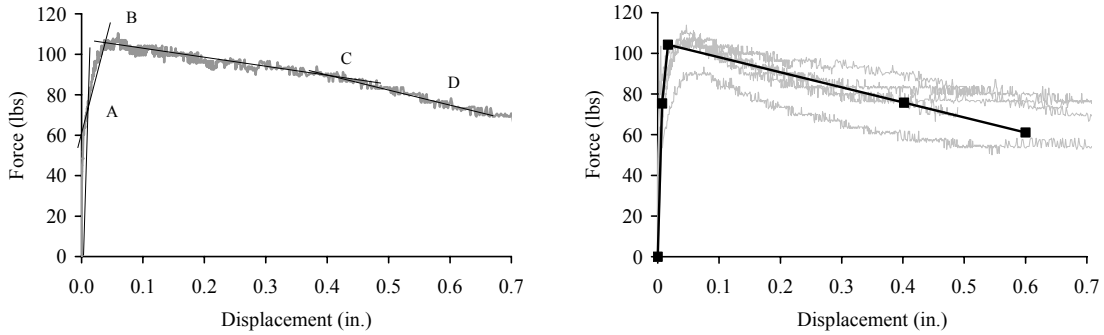

Figure A.1 – Monotonic tension load test results for N(8d)22min type of brick veneer tie connections.

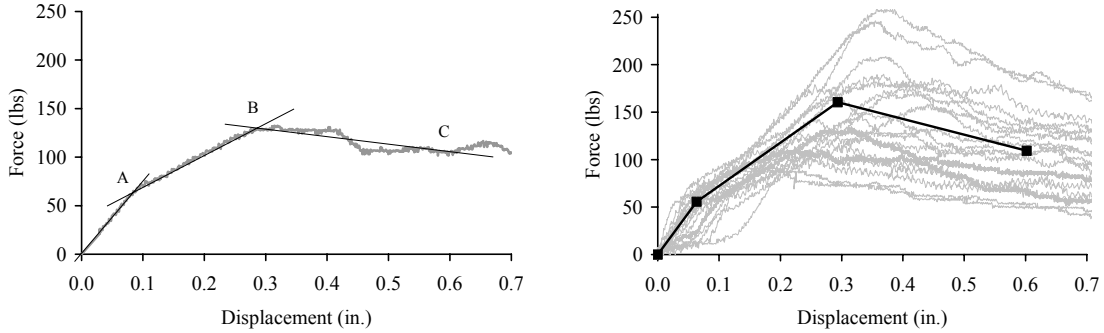

Figure A.2 – Monotonic tension load test results for N(8d)22ecc type of brick veneer tie connections.

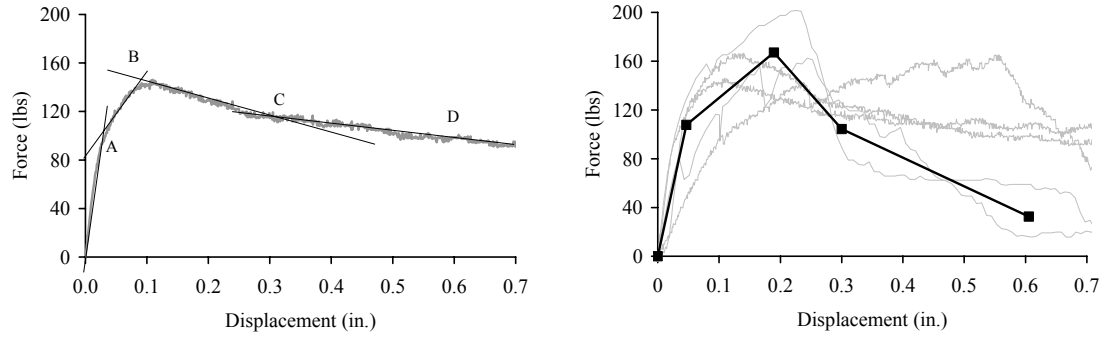

Figure A.3 – Monotonic tension load test results for N(8d)28min type of brick veneer tie connections.

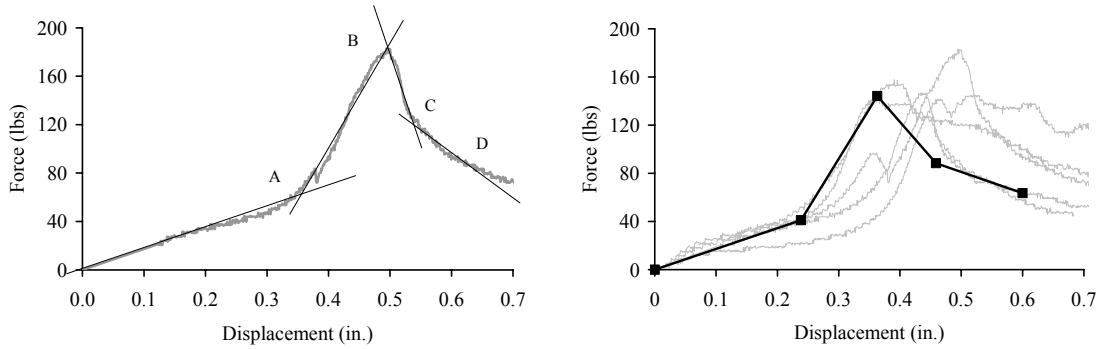

Figure A.4 – Monotonic tension load test results for N(8d)28ecc type of brick veneer tie connections.

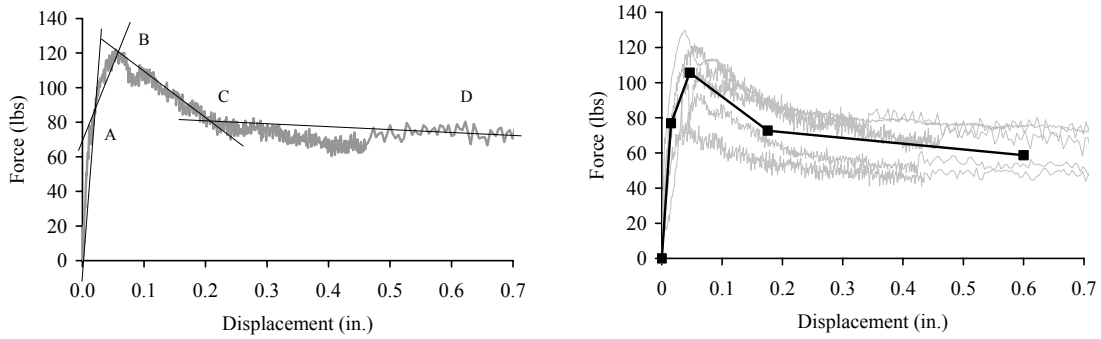

Figure A.5 – Monotonic tension load test results for N(2.5)22min type of brick veneer tie connections.

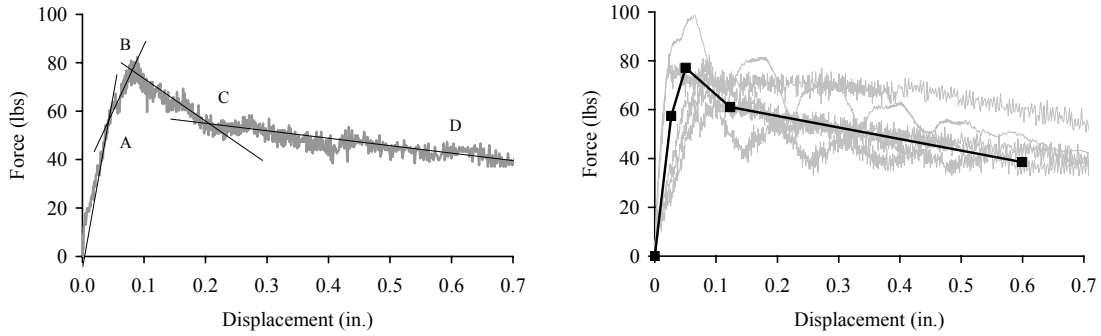

Figure A.6 – Monotonic tension load test results for N(1.5)22min type of brick veneer tie connections.

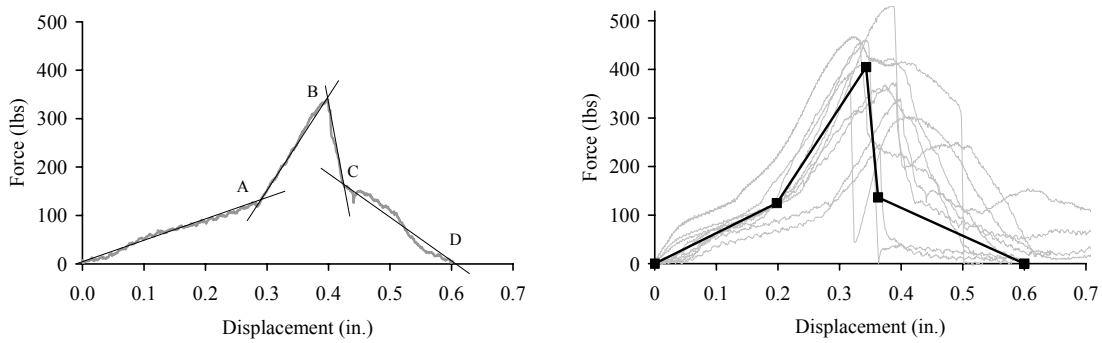

Figure A.7 – Monotonic tension load test results for S(-)22ecc type of brick veneer tie connections.

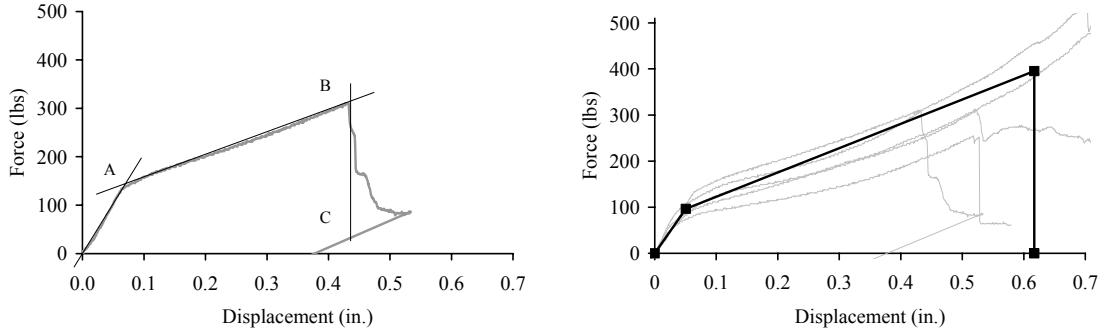

Figure A.8 – Monotonic tension load test results for S(-)16min type of brick veneer tie connections.

EXPERIMENTAL TESTING OF BRICK VENEER

Table B.1 – Brick masonry material strength test results for each wall panel specimen.

Wall-1

Masonry Prism Specimen	Crushing Strength, f'_m (ksi)	Elastic Modulus, E_m (ksi)
CP1	3.78	1831
CP2	4.33	1514
CP3	3.93	2887
CP4	4.27	2212
CP5	3.24	1483
Average	3.91	1986

Wall-2

Masonry Prism Specimen	Crushing Strength, f'_m (ksi)	Elastic Modulus, E_m (ksi)
CP1	3.07	2966
CP2	3.34	1889
CP3	2.96	2809
CP4	2.43	974
CP5	2.82	1577
Average	2.92	2043

Mortar Cube Specimen	Compressive Strength, f_u (psi)
MC1	1015
MC2	953
MC3	999
MC4	924
MC5	816
MC6	870
Average	930

Masonry Prism Specimen	Flexural Strength, f_r (psi)
MC1	103
MC2	83
MC3	87
MC4	73
Average	86

Wall-3

Masonry Prism Specimen	Crushing Strength, f'_m (ksi)	Elastic Modulus, E_m (ksi)
CP1	3.33	1114
CP2	3.07	1356
CP3	3.23	843
CP4	4.75	1374
CP5	3.50	1395
Average	3.58	1216

Mortar Cube Specimen	Compressive Strength, f_u (psi)
MC1	1052
MC2	977
MC3	1053
MC4	1164
MC5	1111
MC6	1173
Average	1088

NOTE: Prism compression strength tests were conducted following ASTM C 1314 (ASTM 2002a), and the modulus of elasticity was evaluated per ASTM E 111 (ASTM 2002b). Mortar cube compression strength tests were conducted following ASTM C 780 (ASTM 2002c), and ASTM E 518 (ASTM 2002d) for prism flexural strength tests.

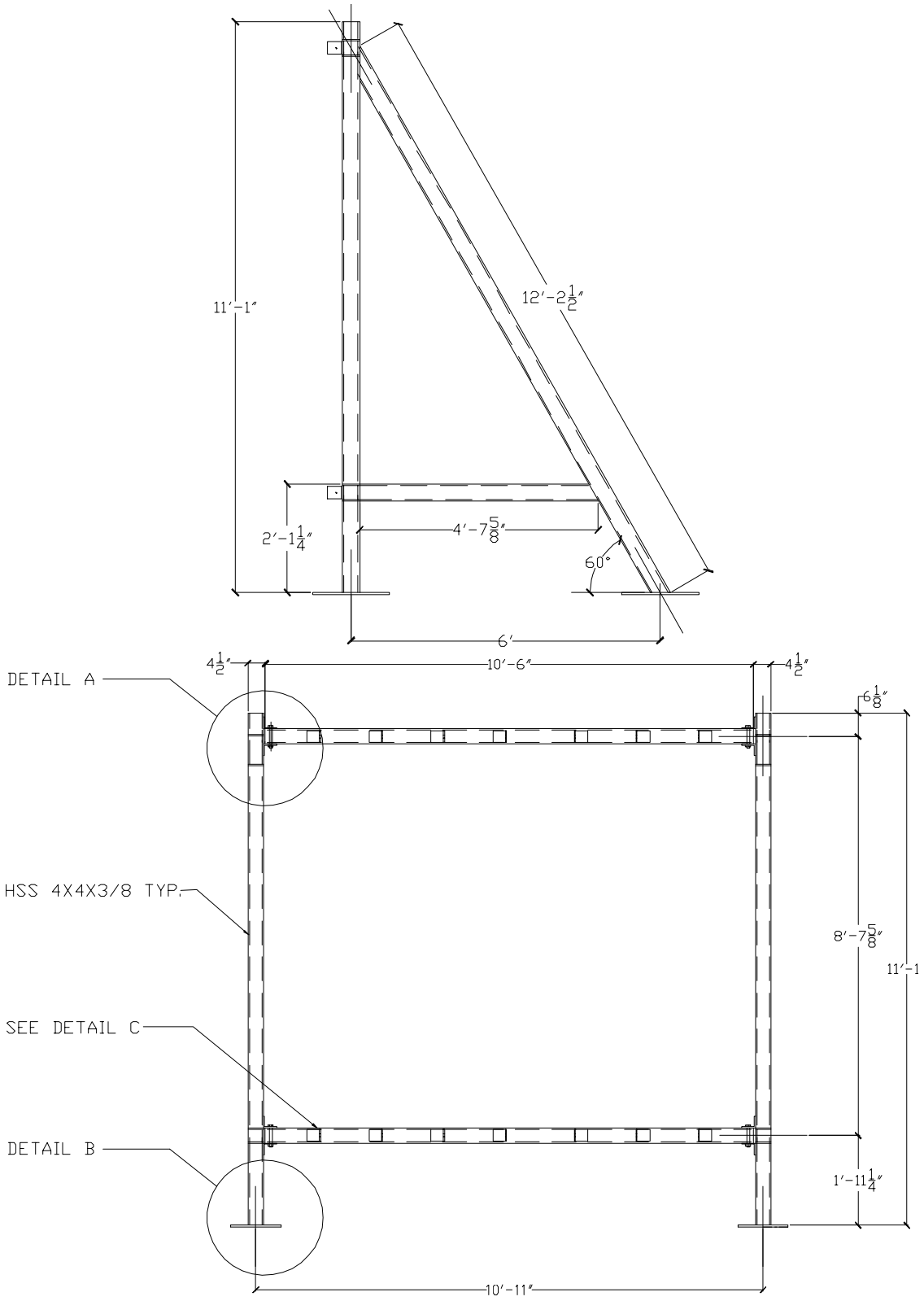

Figure B.1 – Elevation views of steel reaction frame.

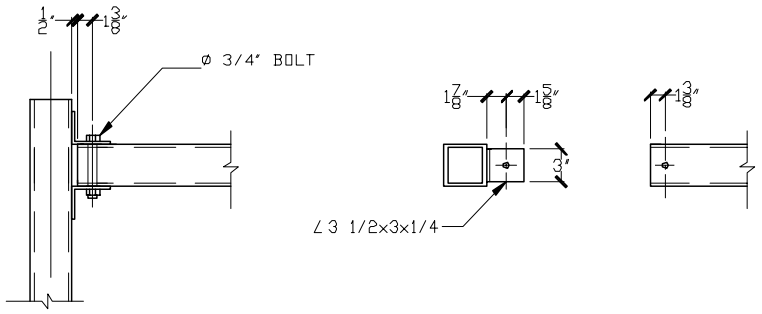

DETAIL A

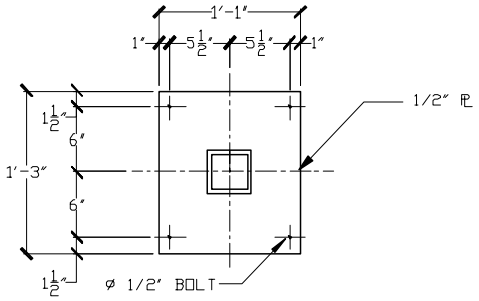

DETAIL B

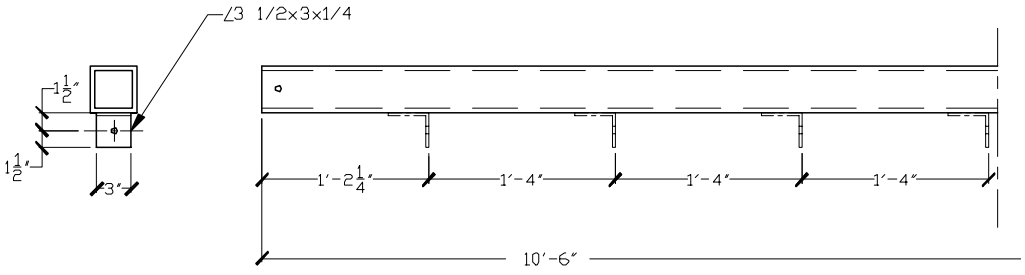

DETAIL C

Figure B.2 – Details of steel reaction frame.

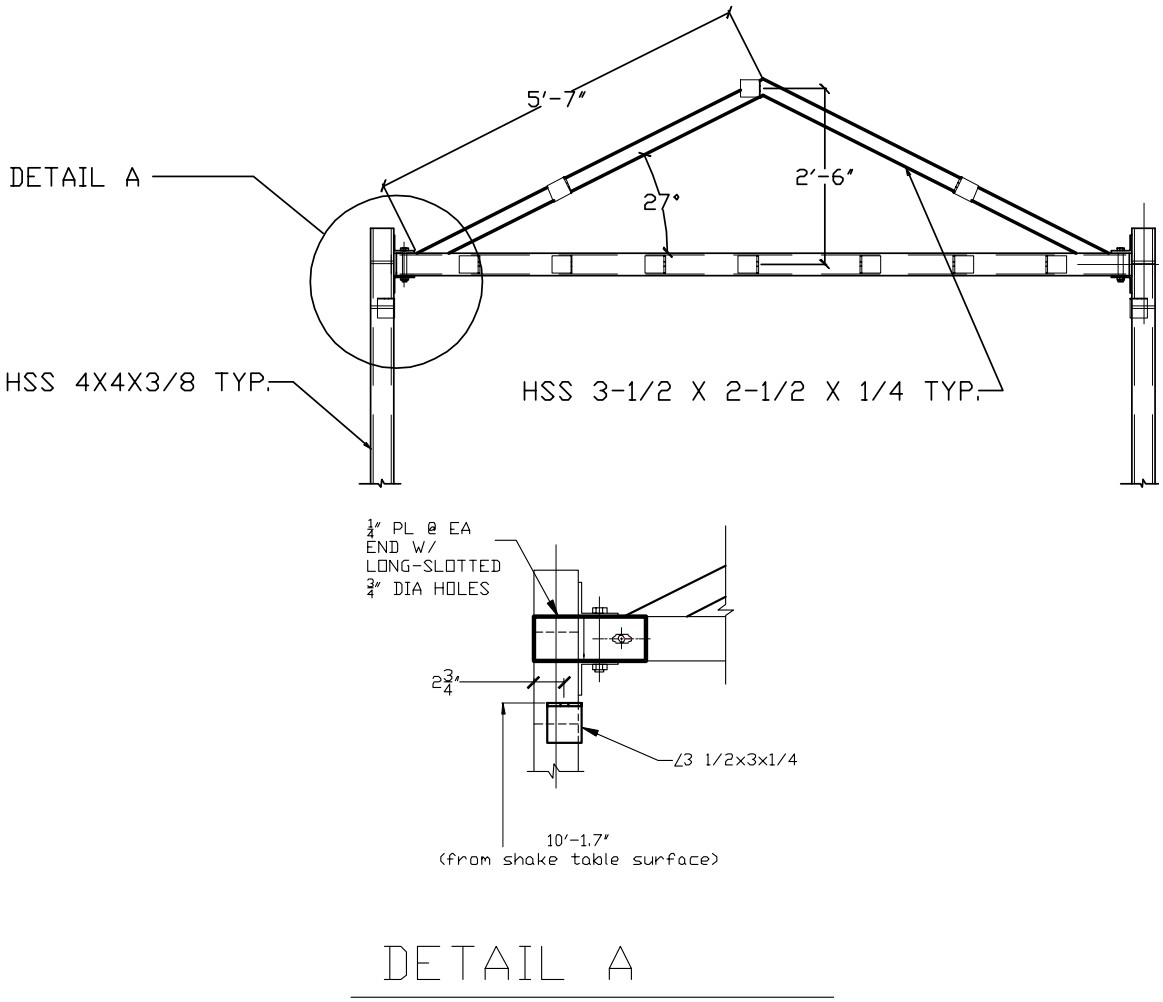

Figure B.3 – Additional details of steel reaction frame for Wall-3.

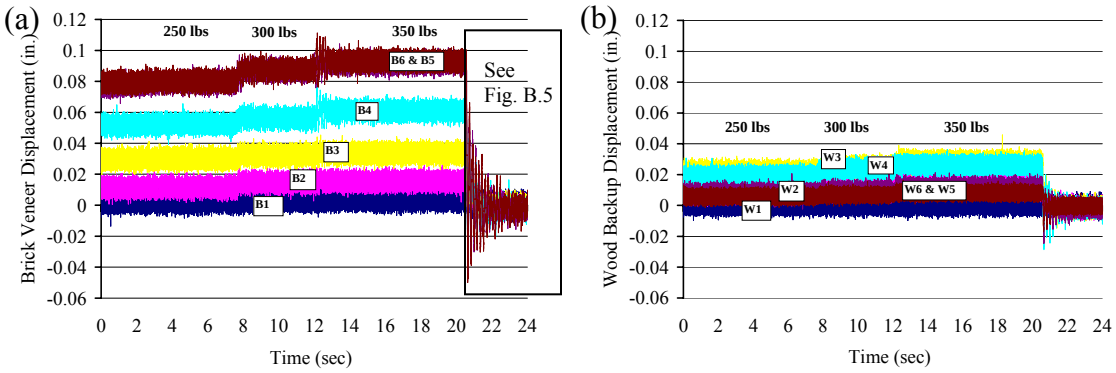

Figure B.4 – Static load displacement time traces for Wall-2 (a) brick veneer and (b) wood frame backup.

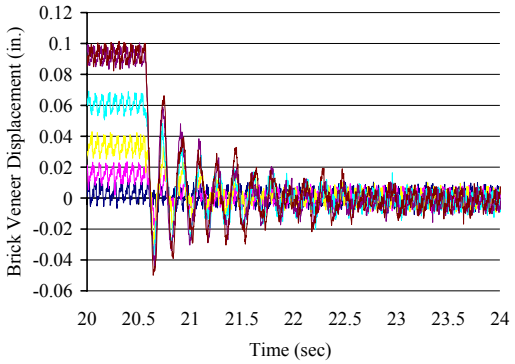

Figure B.5 – Free vibration response of the brick veneer Wall-2 after releasing the static point load.

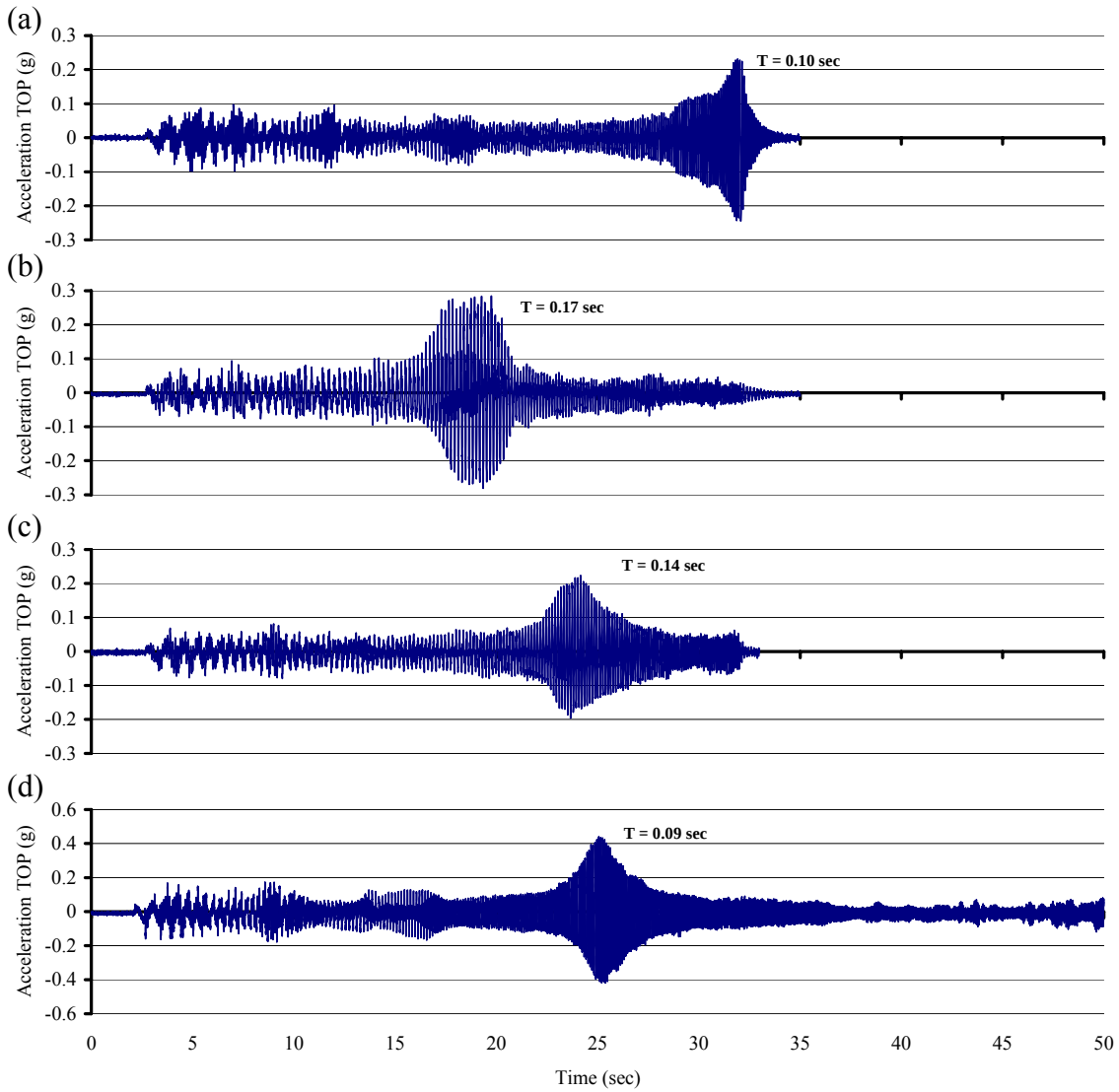

Figure B.6 – Resonant acceleration response and period of vibration of brick veneer walls at onset of dynamic testing, for (a) Wall-1, (b) Wall-2, (c) Wall-2b, and (d) Wall-3.

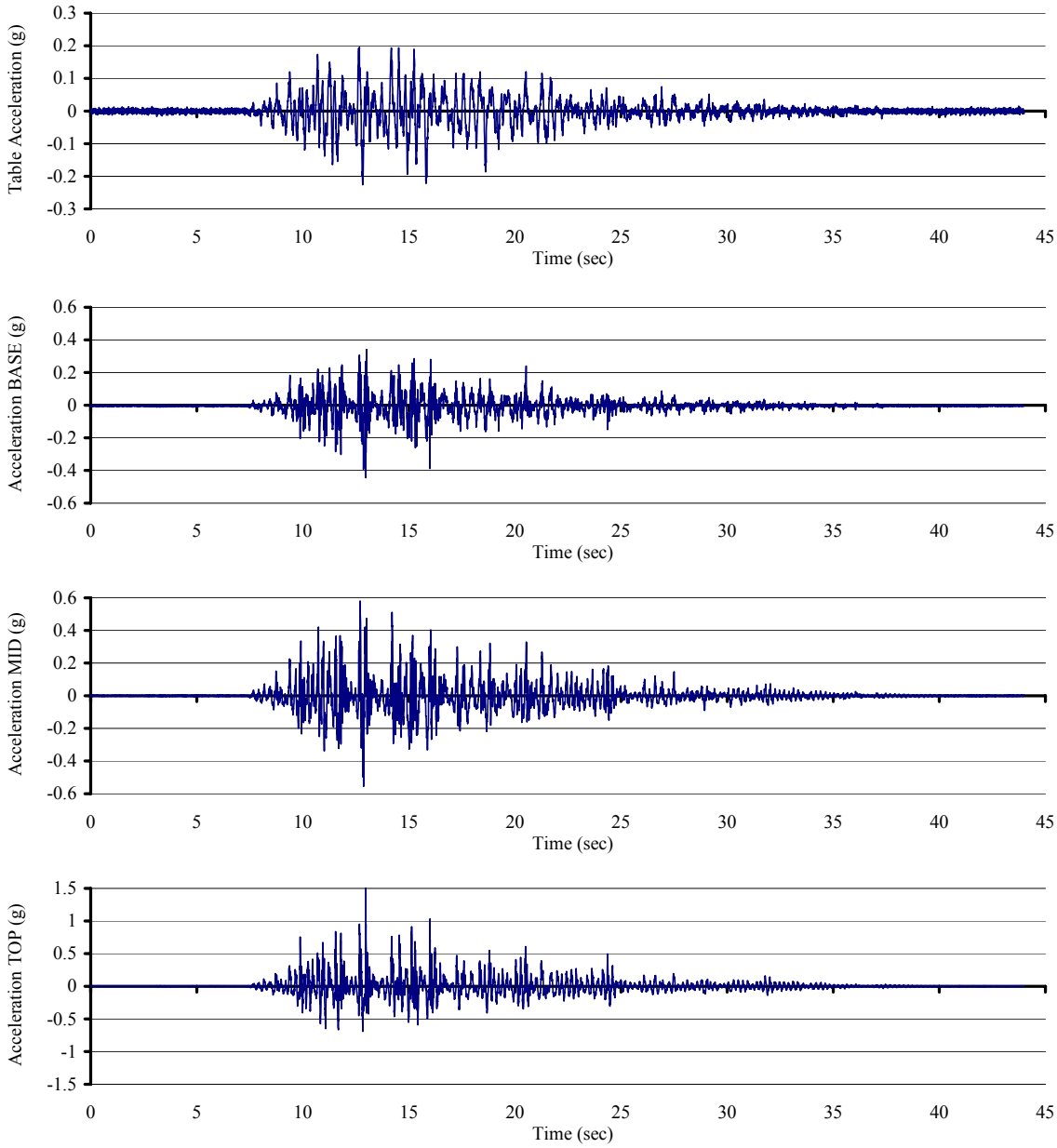

Figure B.7 – Example set of acceleration traces from testing of Wall-2

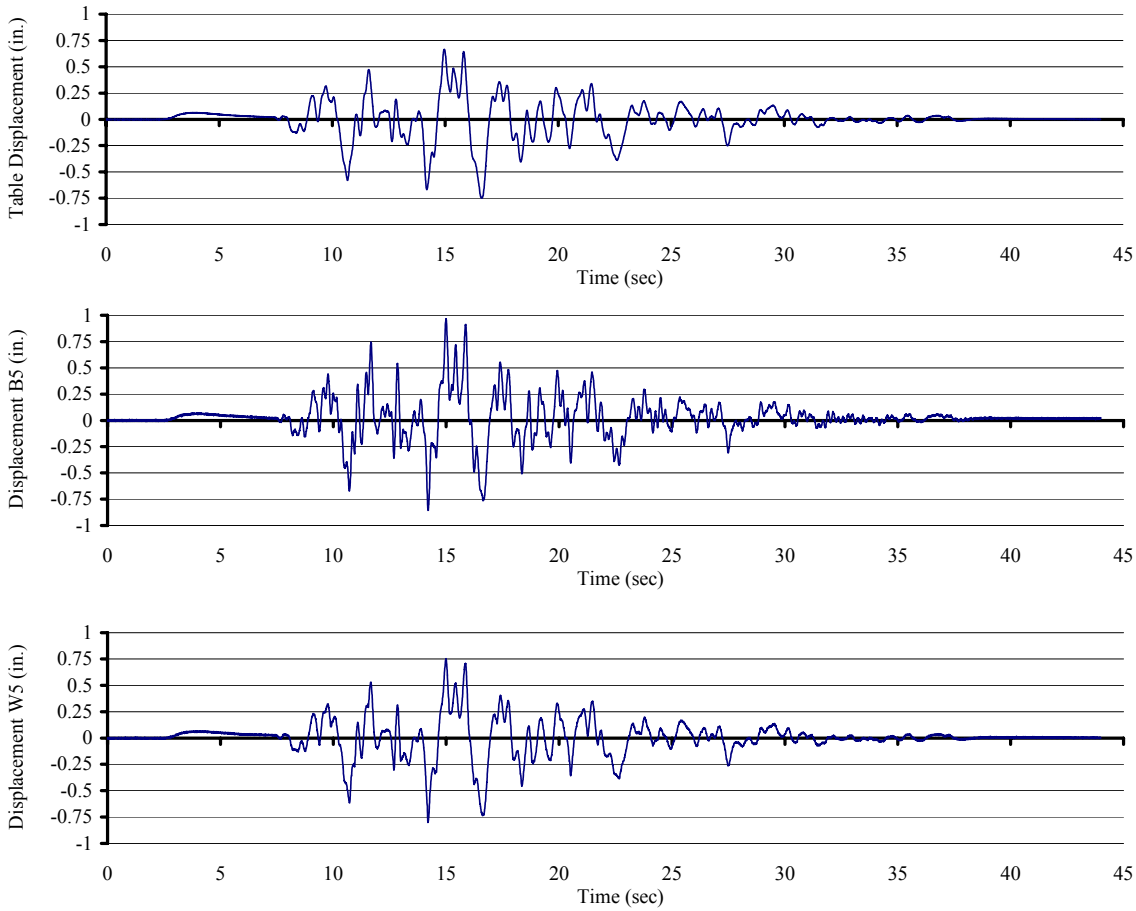

Figure B.8 – Example set of displacement traces from testing of Wall-2.

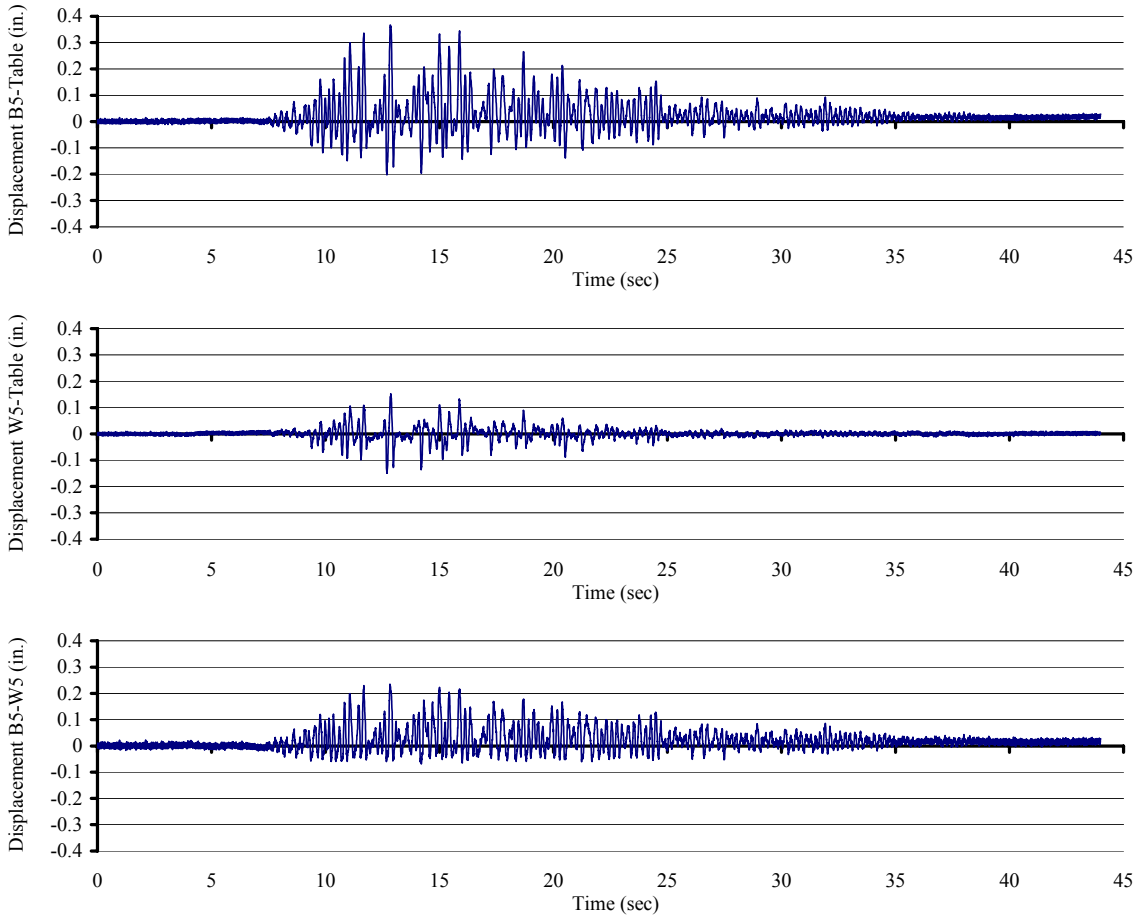

Figure B.9 – Example set of relative displacements from testing of Wall-2.

FINITE ELEMENT ANALYSIS OF BRICK VENEER

C.1 Tie Connection "Material" Model Subroutine (*UMAT*)

During nonlinear FE analysis, the subroutine is called at all material calculation points and produces updates for the axial stress at the end of each increment, by following the hysteresis rules in tension and the linear elastic rule in compression. The subroutine defines the state of element stress based on the previous loading state and the current change in strain. The "material" model subroutine was defined by a state table, as shown in Table C.1, controlled by three load states: (1) initial, (2) tension, and (3) compression. (An example from Dodds (2004) for a Marshall strut nonlinear material model was used to develop this state table.)

Table C.1 – State table used to define the tie connection material model subroutine.

State	Data: + $\Delta\varepsilon$ (IADD = 1)		Data: - $\Delta\varepsilon$ (IADD = 2)	
(1)	CASE 1	STATE = 2, CONTINUE	CASE 4	STATE = 3, CONTINUE
(2)	CASE 2		CASE 5	Compute a test stress ($\sigma_{test} = \sigma_{old} + E_5\Delta\varepsilon$)
	(A)	IF current strain (ε) is greater than or equal to peak strain reached along backbone curve: Select an appropriate modulus of elasticity (E_i, where i = 1 through 4) and compute new stress along the backbone curve, based on backbone stress and strain pairs (σ_j and ε_j, where j = A through D), as $\sigma_{new} = \sigma_j + E_i(\varepsilon - \varepsilon_j)$	(A)	IF test stress is greater than 0.0 and current strain (ε) is greater than 0.0: $\sigma_{new} = \sigma_{old} + E_5\Delta\varepsilon$
	(B)	IF current strain (ε) is less than peak strain reached along backbone curve: Compute the reloading modulus of elasticity (E_r) based on the point where reloading begins to the load reversal point on the backbone curve (at highest previously imposed strain) *Verify that the reloading modulus of elasticity (E_r) is less than the initial modulus (E_1) for low-to-high stiffness ties IF reloading starts from origin, then: $\sigma_{new} = E_r\varepsilon$ or $\sigma_{new} = E_1\varepsilon$ Otherwise: $\sigma_{new} = \sigma_{old} + E_r\Delta\varepsilon$ or $\sigma_{new} = \sigma_{old} + E_1\Delta\varepsilon$	(B)	IF test stress is less than 0.0 and current strain is greater than 0.0: $\sigma_{new} = 0.0$
			(C)	IF current strain (ε) is less than 0.0 (element is no longer in tension): STATE = 3, CONTINUE
(3)	CASE 3	Compute a test stress ($\sigma_{test} = \sigma_{old} + E_5\Delta\varepsilon$)	CASE 6	$\sigma_{new} = E_6\varepsilon$
	(A)	IF test stress is less than 0.0 and current strain (ε) is less than 0.0: $\sigma_{new} = \sigma_{old} + E_6\Delta\varepsilon$		
	(B)	IF test stress is greater than 0.0 and current strain (ε) is greater than 0.0 (element is no longer under compression): Let previous stress (σ_{old}) equal 0.0 STATE = 2, CONTINUE		

An example of the *FORTRAN90* code used to execute the material model subroutine is shown here:

```
C
C*****ABAQUS UMAT SUBROUTINE HEADER*****************************
C
      SUBROUTINE UMAT(STRESS,STATEV,DDSDDE,SSE,SPD,SCD,RPL,
     1 DDSDDT,DRPLDE,DRPLDT,STRAN,DSTRAN,TIME,DTIME,TEMP,DTEMP,
     2 PREDEF,DPRED,CMNAME,NDI,NSHR,NTENS,NSTATV,PROPS,NPROPS,
     3 COORDS,DROT,PNEWDT,CELENT,DFGRD0,DFGRD1,NOEL,NPT,LAYER,
     4 KSPT,KSTEP,KINC)
C
      INCLUDE 'ABA_PARAM.INC'
C
      CHARACTER*80 CMNAME
      DIMENSION STRESS(NTENS), STATEV(NSTATV),
     1 DDSDDE(NTENS,NTENS),
     2 DDSDDT(NTENS), DRPLDE(NTENS),
     3 STRAN(NTENS), DSTRAN(NTENS),TIME(2),PREDEF(1),DPRED(1),
     4 PROPS(NPROPS),COORDS(3),DROT(3,3),DFGRD0(3,3),DFGRD1(3,3)
C
C*****PARAMETER DECLARATIONS*************************************
C
      INTEGER :: STATE, ACTION
      LOGICAL :: AGAIN
C
C*****DEFINE THE TIE CONNECTION PROPERTIES**********************
C
      EMOD1 = PROPS(1)
      EMOD2 = PROPS(2)
      EMOD3 = PROPS(3)
      EMOD4 = PROPS(4)
      EMOD5 = PROPS(5)
      EMOD6 = PROPS(6)
      EA = PROPS(7)
      EB = PROPS(8)
      EC = PROPS(9)
      ED = PROPS(10)
      SA = PROPS(11)
      SB = PROPS(12)
      SC = PROPS(13)
      SD = PROPS(14)
C
C*****INITIALIZE THE STATE HISTORY VARIABLES********************
C
C     STATEV(1) => HISTORY MODULUS
C     STATEV(2) => HISTORY STRAIN
C     STATEV(3) => HISTORY STRESS
C     STATEV(4) => HISTORY STATE
C
      IF (STATEV(2) .LE. 0.0 .AND. STATEV(3) .LE. 0.0) THEN
          STATEV(1) = EMOD1
          STATEV(2) = 0.0
          STATEV(3) = STATEV(1)*STATEV(2)
          STATEV(4) = 1
      END IF
C
C*****COMPUTE CURRENT STRAIN USING CURRENT STRAIN INCREMENT*****
C
      DEPS = DSTRAN(1)
      OLDEPS = STRAN(1)
      EPS = OLDEPS+DEPS
C
```

```
C*****DETERMINE UPCOMING ACTION BASED ON INITIAL OR PREVIOUS****
C*****STATE AND CURRENT STRAIN INCREMENT************************
C
      IF (DEPS .GE. 0.0) IADD = 1
      IF (DEPS .LT. 0.0) IADD = 2
      STATE = STATEV(4)
C
C*****EXECUTE STATE TABLE***************************************
C
      AGAIN = .TRUE.
      DO WHILE (AGAIN)
      ACTION = (IADD-1)*3 + STATE
C
      SELECT CASE(ACTION)
C
      CASE(1)
      STATE = 2
C
      CASE(2)
C
      IF (EPS .GE. STATEV(2)) THEN
        IF (EPS .LT. EA) THEN
           DDSDDE(1,1) = EMOD1
           STRESS(1) = EMOD1*EPS
        ELSE IF (EPS .GT. EA .AND. EPS .LT. EB) THEN
           DDSDDE(1,1) = EMOD2
           STRESS(1) = SA+(EPS-EA)*EMOD2
        ELSE IF (EPS .GT. EB .AND. EPS .LT. EC) THEN
           DDSDDE(1,1) = EMOD3
           STRESS(1) = SB+(EPS-EB)*EMOD3
        ELSE IF (EPS .GT. EC) THEN
           DDSDDE(1,1) = EMOD4
           STRESS(1) = SC+(EPS-EC)*EMOD4
        ELSE IF (EPS .GT. ED) THEN
           DDSDDE(1,1) = -0.0001
           STRESS(1) = SD
        END IF
        AGAIN = .FALSE.
      ELSE IF (EPS .LT. STATEV(2)) THEN
        IF (OLDEPS .LT. 0.0 .AND. EPS .GT. 0.0) THEN
        DELSTRAIN = STATEV(2)
        DELSTRESS = STATEV(3)
        EMODR = DELSTRESS/DELSTRAIN
           IF (EPS .LT. EA .AND. EMODR .GT. EMOD1) THEN
             DDSDDE(1,1) = EMOD1
             STRESS(1) = EMOD1*EPS
             AGAIN = .FALSE.
           ELSE
             DDSDDE(1,1) = EMODR
             STRESS(1) = EMODR*EPS
             AGAIN = .FALSE.
           END IF
        ELSE
        DELSTRAIN = STATEV(2)-STRAN(1)
        DELSTRESS = STATEV(3)-STRESS(1)
        EMODR = DELSTRESS/DELSTRAIN
           IF (EPS .LT. EA .AND. EMODR .GT. EMOD1) THEN
             DDSDDE(1,1) = EMOD1
             STRESS(1) = STRESS(1)+EMOD1*DEPS
             AGAIN = .FALSE.
           ELSE
             DDSDDE(1,1) = EMODR
```

```
              STRESS(1) = STRESS(1)+EMODR*DEPS
              AGAIN = .FALSE.
            END IF
          END IF
        END IF
C
        CASE(3)
        TESTSTRESS = STRESS(1)+EMOD6*DEPS
        IF (TESTSTRESS .LT. 0.0 .AND. EPS .LT. 0.0) THEN
             DDSDDE(1,1) = EMOD6
             STRESS(1) = STRESS(1)+EMOD6*DEPS
             AGAIN = .FALSE.
        ELSE IF (TESTSTRESS .GT. 0.0 .AND. EPS .GT. 0.0) THEN
             STRESS(1) = 0.0
             STATE = 2
        END IF
C
        CASE(4)
        STATE = 3
C
        CASE(5)
        TESTSTRESS = STRESS(1)+EMOD5*DEPS
        IF (TESTSTRESS .GT. 0.0 .AND. EPS .GT. 0.0) THEN
             DDSDDE(1,1) = EMOD5
             STRESS(1) = STRESS(1)+EMOD5*DEPS
             AGAIN = .FALSE.
        ELSE IF (TESTSTRESS .LE. 0.0 .AND. EPS .GT. 0.0) THEN
             DDSDDE(1,1) = 0.0
             STRESS(1) = 0.0
             AGAIN = .FALSE.
        ELSE IF (EPS .LT. 0.0) THEN
             STATE = 3
        END IF
C
        CASE(6)
        DDSDDE(1,1) = EMOD6
        STRESS(1) = EMOD6*EPS
        AGAIN = .FALSE.
C
        END SELECT
        END DO
C
C
C*****RECORD HISTORY DATA FOR NEXT INCREMENT*******************
C
        IF (DSTRAN(1) .GT. 0.0 .AND. EPS .GT. STATEV(2)) THEN
             STATEV(1) = DDSDDE(1,1)
             STATEV(2) = EPS
             STATEV(3) = STRESS(1)
        END IF
        STATEV(4) = STATE
C
        RETURN
        END
```

C.2 Evaluation of Brick Veneer Cracking

Cracking in brick masonry veneer walls has sometimes been represented with a discrete crack model by introducing hinges between wall element nodes, as shown by Arumala (1991) and Junyi et al. (2003). Furthermore, Casolo et al. (2000) showed that the classic plasticity model can effectively be used to represent the pre- and post-cracked flexural behavior of masonry. As part of preliminary FE analyses of brick veneer walls, a discrete crack model was implemented in the brick veneer wall models, representing the rupture strength of masonry and subsequent hinging behavior after the rupture strength was exceeded. Analysis results showed that even though cracking played a role in the response of the wall panels, the tie connection properties dominated the response and ultimate performance of brick veneer walls. Therefore, cracking was not represented in the final analytical program, in order to simplify the wall panel models for various parameter studies, and also because brick veneer wall performance was effectively represented by utilizing detailed nonlinear inelastic FE models for the tie connections.

C.2.1 Overview of FE Model and Analysis Setup

Experimental tests showed that the brick masonry veneer under out-of-plane loading experienced cracking as a result of flexural deformations. A horizontal crack formed in the brick veneer of Wall-1 at approximately 73 in. (1.85 m) from the base of the veneer (below the top two rows of ties) during the collapse earthquake input M10-0.64[0.54]g; in Wall-2, a horizontal crack developed earlier in testing, during the M10-0.30[0.24]g input, at approximately 55 in. (1.40 m) from the base of the veneer (below the top three rows of ties). The brick veneer in Wall-3 first underwent horizontal cracking during the M10-0.63[0.49]g input, along the base of the gable (starting from the top two corners of the window opening). Cracks in the brick veneer generally formed in clearly defined linear patterns, primarily along the brick masonry mortar joints.

In the FE wall panel models, hinges were introduced between the brick veneer shell element nodes, at the locations shown in Figure C.1 (approximately at the locations where cracking was noted experimentally). Additionally, rotational resistance was introduced at the hinge locations with a classic plasticity model, as shown in Figure C.2 from Casolo et al. (2000). The pre-cracked masonry strength was represented with a rupture strength (σ_y) of 75 psi (517 kPa) (rupture strength of brick masonry with type N mortar), and the post-cracked ultimate strength (σ_u) was defined as nearly zero. Time history analyses were then conducted with the FE wall panel models, first to evaluate the load intensity to cause onset of cracking in the brick veneer, and then to compare the total response of the FE wall models with cracking in the brick veneer to those without a cracking model.

C.2.2 FE Analysis Results and Discussion

The FE wall panel models were subjected to the M10 earthquake input, scaled to gradually increasing PGA values, and the flexural stresses in the brick veneer shell elements were recorded. Table C.2 summarizes the M10 input PGAs from the experiments that caused brick veneer cracking, and the FE analyses where the rupture

stress in the brick veneer was exceeded. The vertical location of the maximum computed stresses in the brick veneer of all three wall panel models matched closely with the location of brick veneer cracking in the physical test structures. The FE wall model of Wall-1 predicted cracking at lower PGA values than was observed experimentally. The Wall-2 and -3 models were somewhat closer at predicting the load for onset of cracking. Furthermore, the brick veneer wall models effectively represented the intended pre- and post-cracked behavior of masonry, as shown in Figure C.3. For example, the time trace of the rotation of the top one-third of the brick veneer with respect to the lower portion (in a model of Wall-1) exhibited nearly zero values before cracking (up to approximately 4 sec into the earthquake record), followed by much higher rotation angles after cracks developed. The pre- and post-cracked wall strength behavior was also successfully modeled, capturing the rupture capacity, which then dropped to nearly zero strength (Figure C.3(b)).

The peak overall displacements of brick veneer wall panel models, with and without cracking, are compared in Figures C.4 and C.5. In models of Walls-1 and -3, the presence of a crack hinge allowed the brick veneer to bend and assume a shape more like that of the wood frame backup, reducing the load demand on the upper rows of tie connections. (This type of response was noted experimentally in Wall-3.) Experimental tests, however, showed that the tie connections in the upper regions of the wall panels underwent the highest loads. Therefore, the wall panel models with a continuous brick veneer appeared to actually be more conservative at estimating the demand on the upper rows of ties. This model effectively captured the onset of brick veneer cracking and post cracked hinging behavior. This type of model was not employed in the final analytical program, in order to simplify the wall panel models for various parameter studies, and also because brick veneer wall performance was effectively represented by utilizing detailed nonlinear inelastic FE models for the tie connections.

Table C.2 – Summary of M10 earthquake input PGAs at onset of cracking (experiment vs. analysis).

Wall Panel	Experiment Nominal Scaled PGA (g)	FE Scaled PGA (g)
Wall-1	0.54	0.25
Wall-2	0.24	0.26
Wall-3	0.49	0.40

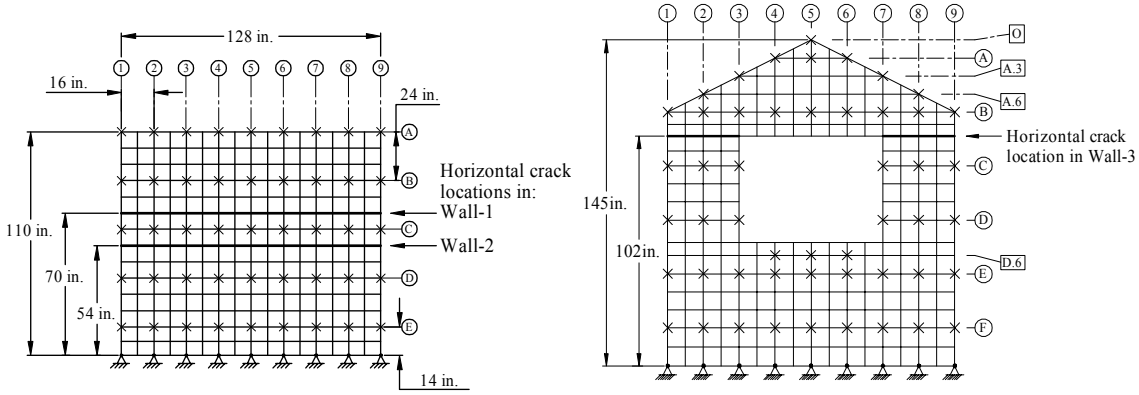

Figure C.1 – Horizontal crack hinge locations in brick veneer wall models.

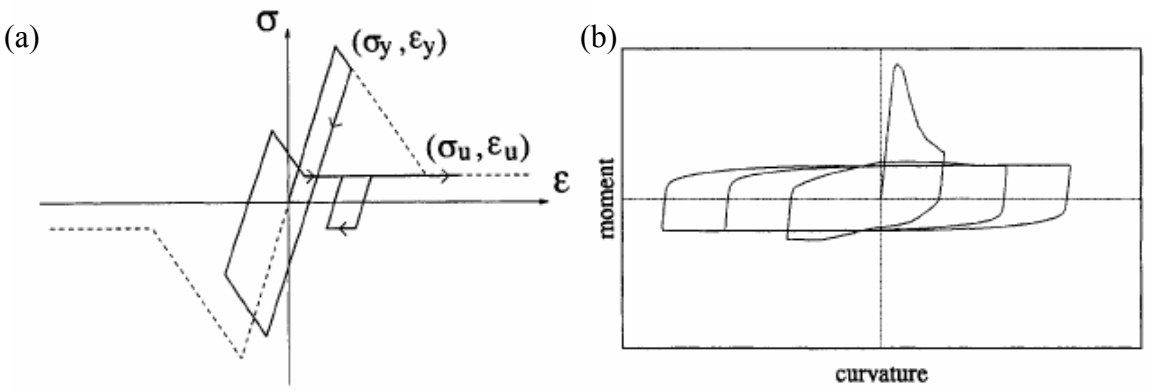

Figure C.2 – Example of brick masonry material cracking model from Casolo et al. (2000): (a) classic plasticity model representing pre- and post-cracked behavior of masonry, and (b) general moment-curvature response with this type of a model.

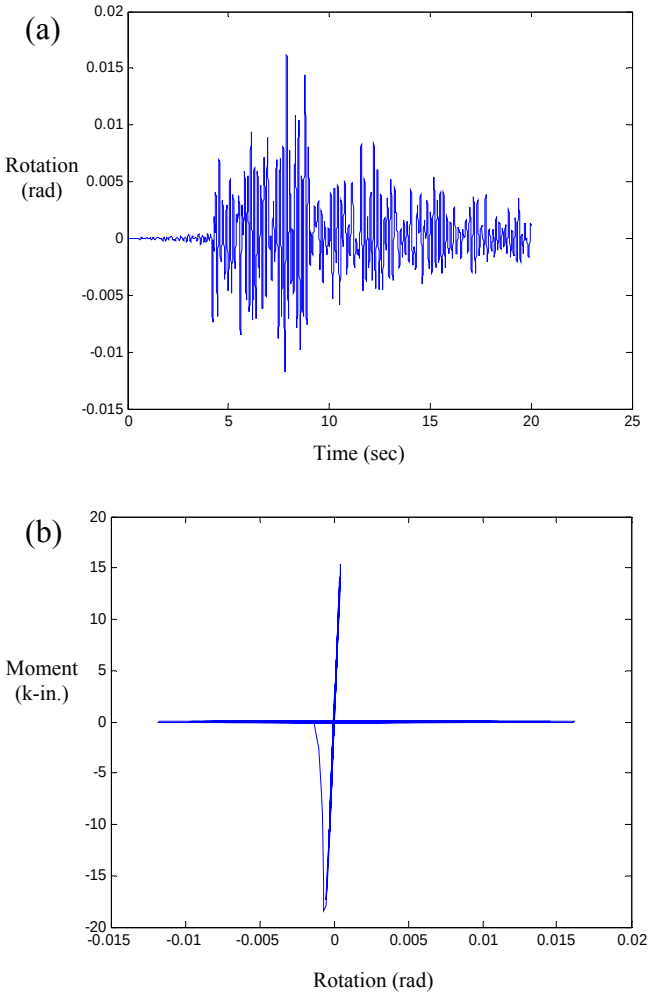

Figure C.3 – (a) Time history trace of angle of rotation between the top one-third and lower portion of the brick veneer of Wall-1 model subjected to M10-0.54g input, and (b) total brick veneer moment vs. rotation at the hinge location, before and after cracking.

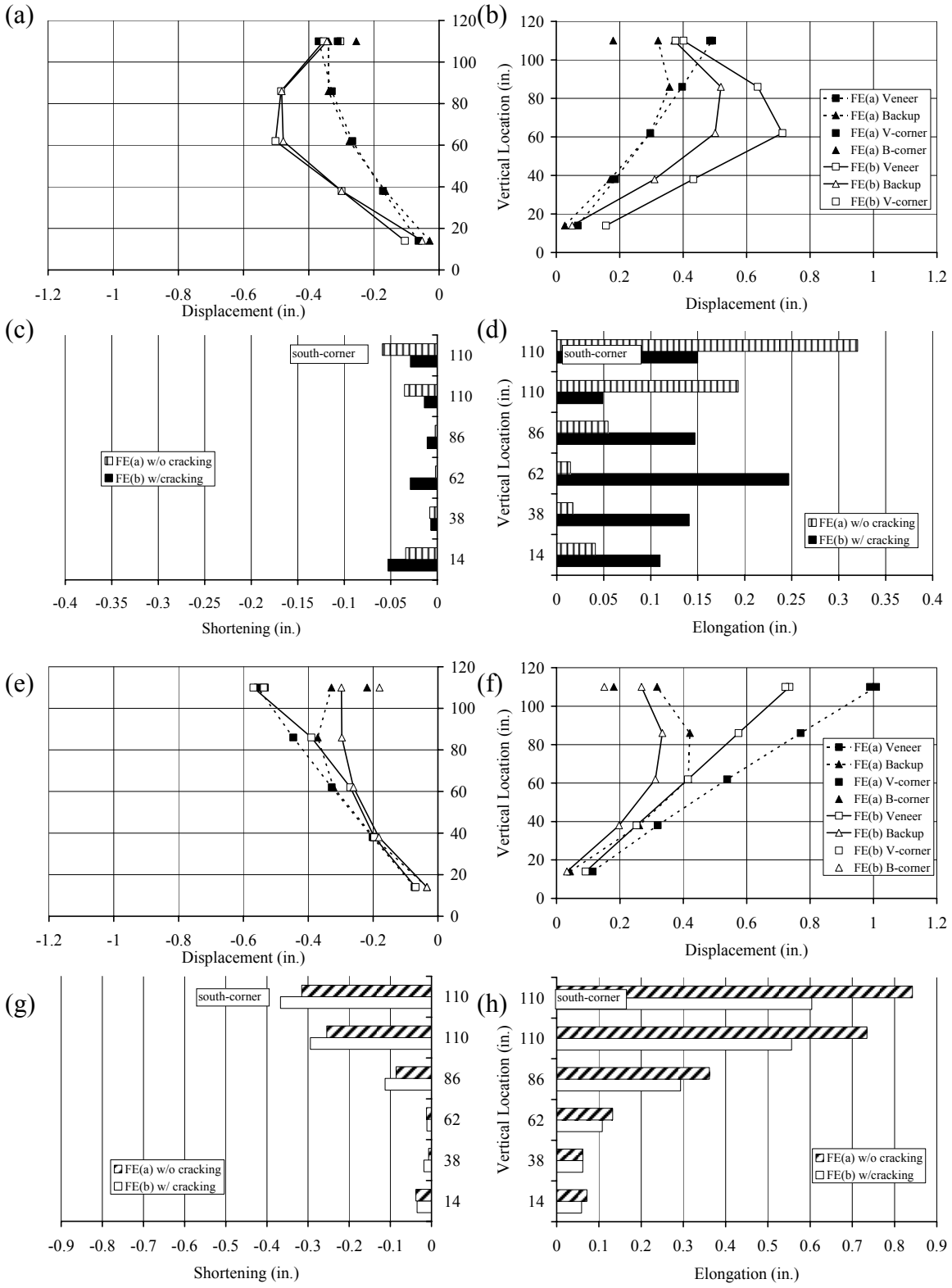

Figure C.4 – Peak displacements and tie deformations in the negative (inward) and positive (outward) directions for (a-d) Wall-1 models during M10-0.54g input and (e-h) Wall-2 models during M10-0.48g input. (FE(a) – wall model without brick veneer cracking; FE(b) – wall model with cracking.)

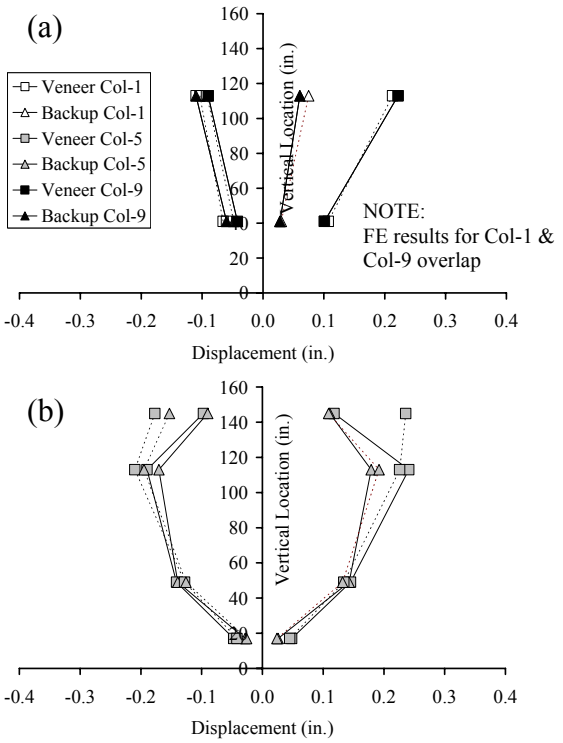

Figure C.5 – Peak negative and positive displacements of the Wall-3 model during dynamic M10-0.55g input along (a) vertical edges, and (b) centerline. (Brick veneer with cracking (solid lines) and without cracking (dashed lines).)

C.3 FE Wall Model Validation Results

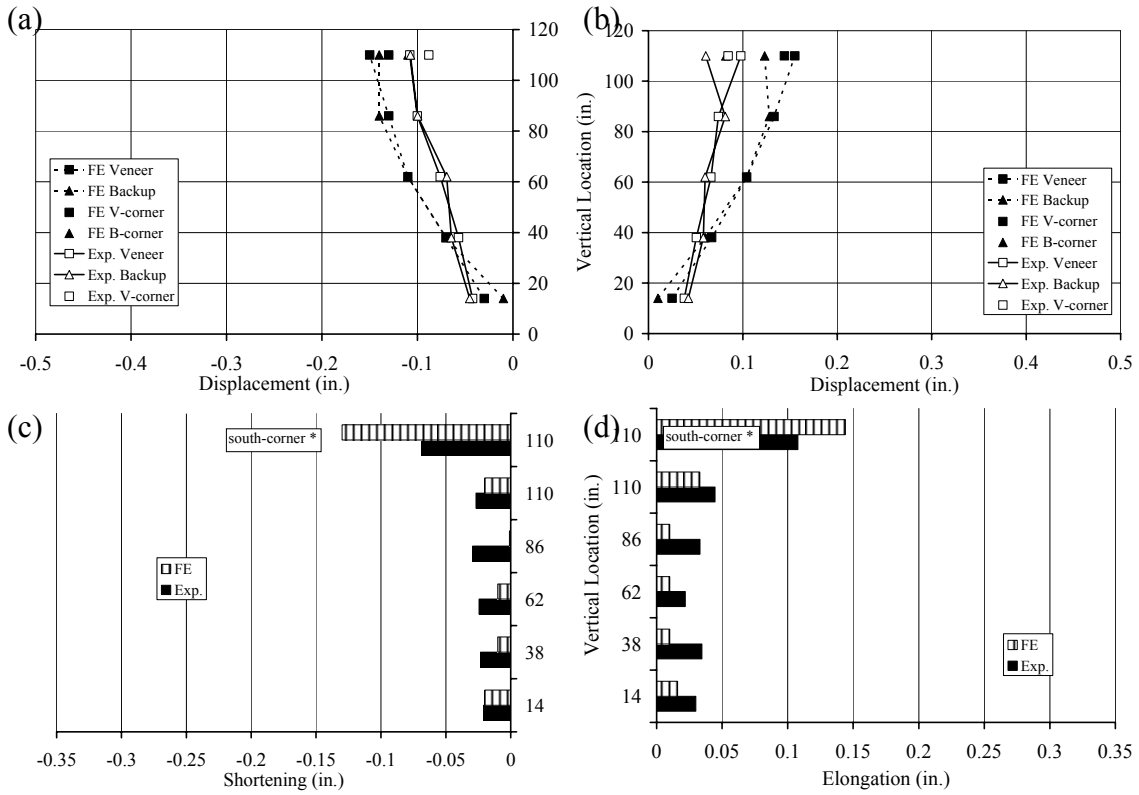

Figure C.6 – Peak displacements and tie deformations in the negative (inward) and positive (outward) directions for Wall-1 during M02-0.34[0.31]g input (* - net brick displacement).

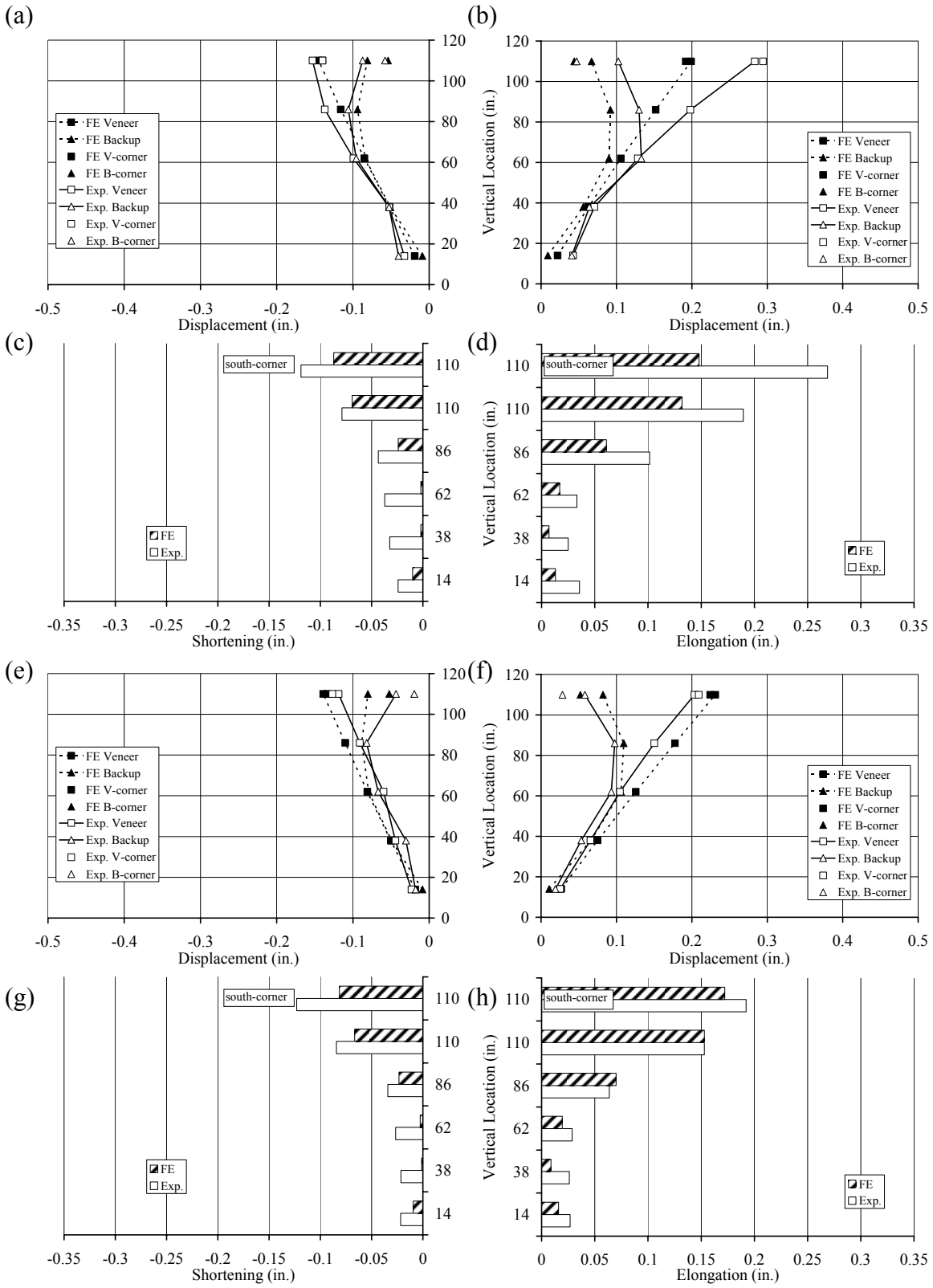

Figure C.7 – Peak displacements and tie deformations in the negative (inward) and positive (outward) directions for Wall-2 during (a-d) M02-0.20[0.18]g input and (e-h) NA-0.15[0.15]g input.

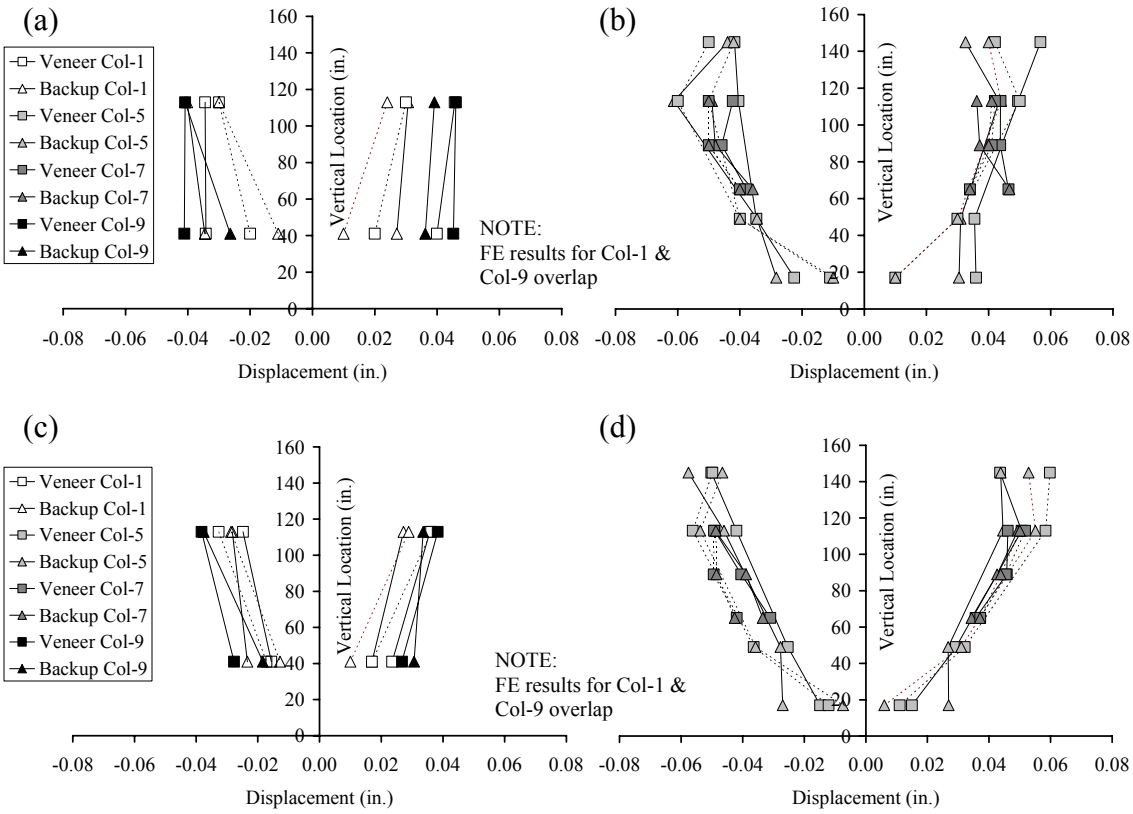

Figure C.8 – Peak displacements in the negative (inward) and positive (outward) directions for Wall-3 during (a-b) M02-0.22[0.22]g input and (c-d) NA-0.16[0.16]g input.

C.4 FE Wall Model Parametric Study Results

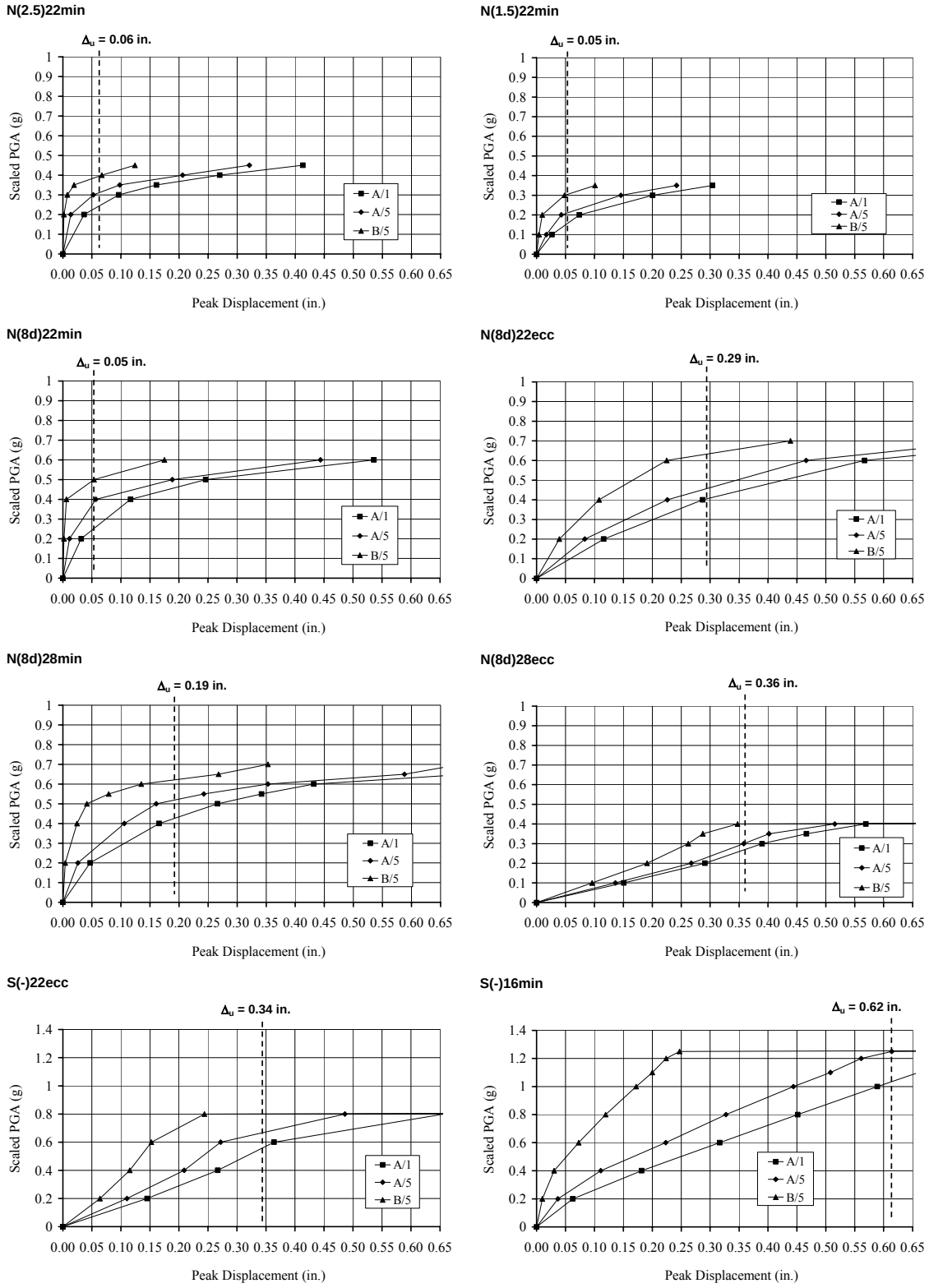

Figure C.9 – M10 earthquake input PGAs vs. key tie elongations used to evaluate damage limit states during parametric studies of solid wall panels with tie layout "A" (24 in. x 16 in. grid).

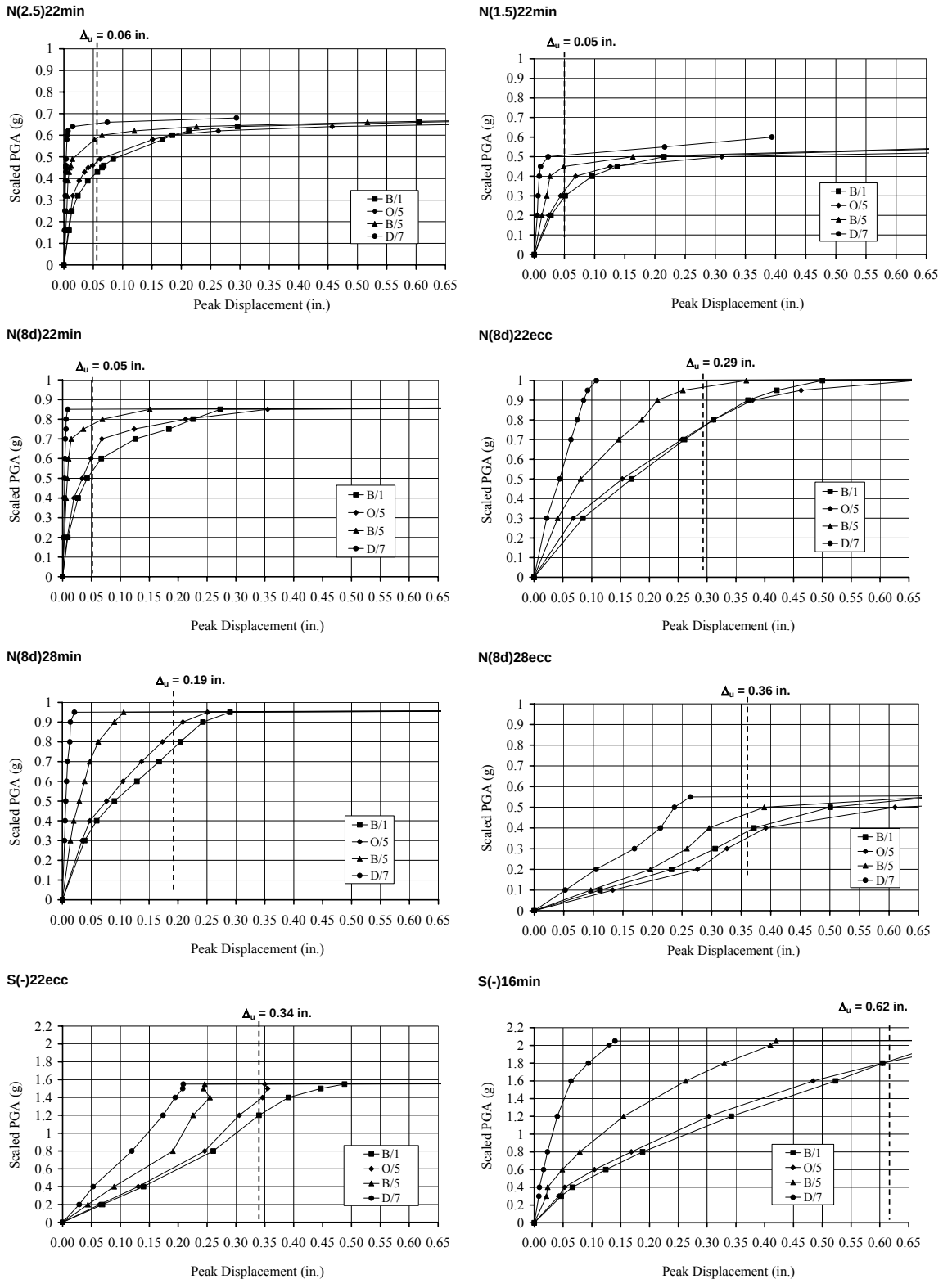

Figure C.10 – M10 earthquake input PGAs vs. key tie elongations used to evaluate damage limit states during parametric studies of wall panels with window opening and gable, with tie layout "AY" (24 in. x 16 in. grid, including additional ties at all edges of the wall).

FRAGILITY ASSESSMENT OF BRICK VENEER

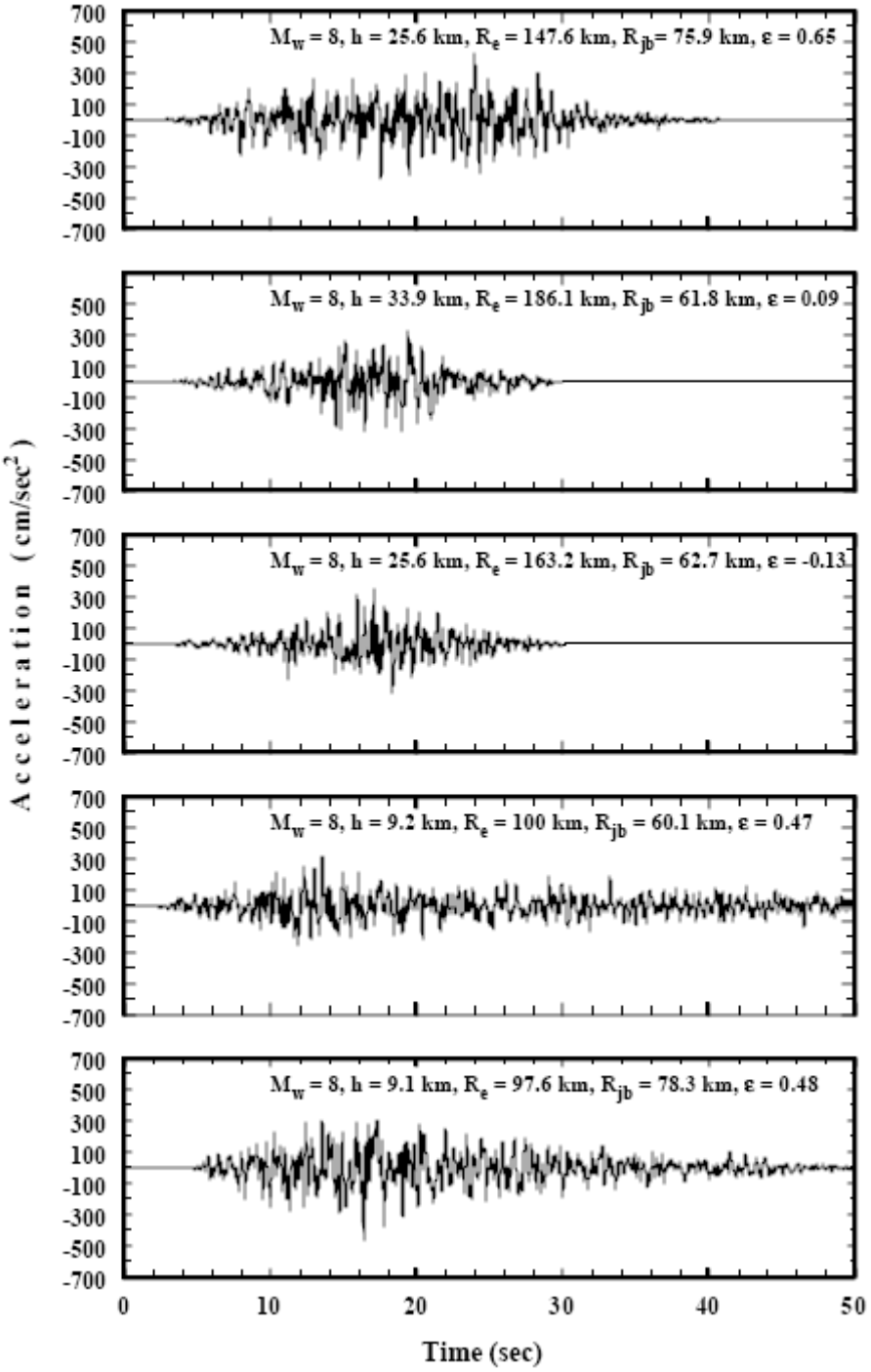

Figure D.1 – Uniform hazard ground motions for Memphis soil site with 2% probability of exceedance in 50 years (Wen and Wu 2001).

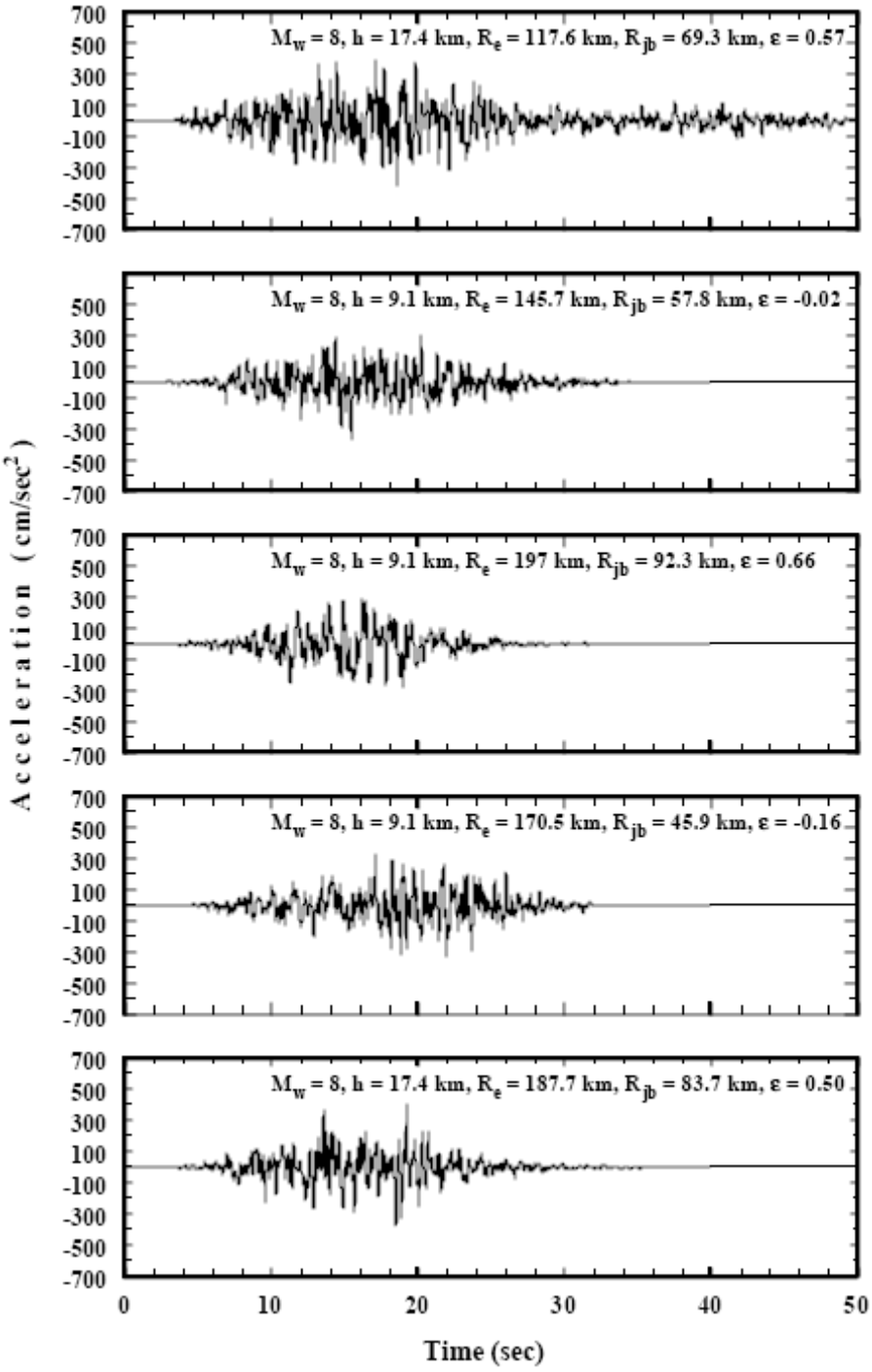

Figure D.1 – (continued).

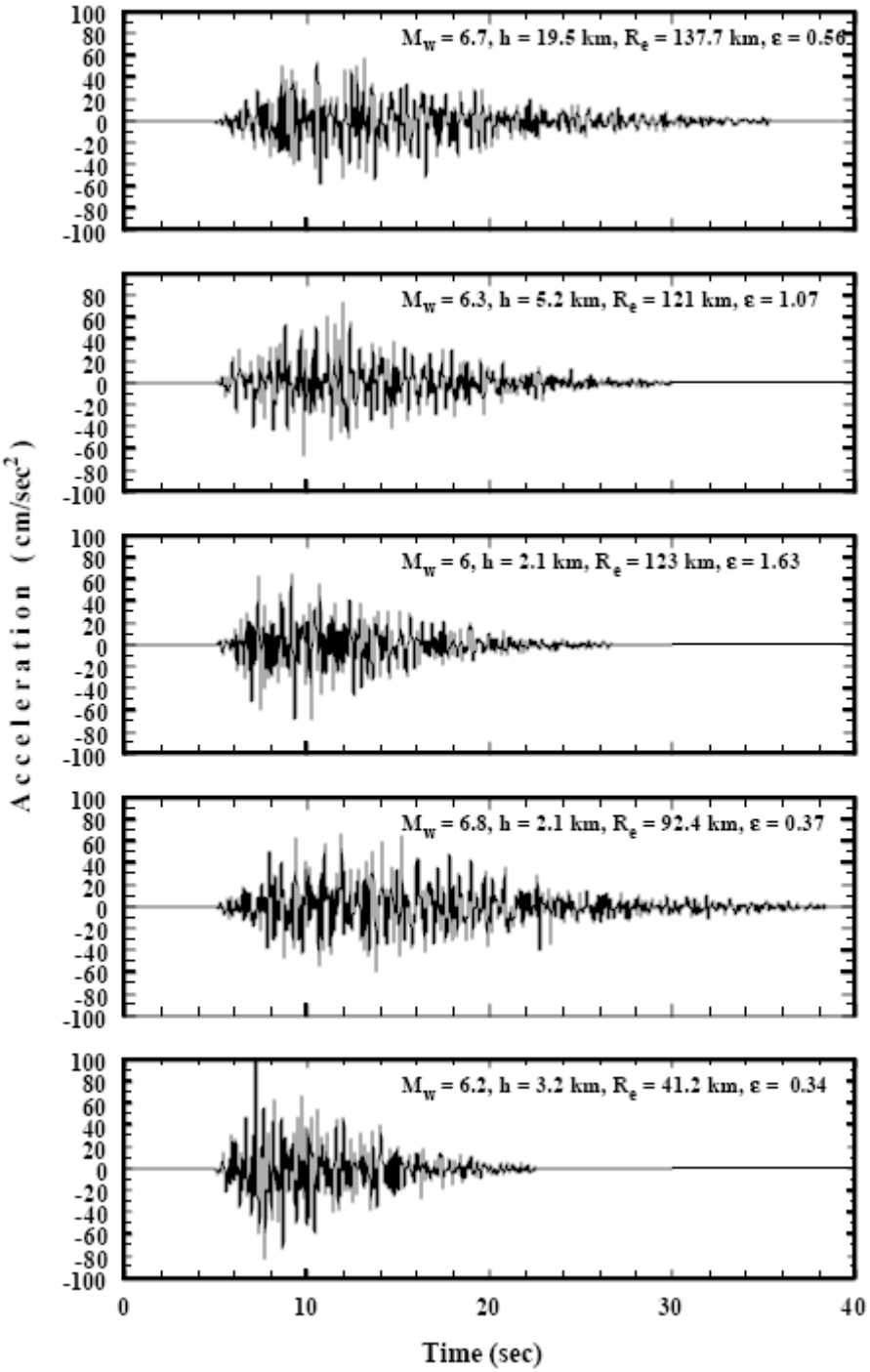

Figure D.2 – Uniform hazard ground motions for Memphis soil site with 10% probability of exceedance in 50 years (Wen and Wu 2001).

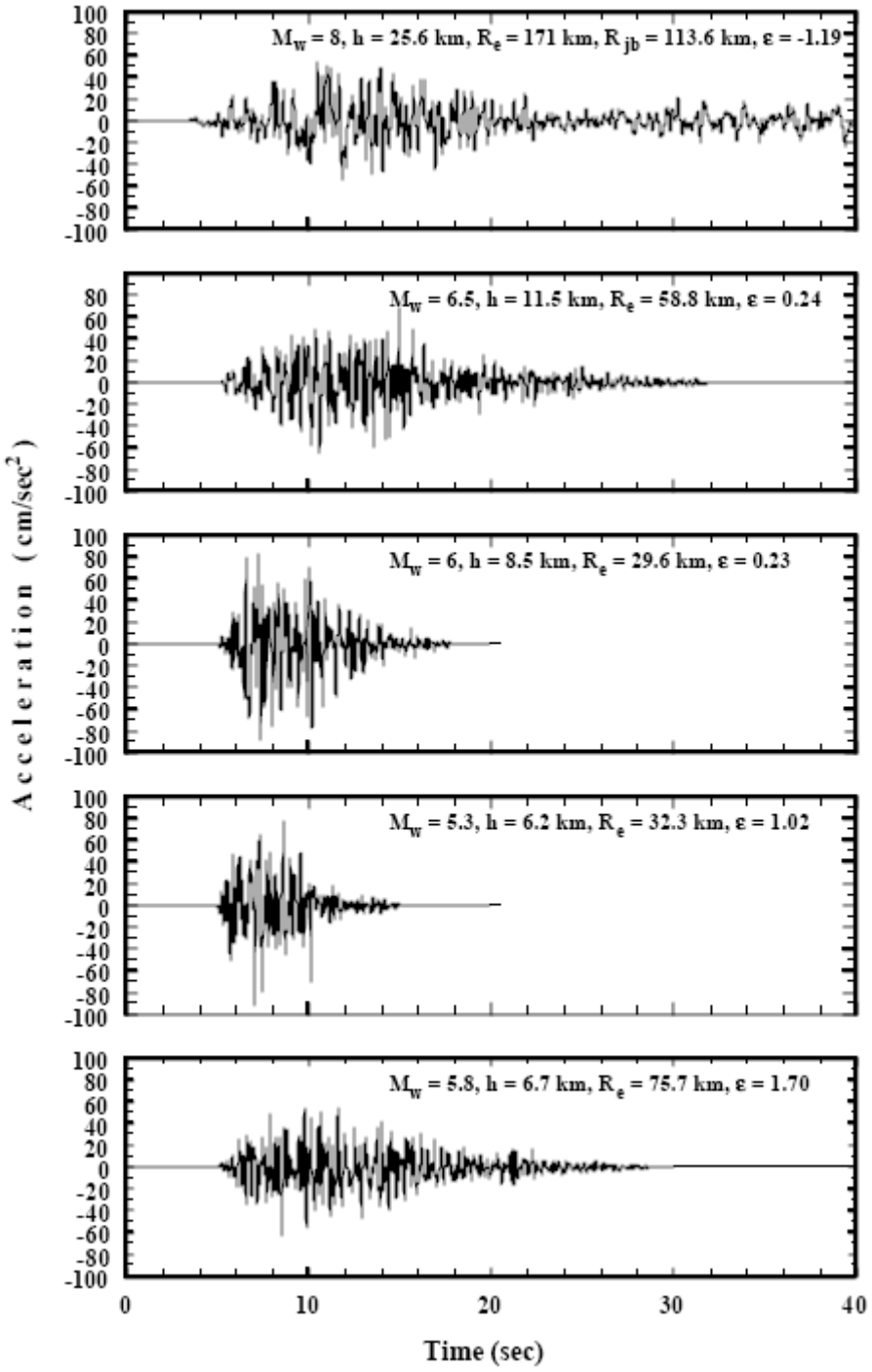

Figure D.2 – (continued).

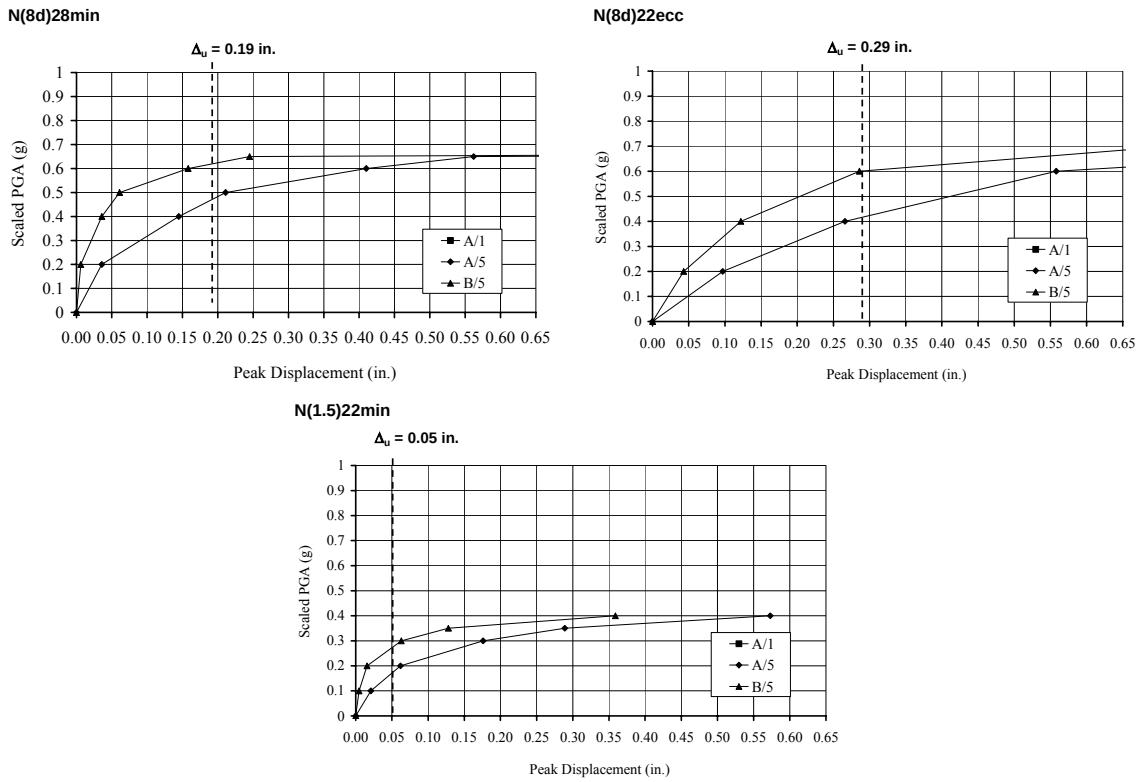

Figure D.3 – M10 earthquake input PGAs vs. key tie elongations used to evaluate damage limit states for simplified wall strip models.

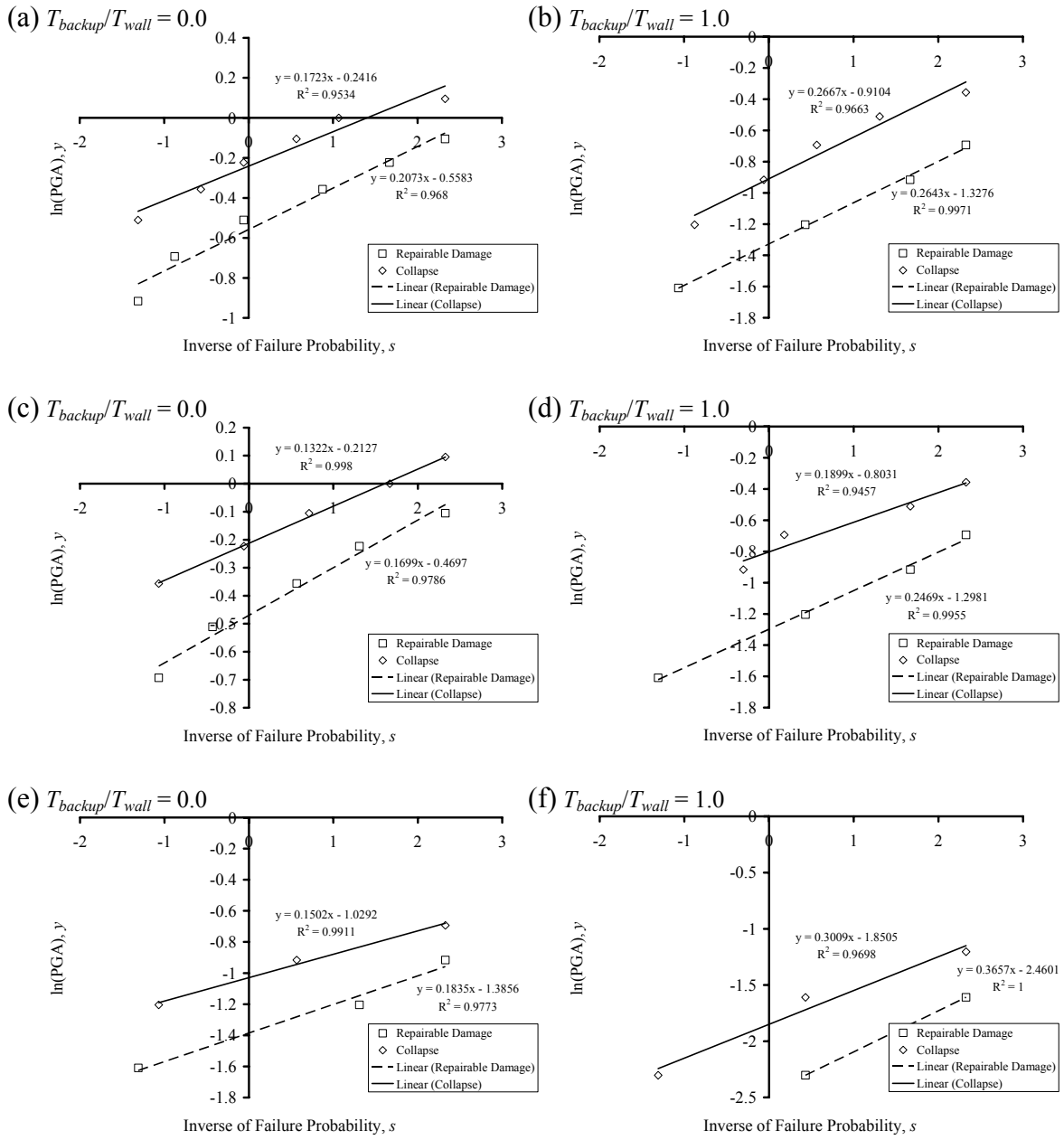

Figure D.4 – Probability paper and lognormal parameter calculations for wall strips with (a-b) N(8d)22ecc, (c-d) N(8d)28min and (e-f) N(1.5)22min types of tie connections with a vertical spacing of 24 in.

(a) $T_{backup}/T_{wall} = 1.0$

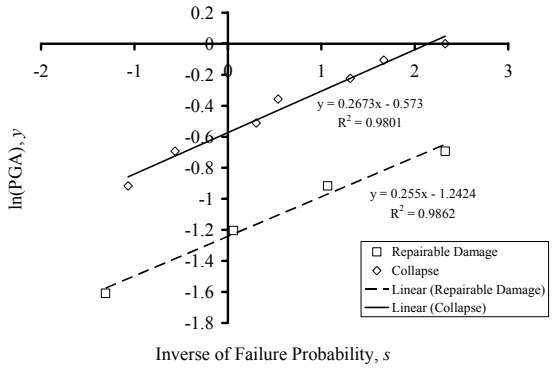

(b) $T_{backup}/T_{wall} = 1.0$

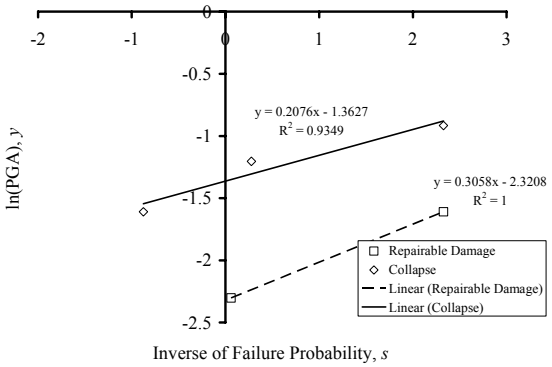

Figure D.5 – Probability paper and lognormal parameter calculations for wall strips with (a) N(8d)22ecc and (b) N(1.5)22min type tie connections with 16 in. vertical spacing.

List of Recent NSEL Reports

No.	*Authors*	*Title*	*Date*
001	Nagayama, T. and Spencer, B.F.	Structural Health Monitoring Using Smart Sensors	Nov. 2007
002	Sun, S. and Kuchma, D.A.	Shear Behavior and Capacity of Large-Scale Prestressed High-Strength Concrete Bulb-Tee Girders	Nov. 2007
003	Nagle, T.J. and Kuchma, D.A.	Nontraditional Limitations on the Shear Capacity of Prestressed, Concrete Girders	Dec. 2007
004	Kwon, O-S. and Elnashai, A.S.	Probabilistic Seismic Assessment of Structure, Foundation, and Soil Interacting Systems	Dec. 2007
005	Nakata, N., Spencer, B.F., and Elnashai, A.S.	Multi-dimensional Mixed-mode Hybrid Simulation: Control and Applications	Dec. 2007
006	Carrion, J. and Spencer, B.F.	Model-based Strategies for Real-time Hybrid Testing	Dec. 2007
007	Kim, Y.S., Spencer, B.F., and Elnashai, A.S.	Seismic Loss Assessment and Mitigation for Critical Urban Infrastructure Systems	Jan. 2008
008	Gourley, B.C., Tort, C., Denavit, M.D., Schiller, P.H., and Hajjar, J.F.	A Synopsis of Studies of the Monotonic and Cyclic Behavior of Concrete-Filled Steel Tube Members, Connections, and Frames	April 2008
009	Xu, D. and Hjelmstad, K.D.	A New Node-to-node Approach to Contact/Impact Problems for Two Dimensional Elastic Solids Subject to Finite Deformation	May 2008
010	Zhu, J. and Popovics, J.S.	Non-contact NDT of Concrete Structures Using Air Coupled Sensors	May 2008
011	Gao, Y. and Spencer, B.F.	Structural Health Monitoring Strategies for Smart Sensor Networks	May 2008
012	Andrews, B., Fahnestock, L.A. and Song, J.	Performance-based Engineering Framework and Ductility Capacity Models for Buckling-Restrained Braces	July 2008
013	Pallarés, L. and Hajjar, J.F.	Headed Steel Stud Anchors in Composite Structures: Part I – Shear	April 2009
014	Pallarés, L. and Hajjar, J.F.	Headed Steel Stud Anchors in Composite Structures: Part II – Tension and Interaction	April 2009
015	Walsh, S. and Hajjar, J.F.	Data Processing of Laser Scans Towards Applications in Structural Engineering	August 2009
016	Reneckis, D. and LaFave, J.M.	Seismic Performance of Anchored Brick Veneer	August 2009